ISTANBUL TECHNICAL UNIVERSITY ★ INSTITUTE OF SCIENCE AND TECHNOLOGY

COPYROLYSIS OF AVGAMASYA ASPHALTITE AND GÖYNÜK OIL SHALE FOR PITCH PRECURSORS: CHARACTERISATION AND CARBON FIBRE PRODUCTION

PhD Thesis by

Mevlude Ebru APAK, MSc.

506942022

Date of submission : 17 December 1999

Date of defence examination: 10 March 2000

Supervisor (Chairman): Assoc. Prof. M. Ferhat YARDIM

Members of the Examining Committee: Prof. Dr. Ekrem EKINCI (I.T.U.)

Prof. Dr. A. Tuncer ERCIYES (I.T.U.)

Prof. Dr. Yuda YURUM (S.U.)

Assoc. Prof. Sunullah OZBEK (TUBITAK)

MARCH 2000

İSTANBUL TEKNİK ÜNİVERSİTESİ ★ FEN BİLİMLERİ ENSTİTÜSÜ

ZİFT ELDESİ İÇİN AVGAMASYA ASFALTİTİ VE GÖYNÜK BİTÜMLÜ ŞİSTİNİN KOPİROLİZİ: ZİFT KARAKTERİZASYONU VE KARBON FİBER ÜRETİMİ

DOKTORA TEZİ

Y. Müh. Mevlude Ebru APAK

506942022

Tezin Enstitüye Verildiği Tarih : 17 Aralık 1999

Tezin Savunulduğu Tarih : 10 Mart 2000

Tez Danışmanı : Doç. Dr. M. Ferhat YARDIM

Diğer Jüri Üyeleri : Prof. Dr. Ekrem EKİNCİ (İ.T.Ü.)

Prof. Dr. A. Tuncer ERCİYES (İ.T.Ü.)

Prof. Dr. Yuda YÜRÜM (S.Ü.)

Doç. Dr. Sunullah ÖZBEK (TÜBİTAK)

MART 2000

PREFACE

This present study consists of an introduction to pitch precursors, covering their production by some methods and characterisation as well as processing one of the pitches into carbon fibre. The primary aim of this research is to appreciate Turkish fossil fuels, which comprise the largest reserves in Turkey, to produce pitch precursors. Therefore, Göynük oil shale which yields in high amounts of tar and Avgamasya asphaltite which has mostly aromatic structures have been selected as alternative raw materials.

During my research, I have had a great deal of help in terms of information, investigation, and guidance from my dearest supervisor Assoc. Prof. M. Ferhat YARDIM. I am grateful to him for his help, supervision, and for his patience.

I would like to thank Prof. Ekrem EKİNCİ for his professional advice, and encouragement. His amazing knowledge has always illuminated me. I am very lucky since he has taught me how to be a scientist.

I am grateful to British Council and Tübitak since they awarded me with their joint scholarship in order to make a research for my PhD study at the University of Leeds, School of Materials and School of Chemistry.

It is a great pleasure for me to thank Prof. Brian RAND who is the head of the School of Materials at the University of Leeds for his spiritual support, precious guidance, and generosity. He accepted me as one of the members of his Carbon Group and he gave me a great courage to complete my thesis with success.

I also would like to thank Prof. Keith BARTLE at the University of Leeds, School of Chemistry for his generosity during my research at his laboratories.

Many thanks to my dearest friends Dr. Andy ROSS, Dr. Shillin LU, and Dr. Ricardo SANTAMARIA for their invaluable helps, immeasurable patience, co-operation, and willingness to pass me their knowledge.

Finally, I would like to thank my mom Ayet and dad Yaşar who have given me endless support all my life long. They have provided me encouragement when my enthusiasm was flagging.

Once again, thank you all very much.

December, 1999 Mevlude Ebru APAK

CONTENTS

ABBREVIATIONS

A	: 100% Avgamasya Asphaltite Tar
A-A1	: Air-blowing Residual Product of A at 250°C for 60 Minutes
AA	: Avgamasya Asphaltite
ASTM	: American Standards Testing Materials
AT	: Air-blowing Temperature
BS	: Benzene Soluble
$CDCl_3$	: Deuterochloroform
CY	: Carbon Yield
db	: Dry Basis
DCM	: Dichloromethane
DDSC	: Dynamic Differential Scanning Calorimetry
DSC	: Differential Scanning Calorimetry
DTA	: Differential Thermal Analysis
DTG	: Derivative Thermogravimetry
EI	: Electron Impact
FAB-MS	: Fast Atom Bombardment Mass Spectrometer
FTIR	: Fourier Transform Infrared Spectrometry
GCMS	: Gas Chromatography Mass Spectrometry
GOS	: Goynuk Oil Shale
GPa	: Giga Pascal
GPCF	: General Purpose Carbon Fibre
HI	: Hexane Insoluble
HPCF	: High Performance Carbon Fibre
HS	: Hexane Soluble
i.d.	: Inner Diameter
IR	: Infrared
MALDI	: Matrix Assisted Laser Desorption Ionisation
MHz	: Mega Hertz
MM	: Molecular Mass
MPa	: Mega Pascal
MS	: Mass Spectrometry
MW	: Molecular Weight
ND	: Not Determined
NT	: Nitrogen-blowing Temperature
NMP	: 1-Methly-2-Pyrrolidinone
NMR	: Nuclear Magnetic Resonance
NOE	: Nuclear Overhouser Enhancement
o.d.	: Outer Diameter
PAH	: Polycyclic Aromatic Hydrocarbon
PAN	: Polyacrylonitrile
PI	: Pyridine Insoluble
ppm	: Part Per Million

QI	: Quinoline Insoluble
RI	: Refractive Index
rpm	: Rate Per Minute
S3A7	: 30% Goynuk Oil Shale + 70% Avgamasya Asphaltite Tar
S5A5	: 50% Goynuk Oil Shale + 50% Avgamasya Asphaltite Tar
S7A3	: 70% Goynuk Oil Shale + 30% Avgamasya Asphaltite Tar
S-A1	: Air-blowing Residual Product of S at 250°C for 60 Minutes
S-A2	: Air-blowing Residual Product of S at 270°C for 90 Minutes
S-V1	: Vacuum distillation Residual Product of S at 300°C for 60 Minutes
S3A7-A1	: Air-blowing Residual Product of S3A7 at 270°C for 90 Minutes
S3A7-V1	: Vacuum distillation Residual Product of S3A7 at 300°C for 60 Minutes
S5A5-A1	: Air-blowing Residual Product of S5A5 at 250°C for 60 Minutes
S5A5-A2	: Air-blowing Residual Product of S5A5 at 250°C for 90 Minutes
S5A5-A3	: Air-blowing Residual Product of S5A5 at 250°C for 240 Minutes
S5A5-A4	: Air-blowing Residual Product of S5A5 at 270°C for 90 Minutes
S5A5-N1	: N_2-blowing Residual Product of S5A5 at 250°C for 60 Minutes
S5A5-N2	: N_2-blowing Residual Product of S5A5 at 250°C for 120 Minutes
S5A5-N3	: N_2-blowing Residual Product of S5A5 at 250°C for 240 Minutes
S5A5-N4	: N_2-blowing Residual Product of S5A5 at 250°C for 480 Minutes
S5A5-N5	: N_2-blowing Residual Product of S5A5 at 300°C for 60 Minutes
S5A5-V1	: Vacuum distillation Residual Product of S5A5 at 300°C for 60 Minutes
S7A3-A1	: Air-blowing Residual Product of S7A3 at 270°C for 60 Minutes
S7A3-A2	: Air-blowing Residual Product of S7A3 at 270°C for 90 Minutes
S7A3-E1	: Solvent Extraction Residual Product of S7A3-V1
S7A3-V1	: Vacuum distillation Residual Product of S7A3 at 300°C for 60 Minutes
S	: 100% Goynuk Oil Shale Tar
SEC	: Size Exclusion Chromatography
SEM	: Scanning Electron Microscopy
SF	: Supercritical Fluid
SFE	: Supercritical Fluid Extraction
TG	: Thermogravimetry
TGA	: Thermogravimetric Analysis
TI	: Toluene Insoluble
THF	: Tetrahydrofuran
TMA	: Thermomechanical Analysis
TS	: Toluene Soluble
UCC	: Union Carbide Company
UV	: Ultraviolet
VDT	: Vacuum-distillation Temperature
VGCF	: Vapour Grown Carbon Fibre
VPO	: Vapour Phase Osmometry

LIST OF TABLES

LIST OF FIGURES

LIST OF SYMBOLS

A_o	:	Aromatic carbon atoms substituted by - OH, ether, -CO and C atoms in carbonyls.
A_1	:	Ring junction carbons, substitutes aromatic ring carbons and halfof the unsubstituted carbons
A_2	:	The other half of unsubstituted (or protonated) aromatic ring carbons
A_3	:	Paraffinic, including cycloparaffinic and carbons of methyl and alkyl substitution on aromatic rings
$A_{14.1}$	:	Terminal methyl carbon - CH3
A_{23}	:	First methylene carbon in long alkyl groups -CH2-CH3
A_{32}	:	Second methylene carbon in long alkyl groups - CH2- CH2-CH3
$A_{29.7}$	:	Third or further methylene carbon in long alkyl groups -(- CH2)n-CH2- CH2-CH3
$A_{19.5}$	:	Internal methyl carbon -CH-CH2 | CH3
A, B	:	Constants
^oA	:	Angstrom
c/2	:	Interlayer distance
C^s_1	:	Weight fraction of non-bridge aromatic rings by alkyl groups
C^u_1	:	Weight fraction of non-bridge aromatic rings which are unsubstituted
C_1	:	Weight fraction of non-bridge aromatic rings which are unbridged
$C_{Al.1}$	:	Methyl carbon
$C_{Al.2}$	:	Methylene carbon
C_{Ali}	:	Aliphatic carbon atoms
C_{Aro}	:	Aromatic carbon atoms
CH_{Aro}	:	Protonated carbon atoms
C_{oq}	:	Outer carbon atoms
C_p	:	Critical point
C_P	:	Heat capacity
C_q	:	Quaternary carbon atoms
C_{qs}	:	Substituted quaternary carbon atoms or internal benzonaphthenic carbons
$+C_s$	:	Caesium ion
C_s	:	Substituted carbon atoms
fa^{13}	:	Aromaticity
f	:	Hydrogen to carbon atomic ratio in alkyl groups
G	:	Gibbs free energy
H_A	:	Hydrogens attached to aromatic ring carbons
H_{CH}	:	Hydrogens in CH groups of saturates
H_{CH2}	:	Hydrogens in CH2 groups of saturates (including cycloparaffins)
H_{OL}	:	Hydrogens attached to carbons forming double bonds

H_α	:	Hydrogens attached to carbons in alkyl substitution α to aromatic ring
$H_{\alpha 1}$	:	Hydrogen in methyl group α to aromatic ring
$H_{\alpha 2}$	:	Hydrogen in CH2 and CH groups of saturates
H_β	:	Hydrogens in alkyl substitution β- or further from aromatic rings
H_γ, H_{CH3}	:	Hydrogen in terminal or isolated CH3 groups of saturates or hydrogens in alkyl groups substituted in position γ- and further from aromatic ring
H	:	Molar enthalpy
H_N	:	Naphthenic methylene and methine (other than α to rings)
H/C	:	Hydrogen to carbon atomic ratio
I_{Ar}	:	Hydrogen aromaticity index
I_S	:	Substitution number
L_a	:	Lamellae size
L_c	:	Stacking height
m/z	:	Mass to charge ratio
M_n	:	Average molecular mass
n	:	Average number of carbon atoms per alkyl substituent
nm	:	Nanometer
P_c	:	Critical pressure
r	:	Number of naphthenic rings per alkyl substituent
R_1, R_2, R_3...	:	Parameters calculated from the intensity ratios of characteristic absorption bands
S	:	Molar entropy
T_c	:	Critical temperature
T_g	:	Glass transition temperature
T_m	:	Melting point temperature
T_s	:	Softening point temperature
V_R	:	Retention volume
V	:	Molar volume
wt%	:	Weight percent
X	:	Isothermal compressibility
X	:	Parameter refer to the H/C atomic ratios for the benzylic carbon structures
Y	:	Parameter refer to the H/C atomic ratios for the non-aromatic carbon structures
ΔH	:	Enthalpy difference
ΔT_g	:	Temperature interval of glass transition
-ΔW	:	Weight loss
α	:	Thermal expansion coefficient
γ	:	Shear rate
γ_{ll}	:	Strain rate tensor
η	:	Shear viscosity
λ	:	Lamda
μm	:	Micro meter
μs	:	Micro second
σ	:	Degree of substitution of non-bridge aromatic ring by alkyl groups
τ	:	Shear stress
τ_{ik}	:	Stress rate tensor

COPYROLYSIS OF AVGAMASYA ASPHALTITE AND GÖYNÜK OIL SHALE FOR PITCH PRECURSORS: CHARACTERISATION AND CARBON FIBRE PRODUCTION

SUMMARY

Formation of broad range of new advanced materials via integrated efforts in synthesis and processing is among the most significant recent advances in materials science and engineering. Materials with a wide spectrum of physical properties are being developed to meet a variety of highly specialised needs. These materials offer the potential for developing fibrous structures with unique combinations of mechanical properties, such as high stiffness and strength, high temperature performance, and optical and electrical properties.

Carbon fibres occupy a premier position among advanced materials especially for composites in that they combine high stiffness and strength with high temperature performance, high corrosion resistance and also offer relatively inexpensive routes for large-scale production. Although a wide range of materials have been used to produce carbon fibres since their introduction in the early sixties, current commercial production is concerned on three major precursor materials; rayon, polyacrylonitrile (PAN), and pitch.

In the present study, two Turkish fossil fuels, Goynuk oil shale (GOS) and Avgamasya asphaltite (AA), have been chosen as raw materials to prepare pitch precursors for isotropic carbon fibre production. In order to produce tar material, ground GOS and AA have been mixed in some ratios. Tar materials have been produced by pyrolysis and co-pyrolysis of GOS and AA in a stainless steel fixed bed retort under the flow of nitrogen. Pitches have been prepared by four different methods. In the first method, selected tars have air-blown. In the second method, selected tars have heat-treated under the nitrogen atmosphere. In the third method, all tars have vacuum-distilled. In the last method, one of the pitches obtained by vacuum distillation has furthermore subjected to solvent extraction with hexane.

The structural characterisation of the tar materials and pitch precursors and the chemical changes occurred due to different processing have studied by elemental analysis, thermogravimetric analysis (TGA), dynamic differential scanning calorimetry (DDSC), softening point measurement (SP), size exclusion chromatography (SEC), mass spectrometry (MS), optical microscopy, scanning electron microscopy (SEM), Fourier transform infrared spectroscopy (FTIR), 1H and 13C nuclear magnetic resonance spectroscopy (NMR).

The co-pyrolysis of GOS and AA mixture in some ratios has not resulted in obvious synergistic effect. However, the yield of all tars decreases as the percentage of the GOS decreases in the raw mixtures.

The H/C atomic ratios and therefore, the softening points of the pitches have been varied with the severity of the air and nitrogen blowing. Air-blowing and nitrogen-blowing have given pitches with higher softening points in the range of 110-160°C. Mild oxidation effect has been observed by air-blowing. Vacuum-distillation has resulted in lowest pitch yields, softening points, and higher H/C atomic ratios.

Depending on the data obtained from FTIR, 1H and 13C NMR analysis, nitrogen-blowing applied to 50%GOS-50%AA tar (S5A5) at 300°C for 60 minutes has resulted in the pitch with the highest aromaticity.

A spinnable pitch with a moderate softening point has been produced by vacuum-distillation followed by hexane extraction (S7A3-E1). The stabilisation of the green fibres obtained by the spinning of this pitch has been done by using nitric acid instead of air or oxygen. The stabilised fibres have been carbonised in a tubular furnace with slow heating steps up to 1000°C. The SEM images of the carbonised fibres have shown some surface distortions due to insufficient stabilisation and/or pitch composition.

In order to observe the effectiveness of supercritical fluid extraction (SFE), the selected pitches have been subjected to 30 minute dynamic SFE with CO2 and with CO2 modified by hexane at different temperatures and pressures. The SFE with CO2 modified by hexane at 150°C and 400 atm has removed higher amounts of light fractions of the pitches. The elemental analysis of the residues of the pitches showed that SFE has resulted in lower H/C atomic ratios in the residues. The SFE of S-A2 pitch with CO2 modified by toluene at 150°C and 400 atm has not been successful since the S-A2 pitch has totally dissolved during the extraction. This should be attributed to the aliphatic nature of S-A2 pitch.

SFE of the selected pitches has shown that SFE can be used alternatively as a clean and effective extraction technique compared to ordinary solvent extraction technique.

ZİFT ELDESİ İÇİN AVGAMASYA ASFALTİTİ VE GÖYNÜK BİTÜMLÜ ŞİSTİNİN KOPİROLİZİ: ZİFT KARAKTERİZASYONU VE KARBON FİBER ÜRETİMİ

ÖZET

Son yıllarda malzeme bilimcilerin ve mühendislerin önem verdiği konuların başında ileri teknoloji malzemelerinin üretimi ve üretim proseslerinin geliştirilmesi gelmektedir. İleri teknoloji malzemelerinin fiziksel özellikleri kullanım alanlarına göre geliştirilmektedir. Bu malzemeler yüksek derecede sıcaklık ve mukavemet gibi mekanik özellikler, yüksek sıcaklıklara dayanıklılık, yüksek optik ve elektriksel özellikler göstermektedirler.

Karbon fiberler yüksek sıcaklık uygulamalarına uygun olmaları, çok iyi bir sertlik ve mukavemete sahip ve korozyona dirençli olmaları nedeniyle ileri teknoloji malzemeleri arasında önemli bir yer almaktadır. Karbon fiberler ticari olarak rayon, polyacrylonitrile (PAN) ve zifften üretilmektedirler.

Bu çalışmada, Türk katı yakıtlarının hammadde olarak kullanılmasıyla zift esaslı izotropik karbon fiber (GPCF) üretimi ve bu üretim için gerekli olan ziftin eldesi ve karakterizasyonu hedef alınmıştır. Katı fosil yakıt olarak Bolu'nun Göynük yöresinden çıkartılan bitümlü şist (GOS) ve Siirt'in Avgamasya yöresinden çıkartılan asfaltit (AA) kullanılmıştır. Bu çalışmada Göynük bitümlü şisti (GOS) ve Avgamasya asfaltiti (AA) öğütülüp elendikten sonra belirli oranlarda karıştırılmış ve azot atmosferi altında sabit yataklı bir reaktörde piroliz işlemi uygulanarak katran üretilmiştir. Zift ise hava üfleme, azot üfleme, vakum destilasyonu, ve vakum destilastonu ile elde edilen ziftlerden birinin hekzan ile ekstraksiyonu sonucu üretilmiştir.

Üretilen katran ve ziftlerin yapısal karakterizasyonu ve farklı işlemler sonucu oluşan kimyasal değişiklikleri elementel analiz, termogravimetrik analiz (TGA), dinamik diferansiyel taramalı kalorimetri (DDSC), yumuşama noktası ölçümü (SP), moleküler dağılım ölçümü (SEC), kütle spektrometrisi (MS), optik mikroskop, taramalı elektron mikroskopu (SEM), Fourier transform infrared spektroskopisi (FTIR), ^{1}H ve ^{13}C nükleer manyetik rezonans spektroskopisi (NMR) ile ölçülmüştür.

GOS ve AA'nın belirli oranlarda karıştırılmasından sonra uygulanan birlikte pirolizi az miktarda sinercitik etkiye neden olmustur. Bunun yanısıra karışım içerisindeki GOS miktarı azaldıkça üretilen katran miktarında da bir azalma olduğu görülmüştür.

Ziftlerin H/C atomik oranları ve dolayısıyla yumuşama noktaları, uygulanan hava ve azot üfleme yöntemlerinin sıcaklık ve zaman parametrelerindeki değişikliğe bağlı olarak farklılık göstermiştir. Hava ve azot üfleme yöntemleriyle yumuşama noktaları 110-160°C olan ziftler üretilmiştir. Hava üfleme yöntemi ile ziftlerde hafif

oksidasyon etkisi görülmüştür. Vakum destilasyon yöntemi ile verimi ve yumuşama noktası en düşük ve H/C atomik oranı en yüksek olan ziftler üretilmiştir.

FTIR, ^{1}H ve ^{13}C NMR sonuçlarından göre %50 GOS-%50 AA karışımından üretilen katrana 300°C'da 60 dakika süreyle uygulanan azot üfleme yöntemiyle aromatisitesi en yüksek olan zift üretildiği anlaşılmıştır.

Üretilen ziftlerden S7A3-E1, fiber çekme deneylerinde kullanılmıştır. Bu zift çekme ünitesinde yumuşama noktasının yaklaşık 20°C üzerinde başarıyla çekilerek yeşil fiber haline getirilmiştir. Elde edilen yeşil fiberler nitrik asit ile stabil hale getirilmiş ve daha sonra 1000°C'da karbonize edilmiştir. Karbonize edilen fiberlerin taramalı elektron mikroskobu ile (SEM) incelenmesiyle fiberlerin yüzeylerinde bazı yarıklar ve pürüzler görülmüştür. Bunlar, ziftlerin yapısından ya da yeterli derecede stabilize edilememiş olmasından dolayı kaynaklanmaktadır.

Süperkritik sıvı ekstraksiyonu (SFE), seçilen ziftlere CO_2 ve hekzan ile modifiye edilmiş CO_2 kullanılarak farklı sıcaklık ve basınçlarda uygulanmıştır. 150°C ve 400 atm'de hekzan ile modifiye edilmiş CO_2 kullanılarak uygulanan SFE, fazla miktarda düşük fraksiyonları ziftlerden uzaklaştırmıştır. Dolayısıyla elde edilen ziftlerdeki H/C atomik oranlarının bir miktar daha düşmesi sağlanmıştır. S-A2 ziftinin 150°C ve 400 atm'de toluen ile modifiye edilmiş CO_2 kullanılarak gerçekleştirilen ekstraksiyonu sonucunda S-A2 ziftinin alifatik yapısından dolayı tüm zift çözünmüştür.

Süperkritik sıvı ekstraksiyonunun, yaygın olarak kullanılan klasik ekstraksiyon yöntemlerine göre daha temiz ve etkili bir yöntem olduğu sonucuna varılmıştır.

1. INTRODUCTION

Today, carbon fibres, advanced composite carbon fibres, fine ceramics, and other high-function materials, collectively known as "advanced or new materials", have begun to attract attention as the third generation of new industrial materials, following in the wake of conventional metals and plastics. Therefore, research and development on a host of new materials is being promoted throughout the world.

The Basic New Material Research Council in its report defines new materials as follows: "New materials are high value-added materials exhibiting epoch-making properties and producing a level of social value never before experienced, which are made from metallic, inorganic, organic, or a combination of such raw material and are the product of high-level manufacturing/processing technology, or commercial application technology" [1].

Carbon materials are characterised by high specific stiffness, specific strength, high conductivity, low density, etc., which result from the fundamental properties of the carbon atom and which confer on them many advantages over other materials. Carbon materials also retain their good mechanical properties at high temperatures (2000°C), under non-oxidative conditions. All these specific properties convert these materials in versatile products with many different uses ranging from the aluminium industry to high technology applications [2-4].

Carbon fibres are primarily used in composites. Composites are structures containing two or more components. Fibre reinforced composites have two components, the fibre and the binder. The advantage of many composites is that they offer a combination of properties that cannot be found in any single material. And the advantage of carbon fibres within a matrix of another substance is that their performance and properties can be even more impressive than those of other types of fibres, such as glass, nylon, rayon, and kevlar. The superior properties of carbon fibre to steel and other metals meant that the aerospace industry was an obvious market for

composite materials. The use of lighter materials in aircraft construction allows for fuel savings or a greater payload [1].

The carbon fibre industry was impacted by significant cutbacks in the military and aerospace industries due to the global economic recession from 1990-1993. The producers of aerospace materials experienced a significant decline in the market for their products because of this unexpected reduction in commercial aircraft orders and military aerospace programs. World-wide carbon fibre capacity in 1993 was 11.3 million kg while the demand was 6.2 million kg. Producers consolidated operations, closed plants, temporarily shut down facilities, and laid off workers to balance inventories [1].

After 1993, the recovery of the commercial aircraft market and the increased use of the composite materials in sporting goods, and industrial equipment sectors helped the industry make a transition from defence to higher-volume, lower-cost applications. This transition led the industry to emphasise the development of cost-effective materials and manufacturing processes. For example, processes that produced low-cost carbon fibres in bundles with an increasing number of filaments were finding applications in high-volume markets [1].

During 1997, the market for composite materials continued to grow. The Society of the Plastics Industry's Composite Institute estimated that U.S.. shipments for composites of all types totalled 1.550.000 metric tons, an increase of about 6% above 1996 levels and 8% above 1995 levels, for the sixth consecutive year increases. In 1996 and 1997 the carbon fibre industry operated at close to capacity. The 1997 gains were most pronounced in the consumer products and transportation sectors, which was reflective of the increased use of composites in sporting goods, and of the upturn in the commercial aircraft market. End-use demand for carbon fibres has shifted significantly in the last few years [1].

More than 30 years have passed since commercially usable carbon fibre appeared. Carbon fibres are now widely used to fabricate reinforcing structural materials, composites, which have extensive use in the aerospace industry [5]. Carbon fibres are produced from precursors such as rayon, polymers (e.g., polyacrylonitrile), carbonaceous gases (e.g., acetylene) or pitch (isotropic or mesophase) [6].

Continuous carbon fibres have been produced by polymers and pitch precursors while discontinuous fibres have been produced by vapour-grown carbonaceous gases. Rayon and isotropic pitch precursors are used to produce low modulus (< 60 GPa) carbon fibres. High modulus carbon fibres are made from PAN or mesophase pitch precursors. In both cases, an oriented precursor fibre is spun, stabilised by slightly oxidising to thermoset the fibres and carbonising to temperatures in excess of 800°C to produce a carbon fibre [7].

The conversion of these precursors to pitch is generally accomplished through the use of heat-treatment and distillation procedures. The final properties of the pitch are to an extent related to the precursor of choice and to the degree of thermal processing. However, even more extreme variations in pitch properties can be achieved by using chemical conversion procedures with such reagents as O_2, S, and certain Lewis acids. Treatment of pitches, thermal or air-blowing, prior to their use in the preparation of carbon materials, considerably improve such properties as carbon yield and density. However, these treatments significantly increase the final price of the pitch. The direct application of specific treatments to parent tar would obviate this problem [8,9].

Its low cost makes pitch fibre attractive in non-structural applications, where high strength and stiffness are not required, such as filters, static dissipation, thermal insulation and brake and clutch frictional materials. However, actual markets continuously require improvement of the quality of the products and a reduction of costs. This can be achievable only from a good knowledge of the physical and chemical properties of pitches relevant to carbon materials and the chemistry involved during their processing [2]. Recently, pitch fibres have been used in cost-driven structural applications, such as carbon fibre reinforced concrete. Also, pitch fibres are potentially attractive as low cost replacement for asbestos in some insulation and roofing material applications. Presently, because of their superior stiffness, mesophase fibres are used in aerospace structural applications, and future reductions in cost should allow them to be used in automotive structures. However, the extremely high thermal conductivity of newer varieties of mesophase fibres makes them uniquely attractive for dissipating heat in high speed machinery, aircraft structures and even electronic packages [10].

Isotropic pitches derived from coal and petroleum are used for the commercial production of general purpose carbon fibres. Although the pitches have different origins and processing histories, they have all been subjected to thermal cracking or catalytic cracking at high temperatures (>850°C). They each have high aromatic, and low aliphatic carbon contents and give high yields on carbonisation. These properties allow the production of carbon fibres with high density and comparatively high strength and stiffness [11].

Recently, activated carbon fibres have found many application areas as their novel properties make them more attractive than conventional forms of activated carbons (powder or large size carbons) for certain applications. Being fibrous in form, they can be incorporated more easily into fabrics, filters, and other articles which would require special designs to include powder or granular products. The isotropic nature of pitch-based fibres makes it possible to create high specific surface areas in the region of 700-2000 m^2/g; because diffusion limitations are minimal, the fibres exhibit very high rates of adsorption and desorption [12,13].

New materials technology is growing up in Turkey as well as all over the world. The developments are made to improve the properties of these materials and also to find alternative precursors which can give the desirable properties in the materials. The high cost of the present carbon fibre precursors, tended researchers to find alternative and cheaper sources. The scientists have begun to search available substitute sources as precursors for the production of carbon fibre in their countries. In this context, hydrocarbon sources of Turkey are investigated as possible carbon fibre precursors. Among many hydrocarbon sources, oil shales and asphaltites seem to be candidate precursors for realisation of this research for the production of carbon related materials.

Such research will definitely improve the economics of oil shale and asphaltite utilisation through broadening the spectrum of products that can be derived from this resource, and producing added-value materials that are either unavailable or more difficult to produce from other sources. The history of oil shale development shows that most attempts to commercialise oil shale technology have relied upon the marketing of by-products. Oil shale comprises the second largest solid fuel reserves in Turkey. Göynük oil shale reserves, approximately 697 million tons, are located

near the city of Bolu [14]. The total estimated asphaltite reserves of Turkey are around 50 million tons and Avgamasya asphaltite comprises the largest reserve with 14 million tons. Avgamasya asphaltite is a representative deposit of the asphaltic substances of Southeastern Turkey, which range from asphaltite to asphaltic pyrobitumen according to their degrees of alteration. It is geochemically classified as a solid aromatic-asphaltic oil containing mineral matter, derived from nearby oil deposits by alteration during burial [15].

Previously, Istanbul Technical University Chemical Engineering Carbon Group has conducted a research using Göynük oil shale and Avgamasya asphaltite, and the results seem to be promising for pitch precursor and therefore, carbon fibre production. However, both sources have some properties which have advantageous and disadvantageous, individually, for pitch preparation.

The aim of this work is to assess the potential for producing new precursors for carbon materials from Turkish oil shale and asphaltite. The present study consists the production of pitch precursors and general carbon fibres and the determination of the chemical characteristics of the pitch precursors. In order to optimise the disadvantages and upgrade the characteristics of Göynük oil shale and Avgamasya asphaltite these two hydrocarbon sources have been copyrolysed and the synergistic effect of copyrolysis has been investigated. This study has also initiated the possibility of the needle coke production from these sources.

2. GENERAL INFORMATION ABOUT CARBON AND CARBON RELATED MATERIALS

2.1 Carbon

Carbon has an atomic weight of 12.011 and is the sixth element in the periodic table. Three isotopes are known to be exist, these being C^{12}, C^{13}, and C^{14}, the first two of which are stable. C^{12} accounts for around 99% of the naturally occurring carbon and is used as the reference definition of atomic mass. It is defined as having the "Relative Atomic Mass" of 12. C^{13} has a magnetic moment (spin = 1/2) which results in its being used as a probe in nuclear magnetic resonance (NMR) studies. The radioactive isotope C^{14} is generated in the earth's upper atmosphere by the interaction of neutrons with nitrogen:

$$N14 + n \rightarrow C14 + H1 \qquad (2.1)$$

C^{14} has a very long half-life of 5730 years is used extensively in the dating of archeological artefacts and as a "label" in the study of organic reaction mechanisms.

The properties of carbon based materials depend upon its electronic configuration. Despite the electronic ground state of carbon being $1s^2$, $2s^2$, $2p^2$, energetic advantage is gained from involving all four outer orbital electrons in bonding between other atoms or carbon atoms themselves. Carbon displays "catenation" (bonding to itself) to such a degree that the number of resulting chains, rings, and networks are almost limitless [7].

2.2 Bonding in Carbon Materials

Bonding in carbon compounds is dominated by two principal regimes as described below:

1- α-bond - diamond or aliphatic type. This results in chains of carbon atoms such as polyolefines, or three-dimensional structures which are rigid and isotropic.

2- α-bond and β-bond - graphite or aromatic type. This results in predominantly layered structures with a h igh degree of anisotropy.

The majority of carbonaceous materials contain examples of both bonding regimes with an immense range of complexity [16].

2.3 Crystal Structures of Carbon

Carbon exists in two regularly ordered crystalline forms, diamond and graphite. At ambient temperatures and pressures, graphite is the most thermodynamically stable allotrope:

$$C\ (\text{diamond}) \rightarrow C\ (\text{graphite}) \qquad \Delta H = -2.1\ \text{kJ/mol} \qquad (2.2)$$

Diamond is made up of a regular three dimensional network of α-bonds providing a very rigid, stable structure (Figure 2.1) making it the hardest material known. Bonding electrons within the diamond lattice are fixed between atoms such that electrical conductivity is very low, tending towards insulation. Diamond, because of its higher density ($3.51 g.cm^{-3}$ compared with 2,25 $g.cm^{-3}$), is the most stable allotrope at high pressures (>600 GPa at 20 °C) [7,16].

In graphite, there is both α- and π-bonding holding the atoms in hexagonal two dimensional networks. These hexagons form aromatic layers called graphenes. These layers are stacked together in a hexagonal compact ABA form in the c-direction as shown in Figure 2.2 [16,17].

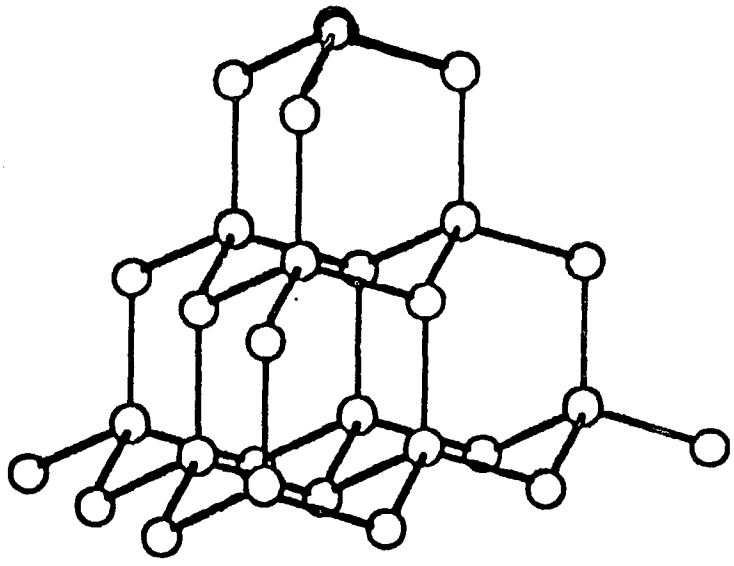

Figure 2.1. Structure of diamond [16].

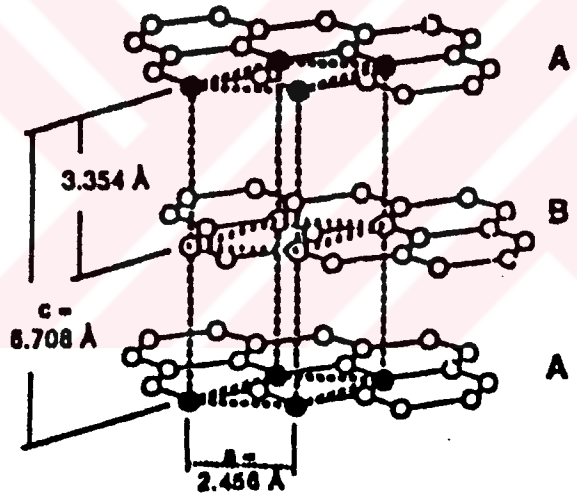

Figure 2.2. Graphite structure [16].

In the graphene layer, each carbon atom exchanges three covalent bonds with its neighbours (C-C distance 1.4211 °A). In the c-direction, the distance between two carbon layers, c/2, is much higher (3.354 °A), due to loose Van der Waals bonds [17]. The most probable value of c appears to be 6.707 °A at room temperature. The lattice constant "a" does not seem to be very much affected by lattice imperfections; the accuracy of the determination can, however, be influenced by line broadening due to disorder effects. The most probable value for this constant

is 2.4614 °A at room temperature, corresponding to a C-C bond length of 1.4211 °A [18].

A small amount of material is stacked according to ABC ABC. This material is known as the rhombohedral form and accounts for less than 10% of the graphite. Graphite is a very soft material with good lubricating properties, since the energy required to slide the layers over one another is very low. The properties of graphite tend to be very anisotropic as a result of its crystal structure. This anisotropic behaviour can be illustrated using the electrical conductivity of graphite. The conjugating π-bonding within the layered configuration results in the delocalization of electrons throughout the structure. A means of electrical conductivity similar to the conduction band in metals is thus provided. In direct contrast, there is no electron movement across the layers, conduction in that direction is minimum [7].

2.4 Order and Disorder in Carbon Materials

Several types of defects, like in-plane rotation, stacking faults, vacancies, non-planarity of the aromatic sheets may disturb the crystalline ordering resulting in an imperfect turbostratic structure (Figure 2.3).

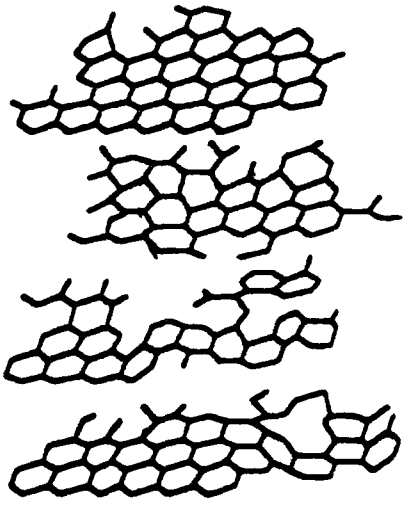

Figure 2.3. Disordered turbostratic carbon [17].

The structure of carbon materials can be schematically described as consisting of carbon layers with locally well-ordered domains, i.e. crystallites, and other domains

with less-order. Crystallites are characterised by the interlayer distance c/2 which is generally much larger than in graphite, the stacking height, L_c, and the lamellae size, L_a, (Figure 2.4). The mutual arrangement of the crystallites is also an important factor since it controls the overall reordering of the carbon structure during heat treatment up to 2800 °C [17].

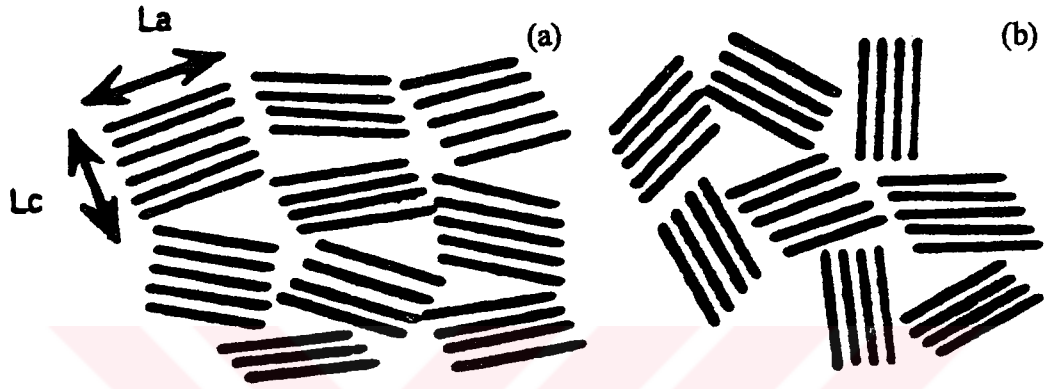

Figure 2.4. Schematic structure of graphitizable carbon (a), and non-graphitizable carbon (b) [17].

2.4.1 More-ordered structures

The principal parts of the more-ordered structures are essentially graphitic. Small volumes often have an almost perfect graphite lattice but, as the volume increases, the presence of defects, distortions, and heteroatoms destroys the regularity giving material, which is very disordered. It can be demonstrated that very little energy is needed to slide the graphitic layers over one another. Similarly, twisting leads so that they are no longer aligned is another possibility. The twisting leads to structures, which have roughly parallel and equidistant layers, but with random orientation. This arises from an irregular disposition of carbon atoms within a layered type of over-structure. The diamond-like parts of most carbon materials tend to have even shorter range than the graphitic regions, although a large proportion of the disordered parts is aliphatic in nature. A whole host of defects and irregularities are again present in any long-range structures [7,19].

2.4.2 Less-ordered structures

For the most part, carbon materials may be regarded as analogous to metal alloys in that they are made up of constituents, which can be separately identified within the overall structure. The principal phases may be described as:

1- ordered or graphitic, in which case there is a high degree of anisotropy;
2- disordered material, which, under most characterisation techniques, exhibits an isotropic structure.

The processes whereby disordered material is converted into an ordered state and vice versa are one of the primary concerns in the fabrication and properties of products made by the carbon industry in general and carbon-carbon composites in particular. Those processes, whether by heat treatment, ageing or some other method of energy input, are again analogous to metals production [7,19].

Generally speaking, a carbon material is obtained after pyrolysis or charring of an organic substance at a temperature close to 900°C (carbonisation). The resulting carbon has a non-graphitic structure. The size of the ordered domains is usually of short range (< 20nm), but it may develop upon treatment up to 2800 °C. The solid state transformation of non-graphitic carbon into graphite by thermal activation is called graphitisation. This process, illustrated in Figure 2.5, illustrates the range of irregular structures. Depending on the ability of a carbon to develop a graphitic structure, one distinguishes between graphitizable and non-graphitizable carbons. The mutual arrangements of the ordered domains in the carbon are a key factor to its graphitizability. A random arrangement of the crystallites is not favourable for the crystallite growth shown in Figure 2.4 (a). In the case of a preoriented structure, Figure 2.4 (b), a significant development above 2000 °C is observed.

The interlayer, c/2, decreases and reaches values close to that in graphite. Also the stacking height of the crystallites, L_c, and the average diameter of the lamellae, L_a, increase significantly. Typical values of crystallite parameters for a graphitizable petroleum coke as determined by X-ray diffraction are listed in Table 2.1 [17]. In the case of non-graphitizable carbon, polyacrylonitrile-based (PAN)carbon fibre, only a slight increase in the crystallinity of the carbon is observed even after heat treatment at 2800 °C (Table 2.1). An intermediate case is observed for mesophase pitch-based

carbon fibre heated at 2800 °C for which the interlayer spacing decreases and becomes close to that of graphite, but the size of the ordered domains still remains the same [17].

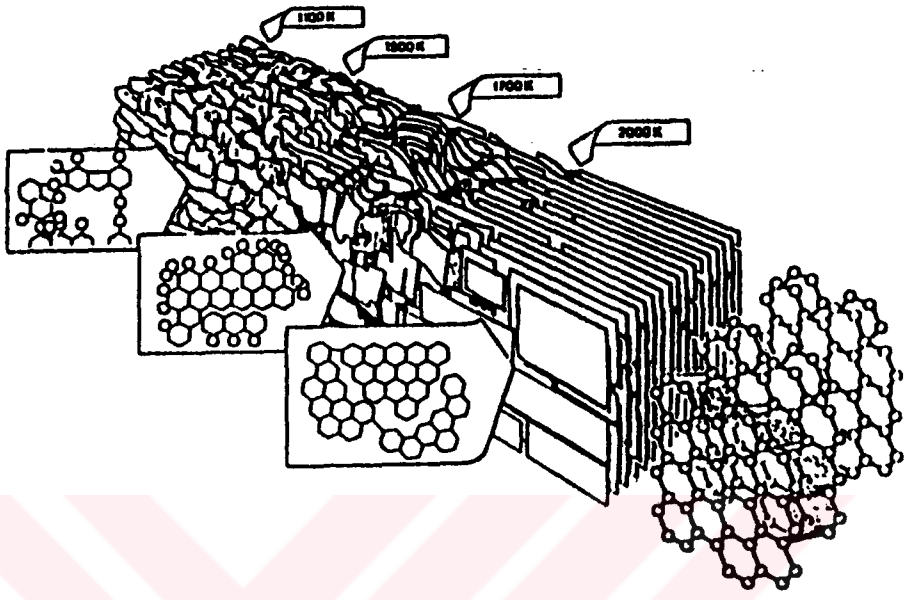

Figure 2.5. Marsh - Griffiths model of carbonisation/graphitisation process [16].

Table 2.1. Crystallographic parameters of typical carbon forms [17].

Carbons	Heat treatment temperature (°C)	Interlayer spacing, c/2 (nm)	Stacking height, L_c (nm)	Crystallite diameter, L_a (nm)
Petroleum coke	1100	0.344	3	5
	2000	0.343	30	20
	2800	0.337	>50	>500
PAN-based carbon fibre	1100	0.360	2	3
	2800	0.350	5	7
Mesophase pitch-based carbon fibre	1100	0.342	12	10
	2800	0.336	26	10

2.4.3 Range of order

The ordered carbons within carbons may be considered as crystallites of graphite. The range of order can be estimated by measuring the size and distribution of the crystallites. A consideration of the orientation of the crystallites is often necessary in the calculation, since the actual range of order may be several orders of magnitude higher than the size of the individual crystallites.

The type and range of ordering considered within the structures will depend very much on the analysis technique employed. When assessing the properties, performance and applications of carbon materials, the degree of isotropy and anisotropy present is of great significance. Although the macroscopic properties of many carbons are isotropic, their structure on a microscopic level exhibits a high degree of anisotropy. This observation can be exemplified by considering the optical microstructure of a carbon when compared with an electron microscope image. Optical microscopes are limited to a resolving power of around 1μm. Some structures may thus be discerned as isotropic using optical microscopy, whereas they may be shown to be highly anisotropic at the nanometer level observed in the electron microscope [7].

2.5 Carbon Forms

2.5.1 Graphitic and non-graphitic carbons

Graphitic carbons are all varieties of substances consisting of the element carbon in the allotropic form of graphite irrespective of the presence of structural defects.

Non-graphitic carbons are all varieties of substances consisting mainly of the element carbon with two-dimensional long range order of the carbon atoms in planar hexagonal networks, but without any measurable crystallographic order in the third direction (c-direction) apart from more or less parallel stacking. Many non-graphitizing carbons can be converted into graphitic carbons by heat treatment to above 2500 K [16].

2.5.2 Graphitizable and non-graphitizable carbons

The broad division of carbons into two types - graphitizing or non-graphitizing, soft or hard, coke or char - has long being recognised.

Graphitizing carbons may be defined as these, which begin to develop three-dimensional atomic order on heating to temperatures near 1700 °C [20]. Most graphitizing carbons pass through a fluid stage during carbonisation. This allows large aromatic molecules to align with each other so forming the mesophase

precursor of the graphitic structure, which is essential to the development of the cake [16].

Substances which form graphitizing carbons in this way include vitrinites of medium-volatile coking coal, high-temperature coal-tar pitch, petroleum bitumen, polymers such as poly(vinyl chloride), and polynuclear aromatic compounds such as naphthacene and dibenzanthrone. The carbons normally obtained by heating these substances are coke-like in appearance and exhibit complex pattern of optical anisotropy under the microscope [20].

Non-graphitizing carbons are those which can not be transformed into graphitic carbon solely by heat treatment up to 3300 K under atmospheric or lower pressure. Non-graphitizing carbons are produced from wood, nutshells, and non-fusing coals. Essentially, the macromolecular (polymeric) structure of these materials remains during heat treatment only losing small molecules by degradation and developing even more cross-linking so that fusion can not take place. The loss of small molecules and the retention of the complex macromolecular structure lead to high microporosity, with surface areas in the order of 1000 $m^2.g^{-1}$ [16].

These two types of non-graphitic carbons are basically different in structure. The most striking difference appears in a comparison of the apparent stack height (average number of layers per stack) is greater for a graphitizing than for a non-graphitizing carbon with a comparable structure of the layers. This difference is observed well below the range of temperatures in which graphitisation can occur. To explain the effect, it is assumed a crystallite growth by migration of whole layers or groups of layers, and there is a higher probability of these migration entities to be fixed on the basal plane of already existing crystallites than to be attached to the edge atoms of layer planes, thus increasing the stack size more rapidly the layer size [18].

Studies on the carbonisation of model compounds (acenapthylene, bifluorenyl) have revealed the importance of size and shape of the reactive intermediates produced in the first stages of carbonisation. It was found that the steric conditions of fitting aromatic molecules together to build up perfect graphitic layers without holes seem to determine to a large extend whether a perfect graphite structure will be formed at higher temperature. The important first steps of layer growth by a sterically favoured

coalescence of aromatic molecules occur in the temperature range 300-500 °C. It is in this temperature range that a migration of particles is taking place, and it appears rather unlikely that a second migration process of particles exists in the temperature range between 1000-2000 °C as previously assumed model. It seems to be more likely that in the latter temperature range the increase in perfection as indicated by the increase of the apparent crystallite dimensions is due to the migration of imperfections (dislocations, vacancies, and interstitials) [18].

2.6 Isotropic Carbons

Isotropic, non-graphitizable carbons originate from materials which are already macromolecular in nature, e.g. the cellulose or lignin components of wood, nuts, and nutshells, or the specific cross-linked (C-O-C bondings) of low rank coals such as peats, lignites, brown coals, and non-caking bituminous coals. Figure 2.6 shows the two dimensional drawing of carbon lamellae to illustrate structure in isotropic carbon.

To prepare an isotropic carbon, the precursor material must be polymeric, either being heavily cross-linked initially or developing cross-linkages in the early stages of carbonisation [21].

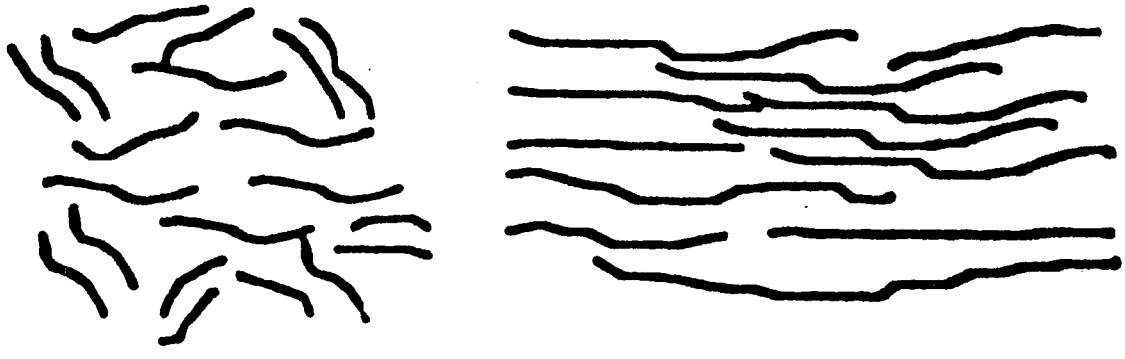

Figure 2.6. Isotropic carbon Anisotropic carbon [21].

When thermosetting polymers are heated in an inert atmosphere, reactions take place such that one or two possibilities generally occur; the polymer chains may degrade into small molecules with the products being evolved as gases leaving little or no

carbon behind, or the carbon-carbon chains remain intact, while heteroatoms are driven off and the carbon chains coalesce with neighbours. The material does not pass through a plastic or liquid state. The final carbon is isotropic if the precursor material is isotropic and can be anisotropic if the precursor is anisotropic. In either case the carbon is non-graphitizable, even when heated to 3000 °C.

The mechanical properties of isotropic carbons are directly related to their structure, which consists of a three-dimensional random network of stacks of graphene layers appearing rather like tangled ribbons, with three types of bonding therein. Between closely spaced parallel ribbons only weal Van der Waal's type forces exist, which can be neglected. Within the ribbons the C-C bond is the stiffest component of the system. In a random configuration of ribbons, the response to an applied stress is related primarily to the ease with which segments can rotate with respect to their environment, which is resisted by carbon bonding between the ribbons. Considering its non-crystalline structure, the Young's modulus and hardness of isotropic carbon are very high. This is due in the main to the presence of cross-links between the ribbon-like bundles of graphene layers, which prevent the layers from shearing past one another. Isotropic carbon, because of its high hardness, relatively high strength and chemical inertness to body fluids, has been employed as a structural material in biomedical implants such as artificial heart valves. The material is somewhat limited when load bearing is required, because of its extreme brittleness. Mechanical failure is almost completely controlled by brittle fracture. The failure occurs with negligible plastic deformation, without prior warning and involves low-energy absorption. Isotropic carbon is much stronger than most other carbon or graphites [7].

2.7 Introduction to Carbon Fibres

Carbon fibre is a material of industrially great importance in virtue of its unique properties, such as high strength, low thermal expansion, and high corrosion [22]. Carbon fibres refer to fibres, which are at least 92% carbon in composition. They can be short or continuous; their structure can be crystalline, amorphous, or partly crystalline. The crystalline form has the crystal structure of graphite, which consists of sp^2 hybridised carbon atoms arranged two-dimensionally in a honeycomb structure in the x-y plane [23].

The high modulus of a carbon fibre stems from the fact that the carbon layers, though not necessarily flat, tend to be parallel to the fibre axis. This crystallographic preferred orientation is known as a fibre texture. As a result, a carbon fibre has a higher modulus parallel to the fibre axis than perpendicular to the fibre axis. Similarly, the electrical and thermal expansion is lower along the fibre axis [23].

The greater the degree of alignment of the carbon layers parallel to the fibre axis, i.e., the stronger the fibre texture, the greater the c-axis crystallite size (L_c), the density, the carbon content, and the fibre's tensile modulus, electrical conductivity, and thermal conductivity parallel to the fibre axis; the smaller the fibre's coefficient of thermal expansion and internal shear strength.

Table 2.2. Properties of various fibres [23].

Material	Density (g/cm^3)	Tensile strength (GPa)	Modulus of elasticity (Gpa)	Ductility (%)	Melting temp. (°C)	Specific modulus (10^6 m)	Specific strength (10^4 m)
E-glass	2.6	3.4	72.4	4.7	<1725	2.9	14.0
S-glass	2.5	4.5	86.9	5.2	<1725	3.6	18.0
SiO_2	2.2	5.9	72.4	8.1	1728	3.4	27.4
Al_2O_3	4.0	2.1	380	0.6	2015	9.9	5.3
Carbon (HM)	1.5	1.9	530	0.4	3700	36.3	13.0
Carbon (HS)	1.5	5.7	280	2.0	3700	18.8	19.0
Boron	2.4	3.4	380	0.9	2030	16.4	12.0
SiC	4.1	2.3	480	0.4	2700	12.0	9.9
Kevlar	1.4	4.5	120	3.8	500	8.8	25.7

Table 2.2 compares the mechanical properties, melting temperature, and density of carbon fibres with other types of fibres. There are numerous grades of carbon fibres; Table 2.2 only shows the two high-performance grades, which are labelled "high strength" and "high modulus". Among the fibres (not counting the whiskers), high-strength carbon fibres exhibit the highest strength while high modulus carbon fibres exhibit the highest modulus of elasticity. Moreover, the density of carbon fibres is quite low, making the specific modulus (modulus/density ratio) of high-modulus carbon fibres exceptionally high. The polymer fibres, such as polyethylene and Kevlar fibres, have densities even lower than carbon fibres, but their melting temperatures are low. The ceramic fibres, such as glass, SiO_2, Al_2O_3, and SiC fibres,

have densities higher than carbon fibres; most of them (except glass fibres) suffer from high prices or are not readily available in a continuous fibre form. The main drawback of the mechanical properties of carbon fibres is in the low ductility, which is lower than those of glass, SiO_2, and Kevlar fibres. The ductility of high-modulus carbon fibres is even lower than that of high-strength carbon fibre [23].

2.7.1 History of carbon fibres

Carbon fibres have been made inadvertently from natural cellulosic fibres such as cotton or linen for thousands of years. However, it was Thomas Edison who, in 1878, purposely took cotton fibres and later, bamboo, and converted them into carbon in his quest for incandescent lamp filaments. Interest in carbon fibres was renewed in the late 1950s when synthetic rayons in textile forms were carbonised to produce carbon fibres for high-temperature missile applications. All these fibres had low elastic moduli (< 50 GPa, or 7 x 10^6 psi) [24].

Initial interest was in the aerospace field, where the advantages of low weight and high strength/stiffness are most obvious. Substantial broadening of the application base has taken place since then to include recreational sports equipment as well as industrial and commercial products [25].

The story with high performance carbon fibres started in the sixties, when Union Carbide Company (UCC) was able to demonstrate, that high modulus can be achieved by hot working of the isotropic carbon fibre, that means by hot stretching of the fibres at graphitisation temperatures. The hot stretched carbon fibre types commercially available from UCC were called THORNELL 25, 50, and 70 indicating the modulus number in million psi [26].

The technical and commercial breakthrough for high performance carbon fibres started in the later sixties after introduction of PAN process, which turned out to be more economical due to the less expensive precursor polymer and to the simpler fabrication process. The carbon yield for PAN is 50% whereas rayon carbonisation provides less than 30% carbon residue only [27].

The carbon fibre industry presently uses three different materials: rayon, PAN and pitch fibres, either isotropic or liquid crystalline (mesophase) [28].

2.7.2 Processing of carbon fibres

Carbon fibres are fabricated from pitch fibres, polymer fibres (e.g., polyacrylonitrile), or carbonaceous gases (e.g., acetylene). Those made from pitch and polymer fibres are in short and continuous forms whereas those made from carbonaceous gases are in the short form only. Fibres made from pitch and carbonaceous gases are more graphitizable then those made from polymers, so they can attain higher thermal conductivity and lower electrical resistivity. The raw materials cost is much lower for making fibres from pitch or carbonaceous gases than from polymers [23].

The fabrication of carbon fibres from pitch or polymers involves pyrolysis of the pitch or polymer. In contrast, the fabrication of carbon fibres from carbonaceous gases involves catalytic growth of carbon [22].

2.7.2.1 Rayon based carbon fibres

Rayon precursors, which are derived from cellulosic materials, were one of the earliest precursors used to make carbon fibres. Their advantages were that they were characterised and readily available; their most significant disadvantage was a relatively high weight loss, or low conversion yield to carbon fibre (30 wt%) [11]. An enormous amount of shrinkage is caused by the mass loss from the structure at the different stages of pyrolysis.

This shrinkage can not be translated completely in a bulk shrinkage of the fibre. The consequence is formation of an extremely porous carbon residue with low density (16 g/cm3) [29].

A quantitative illustration of the mass loss during carbonisation is given in Figure 2.7(a) for rayon [30]. Figure 2.7(b) shows the carbon yields of some aromatic polymers like poly(p-phenylene), phenolics, poly(p-phenyleneacethene) and others, compared with rayon, PAN, and pitch [29].

Figure 2.8 shows the basic elements required for producing carbon filaments from rayon. The first low – temperature treatment takes place at around 300 °C and converts the structure to a form which is stable to higher processing temperatures.

The process involves polymerisation and the formation of cross-links of the fibre mass, 50–60 % is lost to decomposition products such as H_2O, CO, and CO_2 during oxidation. The carbonisation step, resulting in further weight loss, is usually carried out at 1500 °C. The yield after carbonisation is 20–25% of the original polymer weight. At this stage fibres have an essentially isotropic structure. The mechanical properties of carbonised rayon are poor as a direct result of the poor alignment of the graphane layers. Stretching of the fibres during heat treatment to graphitisation temperatures increases both strength and modulus, but is an expensive process. Because of the poor mechanical properties, low carbon yield and expense of graphitisation, rayon based carbon fibres have generally not proved competitive in the market place . Table 2.3 lists typical rayon based carbon fibre properties [7].

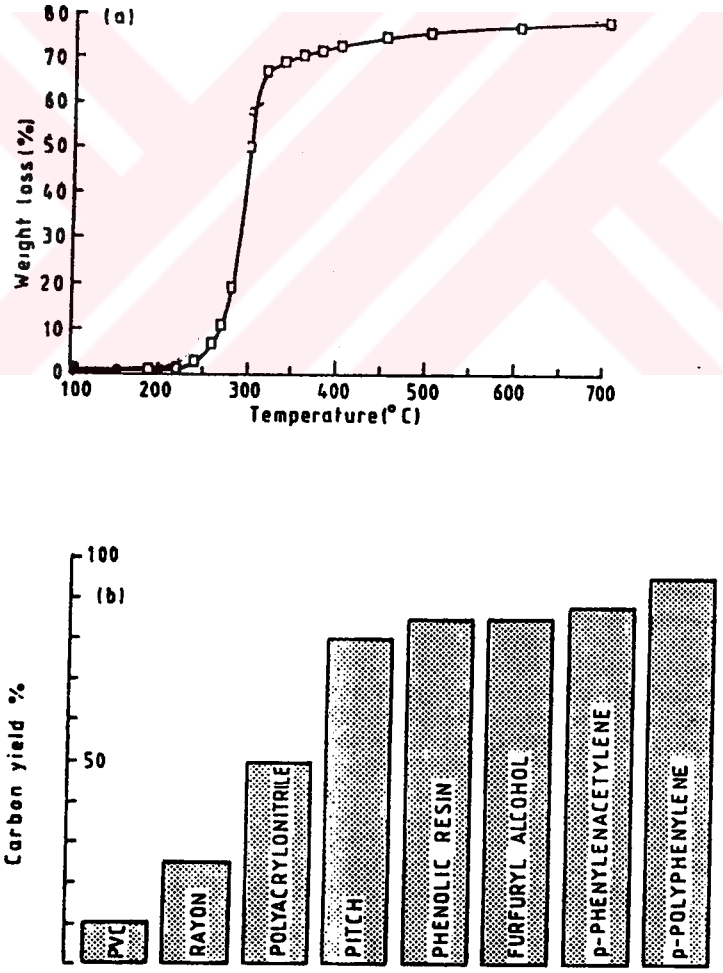

Figure 2.7. Weight loss of rayon during carbonisation (a); carbon yield after carbonisation for some aromatic polymers (b) [29,30].

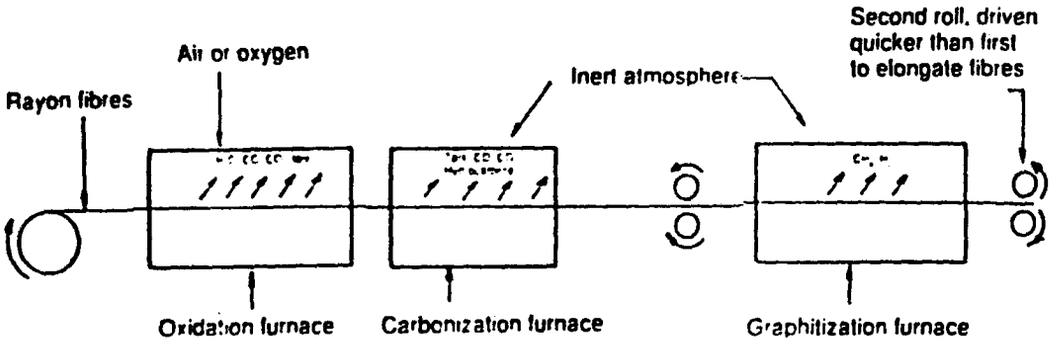

Figure 2.8. Basic elements required to produce carbon fibres from rayon [7].

Table 2.3. Typical properties of rayon-based carbon fibres [7].

Axial	Tensile strength	1.0 Gpa
	Tensile modulus	41.0 Gpa
	Elongation to break	2.5%
	Electrical resistivity	20.0Ω
Bulk	Density	1.6 $g.cm^{-3}$
	Fibre diameter	8.5 μm
	Carbon assay	99.0%

2.7.2.2 Pan based carbon fibres

PAN based carbon fibres are carbon fibres obtained from polyacrylonitrile (PAN) precursor fibres by stabilisation treatment, carbonisation, and possibly final heat treatment at even higher temperature. They provide a carbon fibre conversion yield that is 50 to 55%. These precursors can be thermally rearranged before thermal decomposition, which allows them to be oxidised and stabilised before the carbon fibre conversion process, while maintaining the same filamentary configuration [25].

The process to manufacture PAN carbon fibres is as follows. The first step in the process is to polymerise the precursor material, which starts with the free radical polymerisation of acrylonitrile and suitable comonomers to form PAN. Polymerisation is followed by spinning the precursor polymer into a multifilament strand. The fibres are next thermally stabilised via an oxidation process, which employs temperatures approaching 400 °C. This involves crosslinking of the polymer chains to make the fibre interactable so that it will not melt when subjected to increasingly higher temperatures. The next step of the process is carbonisation,

which takes place in an inert atmosphere at temperatures between 1000 °C and 2000 °C. To achieve very high modulus, a graphitisation step at 2000 °C to 3000 °C is used. The carbon or graphite fibres have achieved their final strength, modulus, and density at this stage of the process [31].

2.7.2.3 Vapour grown carbon fibres

Primitive technology had being used for the preparation of vapour grown fibres as the 1889 patent of Hughes and Chambers, which describes the growth of "hair-like carbon filaments", utilised a feedstock of hydrogen and methane pyrolysed in an iron crucible. The fibres were thought to be suitable for electric light bulb filaments, but lack of modern process controls made them uncompetitive [32].

In 1972, Koyama grow good yields of vapour grown carbon fibres (VGCF) by thermal decomposition of benzene at about 1200 °C [33].

Vapour grown carbon fibres are a promising new technology for the production of strong, stiff, discontinuous carbon fibres, which will be useful in applications where cost is an important consideration.

The basic process for producing vapour grown carbon fibres was developed by Gary Tibbetts at the General Motors NAO Research Labs. In this process, an organometallic compound containing iron is injected into a hydrocarbon vapour at temperatures above 1000 °C. The fibres were lengthen and thicken as they move through the reactor with the gas stream and collected as they exist. However, the process was non-productive; the iron catalyst did not grow filaments profusely enough to be a practical continuous reactor [34].

One of the most important problems in the growth of carbon fibres from catalyst particles is the role of sulphur in the process. As early as 1954, Kauffman and Griffiths were able to increase the fibre fraction of the product grown on silica reactor tube walls tenfold by adding 0.4% by volume H_2S to coke oven gas. During this epoch there was no recognition of the fact that the fibres were growing from small iron particles inadvertently present in the reactor [35]. On the contrary, Katsuki et.al. showed that while iron was indeed a catalyst material, hydrogen sulphide, or sulphur in general, could have an even more crucial role [36]. This group showed

more recently that sulphur addition to the iron catalyst particles alone made fibre growth much more profuse. More recently, Tibbets, et.al observed that 1% addition of hydrogen sulphide to the feedstock of continuous reactor, where abundant fibre nucleation is especially important, is vital to obtaining high yield fibre growth [37].

2.7.2.4 Pitch based carbon fibres

The pitch based carbon fibre was developed by Otani and co-workers in 1963 [38] and now it is recognised as an important industrial material. The pitches used as starting materials for the preparation of carbon fibres are by-products of the coke-making and petrochemical industries. For this reason, these materials have the advantage of being cheap precursors of carbon fibres [39]. Pitch can be defined as a solid, fusible product of the pyrolysis of organic materials [40].

Natural pitch is a high molecular weight by-product of the destructive distillation of petroleum, coal, or natural asphalt [10]. Pitches are composed of a wide variety of different generic classes of compounds ranging from low molecular weight paraffinic material at one extreme to very highly aromatic species at the other [41]. In most types of pitches polycyclic aromatic hydrocarbons (PAH) comprise the dominant class of compounds. Partially hydrogenated PAH occur in petroleum pitches in larger amounts but in high temperature coal-tar pitch the concentrations are low [42]. Pitch can be considered to be composed of four general classes of chemical compounds: saturates, naphthene aromatics, polar aromatics, and asphaltenes. Saturates are the fraction of the pitch which consists of low molecular weight aliphatic compounds. Low molecular weight aromatics and saturated ring structures make up the naphthene aromatic portion of pitch. Polar aromatics, on the other hand, have a higher molecular weight and tend to be more heterocyclic in nature. Asphaltene is the highest molecular weight fraction in a pitch, and it also has the highest degree of aromaticity. Because it tends to consist of large, alkylated, plate-like molecules of condensed aromatic rings, the asphaltene fraction is the most thermally stable portion of the pitch [43].

The complex composition of pitches is the key to their low softening ranges and useful rheological properties, since many of the components can individually have very high melting points. Pitches exhibit both eutectic and glass-like properties. The

glass transitions of pitches can be determined using differential scanning calorimetry (DSC) or thermomechanical analysis (TMA) techniques [44]. Pitches soften over a broad temperature range and isotropic pitches generally exhibit Newtonian flow behaviour with the viscosity changing with temperature [45].

The thermal stability, softening point, and potential carbon yield of a given pitch depend on the relative proportions of the four classes of chemical compounds that it contains. As one would expect, as the asphaltene fraction of a pitch increases, the thermal stability and softening point tend to increase. In addition to increasing the thermal stability and softening of the pitch, a high asphaltene content often results in a high carbon yield when the pitch is converted to fibre. Coal tar pitches are, in general, more aromatic than petroleum pitches. The coal tar pitch has higher benzene and quinoline insoluble content but a lower average molecular weight. Since it is more aromatic and contains a higher benzene and quinoline insoluble content, one might expect coal tar pitch to have a high carbon yield, making it an obvious choice as a precursor for carbon fibres [41]. And also coal tar pitch as a feedstock for the production of carbon fibres provides a relatively cheap raw material available in sufficient quantities, with the prospect of a high carbon yield [42-46].

Carbon fibres based on petroleum pitch have a unique property profile, which includes: very high axial modulus (up to 896 GPa); strongly negative values of axial thermal expansion coefficient; high axial thermal (and electrical) conductivity, and adequate tensile properties [47].

Pitch based carbon fibres having a broad range of microstructure and mechanical properties are available commercially. The fibres have high potential to be used as reinforcement in carbon/carbon composites.

Pitch based carbon fibres have been recognised as a strategic material for the near future because of their excellent tensile properties. Tensile properties, such as Young's modulus and tensile strength of carbon fibres, strongly depend on the degree of preferred orientation in the graphitic layers along the fibre axis [48].

There are two types of pitch based carbon fibres: general purpose carbon fibres (GPCF) and high performance carbon fibres (HPCF) [49]. The first are obtained from conventional isotropic pitches, while the second are prepared from mesophase

pitches. The HPCF are quite expensive compared with the GPCF and their applications are mainly limited to aerospace and sporting goods industries. On the other hand, the GPCF have many potential applications due to their much lower price [50].

Isotropic pitch based carbon fibres (GPCF)

GPCF and HPCF are compared in Table 2.4 according to their physical properties and application areas. In this comparison, all carbon fibres described above belong to the low modulus grade [38].

Table 2.4. Comparison of the two carbon fibres [38].

Type	GPCF	HPCF
Strength (kg/mm^2)	90-85	300-300
Modulus ($10^3 kg/mm^2$)	4.2-3.8	50-20
Present use	Insulation, gasket, fillers in plastics.	Reinforcing elements (sporting goods, aerospace).
Future use expected	Substitution for asbestos and electrodes.	Automobile and others.

Their low cost makes isotropic pitch based carbon fibres an attractive candidate for non-structural applications where high strength and stiffness are not a priority. These applications include: filtration, static dissipation, thermal insulation, and substrate fibres for ceramic fibres, and an asbestos substitute in some insulation and roofing materials. Isotropic carbon fibres have ever been used to reinforce concrete, and recently, they have been utilised to create a new form of activated carbon, which exhibits an extremely high degree of selectivity [51].

There are several reasons why fibres prepared from an isotropic pitch precursor should be less expensive to produce than other continuous carbon fibres. Since, in principle, any spinnable pitch of high coking value can be used as a precursor for isotropic carbon fibres [38], the raw pitch precursor can be relatively inexpensive. In addition, several processes have been developed to lower the cost of converting the raw pitch precursor to a spinnable pitch with a high softening point [52-54]. These processes purify and devolatilise the pitch, reducing filament breaks during spinning and increasing process conversion. Besides purifying the pitch, the preparation process can be designed to produce an isotropic pitch with a high reactivity. This

allows the melt-spun fibre to be stabilised rapidly prior to final heat treatment, further lowering the final fibre cost.

Mesophase pitch based carbon fibres (HPCF)

High performance pitch based carbon fibres are manufactured by carbonising pitch precursor fibres, which are obtained by melt-spinning a mesophase pitch [55-57]. A mesophase pitch of high stabilisation reactivity with a highly oriented structure, low viscosity, high purity, and higher coking value has been required as an appropriate precursor for pitch based carbon fibres with high performance and as a binder pitch of advanced C/C composites [58,59].

The discovery in 1965, by Brooks and Taylor of a mesophase state in pitch, has had a major impact on the technology of carbon and graphite. This phenomenon explained for the first time how isotropic pitches transform to anisotropic carbons [60,61].

The term "mesophase" is used for the substance of which the spheres and the mosaic – before solidification – are formed [62].

The mesophase pitch as a precursor for the high performance pitch based carbon fibre has been prepared from coal tar and petroleum residues through several steps such as hydrotreatment, extensive removal of volatile non-mesogen and extraction of non-fusible non-mesogen [63-68]. When such materials are heat treated at temperatures of about 350-500 °C, mesophase in the form of anisotropic spherules precipitates from the isotropic phase [69,70] and the general pattern of behaviour has been found to be as shown in Figure 2.9 [38]. The substance melts on heating and becomes an isotropic pitch or liquid. As the temperature rises over above 350 °C, optically anisotropic spheres appear in the isotropic matrix. This optically anisotropic phase is called a carbonaceous mesophase.

As the heat treatment progresses, the spherules grow through coalescence (Fig.2.10) [71] and finally transform into irregular regions of coalesced mesophase. Since mesophase is usually obtained through the heat treatment of isotropic pitches, it is important to consider the changes which transpire during pitch pyrolysis. These include both physical and chemical phenomena [72]. The major relevant "physical"

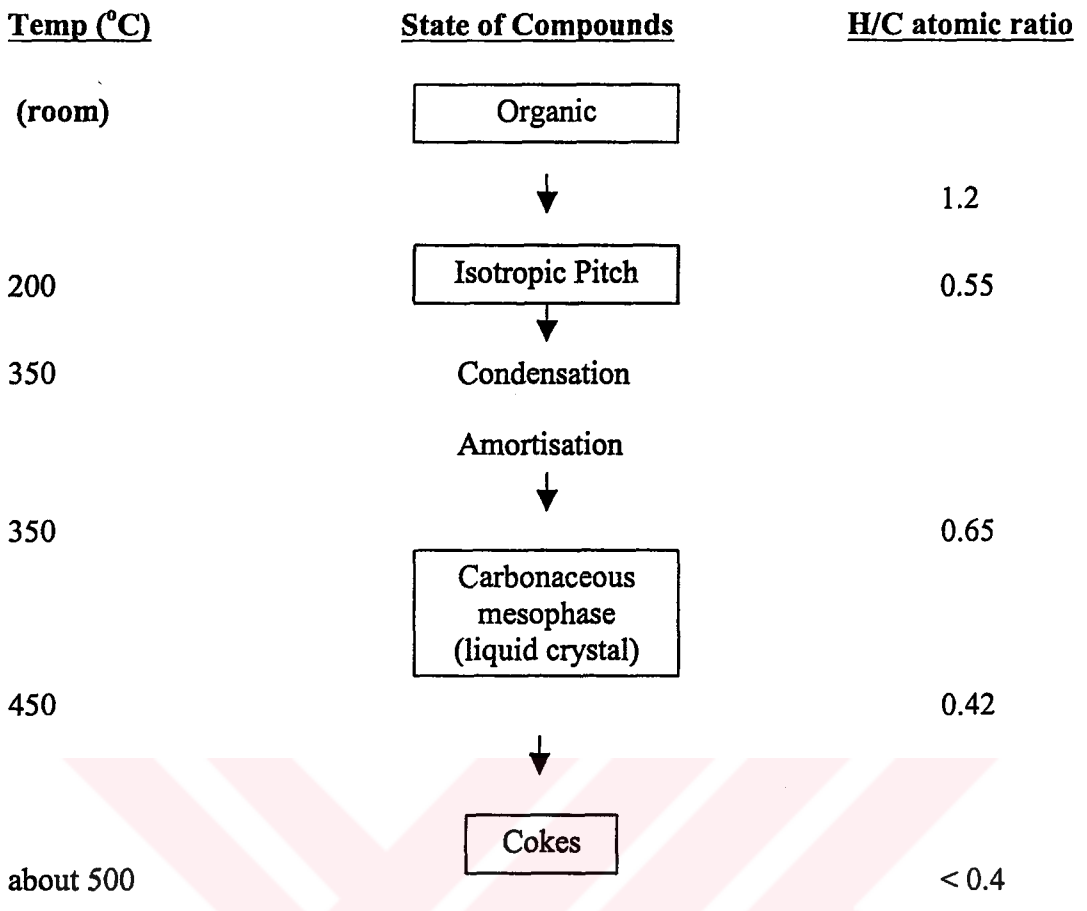

Figure 2.9. Change in non-volatile organic compounds brought about by heating [38].

change, which occurs during heat treatment of pitches at the mesophase stage, is volatilisation of low boiling condensable components and evolution of gases. The volatiles consist largely of low molecular weight components, which distill out of the pitch before they can react. The degree of volatilisation can be altered by the use of pressure [73].

The main chemical process associated with the heat treatment of pitches involves thermally induced polymerisation [74]. The thermal conversion of pitch to mesophase involves both chemical polymerisation and dealkylation reactions [75-77]. Hence, the development in the pitch of long range molecular order, which leads to the physical transformation to liquid crystal, has been attributed both to increasing molecular weight and chemical bonding (side chains on aromatic rings). Such chemical reactions remove mesophase inhibitors and disordering species, and lead to the formation of large planar molecules [78].

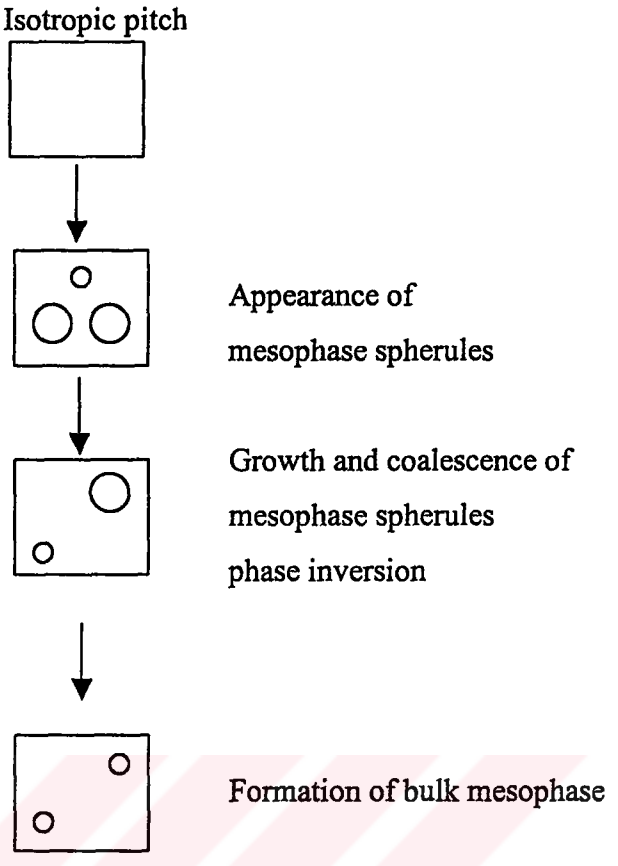

Figure 2.10. The process of mesophase formation [71].

It is known that mesophase formation during the heat treatment of pitches can be related to the increase in the concentration of high molecular weight species generated from low molecular weight molecules by condensation or by distillation of low molecular weight fractions [79]. Chwastiak, et.al referred that Fitzer and others have suggested [80] the chemical basis for mesophase formation is the condensation of small aromatic molecules into larger ones which concentrate into an anisotropic phase, but this does not rule out the presence of some small molecules in the anisotropic phase and some large molecules in the isotropic phase [80].

Because of the apparent insolubility of mesophase spheres in the isotropic pitch, extraction techniques were used initially as a general method for determining mesophase contents of pitches. The decrease in solubility of pitch in excellent pitch solvents such as quinoline and pyridine was used to monitor mesophase development and to determine reaction kinetics [81].

Mesophase pitch, as a precursor for making the high performance carbon fibre, needs to be spinnable at low temperature, highly oriented and reactive for oxidation to promote thermosetting [82].

High performance carbon fibres were mainly developed for aerospace applications because of their high stiffness and low weight. High performance carbon fibres are widely used in polymer-matrix composites for aircraft which are lightweight for the purpose of saving fuel. The aircraft Voyager has 90% of its structure made of such composites and achieved a non-stop, unfueled, round the world flight in 1986. High performance carbon fibres are also used in carbon–matrix composites for high temperature aerospace applications, such as in the space shuttle, as the carbon matrix is more temperature resistant than a polymer matrix [23].

Another promising route for the application of high performance carbon fibres is in the engine itself. One of the results of a large government supported programme in the Federal Republic of Germany is the connecting rod. Medical applications for high performance carbon fibres should be mentioned. Carbon fibre is the material which possesses the best biocompatible properties of all known materials, it is compatible with blood, soft tissue as well as with bones. Two applications are of most interest today, the replacement of ligament, and carbon fibre reinforced bone plates [27].

2.7.3 Spinning of pitch precursors

Spinning is a fibre formation step in which the melt of pitch is spun into fibres by melt spinning, centrifugal spinning or melt blowing. The latter two processes can only produce non-continuous fibres and have low running costs compared with conventional melt spinning, and are most suitable to produce isotropic pitch-based carbon fibres. In these fibre forming processes, the pitch is melted to a carefully controlled viscosity and then forced through a number of fine capillaries to produce the fibres as the pitch re-solidifies. The diameter of the fibre is controlled by drawing the fibre by centrifugal force or a stream of air to blow the fibre onto a moving belt as it forms into a random mat. Extreme care must be taken to control temperature and other parameters.

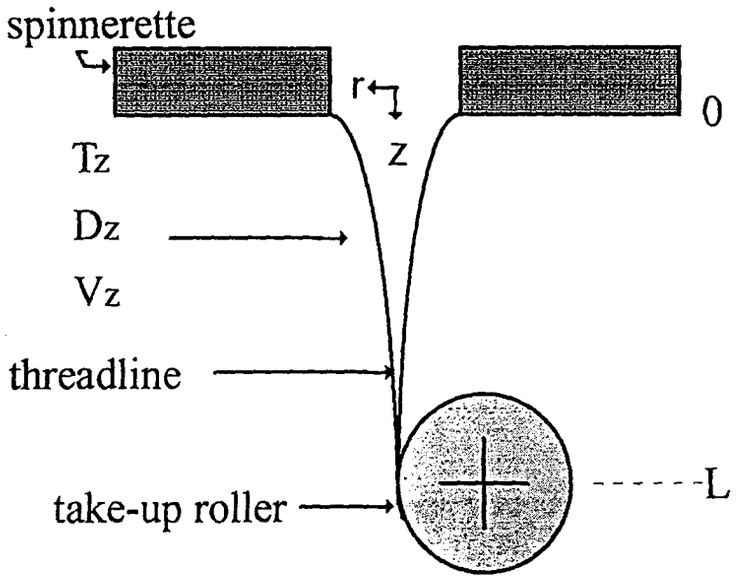

Figure 2.11. Schematic drawing of melt spinning [83].

Mesophase pitch can be formed into fibres through melt spinning. The mesophase pitch melt, having a suitable viscosity at the spinning temperature, is extruded through a multiple hole spinnerette. Under the combined effect of gravity and pulling of the roller, the extrudates draw down as they cool and eventually solidify to form the fibres. A schematic diagram of the process is shown in Figure 2.11.

When the filament draws down, its axial velocity increases until it glassifies, reaching a final diameter where the velocity is at its maximum which is in turn determined by the roller speed. There is an increasing velocity gradient in the filament on leaving the spinnerette, reaching a maximum just above the glassification point. Thus, a maximum tensile stress results where the filament diameter is at its minimum (i.e. from the glassification point downward). For a continuous process, this maximum stress must not exceed the ultimate tensile strength of the "as-spun" filament or else it would break and disrupt the spinning process.

The viscosity of the pitch is extremely important for the spinning of a continuous, thin filament. The viscosity of both mesophase and isotropic pitch is more temperature sensitive than that of organic polymers, and therefore, it is vitally important to carefully control the temperatures of both spinnerette and the surrounding environment.

When molten mesophase pitch is forced through the spinnerette, the planar polyaromatic molecules are lined up in the flow direction. The alignment is further improved during the fibre drawdown. Hence, the polyaromatic molecules are aligned more or less parallel to the fibre axis in the "as-spun" fibres, reducing the energy input required for graphitisation, and producing fibres with exceptional stiffness. The spinning conditions have a strong impact on the degree of preferred orientation of "as-spun" fibres, which is higher when the spinning viscosity is low at a high spinnig temperature. A pitch fibre with larger diameter and lower viscosity during spinning provides a higher degree of preferred orientation because a pitch fibre with a thinner diameter is cooled more rapidly during the elongation process in spinning, and inherits a lower degree of preferred orientation due to disordered states at higher temperature. The molecular structure of mesophase pitch also influences the transverse shape, texture and the degree of preferred orientation of the spun pitch fibres [83].

2.7.4 Oxidative stabilisation of pitch based carbon fibres

For fabrication of pitch-based carbon fibres the pitch precursor must be spinnable and the spun pitch-fibres must be stable in shape or structural configuration during subsequent carbonisation and graphitisation [54,84].

The stabilisation process, occasionally called the infusibilisation or thermosetting step, is the most time consuming step in the production of pitch based carbon fibre [84,85].

The stabilisation step can have a significant impact on the micro structure as well as the mechanical strength of the finished fibre. The chemical and structural mechanisms involved in oxidation during stabilisation are complex. The fibre morphology is largely dependent on the extent of oxygen up-take, precursor composition, and morphology, temperature, environment, and stress [84,86].

The oxidative stabilisation of an as-spun fibre is usually performed, very slowly to prevent spun fibre melting [22] , at a temperature a few tens of degrees below the softening point of the pitch precursor.

The oxidation atmosphere may be ambient air, ozone, oxygen, or pressurised oxygen, with or without additives intended to enhance oxidation [84]. Use of inert environments in early stages of stabilisation has been suggested to yield a more homogeneous stabilised fibre structure. Experimentally, NH_3 gas is known to accelerate stabilisation, but oxygen must be present [86]. The addition of sulphur to isotropic pitch has been reported to shorten the stabilisation time during the production of low strength fibres [54].

Oxidative stabilisation involves two competing reactions, "oxygen uptake" and "fibre burn-off" [87]. Adding oxygen to an organic molecule raises the boiling or melting point or, alternatively, oxygen may promote cross-linking between molecules [88].

Any proposed mechanisms to explain the oxidative stabilisation must support the experimental evidence. Such factors would include a rapid initial weight gain during the early stages of oxidation, accompanied by a loss of methylene hydrogens, and an introduction of oxygen as carbonyl, hydroxyl, and carboxyl. Figure 2.12 accounts for only the rapid weight gain regime. Oxygen uptake reactions are believed to occur first at aliphatic side chains to produce a variety of compounds listed above by oxygen insertion and dehydrogenation, and further aromatisation and cross-linking may take place. The rupture of carbon-carbon bonds allows for the insertion of oxygen between separate pitch molecules and for, ultimately, the formation of oxygen-containing cross-links. Satisfactory mechanisms for oxidative stabilisation must also include a process to account for weight loss which is associated with longer time periods or higher temperatures of oxidation. Weight loss is a result of concerted decarboxylation-type degradations that remove carbon content from the pitch in the form of carbon dioxide and carbon monoxide without rearrangement or randomisation of the lattice [89-93].

Stabilisation of the mesophase pitch, usually by treatment with molecular oxygen, means conversion into a more or less cross-linked polymer with a partial layer structure. The effect of cross-linking can be seen directly in an increase of the glass transition temperature and directly in an increase of the coke yield [94]. Oxidation processing can deliver as much as 20% increase in carbonisation yield. Oxygen absorption and cross-linking reactions, which tend to retain marginally volatile

carbon-bearing species within the pyrolysis residue; and carbon burn-off reactions, which have been found by chemical analyses to occur during both oxidation exposure increases [95].

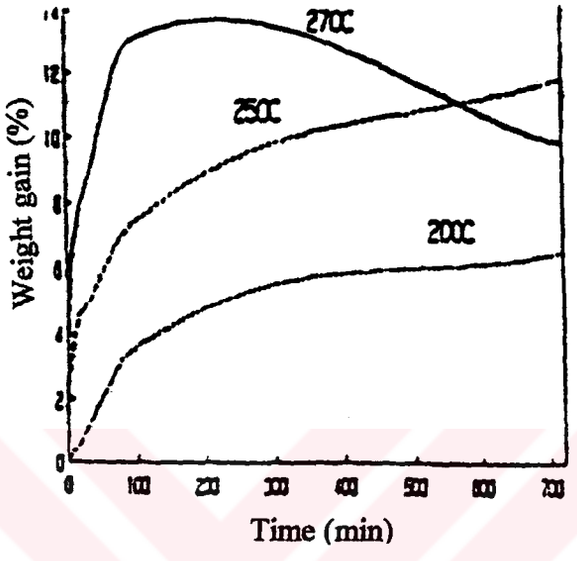

Figure 2.12. Weight changes during stabilisation step [84].

During stabilisation, the solubility characteristics of the fibre change: the proportions of quinoline insoluble (QI) and pyridine insoluble (PI) constituents increase while those of benzene soluble (BS) constituents decrease [85,96].

2.7.5 Carbonisation of fibres

Carbonisation of oxidised pitch fibre is a very important process as well as stabilisation of pitch fibre [97]. Stabilised pitch fibres are infusible but they have poor mechanical properties, e.g., they are fragile and not easy to handle. Therefore, in order to remove the remaining heteroatoms and improve the mechanical properties, carbonisation of the stabilised fibres is necessary. Carbonisation represents the process of elimination of non-carbon atoms, which is completed at around 1500°C.

A number of physical and chemical transformations occur during the carbonisation of pitch between 300°C and 500°C, such as weight loss, evolution of gaseous reaction products, molecular weight increase, and change in physical properties [98].

During carbonisation under an inert atmosphere, the oxygen acquired during stabilisation reacts to produce gaseous species, such as H_2O, CO_2, and CO, while to a lesser extent H_2, and CH_4 are also evolved. These reactions promote further aromatisation and cross-linking of constituent aromatic molecules, leading to the formation of small turbostratic carbon or graphitic crystallites. Increasing the final heat treatment temperature results in an increase in crystallite size and perfection, and in the degree of preferred orientation of layer planes along the fibre axis, resulting in an improvement in mechanical and other properties [99].

3. RELEVANT ANALYTICAL METHODS FOR CHARACTERISATION OF PITCHES

3.1 Determination of the Glass Transition Temperature and Thermal Behaviour of Pitches

Glass transition temperature, T_g, is one of the important parameters for pitch characterisation studies. Different analysis techniques have been used to measure T_g of pitches. Among these techniques DSC (differential scanning calorimetry) has been found to be unsuitable for the determination of T_g for pitches. A new technique which is modified from DSC, called dynamic differential scanning calorimetry (DDSC), is used to examine the applicability of this technique to measure T_g of pitches.

Thermal analysis techniques are those in which a physical property of a substance and/or of its reaction products is measured as a function of temperature while the substance is subjected to a controlled temperature program. It can cover a range of scientific experimentation in which properties are measured with respect to time and temperature and also include isothermal experiments at different temperatures.

The main techniques employed in thermal analysis are TGA, which monitors gain or loss of weight (mass change), and differential thermal analysis (DTA), which monitors changes in specific heat capacity (rate of enthalpy change).

DSC is used to characterise the properties of pitches qualitatively and quantitatively as a function of temperature. Below their glass transition pitches are rigid, because at a molecular level adjacent polyaromatic molecules are frozen in a matrix with insufficient thermal energy for molecular adjustments to occur. With increasing temperature, the thermal energy results in an increasing degree of molecular motion, including co-operative movements between the rigid disc-like molecules. This overall process is accompanied by increasing volume (the s-called "free volume

concept") and heat capacity, and decreasing resistance to eternally applied stresses [100].

Polymeric materials usually do not degrade at a measurable rate until they are heated to about 100°C above their softening temperatures. Polymers are often in the liquid state at reaction temperature, and even below their melting temperatures there can be considerable segmental motion. Because of the complex molecular structure of polymers, physical changes take place much more sluggishly and over broader temperature ranges than in the case for lower molecular weight substances. Glass transitions and even melting transitions extend over broad temperature ranges and exhibit fine structure. Furthermore, many of the changes that affect their properties take place in the condensed phase without significant mass change so that other thermal analysis techniques besides TGA are employed [100].

3.1.1 Thermogravimetric analysis (TGA)

Thermal analysis techniques are already widely used in materials science and technology for both research and commercial applications, especially in polymer and plastic field. Most of the basic techniques and methods used in thermal analysis can be used for all materials, whether inorganic, organic or polymeric. However, there are important differences in thermal behaviour between these different types.

Thermogravimetry may be defined as "a technique whereby the weight of a substance, in an environment heated or cooled at a controlled rate, is recorded as a function of time or temperature". Thus the two basic requirements are a method of heating (or cooling) and a means of weighing. The basic instrumental requirements for thermogravimetry are a precision balance, a furnace capable of being programmed for a linear rise of temperature with time, and a recorder [101].

Thermogravimetry provides information in a wide variety of chemical investigations. Some of the many applications of thermogravimetry are listed below [102]:

1. thermal decomposition of inorganic, organic, and polymeric substances,
2. distillation and evaporation of liquids,
3. pyrolysis of coal, petroleum, and wood,
4. determination of moisture, volatiles, and ash contents,

5. thermal oxidative degradation of polymeric substances,
6. reaction kinetics studies,
7. thermal stability.

Thermogravimetry is also used to characterise the carbonisation behaviour of pitches and pitch fractions [103].

The prediction of pitch behaviour in the thermal processes required for their utilisation is a difficult task due to their complex composition and the innumerable interactions among their components. An adequate characterisation will require the joint application of various methodologies. Thermal analysis could be one of the most relevant, because of its close relationship with the pyrolysis of pitches [104].

Combined thermogravimetry (TG)/derivative thermogravimetry (DTG)/ differential thermal analysis (DTA) have shown their suitability in the interpretation of different phenomena occurring during pyrolysis of different pitches and some of their fractions [105,106].

3.1.2 Differential scanning calorimetry (DSC)

The main aim of using the differential scanning calorimetry (DSC) technique is to examine the applicability of a new method derived from it, called dynamic differential scanning calorimetry (DDSC), to pitches.

Differential scanning calorimetry is an important technique for the thermal analytical investigation of many materials, and is used a great deal in the study of polymeric materials. It measures the difference in energy input between a substance and a reference material as they are subjected to a controlled temperature program. Practically all physical and chemical processes involve changes in enthalpy or specific heat, and the applicability of DSC to condensed-phase systems is almost universal. Its measurement process is quantitative and the change of enthalpy is usually a linear function of the reaction co-ordinate.

DSC technique measures the temperature difference between temperature sensors- one in a specimen and the other in a reference material- as they are subjected to the same programmed temperature change.

DSC measures all enthalpic events, e.g., chemical reactions, physical transitions, release of strains, so that the interpretation of the reaction of interest maybe obscured by side reactions. Mass gain or loss during reaction or transition changes the heat capacity, and produces errors in baseline subtraction.

Dynamic differential scanning calorimetry (DDSC) is a term used to describe a series of techniques whereby a sample is subjected to a repetition of program steps. From analysis of the heat flow response, the specific heat capacity can be determined independently of continuous, long-term enthalpy effects. The DDSC method allows the separation of overlapping events in a material such as simultaneous melting and crystallisation or to isolate the specific heat change of a glass transition form non-repeatable processes, such as reactions, moisture loss, decomposition and crystallisation.

The repeat temperature program can be one of two types, an iso-scan or a heat-cool program. In the repeat program the number of repetitions that are to be performed can be specified. The iso-scan repeat program is used when heating through a crystalline melting transition or when cooling through the re-crystallisation of a crystalline material. The heat-cool type program is used to extract the glass transition event from other events that maybe obscuring the T_g, such as re-crystallisation on heating or enthalpy effects caused by prior thermal and mechanical history [100].

Since pitch materials generally have a very complex composition with molecular mass ranging from a few hundred to several thousand units, it is thought of interest to determine their thermal behaviour and the characteristics related to their glassy transformation [107].

When a polymeric material undergoes heating, the transition from the glassy to rubbery state is referred to as the glassy transition of that material. The transition occurs over a range of a few degrees of temperature. The mid-point or the point of inflection of the transition (depending on the technique employed) is called the glass transition temperature, T_g [108].

It is easy to visualise that the liquid is a condensed gas, i.e., neighbouring molecules touch, but still move randomly, similar to the gas. They can not fly apart because of the attractive forces (bonds). When the temperature is lowered, the translational

motion decreases, the liquid becomes macroscopically more viscous. Finally, the large scale motion becomes practically impossible. The molecules cannot change their position anymore and the substance is a solid in this case an amorphous glass. The structure is still the same as that of a liquid, but the changes in position and orientation of the molecules have stopped. Such a liquid-to-solid transformation occurs at the glass transition temperature, T_g [109].

Occurrence of the glass transition phenomenon:

The variation of enthalpy versus decreasing temperature for a pure liquid exhibits an abrupt variation at the freezing temperature (enthalpy of crystallisation). For many materials such as polymers, or pitches, the enthalpic diagram is somewhat more complex. Provided that the results are interpreted carefully, these diagrams are extremely useful for the description of the molecular configuration of these systems. For glassy materials (Figure 3.1a), no crystallisation occurs. The enthalpy of the frozen liquid goes on decreasing without any discontinuity. The mobility of molecules decreases progressively, and the frozen liquid is transformed into a vitreous material.

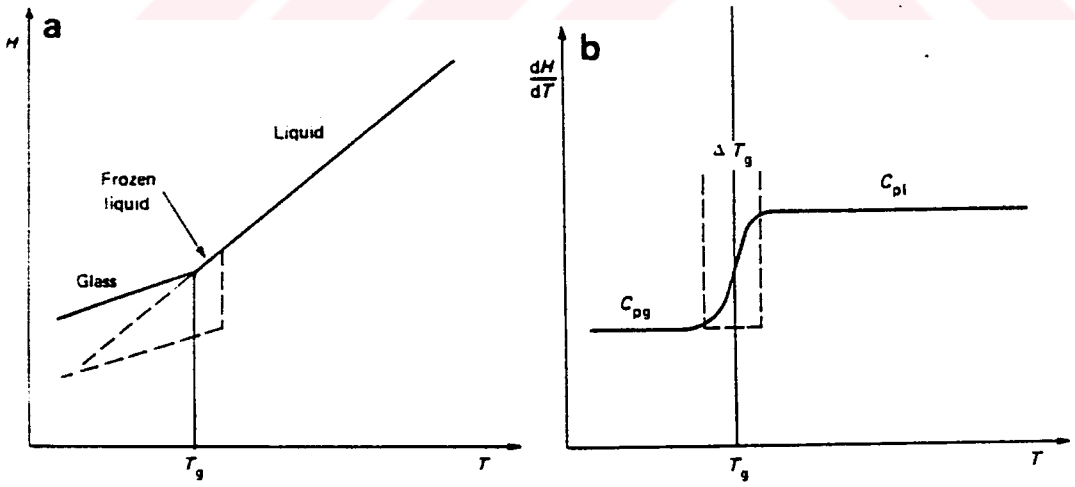

Figure 3.1. Domain of glass transition (a); Enthalpy versus temperature; (b), heat capacity versus temperature [110]

In the plot of heat capacity (C_P) versus temperature (Figure 3.1b), the glass transition temperature T_g is defined at the inflection point. The temperature interval of the glass

transition (ΔT_g) can be characterised by the temperature interval defined by the intercept between the tangent to the inflection point, on the one hand, and the liquid and glass C_P lines, on the other. It should be noted that T_g corresponds to the temperature when the mobility of the molecules or segments rearrangement is close to the cooling rate. Therefore, the T_g value is affected by the cooling rate, and cannot be considered as an absolute parameter. The glass transition interval, ΔT_g, is not significantly affected by heating rate. The molecular relaxation occurring during the interval ΔT_g is both time and temperature dependent [111]. Once cooled to a temperature below T_g, the glass is out of equilibrium [110].

Although pitch materials are organic glasses at low temperatures, few attempts have been made to characterise them in terms of their glass transition temperature, T_g [44]. In general, pitches are very complex in composition, with molecular mass ranging from a few hundred to several thousand units, and are glassy in solid state. Thus, isotropic pitches do not show a defined melting point on heating but pass through a glassy transition region into a relatively low viscosity liquid. The basic constituent compounds belong mainly to planar polycyclic aromatic hydrocarbons [112].

At the present time, however, compositional changes occurring during thermal evolution of pitch, and their influence on pitch rheology and glass transition are incompletely understood. Glass transition temperatures, T_g, of pitches, and their pyrolysis products, have been reported in references 44, 110, 113-116. It was found that T_g increases with an increasing average molecular weight [114], and the range of the glass transition temperature, ΔT_g, increases with the broadening of the molecular size distribution [110].

3.2 Rheological Characteristics of Pitches

The measurement of rheological properties of pitch based precursors for carbon materials is important in terms of providing a fundamental understanding of these materials [117] and they are of major significance in the processing of advanced carbon materials [118].

Lewis [69] indicated that the isotropic phase always has a lower viscosity than the mesophase. Mesophase pitches possess high temperature elastic effects, whereas

optically isotropic pitches were thought to behave as a Newtonian fluid [119]. But recent work [120,121] has shown that heat- treated isotropic pitches can also show this effect. When a pitch is heat treated, it begins to release the light fraction component from its structure by evaporation and condensation reactions, thereby increasing its average molecular weight (MW) and achieving a more narrow MW distribution. As this occurs, rheologically, the elasticity of the system increases [122]. Collet and Rand [123] have shown Newtonian behaviour of pitches up to temperatures of 250 °C and non-Newtonian behaviour only at further increased temperatures. This was also confirmed by Balduhn, and Fitzer [124].

Shear viscosity for a homogeneous, incompressible, isotropic, and Newtonian fluid is defined as the ratio of the shear stress to the shear rate. Therefore:

$$\tau = \eta \dot{\gamma}, \tag{3.1}$$

where; τ, is the shear stress; $\dot{\gamma}$, is the shear rate; and viscosity, η, is dependent of the shear rate. A Newtonian fluid is inelastic and has a zero response time. Therefore, assuming a negligible response time for the measuring apparatus, equation (3.1) applies at any time during the experiment. Hence, shear viscosity, η, is sufficient for total rheological characterisation of a Newtonian fluid.

Since molten mesophase pitch is anisotropic, shear viscosity does not suffice for its total rheological characterisation. In analogy with equation (3.1), a constitutive equation for an inelastic, anisotropic fluid is:

$$\tau_{ik} = \eta \dot{\gamma}_{jl}, \tag{3.2}$$

where; τ_{ik} and $\dot{\gamma}_{jl}$ are stress and strain rate tensors, respectively [125].

3.2.1 Softening point

The softening point ,T_s, of an amorphous material is usually understood to mean the temperature at which the material changes from a non-crystalline solid into a fluid. All the standard methods adopted to measure the softening point temperature, e.g., the ball and ring method [126], cube and air method, and Kraemer-Sarnow method [127], determine the macroscopic fluidity and/or deformability of the material from a

mechanical point of view. The softening temperature does not have a thermodynamic basis, and its determination is usually empirical. Thus, the T_s obtained will depend on the particular standard method employed for its measurement.

T_s is different from the melting temperature, T_m, of a crystalline material, and from the glass transition temperature, T_g, of an amorphous state material, both of which have a definite molecular interpretation and thermodynamic basis. The ordered molecular structure becomes disordered when a crystalline material is transformed into a liquid. At T_g, molecular segments of a material in the amorphous state attain some mobility, whereas below T_g, the molecular segments are "frozen" [128].

T_s and T_g can be used to follow the changes in pitches during processing and/or heat treatment. For instance, pitches of increasing softening point can be prepared by atmospheric distillation and heat treatment in a closed system. In both cases, the amount of insoluble content increases with the softening point, indicating that the average molecular mass of the pitch tends to increase either by removal of light molecules by distillation or by polymerisation and condensation reactions during heat treatment. Similarly, the glass transition temperatures of the pitches becomes higher.

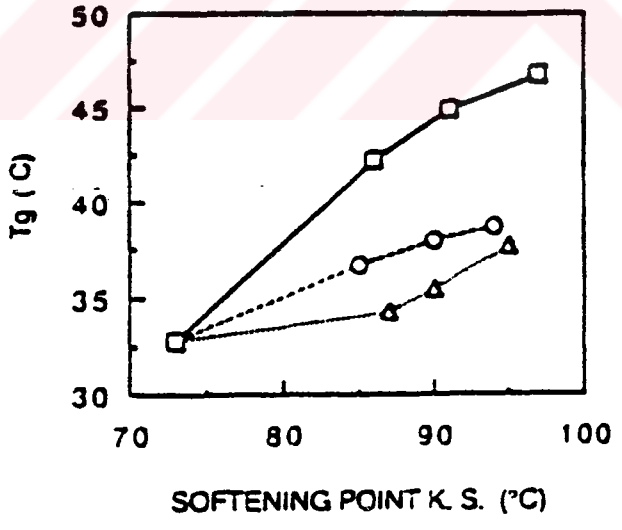

Figure 3.2. Glass transition temperatures for pitches of similar softening points but prepared in different conditions: ( ), atmospheric distillation of a coal-tar; (Δ), atmospheric distillation and heat treatment at 380°C; (O), atmospheric distillation and heat treatment at 410°C [115].

The T_g values for pitches prepared under different conditions are shown as a function of their softening point measured by the Kraemer Samow (KS) method in Figure 3.2.

The relationship between KS and T_g depends on the operating conditions for pitch preparation. Since T_g and KS are isoviscous temperatures, it can be deduced that the decrease in viscosity is much more pronounced for pitch samples prepared by mere distillation than by heat treatment [115].

3.3 Structural Analysis

3.3.1 Size exclusion chromatography (SEC)

Chromatography is widely used in the separation, fractionation, and characterisation of complex mixtures of organic molecules. Size exclusion chromatography (SEC), as known gel permeation chromatography (GPC), is a technique in which molecules are separated on the basis of their ability to penetrate a porous gel. Large molecules cannot penetrate the gel and are confined to the mobile phase resulting in them travelling through the column at the same speed as the mobile phase. Smaller molecules enter the stationary solvent trapped in the gel pores and their elution is retarded by the gel to an extent which is dependent on their molecular size and the distribution of pore sizes in the gel. This method provides a separation mainly on the basis of molecular size which corresponds to separation on the basis of molar mass.

SEC has been extensively used for the separation, fractionation, and characterisation of coal and petroleum derivatives [129]. Greinke has reported the kinetics of petroleum pitch polymerisation by SEC [75]. In general, investigations have shown [130] that the determination of molar mass distributions by SEC needs considerable care in the selection of the mobile and stationary phases. THF is a good solvent for most structures found in coal derivatives and it is compatible with most of the gels used as stationary phases in SEC. However, separation can still occur partially on the basis of functionality as well as on molecular size [129]. Divinylbenzene and polystyrene gels have been found useful for the SEC separations of hydrocarbon fuels [131,132]. Polar solvents are the most satisfactory since irreversible adsorption is minimised [133].

Pitch is a complex material comprised of thousands of components, mainly polyaromatic hydrocarbons and their heterocyclic analogs. Even though pitch has a complex molecular composition, it becomes homogeneously; that is, its properties

tend to change with increasing molecular weight [134]. Due to the complexity of pitch, very few analytical techniques provide much information about composition. However, SEC provides a "fingerprint" of pitch with respect to its molecular composition [135].

SEC separates molecules based on size, but with appropriate calibration procedures can be used to provide molecular weight distribution data for pitch materials [136]. For pitches, interpretation of SEC is not easy. Some of the difficulties are: the entire pitch cannot be characterised because of incomplete solubility in common solvents; SEC detection options that may result in more molecular weight information are limited due to low average molecular weight; pitch components exhibit some non-ideal elution behaviour resulting in molecules not being eluted have varying refractive indices which result in different detector responses for the same number of molecules. Due to varying refractive indices and non-ideal elution behaviour, absolute ratios of "small" vs. "large" molecules cannot be obtained [135]. The other drawback of SEC, however, is that it is still difficult to apply on a large scale to produce sufficient amounts of fractions for further experiments [137].

Despite its limitations, SEC provides discrete information on the composition, which can be related to processes and properties, unlike most analytical determinations of molecular weight that give only an average value [135]. Besides SEC, vapour phase osmometry (VPO), which is another classical technique, and Matrix Assisted Laser Desorption Ionisation Mass Spectrometry (MALDI) which is a new technique, are being used to determine the molecular weight of carbonaceous pitches [138].

SEC allows the determination of molecular mass (MM) distributions, and hence weight average molecular weight ($\bar{M}_w$), so that the heterogeneity index ($\bar{M}_w / \bar{M}_n$) can be calculated where $\bar{M}_n$ is the number-average molecular weight.

In the SEC of a wide variety of polymers it has been found [139,140] that the retention volume (V_R) is related to the logarithm of MM:

$$\text{LogMM} = A - BV_R \qquad (3.9)$$

where A and B are constants. Calibration plots are most reliably constructed from the retention volumes of narrow MM distribution fractions of the same material with

known MM, determined by an independent method. If the standards are sufficiently close to being monodisperse (i.e. $\bar{M}_w / \bar{M}_n < 1.1$) then:

$$M_{peak} \cong \bar{M}_w \cong \bar{M}_n \qquad (3.10)$$

where M_{peak} is the molecular mass corresponding to the peak of the size exclusion chromatography [141].

3.3.2 Infrared spectroscopy

The infrared region of the electromagnetic spectrum extends from the red end of the visible spectrum to out of the microwave region. The region includes radiation at wavelengths between 0.7 and 500 μm or, in wave numbers, between 14,000 and 20 cm^{-1}. The spectral range of greatest use is the mid-infrared region, which covers the frequency range from 200 to 4000 cm^{-1} (50 to 2.5 μm). Infrared spectrophotometry involves the twisting, bending, rotating, and vibrational motions of atoms in a molecule (Figure 3.3). Upon interaction with infrared radiation, portions of the incident radiation are absorbed at particular wavelengths. The multiplicity of vibrations occurring simultaneously produces a higher complex absorption spectrum, which is uniquely characteristic of the functional groups comprising the molecule and of the overall configuration of the atoms as well.

Atoms or atomic groups in molecules are in continuous motion with respect to each other. The possible vibrational modes in a polyatomic molecule can be visualised from a mechanical model of the system, shown in Figure 3.3. Atomic masses are represented by balls, their weight being proportional to the corresponding atomic weight, and arranged in accordance with the actual space geometry of the molecule. Mechanical springs, with forces that are proportional to the bonding forces of the chemical links, connect and help the balls in positions of balance. The infrared spectrum of a compound is essentially the superposition of absorption bands of specific functional groups, yet subtle interactions with the surrounding atoms of the molecule impose the stamp of individuality on the spectrum of each compound. For quantitative analysis, one of the best features of an infrared spectrum is that the absorption or the lack of absorption in specific frequency regions can be correlated with specific stretching and bending motions. Thus, by interpretation of the

spectrum, it is possible to state that certain functional groups are present in the material and that certain others are absent [129].

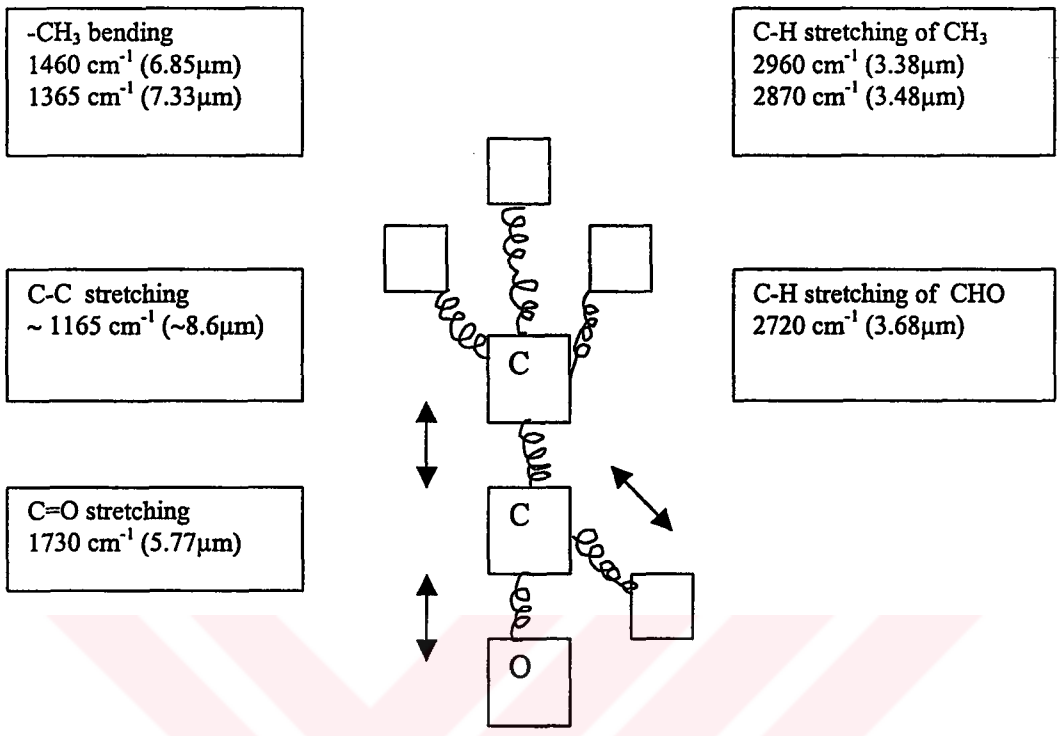

Figure 3.3. Vibrations and characteristic frequencies of acetaldehyde [142].

Fourier transform infrared spectroscopy, which provides information about functional groups in a substance, is one of the most versatile analysis techniques available for the study of complex mixtures such as coals, pitches, and related materials. It must be taken into account that all carbonaceous solids essentially give the same bands in their IR spectra, differing in intensity. Hence, a study of band intensity is necessary when using this technique for the characterisation of these solids. Band intensity can be quantified by measuring absorption coefficients, the determination of which is the principal problem in quantitative infrared spectroscopy. However, in all instances these coefficients have been calculated by approximation, based on assumption that each functional group has a characteristic intensity which does not vary greatly from one molecule to another when they have a similar environment [143].

In spite of this, for coal tar pitches and for comparative studies the determination of absorptivities is not necessary; good results can be obtained taking into account the absorbance values for the different bands. It must be considered that the constituents

of pitches can be grouped into relatively few classes of compounds. Moreover, a study of the volatile fraction of several pitches has shown that, qualitatively, their composition is the same [144]. On the other hand, another infrared study on coal tar pitch and its fractions shows that the volatile fraction of coal tar pitches may also be composed of members of the families of compounds identified by GC-MS in the volatiles with a higher number of aromatic rings [144-146].

3.3.3 Nuclear magnetic resonance spectroscopy (^{1}H and ^{13}C NMR)

Nuclear magnetic resonance spectroscopy arises from interaction of the magnetic component moments possessed by atomic nuclei of isotopes with a nonzero spin quantum number I. Discrete nuclear magnetic moment orientation levels have an energy separation, and hence, a resonance frequency, proportional to the magnetic field B_0 applied. Assemblies as such nuclear moments can give rise to measurable macroscopic changes. According to the size of B_0 and the particular nuclear species, resonance frequencies are usually in the ratio-frequency range 10-300 MHz or so. Thus the quanta are small, so that little disturbance is caused to the system. Development of ^{13}C NMR occurred much later than that of ^{1}H NMR because, in a given magnetic field, ^{13}C NMR has sensitivity about 6000 times less than that of ^{1}H NMR for unenriched samples.

The value of high resolution ^{1}H NMR in providing chemically useful information about individual hydrocarbons, especially cyclic compounds, has been established for many years. Full analyses are often difficult but spectra can generally be solved with the help of high magnetic fields, double resonance experiments, and so on. Remarkably interesting results have been achieved from such superficially unpromising samples as complex mixtures of hydrocarbons extracted from coal and coal products. Over the last decade, ^{13}C NMR has established itself as a complement to ^{1}H NMR and is becoming almost as widely used for organic compounds. Current instrumentation makes the combination of ^{1}H NMR and ^{13}C NMR spectroscopy one of the most valuable non-destructive techniques for studying the composition and structure of solutions of hydrocarbons extracted from coal. In the solid state, early experiments showed that broad-line ^{1}H NMR could be applied to whole coals to measure the moisture content. Very recently, preliminary high resolution ^{13}C NMR

experiments on solid coal samples with new pulse and magic angle techniques have already given very valuable direct indications of aromatic content in coals [147].

3.3.3.1 ^{1}H NMR spectroscopy

Proton magnetic resonance (^{1}H NMR) spectroscopy is particularly important field of NMR spectroscopy. ^{1}H NMR spectroscopy has proven a powerful tool for investigating composition of both coal-and-petroleum derived heavy residues [148].

Organic compounds contain, practically without exception, hydrogen atoms. Hydrogen is the most frequent nucleus of molecules, and it occurs in the most varying chemical environments. The large natural abundance of the ^{1}H isotope (99.8%) and consequently its high sensitivity in nuclear resonance also facilitate the measurements [149].

Three of the more important parameters were proposed by Brown and Ladner [148]: (1) f_a; the ratio of aromatic carbon (C_{Ar}) to total carbon (C), (2) the degree of substitution of the aromatic rings (σ)defined as that fraction of aromatic-edge carbons carrying substituents, and (3) the H/C atomic ratio of the hypothetical unsubstituted aromatic rings (H_{Aru}/C_{Ar}) where H_{Aru} is the number of hydrogens for the hypothetic ensubstituted aromatic system. The latter parameter indicates the size of the condensed aromatic ring structures. The elemental hydrogen, carbon, and oxygen contents of the tars, together with reasonable derived from the proton spectra, are necessary for application of the derived equations. In their original work, Brown and Ladner divided the proton spectra into three regions representing the fractions of aromatic, α-aliphatic, and "other" aliphatic hydrogens, respectively (Table 3.1). They assumed that 60% of the total oxygen atoms occurred as phenolic hydroxyl groups and that this hydrogen was included with the aromatic protons [150]. The Brown-Ladner method makes use of the quantitative determination of the fractions of the total hydrogen present on aromatic rings and as phenolic OH on benzylic carbons and on other non-aromatic carbons. The Brown-Ladner equations are:

$$f_a = [(C/H) - (H^*_\alpha/X) - (H_\beta^*/Y)] / (C/H) \quad (3.11)$$

$$\sigma = [(H^*_\alpha/X) + (O/H)] / [(H^*_\alpha/X) + (O/H) + H^*_{ar}] \quad (3.12)$$

Here, $H^*_\alpha = H_\alpha/H$, the ratio of alpha type hydrogen to total hydrogen; $H_\beta^* = H_\beta/H$, the ratio of beta type hydrogen to total hydrogen; and $H^*_{ar} = H_{ar}/H$ is the ratio of aromatic to total hydrogen. The parameters X and Y refer to the H/C atomic ratios for the benzylic carbon structures and for the other non-aromatic carbon structures, respectively. For the materials derived from coal, X and Y are generally taken to be 2 on the assumption that the aliphatic structures are predominantly methyl groups.

$$H^*_\alpha = H_\alpha/H \tag{3.13}$$

$$H_\beta^* + H_\gamma^* = (H_\beta/H) + (H_\gamma / H) \tag{3.14}$$

which represent the normalised integrated intensities of the α-alkyl and other alkyl hydrogen, respectively [150].

Table 3.1. ^{1}H NMR signals and assignment of protons [147].

Range of band δ (ppm)	Symbol	Assignment of protons
5.5 - 9.0	H_A	Aromatic and phenolic
4.7 - 5.5	-	Olefinic
3.3 - 4.5	$H_{\alpha,2}$ or H_F	Methylene groups α to two rings (e.g., of fluorene)
2.0 - 3.3	H_α	Hydrogen on carbon atoms α to ring
1.6 - 2.0	H_N	Naphthenic methylene and methine (other than α to ring)
1.0 - 1.6	H_β	Methylene β or more remote from ring; methyl groups β to ring
0.5 - 1.0	H_γ	Methyl γ or further from ring.

3.3.3.2 ^{13}C NMR spectroscopy

The structural analysis of average (hypothetical molecules) representing mixtures has become more popular as a technique in NMR has been developed. The ability to obtain quantitative ^{13}C NMR measurements by suppression of Nuclear Overhauser Enhancement (NOE) and the use of paramagnetic relaxation agents to reduce relaxation times has made ^{13}C NMR a routine analytical tool for analysis of coal derived products. The most important feature of both proton and carbon NMR is the ability to calculate aromatic/aliphatic ratios. Brown and Ladner [148] developed formula for calculating the total aromaticity of samples using NMR and elemental

analysis; although it required certain assumptions and it gave good comparative results.

Table 3.2. ^{13}C NMR spectral assignments [152].

A_o: 150-170 ppm	Aromatic carbon atoms substituted by - OH, ether, -CO and C atoms in carbonyls.
A_1: 130-150 ppm	Ring junction carbons, substitutes aromatic ring carbons and half of the unsubstituted carbons.
A_2: 100-130 ppm	The other half of unsubstituted (or protonated) aromatic ring carbons.
A_3: 9-60 ppm	Paraffinic, including cycloparaffinic and carbons of methyl and alkyl substitution on aromatic rings.
$A_{14.1}$ close to 14.1 ppm peak	Terminal methyl carbon - CH_3
A_{23} close to 23 ppm peak	First methylene carbon in long alkyl groups $-CH_2-CH_3$
A_{32} close to 32 ppm peak	Second methylene carbon in long alkyl groups $-CH_2-CH_2-CH_3$
$A_{29.7}$ close to 29.7 peak	Third or further methylene carbon in long alkyl groups $-(-CH_2)_n-CH_2-CH_2-CH_3$
$A_{19.5}$ close to 19.5 peak	Internal methyl carbon $-CH(CH_3)-CH_2$

The ability to calculate aromaticities directly from quantitative ^{13}C NMR enabled more accurate data to be accumulated. Quantifiable ^{13}C has been developed by many workers. The main difficulties involved are different carbon environments, some of which are very long, and secondly when performing proton decoupled spectra, heteronuclear coupling between carbon and hydrogen can enhance some peaks leading to some shifts not being proportional to the amount of that particular carbon environment. This phenomenon is called "Nuclear Overhauser Enhancement". There are many ways of overcoming the differences in nuclei relaxation times. One would be to use very long relaxation but this would create very long acquisition times due to the need to collect a high number of counts for Fourier Transformed spectra.

Another more practical way is to introduce paramagnetic species reduce the relaxation times by introducing an alternative relaxation process to the H-dipolar mechanism. One such relaxation agent is chromium acetylacetonate. NOE effects can be suppressed using techniques of heteronuclear gated decoupling [151].

3.3.4 Mass spectroscopy (MS)

A mass spectrum is a record of the damage done when high energy electrons impinge upon a molecule in the gas phase. The impact of the electron produces highly energetic positively charged ions (molecular ions) which then break up into smaller ions (fragment ions). The fragmentation is governed by the even electron rule which states that odd electron species can fragment by loss of radicals or molecules but even electron species fragment by loss of molecules only. The molecular ions and ragment ions are separated according to their mass/charge (m/z) ratio in a variable magnetic field to focus the particles in sequence of m/z on a detector. The vast majority of the gaseous ions are slightly charged, thus the mass-charge ratio of those ions is equal to the mass of the ions.

The mass spectrometer is designed to perform three basic functions: to vaporise compounds of widely varying volatility; to produce ions from the resulting gas-phase molecules; and to separate ions according to their m/z ratios, and subsequently detect and record them. There are many methods commonly used to produce ions from thermally volatile materials such as electron impact (EI) [142].

3.3.5 Optical microscopy

For many years, the optical microscope has proved extremely useful in studies of the optical texture, using polarised light, i.e., in the anisotropic structural components in carbons and cokes.

The size of these anisotropic structural components, when viewed in polished section, varies from less than 1μm to over 300 μm. The size and shape of these components constitute the optical texture. The mechanism of formation of these anisotropic components, large and small, from the fluid phase of carbonisation is via the nematic liquid crystal and mesophase.

When a polished section of an anisotropic carbon is viewed in plane polarised light, with the polariser and the analyser crossed, then patterns of extinction contours are to be seen. Using a rotating stage it is possible to map out how the stacking of the structural planes, i.e., the lamelliform structure, varies within the material.

A related technique, which employs a retarder plate in the optical system, has been increasingly used. This technique allows an assessment of the orientation of the lamelliform structures at the surface because different orientations have different colours, e.g. yellow, blue, and various purples. It has been found that a purple coloration originates at a surface of isotropic carbon or when basal planes are parallel to the polished surface, this coloration being unchanged by rotation of the specimen stage of the microscope. Yellow and blue colours are seen when a prismatic edge is presented at the surface. A rotation of the microscope specimen stage by 90° will change a yellow colour into a blue colour (through an intermediate purple [153].

3.3.6 Scanning electron microscopy (SEM)

Examination of carbons by electron microscopy presents excellent opportunities for the structural study, and to discover the problems in specimen preparation and interpretation of the images produced.

Scanning electron microscopy (SEM) is established as a means of surface topography, mainly because of the large depth of focus available and the high magnifications currently possible (up to X 200.000).

SEM uses the scattering of electrons from the surface of the sample to reveal the topography of material. It also utilises the scattering power of different materials to distinguish them.

SEM is an excellent method for monitoring the morphological changes occurring during carbonisation, graphitisation, gasification, etc. [154].

3.4 Supercritical Fluid Extraction

Soxhlet extraction is one of the oldest and most commonly used extraction techniques. It has several disadvantages such as being time consuming, non-

selective, toxic, and consuming large amounts of solvents. Supercritical fluid extraction (SFE) is becoming an increasingly important tool in analytical science [155]. SFE is a separation technique that uses the large changes in solvent strength a compressed fluid can exhibit near its critical point [156].

SFE has several advantages over classical extraction techniques owing to the three basic characteristics of supercritical fluids (density, temperature, and composition) the proper adjustment of which enables the extraction power to be finely turned [155]. These advantages include more rapid extraction rate, the possibility of more efficient extractions, increased selectivity, and possible analyte fractionation during extraction [157]. Besides these advantages SFE uses compounds such as carbon dioxide (CO_2) and/or water without consumption of any harmful or restricted compounds. CO_2 has added some advantages in that it is non-flammable, non-toxic, has no associated disposal problems and is extremely low cost. SFE has been investigated as an approach to extracting selected components from bulk samples as a process engineering tool [158].

SFE is influenced by three inter-related factors; solubility, diffusion, and matrix effects. Firstly, solute must be sufficiently soluble in the supercritical fluid for a successful extraction. This factor is particularly important during the initial stages where extraction occurs at a higher rate. Secondly, the solute must be transferred rapidly by "diffusion" from the interior of the matrix in which it is contained. The diffusion process may be normal diffusion of the solute or it may involve diffusion of the fluid into the matrix and perhaps subsequent replacement of the solute by solvent molecules on surface sites. The final factor is that of the matrix. Matrix effects mean that, although in many cases SFE will extract all of a particular compound in a sample, in some cases not all of the compound is extractable; the rest is locked into the structure of the matrix or too strongly bound to its surface [159].

Supercritical Fluids:

Over the last 10-15 years, essential studies have been conducted in a wide variety of areas using supercritical fluids (SF) which offer a convenient way to achieve solvating properties without actually changing structure. By proper control of pressure and temperature, we can access a significant range of physicochemical

properties (density, diffusivity, dielectric constant, etc.) without ever passing through a phase boundary, changing from gas to liquid form. Therefore, SF can be considered as a continuously adjustable solvent [160].

A pure supercritical fluid is a substance above its critical temperature and pressure. At the critical temperature it does not condense or evaporate to form a liquid or a gas, but is a fluid with properties changing continuously from gas-like to liquid-like as the pressure increases. Figure 3.4 shows the phase diagram of a single substance [160].

At the critical point, C_P, the densities of the two phases become identical and the distinction between the gas and liquid is lost and the material becomes a supercritical fluid. The critical point is characterised by its two co-ordinates on the diagram, the critical temperature, T_C, and critical pressure, P_C [160].

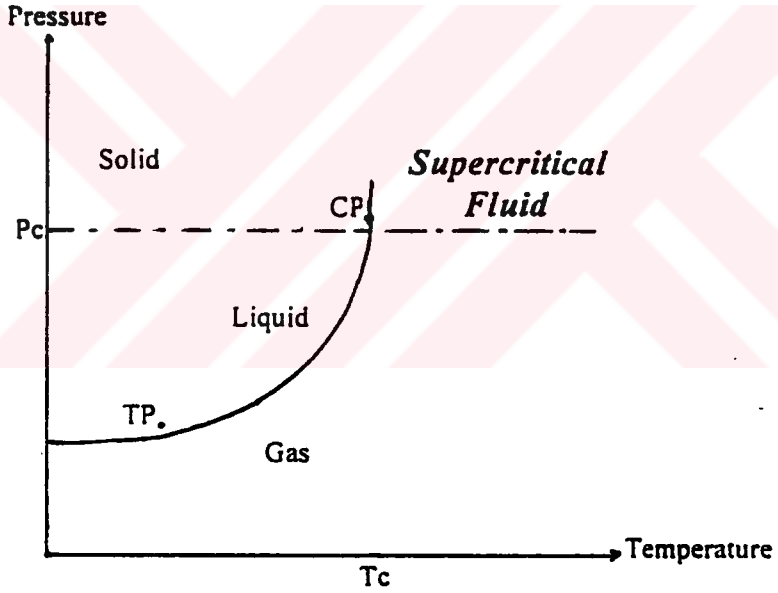

Figure 3.4. Schematic phase diagram of a single substance [160].

SFs have lower viscosities and higher solute diffusivities that liquid solvent, which improves mass transfer, and reduces the extraction time needed. The most widely used SF is carbon dioxide, as it meets most of these criteria and has critical temperature and pressure of 31 °C and 73 atm, respectively [158].

One of the primary advantages of supercritical fluid extraction is that the fluid density can be varied continuously from liquid-like to gas like densities by either

varying the temperature or pressure [156,161]. At 80 atm and 30 °C, the solubility of naphthalene is about 2.4wt%. At 80 atm and 40 °C, the solubility decreases by an order of magnitude to less than 0.3wt%. Alternatively, if the temperature is held constant at about 35 °C, a comparable solubility decrease occurs as the pressure is decreased from 90 to 72 atm [162].

This effect of solvent density on solubility can be used to separate mixtures of homologous compounds with a range of molecular weights. As the density is decreased, the compounds precipitate in the order of decreasing molecular weight.

SFE has been used successfully on an industrial scale in several separation processes. The success of these processes clearly demonstrates the capability of supercritical fluids to fractionate high molecular weight mixtures. To successfully fractionate petroleum pitch by this technique, all the desirable constituents must be dissolved in supercritical fluid solvent [156]. The above processes and the other data for the solubility of heavy hydrocarbons in supercritical fluid solvents indicate that aromatic solvents with relatively high critical temperatures are required to dissolve the pitch. Hutchenson et.al [156] and Bolanos et.al [163] have chosen toluene (T_C= 319 °C) as the solvent in their research.

4. EXPERIMENTAL

4.1 Samples

The sample of Göynük oil shale was collected from excavated open-cast seams in Göynük, which is situated near Bolu. Göynük is the largest reserve in Turkey with an estimated 697 million tonnes.

The asphaltite samples used in this study were originated from a mine located in Avgamasya vein near Sirnak in the Siirt province.

Before the experiments, the bulk samples were crushed, ground, and screened to size distribution of -150μm + 300μm particle size and then, stored in sealed containers to retard oxidation.

The proximate and ultimate analyses of Göynük oil shale (GOS) and Avgamasya asphaltite (AA) are given in Table 4.1 and 4.2, respectively.

Table 4.1. Proximate and ultimate analyses of Göynük oil shale (db)..

Ultimate analyses		Proximate analyses	
Component	(wt%)	Component	(wt%)
C	55.96	Moisture	10.13
H	6.73	Ash	15.48
N	1.20	Volatile matter	61.52
S	1.50	Fixed carbon	12.87

db: dry basis.

Table 4.2. Proximate and ultimate analyses of Avgamasya asphaltite.

Ultimate analyses		Proximate analyses	
Component	(wt%)	Component	(wt%)
C	42.14	Moisture	1.12
H	3.50	Ash	47.42
N	0.76	Volatile matter	39.50
S	6.76	Fixed carbon	11.96

4.2 Preparation of Tar

In order to produce tar material, Göynük oil shale and Avgamasya asphaltite were mixed in some ratios. Table 4.3 gives the notation of all tar materials produced from various GOS and AA mixtures.

Table 4.3. Notation for produced tar materials.

Notation	Tar material (wt%)
S	100% GOS
S7A3	70% GOS + 30% AA
S5A5	50% GOS + 50% AA
S3A7	30% GOS + 70% AA
A	100% AA

Tar materials were produced by pyrolysis and co-pyrolysis of Göynük oil shale and Avgamasya asphaltite in a stainless steel fixed bed retort under the flow of nitrogen. Figure 4.1 gives a schematic representation of the pyrolysis unit.

The pyrolysis temperature was controlled using a temperature controller connected to a thermocouple inside the retort and the liquid traps were cooled by dry ice. An amount of 150g of sample was used in all experimental runs. The retort was heated at 5 °C/min to 550 °C. 30 minutes of holding soak time was used for each experiment.

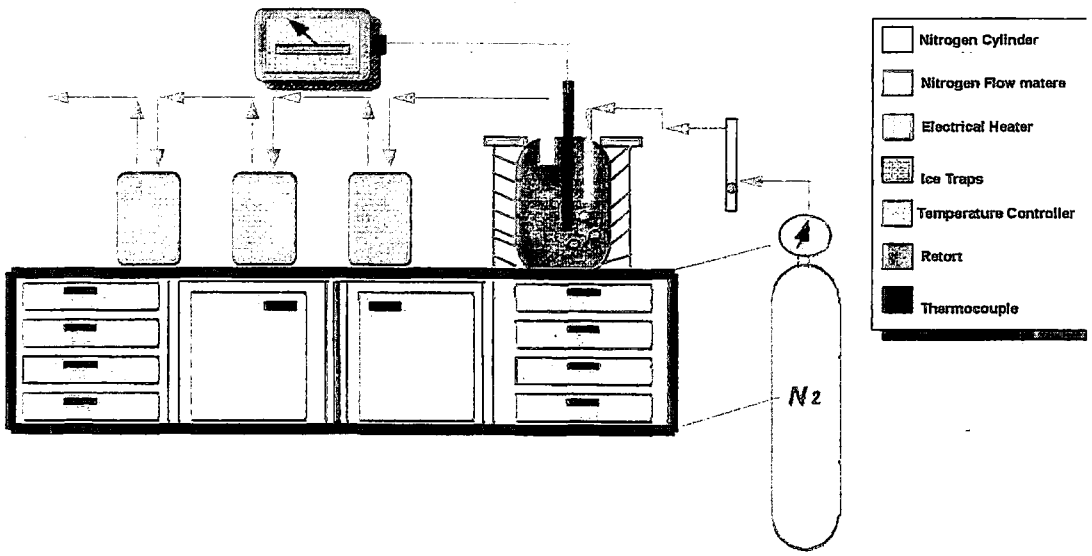

Figure 4.1. Schematic representation of pyrolysis unit.

4.3. Pitch Preparation

To get desirable carbon materials, one may modify the molecular structure and molecular aggregation state of pitch by various methods [164].

Pitches were prepared by four different methods. In the first method, selected tars were air-blown. In the second method, selected tars were heat-treated under the nitrogen atmosphere. In the third method, all tars were vacuum-distilled. In the last method, one of the pitches obtained by vacuum distillation was furthermore subjected to solvent extraction. Figure 4.2 shows the flow chart of the preparation of pitches from Göynük oil shale and Avgamasya asphaltite.

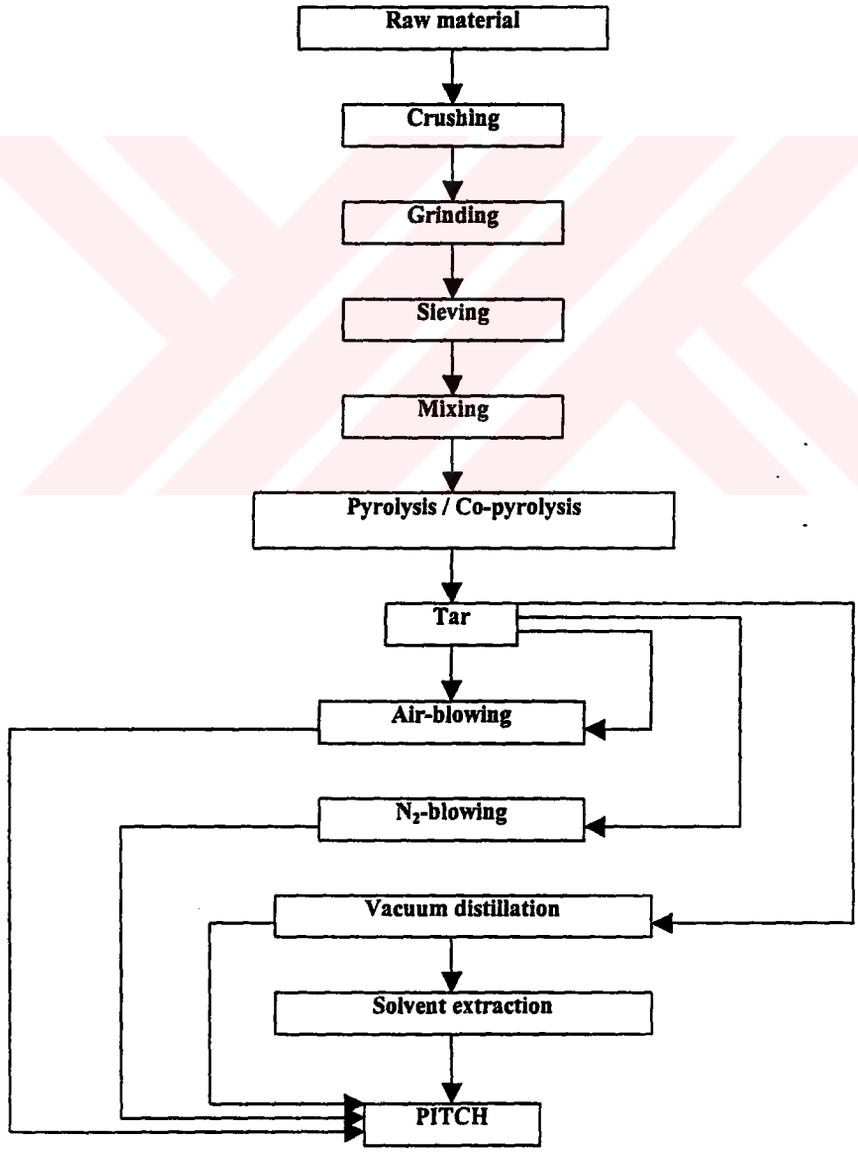

Figure 4.2. Flow chart of pitch preparation.

4.3.1. Production of pitch by air-blowing

Air-blowing reaction is an effective method to elevate the softening point of pitches and to give pitches in isotropic molecular aggregation state. In the air-blowing reaction, heat (or temperature), air (or oxygen), and distillation (or low pressure) are important factors to determine chemical and physical properties of the pitch [164].

The oxidation treatment was conducted by heating the tars in a stainless steel reactor, which has an inner diameter of 3.5 cm and a length of 30 cm. 50g of tar samples were subjected to air-blowing at 250 °C, and 270 °C, respectively, in a vertical electric furnace for 60, 90, and 240 minutes. A thermocouple was directly immersed into the liquid pitch for exact measurement of pitch temperature. Stirring was maintained at 260 rpm for all the experiments.

The rate of heating was carried out at 5 °C/min until the desired temperature was achieved and then was maintained at the various soak time. The blown air was introduced into the bed of pitch at room temperature at calibrated flow rate of 1 l/min.

Figure 4.3 shows the schematic representation of air-blowing unit used for the preparation of air-blown pitches.

4.3.2 Production of pitch by N_2 – blowing

In this study, selected tars were blown under a nitrogen flow of 1l/min in the stainless steel reactor, which was also used for air-blowing reactions. The N_2-blowing experiments were carried out at 250 and 300°C, respectively, at varying time. Stirring was maintained at 260 rpm for all the experiments. Figure 4.3 shows a schematic set up of the N_2-blowing (air-blowing) system used.

The N_2-blowing experiments were conducted for 60, 120, 240, and 480 minutes. The rate of heating was carried out at 5°C/min until the desired temperature was achieved and then was maintained at the various soak time given above.

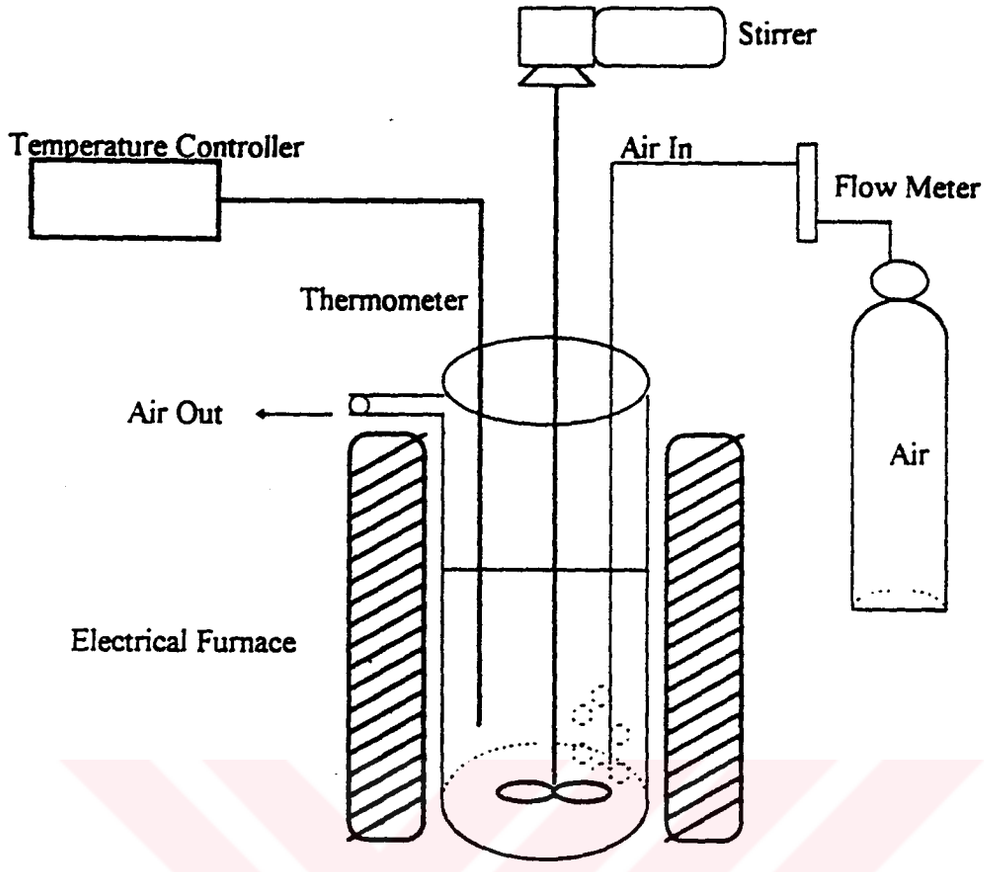

Figure 4.3. Schematic set up of air-blowing / N_2-blowing unit.

4.3.3 Production of pitch by vacuum distillation

All tars were vacuum-distilled under 3 torr and at 300°C for 60 minutes in order to obtain the pitch precursors. Figure 4.4 gives a schematic representation of the vacuum distillation unit. Yields were calculated by using the initial weight of the tar and the weight of the pitch remaining in the flask after distillation.

4.3.4 Production of pitch by solvent extraction

Diefendorf and Riggs used solvent extraction of petroleum pitch at ambient temperature to remove the lower molecular species and to concentrate the higher molecular species ("heavies") in the insoluble fraction [165].

S7A3-V1 pitch, which was prepared by vacuum distillation, was selected to be extracted with hexane as the pitch yield of S7A3-V1 pitch was the highest (20.5%) among the other vacuum-distilled pitches. 30g of S7A3-V1 pitch was heated with 1l. hexane at its boiling point (69°C) and at atmospheric pressure in 2 l. flask for 7

hours. The yield of the solvent-free extract was 14.5% on original basis. The solvent was removed from the extract by rotary evaporation, and then the extract was further placed in a vacuum oven to ensure complete removal of traces of the solvent. Table 4.4 gives the notation of all the pitches produced by various methods.

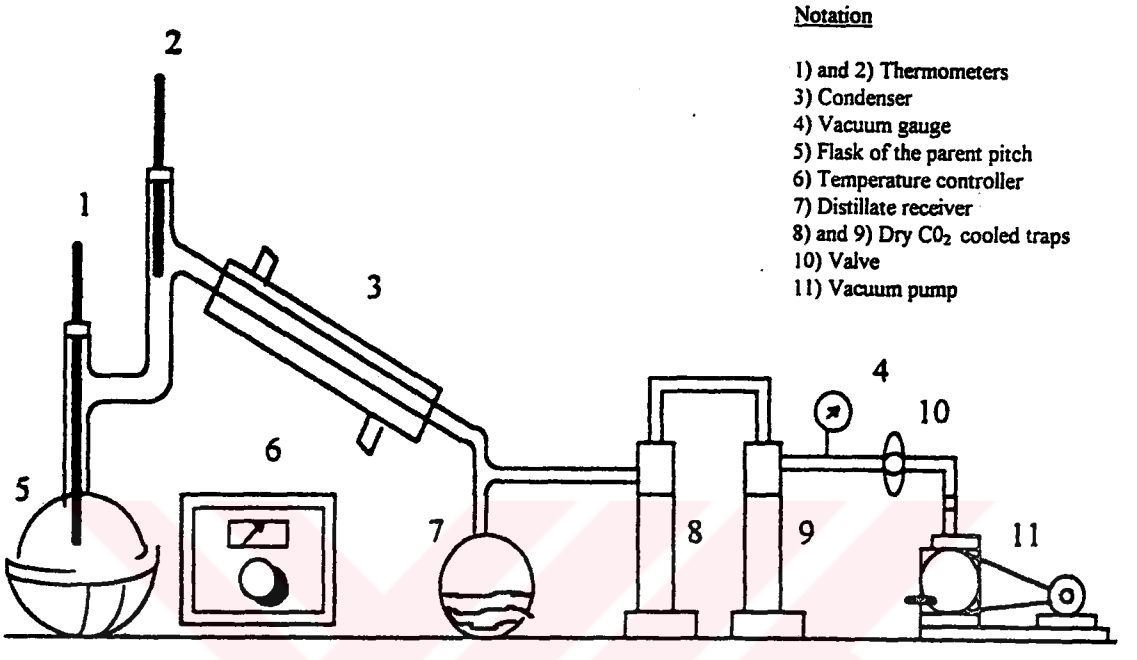

Figure 4.4. Schematic representation of vacuum distillation unit.

4.4 Sample Analysis and Characterisation

The structural characterisation of the parent tars, and pitches and the chemical changes occurred due to different processing were studied by elemental analysis, thermogravimetric analysis (TGA), dynamic differential scanning calorimetry (DDSC), softening point (SP) measurement, size exclusion chromatography (SEC), supercritical fluid extraction (SFE), mass spectrometry (MS), optical microscopy, scanning electron microscopy (SEM), Fourier transform infrared spectroscopy (FTIR), ^{1}H and ^{13}C NMR.

4.4.1 Elemental analysis

The parent tar and pitches were analysed for carbon, hydrogen, nitrogen, and sulphur with a Carlo-Erba Model 1106 elemental analyser using a standard ASTM procedure.

Table 4.4. Notation for the derived pitches.

S-A1	Air-blowing residual product of S at 250°C for 60 minutes
S-A2	Air-blowing residual product of S at 270°C for 90 minutes
S7A3-A1	Air-blowing residual product of S7A3 at 270°C for 60 minutes
S7A3-A2	Air-blowing residual product of S7A3 at 270°C for 90 minutes
S5A5-A1	Air-blowing residual product of S5A5 at 250°C for 60 minutes
S5A5-A2	Air-blowing residual product of S5A5 at 250°C for 90 minutes
S5A5-A3	Air-blowing residual product of S5A5 at 250°C for 240 minutes
S5A5-A4	Air-blowing residual product of S5A5 at 270°C for 90 minutes
S3A7-A1	Air-blowing residual product of S3A7 at 270°C for 90 minutes
A-A1	Air-blowing residual product of A at 250°C for 60 minutes
S5A5-N1	N_2-blowing residual product of S5A5 at 250°C for 60 minutes
S5A5-N2	N_2-blowing residual product of S5A5 at 250°C for 120 minutes
S5A5-N3	N_2-blowing residual product of S5A5 at 250°C for 240 minutes
S5A5-N4	N_2-blowing residual product of S5A5 at 250°C for 480 minutes
S5A5-N5	N_2-blowing residual product of S5A5 at 300°C for 60 minutes
S-V1	Vacuum distillation residual product of S at 300°C for 60 minutes
S7A3-V1	Vacuum distillation residual product of S7A3 at 300°C for 60 minutes
S5A5-V1	Vacuum distillation residual product of S5A5 at 300°C for 60 minutes
S3A7-V1	Vacuum distillation residual product of S3A7 at 300°C for 60 minutes
S7A3-E1	Solvent extraction residual product of S7A3-V1

4.4.2 Thermogravimetric analysis

The thermal analysis technique of thermogravimetry (TG) is one where the change in sample mass is recorded as a function of temperature. The resulting mass-change versus temperature curve provides information concerning the thermal stability and composition of the initial sample and the resultant product.

In order to get knowledge of the chemical composition of the selected pitches, pitches were characterised by thermogravimetric analysis. TGA measurements were conducted in a Perkin-Elmer thermoanalyser. The pyrolysis experiments were carried out under nitrogen at flow rate of 200 ml/min using heating rate of 2°C/min over the 20-1000°C temperature interval. The system used allowed continuous measurement of sample weight as a function of temperature, and electronic differentiation of the weight signal gave the rate of weight loss.

Coking yield and the H/C ratio

The coking yield is the %weight of carbon char remaining after the pyrolysis of a sample of carbon containing material [166].

The coking yield was calculated from the data which was obtained by TGA. The following formula gave the coke yield:

Coke yield (%) = (Residual weight at 1000°C / Starting pitch weight) * 100 (4.1)

The H/C ratio of pitches was measured by the elemental analysis.

4.4.3 Glass transition temperature measurement by DDSC

The glass transition temperatures of the selected pitches were measured with Dynamic Differential Scanning Calorimetry (DDSC).

A UNIX operated Perkin - Elmer DSC 7 Differential Scanning Calorimeter used in this study was equipped with the DSC operating in the dynamic mode, called the Dynamic Differential Scanning Calorimetry (DDSC).

The DSC 7 is a computer controlled scanning enthalpic instrument using the power compensating "null balance" DSC principle. This consists of twin microcalorimeters kept in a stable environment. Each calorimeter contains a temperature sensor, a heater and a holder for the sample and reference materials. The energy absorbed or evolved by the sample is compensated by adding or subtracting an equivalent amount of electrical energy to a heater located in the sample holder. Thus, the sample and reference calorimeters are each maintained at approximately the same programmed temperature by electrical power. The difference in power supplied to the two platinum resistance heaters measures the rate of energy change in the sample. The platinum resistance heaters and platinum resistance thermometers are used in the DSC 7 to accomplish the temperature and energy measurements in the design. The continuous and automatic adjustment of heater power (energy per unit time) necessary to keep the sample holder temperature identical to that of the reference holder provides a varying electrical signal equivalent to the varying thermal behaviour of the sample. The measurement is made directly in differential power units (milliwatts), providing true electrical energy measurement of peak areas.

2-10 mg of the samples were encapsulated in standard crimped aluminium pans and placed in the sample holder in the DSC 7. An empty closed aluminium reference pan of the same type as the sample pan was placed in the reference holder. During the

experiment the sample area was purged with nitrogen gas. Prior to DDSC experiment on a pitch sample, a baseline experiment was carried out, where a DDSC run is carried out with a closed empty pan in both the sample holder and reference holder. This needs to be carried out using the same conditions and for the same temperature range as will be used on the sample. This baseline curve is used to take account of the heat flow curve that is achieved when there is no sample present. This baseline can then be added to the run procedure during a DDSC experiment on a sample to give a true heat flow curve.

Since the primary purpose of using the DDSC mode was for the determination of T_g, the heat-cool repeat program was used. The repeat program was to heat a rate of 10°C/min to increase the temperature by 5°C, then to decrease the temperature at a rate of 10°C/min by a step of 5°C. This procedure was carried out for each baseline and each pitch sample.

4.4.4 Softening point measurement

The standard methods such as the ball-and-ring method, cube-and-air method, Kraemer Sarnow method, and Mettler softening point and hot stage microscopy are used to determine the softening point temperatures. But the temperatures measured by these methods vary somewhat from each other.

In this study, the softening point of pitches was determined by a simple technique. ~1g pitch sample was put on a copper disc, which has 5 cm diameter and 1 cm height. The disc was placed on a hot plate. In order to measure the temperature during heating, a thermocouple was inserted to the hole on the disc, and the thermocouple was connected to a temperature controller. In order to prevent oxidation, a glass funnel was placed above the disc, and the funnel was connected to a N_2 cylinder. The heating of the pitch samples was carried out under the nitrogen flow at a flow rate of 200ml.min^{-1}. The softening temperature was reported as the temperature at which the pitch samples began to soften. Figure 4.5 shows the schematic simple apparatus.

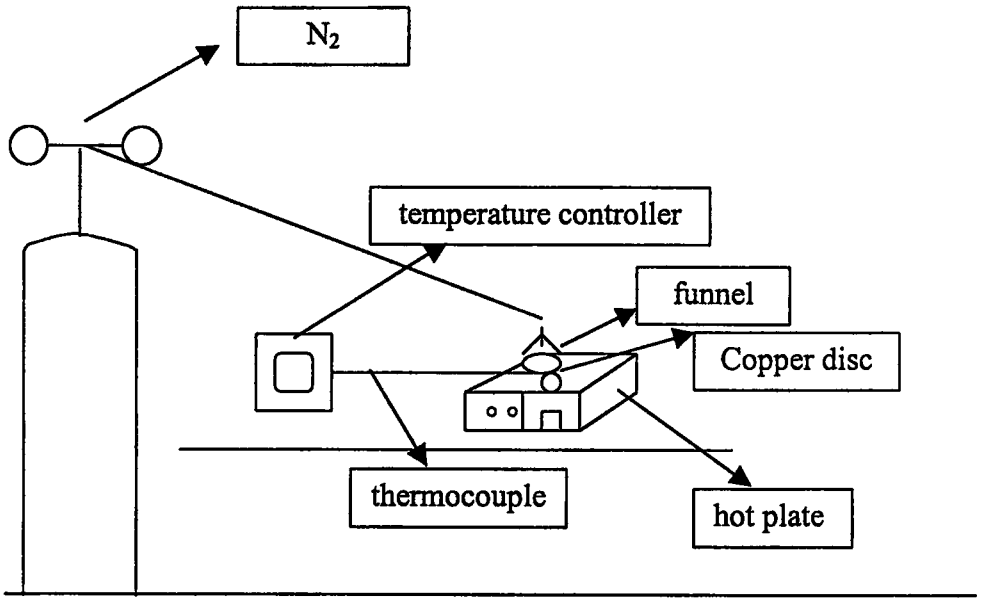

Figure 4.5. The apparatus used for the measurement of the softening point.

4.4.5 Size exclusion chromatography

All size exclusion chromatography (SEC) analysis was performed on a Polymer Labs Mixed E Bed Column (polyvinylbenzene co-polymer packing) with an attached guard column, with 1-methly-2-pyrrolidinone (NMP) pumped at 0.5ml.min^{-1} (Merck Hitachi L6000A Pump). UV absorption at 298 nm (Severn Analytical SA6504 Programmable UV-Absorption Detector) and Refractive index detection (ERMA ERC-7520 Type RI Detector) provided the detection of the samples. The system was operated at 80°C to facilitate pumping of the viscous solvent, to increase the sample solubility and to remove any column-solute interactions which may destroy the size exclusion separation mechanism. The pump pressure was maintained at 108 bar. The signals from the detector were sent to a PC with data capture unit and a custom mode data capture program. The SEC system is shown in Figure 4.6.

2g of each selected pitch was dissolved in 200ml of tetrahydrofuran (THF). In order to create a matrix, 50g of silica sand, which was washed with hexane and then dried at 110°C, was added to that pitch-THF solution. The flask was left in ultrasonic bath to let the dissolved pitch material to be adsorbed on the silica sand. After adsorbing, the THF was evaporated using rotary evaporator above its boiling point (65°C).

2 g of matrix material was extracted for 3 hours using 150 ml of hexane. The extract was dissolved in the eluent (NMP). The residue was extracted with NMP in ultrasonic bath for 2 hours.

Both extracts and residues were injected into the column (Rheodyne 7125 valve, 20µl sample loops) with care being taken not to overload the column.

The calibration curve of the SEC at 80°C based on polystyrene is given in Figure 4.7.

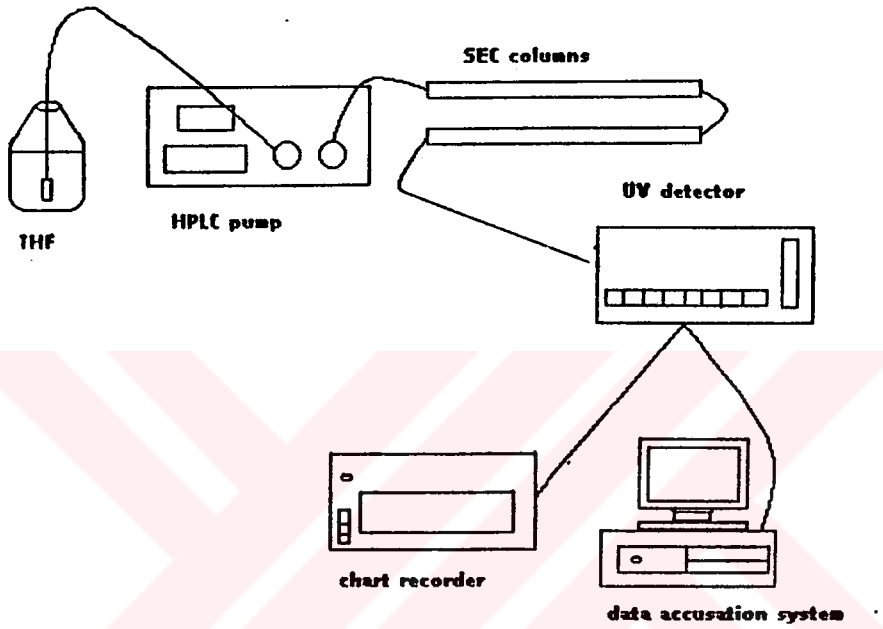

Figure 4.6 Diagram of size exclusion chromatography (SEC) equipment.

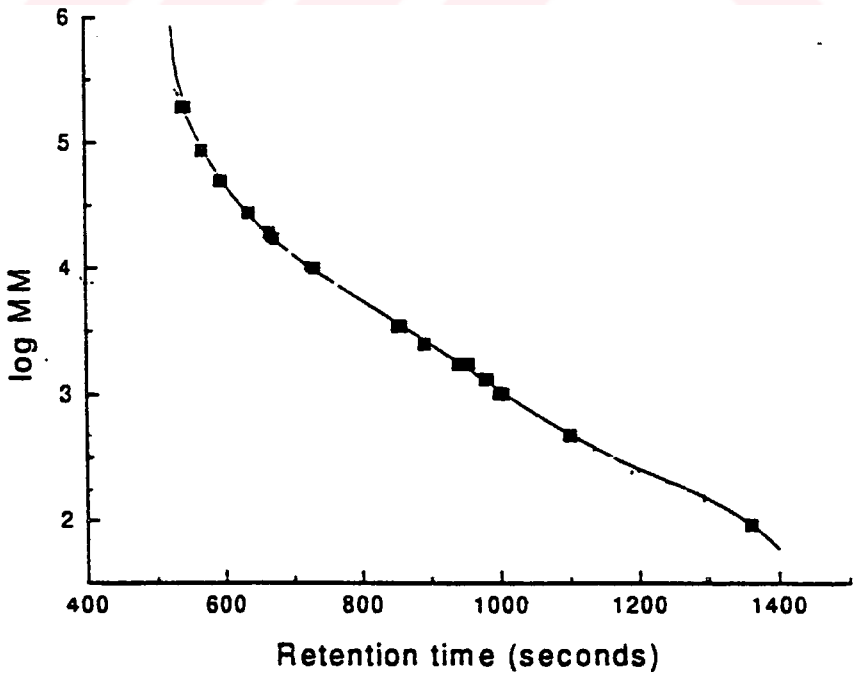

Figure 4.7 Calibration curve of SEC in NMP using polystyrene standards, 80°C.

4.4.6 Mass spectroscopy

Fast Atom Bombardment – Mass Spectrometer (FAB-MS) was used to see the average molecular weights of the selected pitch samples and their SFE extracts and residues using a VG Autospec (Fisons) Mass Spectrometer. The impact of a primary beam of fast ions [Caesium (Cs^+) ions pellet was used] on a target matrix (substrate and solvent) causes desorption of molecular or quasimolecular ions characteristic of the substrate. The process is called FAB for atom bombardment. Molecular masses up to 2000 are fairly routine; above this value, the efficiency of the process drops off but is still useful up to about 30-30,000 [167].

4.4.7 Infrared spectroscopy

Fourier transform infrared spectroscopy was used to provide information about functional groups in the pitch precursors. Infrared spectra of tars and pitch precursors were obtained with a NICOLET AVATAR 360 FTIR spectrophotometer. The solid pitch samples were prepared for FTIR analysis by the traditional procedure. For this type of materials, standard potassium bromide pellets were prepared. The pitch : KBr ratio was 1:100. The mixture was pressed into a disc using a hydraulic press. The paste-like pitch precursors were transferred to the NaCl windows and the NaCl windows were squeezed together to adjust the thickness of the sample. Sample thickness should be adjusted so that the strongest bands display between 60 and 80% absorption. After adjusting the sample thickness these two transmitting windows were mounted in the spectrometer in a suitable holder. Plates need to have high polish, but must be flat to avoid distortion of the spectrum.

4.4.8 ^1H and ^{13}C NMR spectroscopy

S-A2, S5A5-A4, S5A5-N5, S7A3-V1, and S7A3-E1 pitches have been examined by ^1H and ^{13}C NMR spectrometry. From the resulting spectra, a series of structural parameters has been derived, which allow the pitch precursors to be characterised and compared. The ^1H and ^{13}C NMR spectra were recorded on a Bruker ARX250, 250 MHz instrument. Samples were dissolved in deuterochloroform to give approximately 25wt% solutions; these were run in 5mm o.d. tubes. To obtain quantitative ^{13}C NMR data, a paramagnetic relaxation agent, chromium

acetonylacetonate, $Cr(acac)_3$, was added to the deuterochloroform solution to give 0.1 M solution. The proton decoupler was gated.

Thirty degree pulses (6.5 μs for ^{13}C and 9 μs for ^{1}H) were used. The delay between individual pulses was 5 seconds. 62 MHz observation frequency was used. The scans were 8192 and 128 for ^{13}C and ^{1}H, respectively.

4.4.9 The carbonisation of pitches and observation of optical texture of cokes

S5A5-A4, S5A5-N3, S5A5-V1, S7A3-V1, and S7A3-E1 pitches were selected as samples of typical types of pitches in order to determine the optical structures of cokes.

The pitches were carbonised in a Carbolite horizontal electrical tube furnace. All carbonisation runs were carried out in nitrogen atmosphere. Specimens were heated with the heating rate of 2°C/min from room temperature to 1000°C and were maintained for 2 hours at the final temperature. The heated materials were allowed to cool to room temperature before examination. All carbons formed were mounted in epoxy resin, polished and examined optically. Microscopic observation was done with a NIKON OPTIPHOT microscope using cross- polarised light (1λ plate).

4.5 Melt Spinning

The isotropic pitch S7A3-E1 was spun through a single hole spinneret with a nozzle diameter of 100μ and a length of 200μ. The pitch was spun at 155°C, under the flow of nitrogen. The spinning speed was low, around 60m/min. Ambient air quenched the fibre as it is extruded from the nozzle and the quenched fibre was wound on the fibre wind-up device. Figure 4.8 shows the apparatus for melt spinning used in this study.

4.6 Stabilisation

The green fibre S7A3-E1 was prepared by melt-spinning. The bundles of the green pitch fibres were chopped ~50mm and were stabilised by nitric acid. Three different strengths of acid were used; concentrated nitric acid, a mixture of 2 parts concentrated nitric acid to 1 part water, and a mixture of 1 part concentrated acid to 9

parts of water. The green fibres were stabilised in concentrated nitric acid for 1 minute, in 2 parts nitric acid to 1 part water for 10 minutes, and for 30 minutes, and in 1 part nitric acid to 9 parts water for 5 minutes. To ensure that all the fibres came into contact with the acid the fibres were dipped carefully into the solution without breaking.

After stabilisation the fibres were filtered and then washed with distilled water. With all concentrations of acid used the flask became hot indicating an exothermic reaction. The reaction with the concentrated acid was more vigorous.

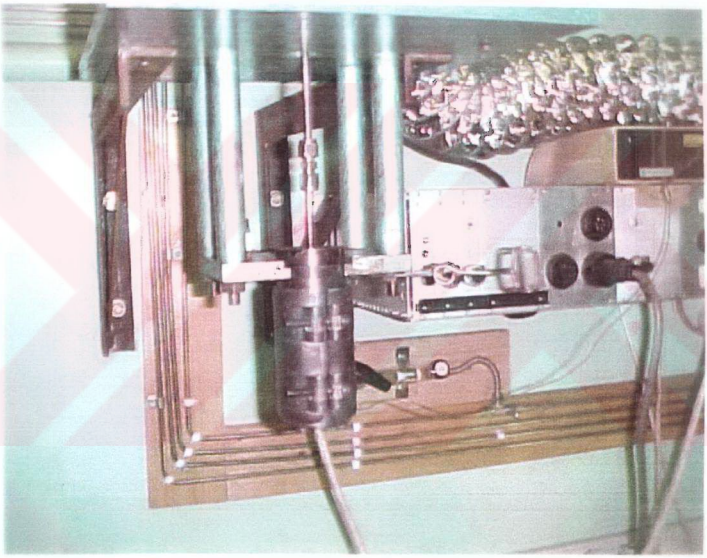

Figure 4.8. The picture of the melt-spinning unit.

4.7 Carbonisation

The stabilised pitch fibres were heated to 100°C at a rate of 2°C/min and then heated to 110°C with 0.1°C/min and was exposured to 110°C for one hour. After waiting for one hour the fibres were heated to 120°C at a rate of 0.1°C/min and held at that temperature for an hour. They were heated from 120°C to 130°C with 0.1°C/min and

from 130°C to 150°C with 0.5°C/min, from 150°C to 200°C with 1°C/min and finally, from 200°C to 300°C with 1°C/min. And each case, the fibres were exposured at the related temperature for one hour to a current of air.

The above process has been designated as the pre-treatment. When this pre-treatment was completed, the filaments were then continuously heated at the rate of 10°C/min under the nitrogen up to the final carbonisation temperature 1000°C and held at that temperature for one hour.

4.8 Scanning Electron Microscopy

The fibre diameter and structure were examined using CAMSCAN Series 4 SEM. A bundle of fibres (approximately 8 mm) was mounted on an aluminium stud with conductive carbon cement. Once set, they were gold coated to prevent build-up of electrostatic charge and to improve resolution under the SEM.

4.9 Supercritical Fluid Extraction of Pitch Materials

Supercritical fluid extraction was performed with an ISCO Model 260D syringe pump (Figure 4.9) delivering pressurised CO_2 to an extraction cell. The cell was

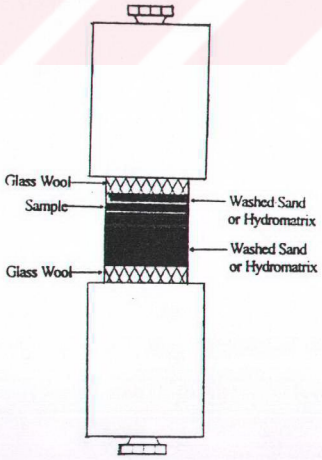

Figure 4.9. Schematic diagram of a packed extracting cell.

made of stainless steel tube (Figure 4.10) and kept in an oven. A restrictor (20 cm length, 50μm i.d. x 375μm o.d. fused silica capillary) was fitted to the extraction cell in order to maintain the pressure in the extraction cell. The end of the restrictor was immersed in collection solvent. The flow rate of the fluid (CO_2) was measured by the pump automatically.

An air-blown pitch (S-A2), a nitrogen-blown pitch (S5A5-N5), and vacuum-distilled and hexane-extracted pitch (S7A3-E1) were extracted using CO_2 and CO_2 modified with hexane at different temperatures and pressures.

For each extraction process, 1g of pitch precursor supported on 2g of pelletised diatomaceous earth hydromatrix directly in the 5ml extraction cell. Modifier was spiked onto the sample matrix mixer in the extraction cell. Extractions were performed at various temperatures (100, 150°C) and pressures (200, 400 atm). Extractions were carried out dynamically for 30 minutes. In order to investigate the efficiency of SFE, S-A2 pitch, which contains more amounts of light molecules, was extracted at 150 °C, 400 atm with CO_2 modified by hexane for 15 minutes. The extracts were trapped in vials containing 5-10ml of DCM (dichloromethane). DCM was chosen as a collecting solvent as it is suitable for trapping the analytes of interest

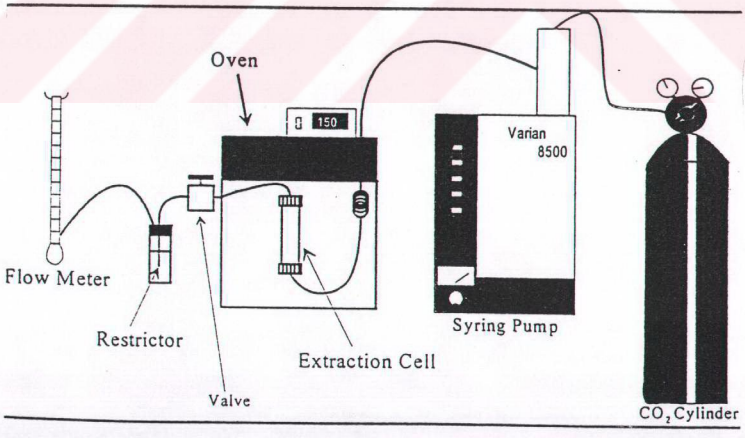

Figure 4.10. Diagram of supercritical fluid extraction equipment.

After the extraction had been carried out for the desired period, the pump was switched off and the pressure lowered in the system. When the system had cooled, the extraction cell was then taken out of the system. The residue was scraped out of the cell, carefully dried in an oven and weighed. The amount of the extracted materials were determined by evaporating DCM under a N_2 stream on a hot plate and weighing the extract obtained to determine the recovery. The remaining material was washed with toluene and then filtered in order to separate the residue and the matrix material. These pitches were also compared to a high softening point pitch, Aerocarb75.

5. RESULTS AND DISCUSSION

5.1 General Properties of the Co-Pyrolysis Products

Some properties of the tars, which were produced by the co-pyrolysis of Göynük oil shale (GOS) and Avgamasya asphaltite (AA), are compiled in Table 5.1. The asphaltite tar has lower C, H, and N content compared to the GOS tar, on the other hand, the sulphur and oxygen contents are higher for the AA. The carbon content of the tar decreased as the percentage of the GOS decreased in the raw mixture. As seen from Table 5.1, tar produced from GOS by pyrolysis was highly aliphatic in character (H/C=2.03). The lowest H/C atomic ratio was obtained for S5A5 tar suggesting that this tar is less aliphatic than the others are.

Table 5.1. Elemental analysis of the tars.

Sample	C (wt%)	H (wt%)	N (wt%)	S (wt%)	[a]O (wt%)	H/C
S	70.50	11.90	0.96	1.70	14.94	2.03
S7A3	64.71	9.60	0.67	2.30	22.72	1.78
S5A5	62.90	8.28	1.06	2.80	24.96	1.58
S3A7	61.13	9.46	1.13	3.30	24.98	1.85
A	69.76	9.38	0.30	4.60	15.96	1.61

[a]: by difference

The yield and the synergistic effect of the co-pyrolysis are given in Table 5.2. As seen from the table, there is a slight difference between the experimental yield and calculated yield, which means the synergistic effect in the yield was not very significant. The only noticeable indication is that as the percentage of the GOS decreases in the raw mixture, the yield decreases.

Table 5.2. Yield and synergistic effect of the co-pyrolysis.

Sample	Yield (wt%)	Calculated yield (wt%)
S	26.88	-
S7A3	24.34	22.58
S5A5	20.00	19.73
S3A7	17.50	16.86
A	12.57	-

5.2 General Properties of the Air-Blown Pitches

In order to optimise pitch utilisation several procedures (i.e., extensive removal of volatile fractions, and controlled condensation)have been developed to modify pitch properties to achieve the preceding requirements (e.g., high aromaticity, high softening point, spinnable) [168]. Thermal treatment (nitrogen-blowing) and air-blowing are the methods more extensively used [169].

The pitch precursors used for general-purpose carbon fibre are prepared by an air-blowing reaction on an industrial scale. The air-blowing reaction mechanism is complicated because of the contact with oxygen, the simultaneous effects of heat treatment, and distillation that is caused by a pressure drop in the system due to air-blowing [170]. In the air-blowing reaction, heat (or temperature), air (or oxygen), and distillation (or low pressure) are important factors to determine chemical and physical properties of pitch [164].

Pitch oxidation by air-blowing promises to be very effective. The main purpose of air-blowing is to produce pitches of high molecular weight, where the oxygen promotes the formation of cross-links between large adjacent aromatic molecules which suppresses the evaporation of the light fractions. Thus, the stacking of large aromatic molecules to form the liquid crystalline mesophase is greatly retarded. The amount of oxygen incorporated into the structure during air-blowing appears to be minimal, since it promotes dehydrogenative condensation of polyaromatic hydrocarbons (PAHs) with water being a product. Such treatments result in a viscosity increase and, simultaneously, the lamellar orientation of the aromatic molecules becomes more difficult to achieve [168,171,172].

Air-blowing promotes the condensation of molecular components of pitch resulting in an increase in the average molecular weight and consequently, an increase in pitch carbon yield. Air-blowing reaction is an effective method to increase the softening point of pitches and to give pitches in isotropic molecular aggregation state [169].

It must be noted that it is never easy to prepare such an isotropic pitch from coal tar by conventional methods such as distillation or heat treatment in an inert atmosphere, because mesophase spheres appear very easily by heating above a certain level of temperature. Air-blowing has been successfully applied in preparing precursors for isotropic carbon materials, and in raising the softening point of coal tar and petroleum feedstocks [173]. Additionally, this process has been shown to be suitable as it considerably increases the final price of the pitch. The direct application of specific treatments like air-blowing to parent tar, instead of the commercial pitch, would be simply the preparation procedure and consequently, would reduce the tailor specific pitch properties regarding to further applications [169].

Table 5.3 summarises the air-blowing conditions and some general properties of the resultant pitches. Air-blowing increased the softening point, contents of insoluble fractions, and decreased the atomic ratio of H/C according to the severity of the conditions. The yields of air-blown pitches decreased proportionally with the rise of the softening point. The higher air-blowing temperature for S5A5 pitch rapidly increased the softening point in shorter periods, giving a lower yield of the blown pitch. For example, 4h air-blowing at 250°C resulted in softening point around 45°C, giving a yield of 50.5%, while it took only 1.5h at 270°C to get a softening point of 130°C, giving a yield of 21.3%. However, air-blowing time had a significant influence on pitch yields for S5A5 pitch. The yields of S5A5 pitches decreased with the air-blowing time, as shown in Figure 5.1.

Table 5.3. Air blowing conditions and properties of the air blown pitches.

Air-blowing conditions			Properties									
Sample	AT (^{O}C)	t (min)	C (wt%)	H (wt%)	N (wt%)	S (wt%)	[a]O (wt%)	H/C	O/C	CY (wt%)	PY (wt%)	TI (wt%)	SP (^{O}C)
S-A1	250	60	87.05	9.70	1.10	2.10	0.05	1.34	0.04	ND	36.00	ND	45
S-A2	270	90	87.55	9.60	1.05	1.70	0.10	1.32	0.08	16.84	30.88	ND	110
S7A3-A1	270	60	85.30	9.00	0.55	2.55	2.60	1.27	2.28	ND	34.60	ND	45
S7A3-A2	270	90	86.05	9.60	0.90	2.30	1.15	1.34	1.00	15.24	34.36	ND	70
S5A5-A1	250	60	86.25	10.45	0.65	2.10	0.55	1.45	0.48	8.36	62.88	10.03	45
S5A5-A2	250	90	84.10	10.40	0.55	2.60	2.35	1.48	2.10	ND	56.28	9.00	60
S5A5-A3	250	240	85.80	9.45	0.55	3.05	1.15	1.32	1.01	15.00	50.48	10.32	45
S5A5-A4	270	90	85.65	8.65	0.75	3.10	1.85	1.21	1.62	19.80	21.28	21.96	130
S3A7-A1	270	90	84.80	9.85	1.35	4.00	0.00	1.39	0.00	ND	66.48	ND	35

AT: air-blowing temperature; [a]: by difference ; ND: not determined; CY: carbon yield; PY: pitch yield; TI: toluene insolubles; SP: softening point.

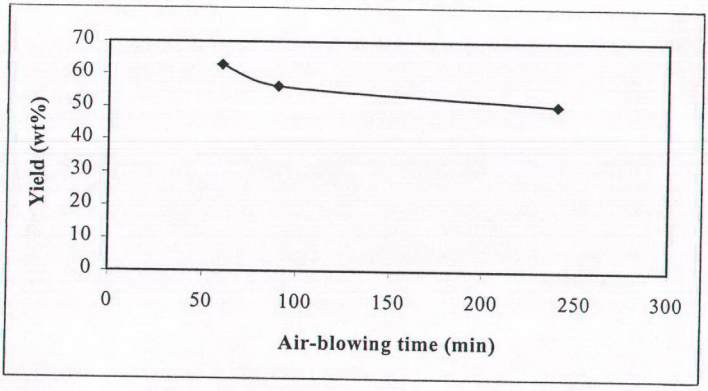

Figure 5.1. Relationship between pitch yield and air-blowing time for S5A5 pitches produced at 250°C.

Coking capacity of S5A5 pitches, as measured by the carbon yield (CY) obtained on pyrolysis at 1000°C, increased with air-blowing time and also air-blowing temperature.

Solubility tests in toluene show that the toluene-insoluble content of pitches increased as the H/C atomic ratio decreased in S5A5 pitch, as shown in Figure 5.2.

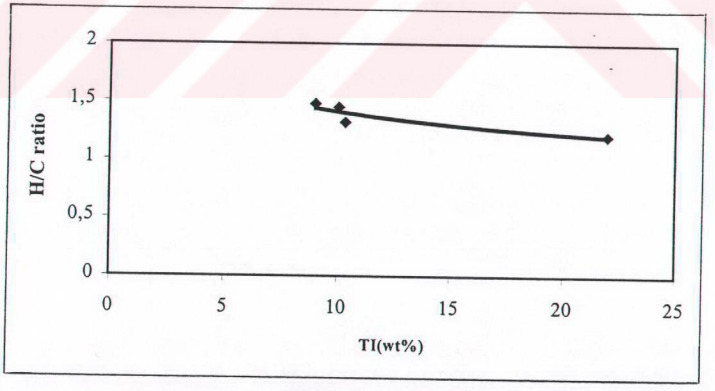

Figure 5.2. The variation of toluene-insoluble content with H/C ratio for S5A5 pitches.

Atomic H/C ratio decreased with air-blowing in all types of pitches with some variations, suggesting a dehydrogenative condensation of pitch content. It is generally known that the lower the H/C ratio, the greater the degree of ring condensation, regardless of the rings are aromatic or naphthenic in character. Air-blowing at higher temperatures accelerated the dehydrogenation. For example, 90 min air-blowing at 250°C resulted in H/C ratio of 1.48 while at 270°C gave a H/C atomic ratio of 1.21 for S5A5 pitch. Almugerhiy has obtained similar results for the pitches produced by air-blowing of Göynük oil shale. 45 min air-blowing at 295°C resulted in H/C ratio of 1.43 while at 325°C resulted in H/C ratio of 1.28 [174].

The H/C ratio of the resultant pitches shows a relationship with the H/C ratio of the tars produced by mixing GOS and AA (Figure 5.3). The S3A7 tar contains the highest H/C ratio (1.85%) while S5A5 tar contains the lowest ratio (1.58%), which means the former tar is the most aliphatic one. This result is consistent with the pitches produced at 270°C, 90 min since S3A7-A1 pitch showed the highest H/C ratio (1.39%) and S5A5-A4 pitch showed the lowest H/C ratio (1.21%). The high H/C ratio of S3A7-A1 pitch is consistent with its highly paraffinic nature. The difference in H/C ratios between the pitches exhibits that S5A5-A4 pitch is the most aromatic pitch since the decrease in H/C ratio is thought to be caused by an increase in aromaticity. This observation is in agreement with the evolution of toluene-insolubles and with FTIR measurements in S5A5-A4 pitch.

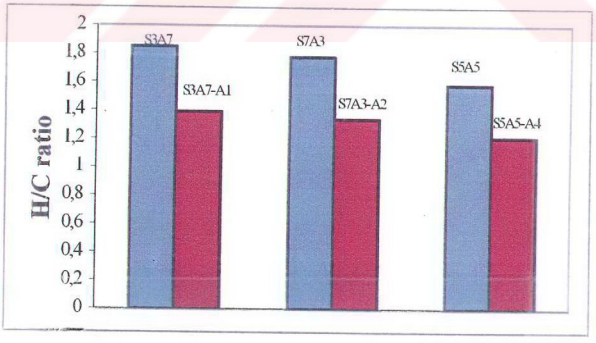

Figure 5.3. The variation of H/C ratio with tars and pitches.

A slight increase in sulphur content in the pitches observed with the air-blowing time and temperature. The increase in temperature resulted in insignificant increase in

nitrogen content in S5A5 pitches. The FTIR spectra of air-blown pitches (S-A2 and S5A5-A4) show a slight increase in the oxygen content compared to the tar material.

The results obtained showed good agreement with the mechanism proposed by Barr and Lewis [172]. As known from the literature, although oxygen substitution is a likely first step, the principal role of oxygen is to bring a dehdrogenative polymerisation like proposed by the chemical equation given below:

$$2ArH + ½\ O_2 \rightarrow Ar\text{-}Ar + H_2O \qquad (5.1)$$

Oxygen groups by oxidation of alkyl side-chains and naphthenic structures decompose to give Ar-Ar [168]. In addition to providing a site for oxygen attack, alkyl substituents can also activate the aromatic rings, thus facilitating the subsequent oxygen-induced hydrogenation [172].

5.3 General Properties of the Nitrogen-Blown Pitches

As previously mentioned in section 5.1, several methods are described to modify pitch composition in order to improve pitch properties as a precursor of high performance carbon materials. Thermal treatment is one of these methods which is more extensively used.

To distinguish the relation between the air-blowing and temperature, S5A5 parent tar was thermally treated under nitrogen at 250°C and 300°C at various periods. Table 5.4 summarises the nitrogen-blowing conditions and the main properties of the nitrogen-blown pitches. Nitrogen-blowing resulted in a decrease in the pitch yield, which was proportional with the raise of the softening point, as the treatment time increased. The longer nitrogen-blowing time (480min) at 250°C increased the softening point, giving a lower pitch yield of 15.2% which indicates a significant distillation during the nitrogen-blowing. However, the higher nitrogen-blowing temperature (300°C) rapidly increased the softening point in shorter periods (60min). Nitrogen-blowing temperature seemed to have a significant effect on the softening point rather than time . The nitrogen-blowing time had an obvious influence on the pitch yield. The pitch yield decreased from 44.2% to 15.2% for S5A5 derived pitches

at 250°C as the nitrogen-blowing time increased from 60 min to 480 min. The variation of pitch yield with nitrogen-blowing time is shown in Figure 5.4.

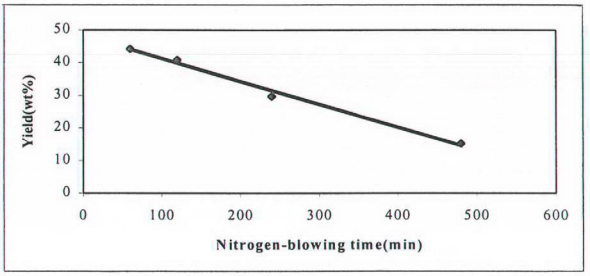

Figure 5.4. Relation between nitrogen-blowing time and pitch yield.

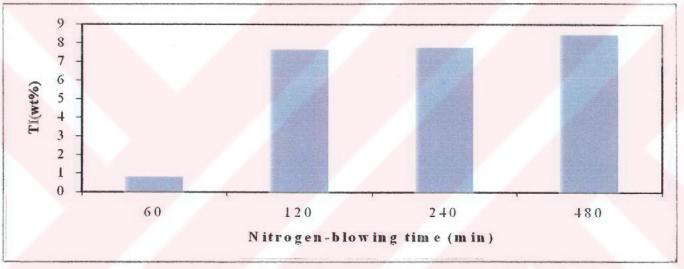

Figure 5.5. Relation between nitrogen-blowing time and toluene-insolubles.

Carbon yield of nitrogen-blown pitches increased in the same sense as the softening point. Variations in toluene insolubles (Figure 5.5) and carbon yields (Figure 5.6) showed that as treatment time increased, nitrogen-blowing produced only little increase in both of these parameters. The increase in TI contents and carbon yields became more important at 300°C for short nitrogen-blowing period (1h). It is to be noted that for S5A5-N1 and S5A5-N5 pitches an increase in temperature from 250 to 300°C produced a rise in CY, TI, and SP as 57.5%, 43.1%, and 160°C, respectively. Under the nitrogen atmosphere, the slight increases in CY and TI are mainly due to volatile release during treatment. Insoluble fractions of air-blown pitches are much greater than those of the nitrogen-blown pitches, which means that chemical reactions caused by air-blowing transform a considerable amount of TS.

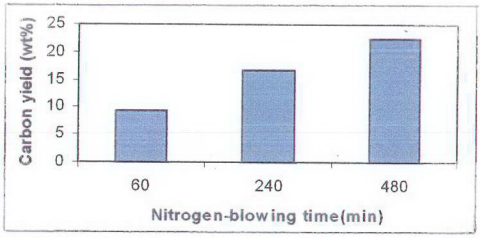

Figure 5.6. Relation between nitrogen-blowing time and carbon yield.

H/C atomic ratio of nitrogen-blown pitches exhibited a close relationship with TI content. Figure 5.7 illustrates the evolution of the H/C atomic ratio with toluene insolubles. A decrease in H/C ratio is thought to be caused by an increase in aromaticity and dehydrogenation. Nitrogen-blowing produces volatilisation of light fractions of the pitch and cracking of aliphatic and aromatic groups with a low degree of condensation [50].

Nitrogen and sulphur contents were increased a little amount with the increase in blowing time. There was a dramatic decrease in oxygen content in nitrogen-blown pitches compared to the parent tar as happened in the air-blown pitches. The decrease in oxygen content is supposed to be the distillation of light compounds having oxygen functional groups.

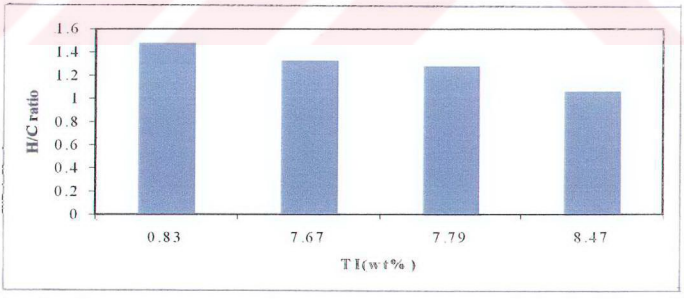

Figure 5.7. The variation of toluene-insoluble content with H/C ratio for S5A5 derived pitches prepared at 250°C.

Table 5.4. Nitrogen blowing conditions and properties of the nitrogen blown pitches.

N_2-blowing conditions			Properties									
Sample	NT (^{O}C)	t (min)	C (wt%)	H (wt%)	N (wt%)	S (wt%)	[a]O (wt%)	H/C	O/C	CY (wt%)	PY (wt%)	TI (wt%)	SP (^{O}C)
S5A5-N1	250	60	84.85	10.45	0.35	2.80	1.55	1.48	1.37	9.39	44.20	0.83	40
S5A5-N2	250	120	86.00	9.55	0.50	2.90	1.05	1.33	0.92	ND	40.80	7.67	40
S5A5-N3	250	240	86.05	9.25	0.35	2.90	1.45	1.28	1.26	16.70	29.71	7.79	45
S5A5-N4	250	480	87.50	8.65	0.55	3.05	0.25	1.06	0.21	22.50	15.22	8.47	120
S5A5-N5	300	60	86.45	7.10	1.25	3.30	1.90	0.98	1.65	57.45	16.69	43.05	160

NT: N_2-blowing temperature; [a]: by difference ; ND: not determined; CY: carbon yield; PY: pitch yield; TI: toluene insolubles; SP: softening point.

5.4 General Properties of the Vacuum-Distilled Pitches

Properties of pitches, prepared by vacuum distillation, were compared with those of air-blown and nitrogen-blown pitches. The summary of properties of vacuum-distilled pitches is illustrated in Table5.5.

Comparison of vacuum-distilled pitches with their respective tars shows that the carbon content of the distilled pitches increased considerably. However, significant change in hydrogen, nitrogen, and sulphur contents was not observed. The carbon content was the highest for the S-V1 pitch (85.5%). The only noticeable difference for vacuum-distilled pitches is that the sulphur contents were higher than the oxygen and nitrogen contents in all distilled pitches. The higher content of sulphur in the vacuum-distilled pitches may be attributed to the distillation of the light non-sulphur containing compounds.

The vacuum-distillation yield was low for all types of distilled pitches, indicating a significant removal of volatiles during the distillation. Compared with air-blown and nitrogen-blown pitches, vacuum-distilled pitches had the highest H/C ratio, the lowest toluene-insoluble content, and therefore, the lowest softening point. Figure 5.8 shows the variation of H/C ratios of the various pitches.

The results show that vacuum distillation did not result in qualified pitches as air-blown and nitrogen-blown pitches.

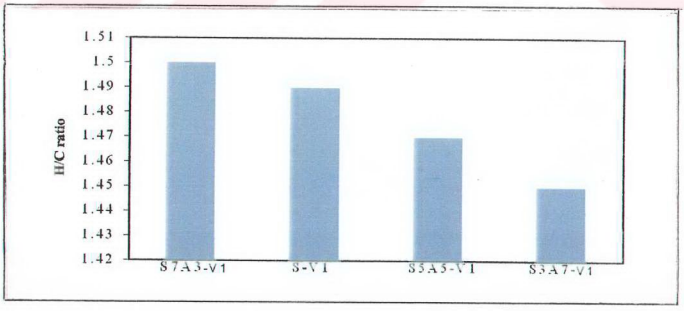

Figure 5.8. The variation of H/C ratio with the various vacuum-distilled pitches.

Table 5.5. Vacuum distillation conditions and properties of the vacuum-distilled pitches.

Vacuum distillation conditions			Properties										
Sample	VDT (^{O}C)	t (min)	C (wt%)	H (wt%)	N (wt%)	S (wt%)	[a]O (wt%)	H/C	O/C	CY (wt%)	PY (wt%)	TI (wt%)	SP (^{O}C)
S-V1	300	60	85.50	10.60	0.95	1.70	1.25	1.49	1.10	9.61	18.62	2.43	40
S7A3- V1	300	60	83.75	10.45	1.15	3.15	1.50	1.50	1.34	12.40	20.49	3.51	50
S5A5- V1	300	60	83.90	10.30	0.90	2.85	2.05	1.47	1.83	13.40	17.09	1.00	50
S3A7- V1	300	60	84.25	10.20	0.80	3.85	0.90	1.45	0.80	8.24	16.84	1.23	40

VDT: vacuum distillation temperature; [a]: by difference ; ND: not determined; CY: carbon yield; PY: pitch yield; TI: toluene insolubles; SP: softening point.

5.5 General Properties of the Vacuum-Distilled and Solvent Extracted Pitches

In order to increase the aromaticity and therefore, the softening point, S7A3-V1 pitch was extracted by hexane at its boiling point. Comparison the hexane-insoluble fraction of S7A3-V1 pitch itself showed a significant reduction in hydrogen content and a great increase in TI content. The hydrogen content decreased from 10.45% to 7.35% while the toluene-insoluble content increased from 3.5% to 37.9% as reported in Table 5.6. This reduction in hydrogen content and the increase in TI content were reflected in the significant decrease of H/C ratio. The softening point of the hexane extracted S7A3-V1 pitch increased from 50 to 136°C with decreasing H/C ratio. This indicates that the S7A3-E1 pitch is much more aromatic than S7A3-V1 pitch and this result is consistent with FTIR results shown in section 5.7.3.

Table 5.6. The comparison of properties of. S7A3-E1 and S7A3-V1 pitches.

Content	S7A3-E1	S7A3-V1	Content	S7A3-E1	S7A3-V1
C(wt%)	81.95	83.75	O/C	4.07	1.34
H(wt%)	7.35	10.45	CY(wt%)	37.80	12.40
N(wt%)	2.40	1.15	Yield(wt%)	12.45	20.49
S(wt%)	3.85	3.15	TI(wt%)	37.85	3.51
[a]O(wt%)	4.45	1.50	SP (°C)	136.00	50.00
H/C	1.08	1.50			

[a]: by difference.

The H/C ratio is lower than that of the S7A3-V1 pitch suggesting that S7A3-V1 pitch contains higher amounts of aliphatic components which were removed by the extraction with hexane.

Coking capacity of the S7A3-E1 pitch increased significantly in the same sense as the softening point. The increase in TI content and carbon yield indicates that S7A3-E1 pitch contains fewer amounts of low molecular components.

5.6 Thermal Analysis

5.6.1 Characterisation of Pitches by Thermogravimetric Analysis

In order to characterise the carbonisation behaviour of pitches, thermogravimetric analysis (TGA) was performed. Figure 5.9 shows the TG curves obtained during pyrolysis of some of the air-blown pitches. TG curves show that the weight loss of S-A2, S7A3-A2 pitches, and S5A5-A1, S5A5-A3 pitches occurred in two different steps. These steps were in the temperature range of 150-500°C and 140-450°C for each group of pitches, respectively. Above 500°C the weight loss was much smaller. S5A5-A1 pitch exhibits a considerably larger weight loss (90%) than the rest of the pitches over the whole temperature interval studied. This agrees with the fact that this sample contains more volatile constituents than the other pitches which is in good agreement with softening point and TI content. On the other hand, TG curves for S-A2 and S7A3-A2 pitches were quite parallel to each other despite the different parent tars. However, these two samples were undergone the same thermal treatments (270°C, 1.5h). At higher air-blowing temperature, as in the case of S-A2 and S7A3-A2 pitches, the weight loss was lower than S5A5-A1 and S5A5-A3 pitches, which were treated at lower temperature, 250°C. However, the weight loss of S5A5-A3 pitch was less than S5A5-A1 pitch as it was treated at 250°C for a longer period than S5A5-A1 pitch. This result is related to the polymerisation and condensation reactions which is the consequence of longer air-blowing periods. The lower weight loss of S-A2 and S7A3-A2 pitches indicate that these pitches contain less lighter components compared to the other two pitches. This is in agreement with higher softening points than those of the others.

S5A5-A1 pitch, which was produced at mild air-blowing conditions, constitutes the most outstanding case among all other pitches, as it undergoes a much larger total weight loss. This result may be due to the insufficient time or temperature of air-blowing. This is also confirmed by the lowest softening point which indicates the presence of more volatile constituents in S5A5-A1 pitch.

Figure 5.10 shows the TG curves of pitches obtained at 250°C and 300°C, under various nitrogen blowing times. S5A5-N1 pitch exhibits a considerably larger weight loss (88%) than the other pitches. S5A5-N1 pitch undergoes weight loss in a simple

step covering the 140-450°C interval; above 450°C significant weight loss was not observed. The weight loss starts at a temperature of about 140°C and gradually increases up to 250°C. From 250°C to 450°C, the weight loss is quite sharp.

In the case of S5A5-N4 pitch, the weight loss starts at a temperature of 150°C and gradually increases up to 220°C. After 220°C, a major loss of weight was observed due to the main devolatilisation which completes around 500°C. S5A5-N4 pitch undergoes overall weight loss at around 79.5%. These results agree with the fact that S5A5-N1 pitch was produced at milder thermal treatment than the S5A5-N4 pitch. Although both pitches were treated at 250°C, the longer nitrogen-blowing time was resulted in lower H/C ratio, higher softening point, and therefore, the lower weight loss.

S5A5-N5 pitch, which was prepared at 300°C, undergoes the least weight loss (42%). The thermal decomposition of S5A5-N5 pitch starts at around 150°C. The weight loss generates slower than that of S5A5-N4 pitch and completes by 550°C. Although the parent material is the same, it is convenient to remark that the less weight loss for S5A5-N5 pitch is in good agreement with the less severe thermal treatment applied to S5A5-N4 pitch.

The TG curves for the vacuum-distilled pitches (Figure 5.11) show that the weight loss of all pitches occurs in a simple step. All the vacuum-distilled pitches have high H/C ratios and low softening points. This is resulted in high weight losses. The thermal decomposition of the pitches starts at around 200°C, and gradually increases up to 300, 350, 360, and 400°C for S3A7-V1, S7A3-V1, S-V1, and S5A5-V1 pitches, respectively. The total weight loss is quite sharp (91%, 88%, 90%, and 84%) and completes at around 440, 460, 480, and 500°C for S3A7-V1, S7A3-V1, S-V1, and S5A5-V1 pitches, respectively.. The lowest weight loss (62.2%) was observed for vacuum-distilled and then hexane extracted pitch. The thermal decomposition of S7A3-E1 pitch starts at earlier temperatures (150°C) than the others, gradually increases up to 300°C and completes at around 550°C.

From the overall results, it is evident that the weight loss of a pitch decreases with increasing aromaticity in the pitch as indicated in Table5.7.

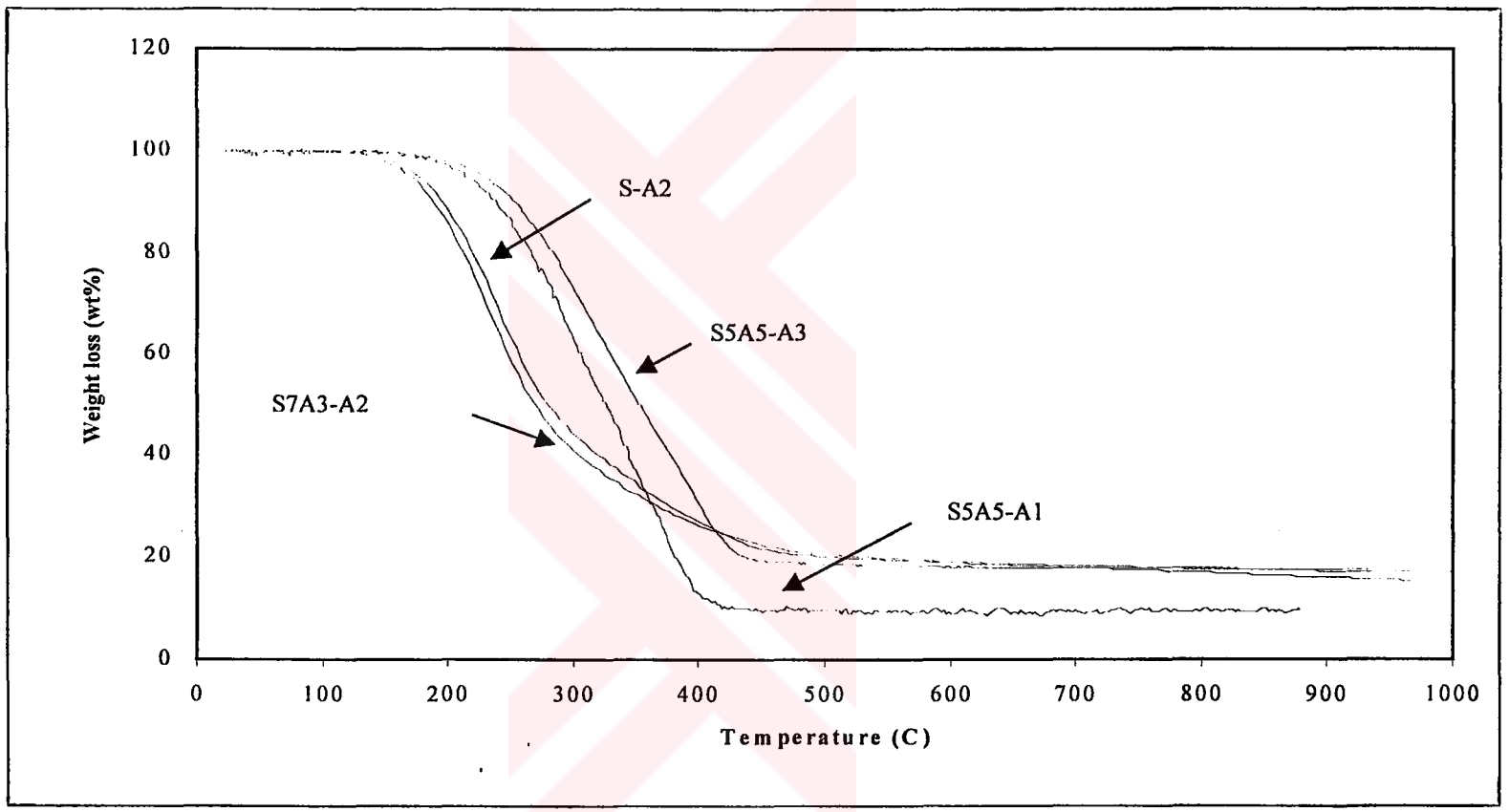

Figure 5.9. Thermogravimetric curves of some air-blown pitches

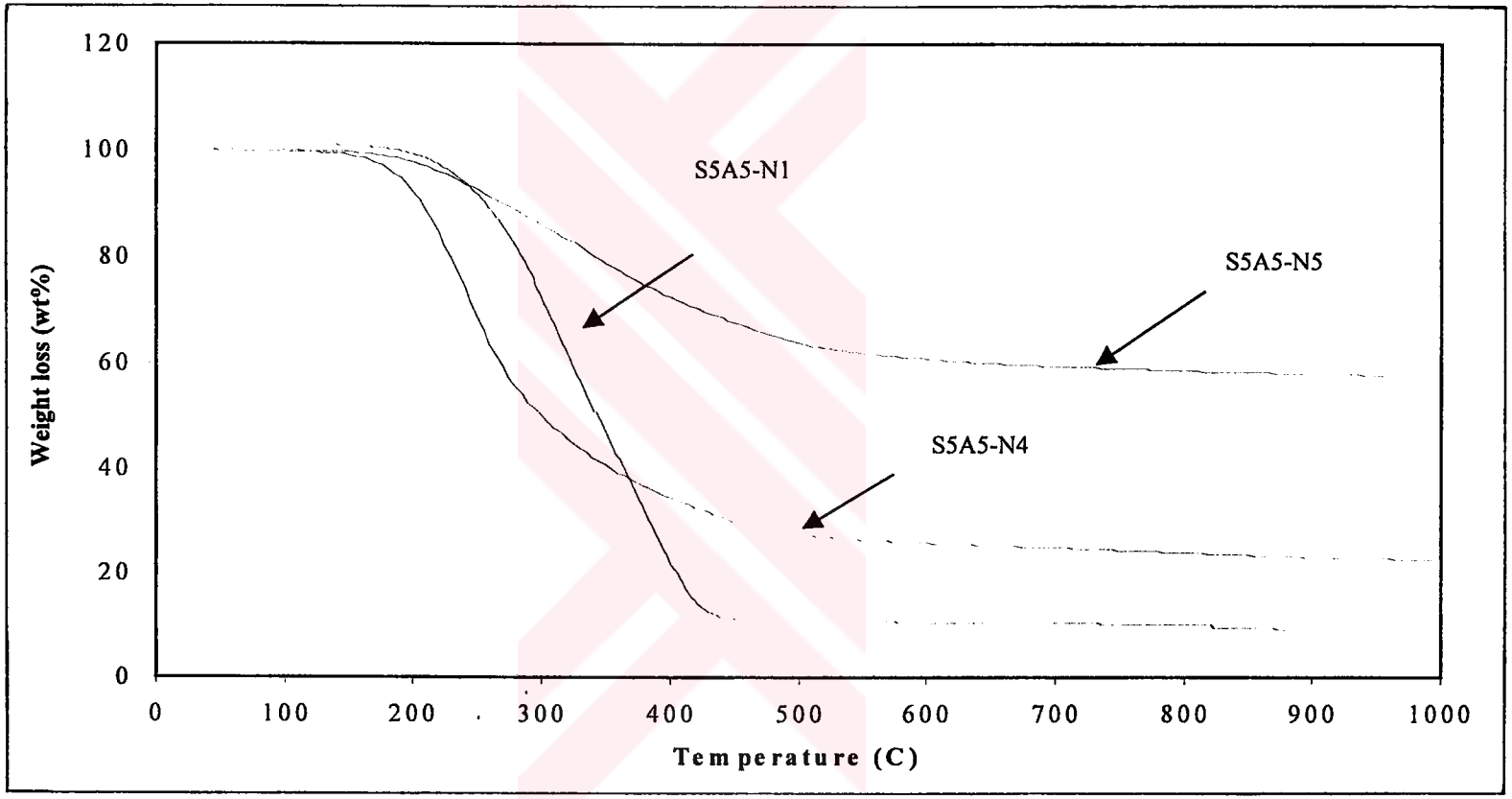

Figure 5.10. Thetmogravimetric curves of nitrogen-blown pitches.

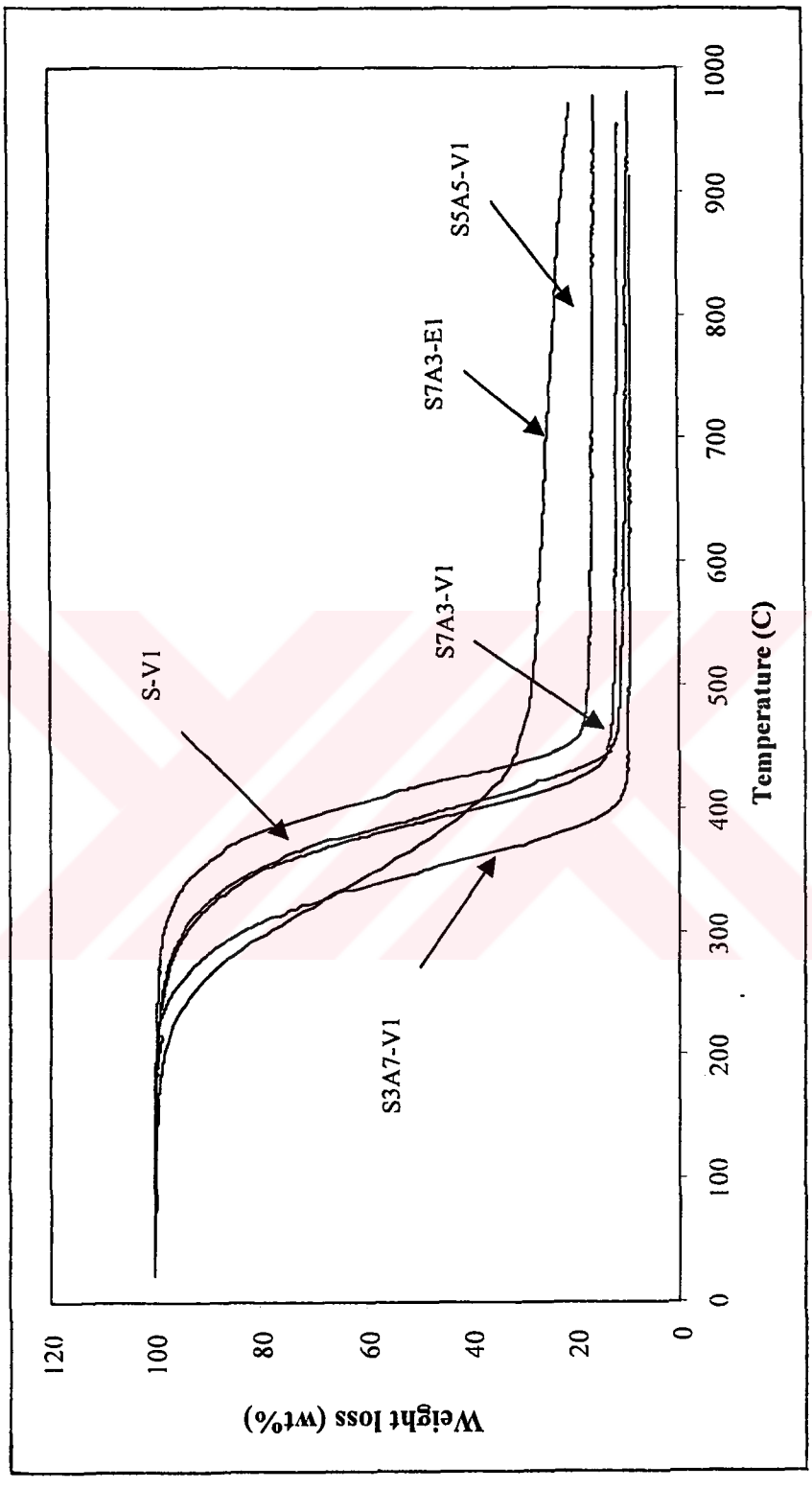

Figure 5.11. Thetmogravimetric curves of vacuum-distilled pitches.

Table 5.7. The relation of weight loss with the H/C ratio of some pitches.

Pitch	H/C	Weight loss (%) (-ΔW%) at 950°C	Carbon yield (wt%)
S-V1	1.49	90.0	10.0
S5A5-A3	1.32	85.0	15.0
S7A3-E1	1.08	62.2	37.8
S5A5-N5	0.98	42.2	57.6

The coking capacity of the pitches as measured by the carbon yield (CY) obtained by pyrolysis at 1000°C was increased with decreasing H/C ratio. It is also noted that the carbon yield increased with increasing severity of air-blowing and nitrogen-blowing (Figure 5.12). As previously reported the major influence of air-blowing on CY is revealed by the noticeable difference between the values obtained at different air-blowing time for the same parent material. In the case of nitrogen blowing, the major influence on CY is observed by the significant difference between the values obtained at different nitrogen-blowing temperatures.

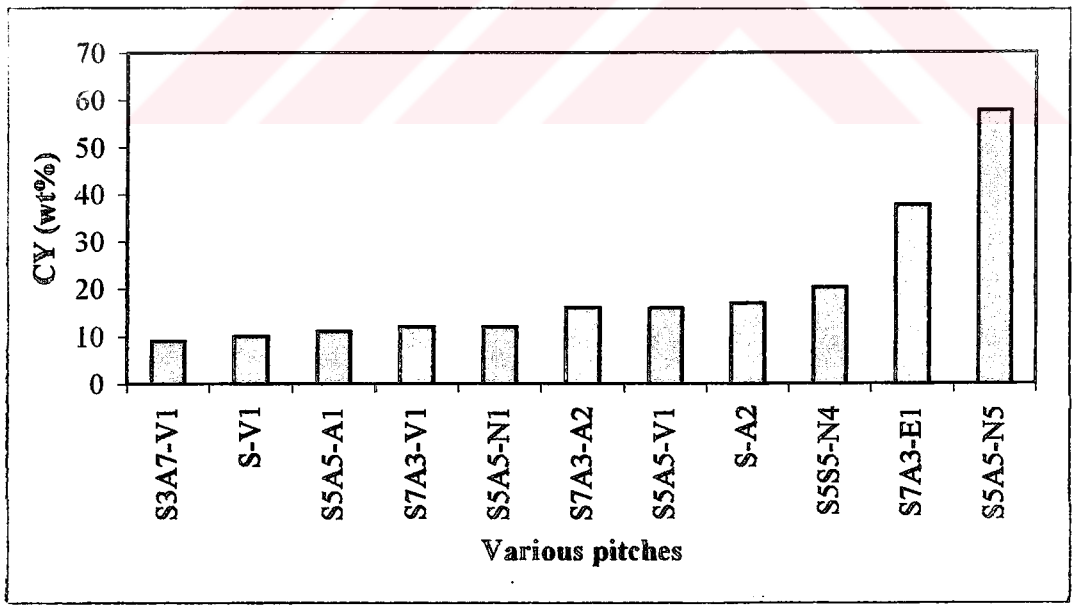

Figure 5.12. Variation of carbon yield of the various pitches.

5.7 Structural Characterisation

5.7.1 Size Exclusion Chromatography

Size exclusion chromatography (SEC) has become the most widely used method for determining the molecular weight distributions of polymers and coal-derived liquids [175]. The operation of SEC involves the molecular size separation of a polymer solution with the use of columns packed with rigid, crosslinked polystyrene gels. The size separation depends on the extent to which the different molecular species permeate the pores of the gel. The pores of the gel exclude molecules greater than a certain critical size whilst smaller molecules can diffuse into the gel structure. Thus, in SEC excluded molecules pass through the column more rapidly than the smaller ones, which permeate the gel. Because of different dimensions are randomly distributed throughout the gel structure, diffusion within the gel also varies with molecular size and shape. Smaller molecules are hence eluted at rates which depend on the degree to which they permeate the gel, and components of a mixture are eluted in sequence of decreasing size (or MM) [131].

Pitches are not high polymers; however, related polymeric products such as asphalts and asphaltenes have been successfully fractionated and analysed by SEC [176].

Some of the air-blown pitches, nitrogen-blown pitches, and vacuum distilled pitches were analysed by SEC in order to compare the molecular weight distributions. Eluted components were detected by monitoring a physical property such as UV absorption and refractive index.

Figure 5.13(1) and (2) compares the SEC chromatograms of S5A5-A4 pitch, NMP-soluble portion of the hexane-soluble (HS) components of the pitch (extract), and NMP-soluble portion of the hexane-insoluble (HI) components of the pitch (residue), obtained with UV and RI detections, respectively.

In Figure 5.13(1), the peaks between 500-700s correspond to eluting material at the exclusion limit of the column. It is important to note that the signal for the excluded material should not be interpreted as a sudden surge of sample with closely bunched molecular masses, but as material that the column was unable to resolve. It is likely that, if resolved, this material would appear as a long trailing distribution of larger

molecular mass (MM) material distributed over a long span of elution times [175]. The elution curves of excluded materials for the pitch, extract, and the residue differ in the ratios, indicating different proportioning of their component species. For the residue and the pitch, the peaks corresponding to excluded material were greater than that of the extract, and also excluded material peak for the residue was as greater as the retained (separated) material peak. This suggests that the excluded material to contain greater concentrations of larger aromatic structures and also possibly greater heteroatom content. There is a significant shift to higher masses for the residues compared to extracts.

For S5A5-A4 pitch, when compared with polystyrene standards (Figure 4.7) the lower MW peak maximum corresponds to 200, while the corresponding peaks for the extract and residue are at 500 and 2000, respectively. The apparent molecular weight distribution for the residue is between 200-8000 for UV detection, and 200-16000 for RI detection. All; extract, residue, and original pitch showed the evidence of excluded material above 20000 by UV detection. The maxima of the peaks shift to shorter elution times, in other words to the higher masses in RI detection, which is seen in Figure 5.13(2). This is thought to be due to material with low UV absorbance and higher MW which is more prominent in the RI chromatogram. Additionally, it should be noted that the specific response of the UV and RI detectors varies markedly with MM.

Figure 5.14(1) and (2) display the SEC for the S5A5-N3 pitch, NMP-soluble portion of the hexane-soluble (HS) components of the pitch (extract), and NMP-soluble portion of the hexane-insoluble (HI) components of the pitch (residue), obtained with UV and RI detections, respectively.

In Figure 5.14(1), the peaks between 500-700s correspond to excluded material. For the residue, the ratio of area under the peak corresponding to excluded material was greater than that by the retained (separated) material, suggesting the excluded material to contain greater concentrations of larger aromatic structures, and different proportioning of their component species.

It may also be noted that the excluded material peak for the parent pitch is larger than that of for the extract, supporting the observation that materials appearing at the exclusion limit of the column contain aromatic ring systems.

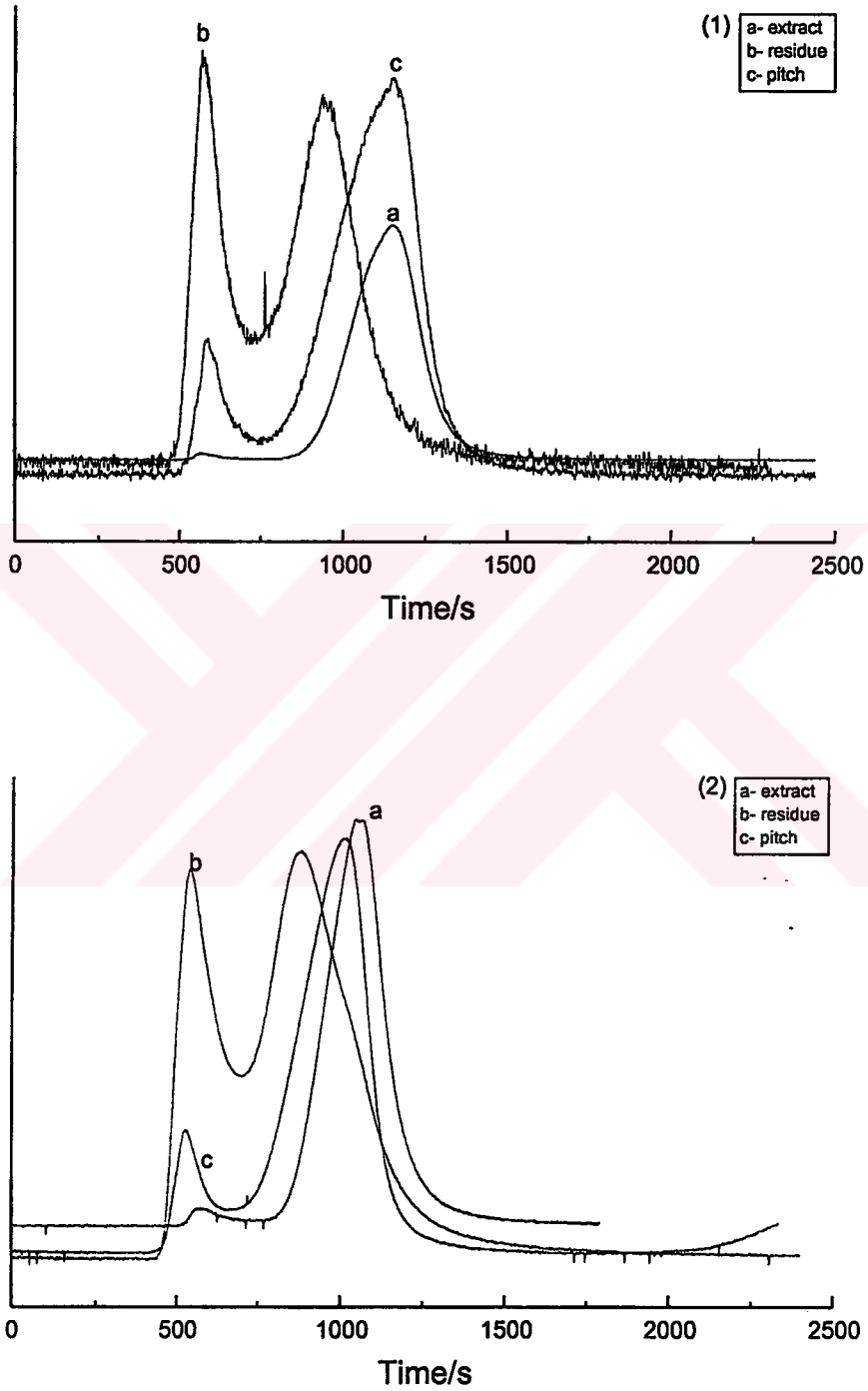

Figure 5.13. SEC chromatogram of S5A5-A4 pitch, extract, and residue : (1) ;UV detection, (2) ; RI detection.

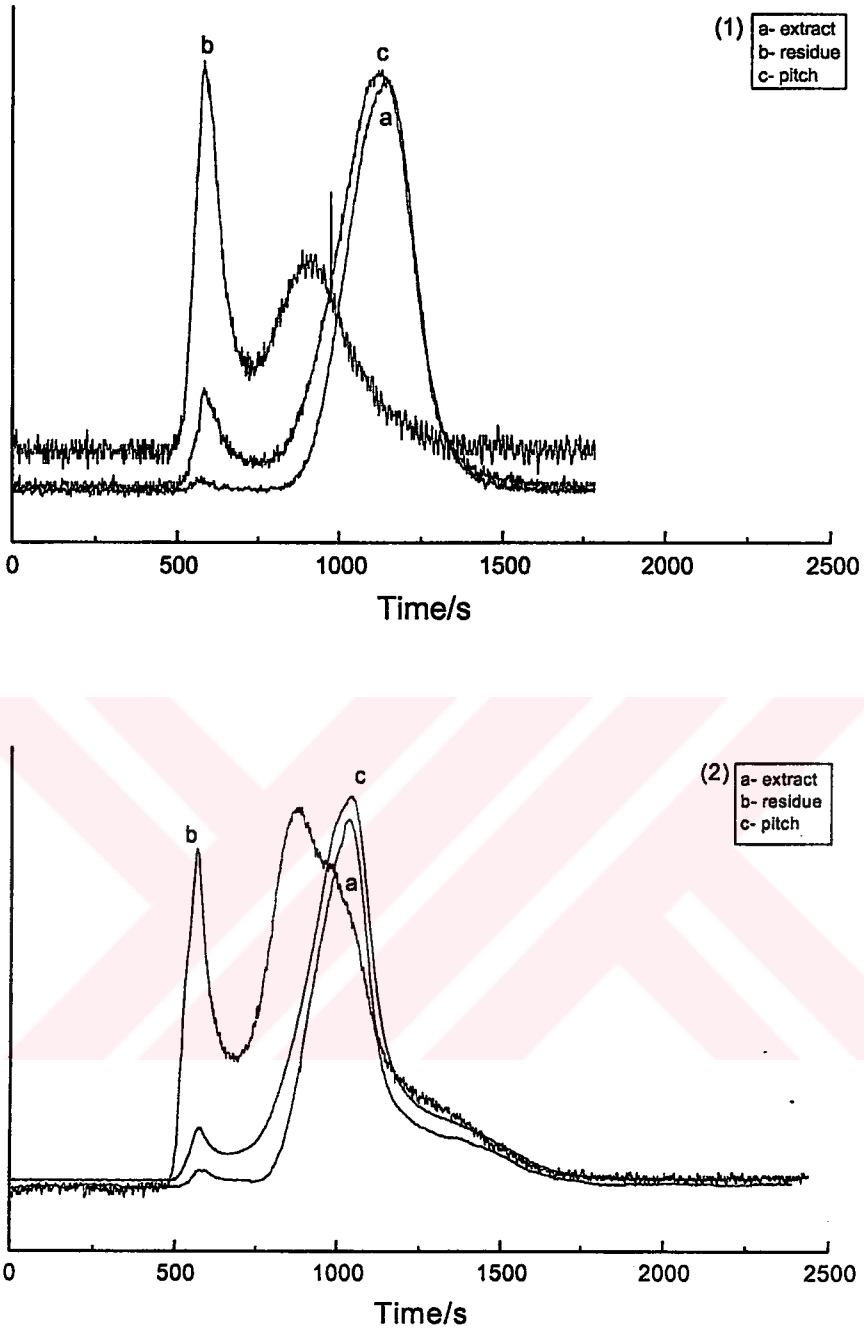

Figure 5.14. SEC chromatogram of S5A5-N3 pitch, extract, and residue : (1) ;UV detection, (2) ; RI detection.

There is a significant move to shorter elution times for the residues compared to extracts observed for both UV and RI detections. The apparent molecular weight distribution for the residue was between 200-8000 for UV detection, and 200-20000 for RI detection. The peaks apparently shift to the higher masses when RI detection was employed.

For S5A5-A4 pitch, since the H/C atomic ratio is lower and the softening point and the TI content are greater than those of S5A5-N3 pitch, the elution curves of S5A5-A4 pitch, and its residue became broader and taller. The position of the maxima of the residue and the pitch shifted to lower elution times. This could be due to larger molecular sizes, or more highly substituted or unsymmetrical molecules as the molecular size and shape are the parameters in the separation by SEC. Another reason should be the presence of components that are either not soluble in, or not eluted by NMP. However, the FTIR results confirmed that S5A5-A4 pitch is more aromatic than S5A5-N3 pitch as the aromaticity index are 0.24 and 0.13 for S5A5-A4 and S5A5-N3 pitches, respectively.

Figure 5.15(1) and (2) presents the size exclusion chromatograms of S5A5-V1 pitch, NMP-soluble portion of the hexane-soluble (HS) components of the pitch (extract), and NMP-soluble portion of the hexane-insoluble (HI) components of the pitch (residue), obtained with UV and RI detections, respectively.

The extract gave an insignificant indication of the presence of excluded material. between 550-650s. Signal from the retained (separated) material was intense between 750-1500s. The peak corresponding to excluded material become clearer when RI detection was employed.

The residue contains two fractions; the first fraction is excluded material with molecular weight distribution around 20000. The second fraction has a molecular weight distribution between 100-16000. The elution curves of the excluded material differ in the ratios of the residue, extract, and the pitch. The peak for the excluded material of the residue is larger than that of for the extract and also for original pitch. This should be due to different proportioning of their component species. The shift to shorter elution times observed between 450 and 650s when RI detection was employed. This should be due to low UV absorbance material in the fractions.

Figure 5.16 (1) and (2) illustrates the SEC of S7A3-V1 pitch, NMP-soluble portion of the hexane-soluble (HS) components of the pitch (extract), and NMP-soluble portion of the hexane-insoluble (HI) components of the pitch (residue), obtained with UV and RI detections, respectively.

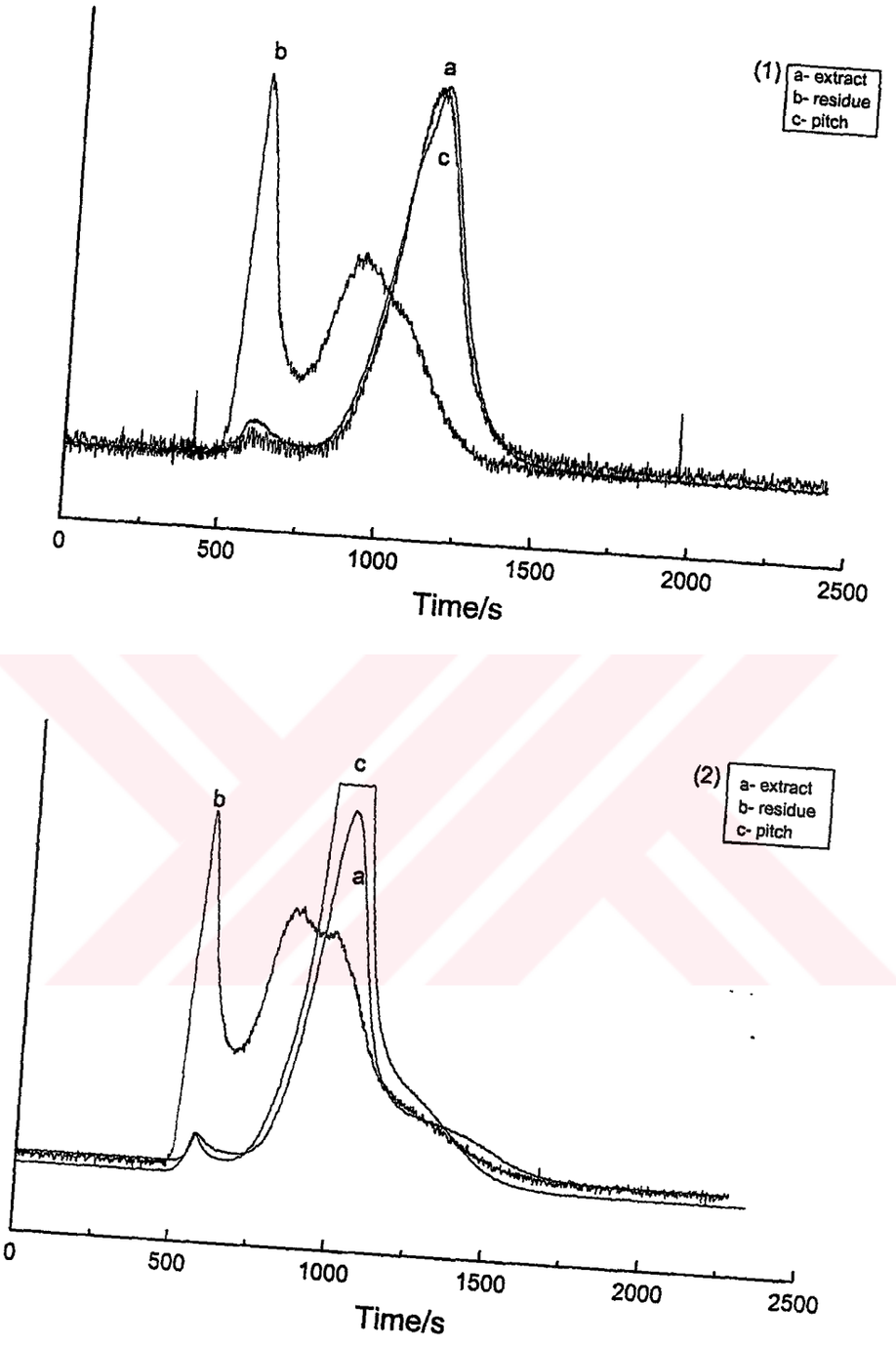

Figure 5.15. SEC chromatogram of S5A5-V1 pitch, extract, and residue : (1) ;UV detection, (2) ; RI detection.

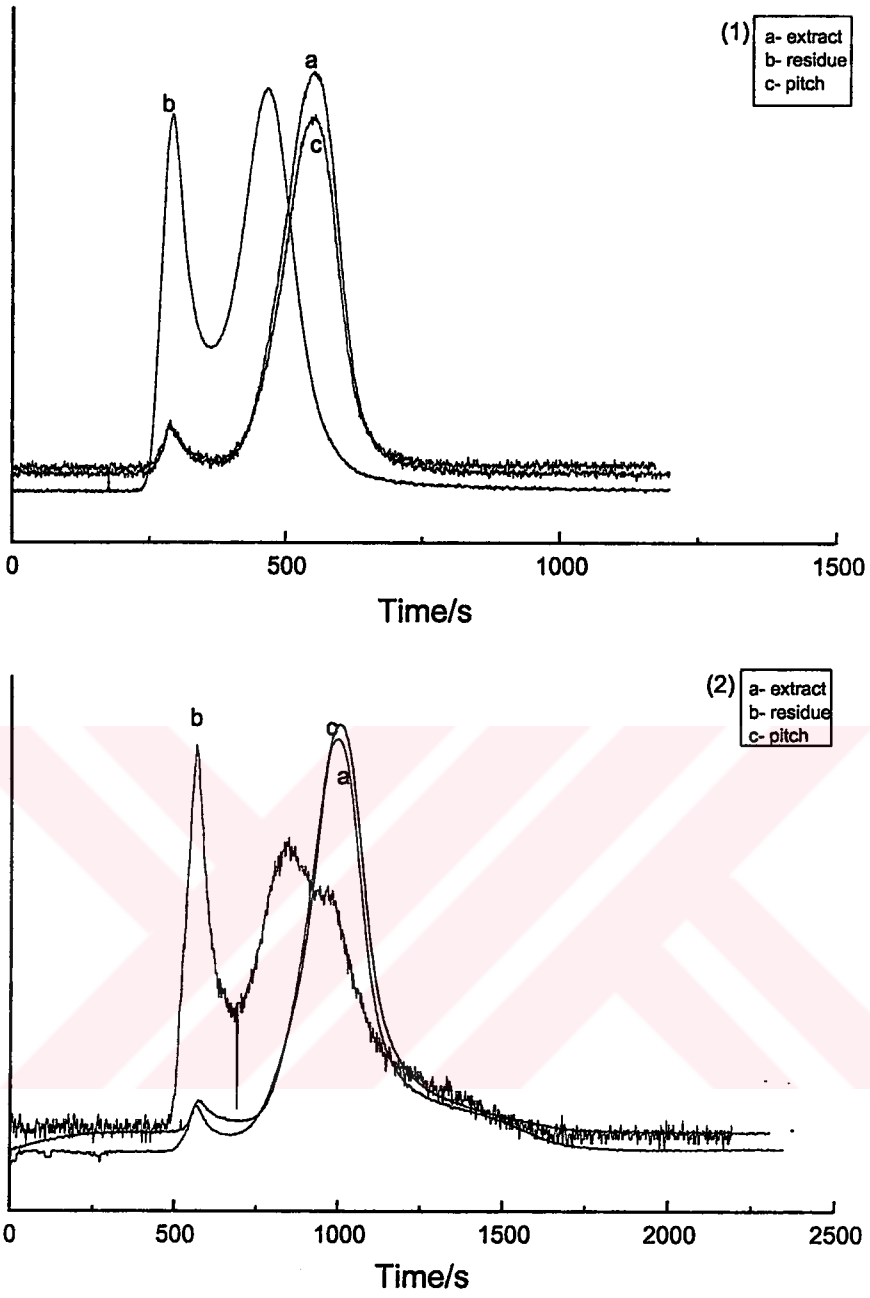

Figure 5.16. SEC chromatogram of S7A3-V1 pitch, extract, and residue : (1) ;UV detection, (2) ; RI detection.

For the residue, the ratios of areas under the peaks corresponding to excluded material to those of the retained material were similar, suggesting the excluded material not to contain greater concentrations of aromatic or larger molecules than the retained material. The extract, and the pitch eluted at longer times than the residue did, indicating molecular size reductions.

When compared with the SEC of S5A5-V1, S7A3-V1 contains more amounts of higher molecular weight components than S5A5-V1 as the eluting peaks shifted to early elution times. The excluded material peak for the residue of S7A3-V1 pitch showed a considerable shifting to the lower elution times end. This could be due to larger molecular sizes or more highly substituted or unsymmetrical molecules or higher content of heteroatoms. The higher heteroatom and TI content of S7A3-V1 than S5A5-V1 pitch confirms this hypothesis.

As seen from all the size exclusion chromatograms, the proportions of retained and excluded material vary with the sample. The peaks apparently shift to the higher masses if RI detection was employed.

The results have shown that the size exclusion chromatography in NMP is suitable for characterising pitch materials, whereas the use of tetrahydrofuran (THF) as mobile phase in SEC has been found to lead to partial loss of sample. The problem has been resolved by using NMP as mobile phase in SEC, showing significant fractions of sample eluting at the exclusion limit of an identical SEC column [175]. A significant shift to higher masses for the residue compared with the extracts is found. The findings indicate that all the pitch materials contain molecules, which elute at or near the exclusion limit of the SEC column, when sufficiently powerful solvent is used.

5.7.2 Mass Spectroscopy

Clearly, to detect as large as a distribution of molecular ions as possible, it is necessary to minimise fragmentation of the sample molecules during vaporisation and ionisation. The fast atom bombardment mass spectrometry (FAB-MS) has been generally used for polar molecules rather than neutral ones; however, the method has been used for polynuclear hydrocarbons and has given molecular ions possibly because the molecular ions formed from large fused aromatic system are particularly stable.

Figures from 5.17 to 5.20 show the mass spectra of S5A5-A4, S5A5-N3, S5A5-V1 and S7A3-V1 pitches and their hexane soluble fractions.

(a)

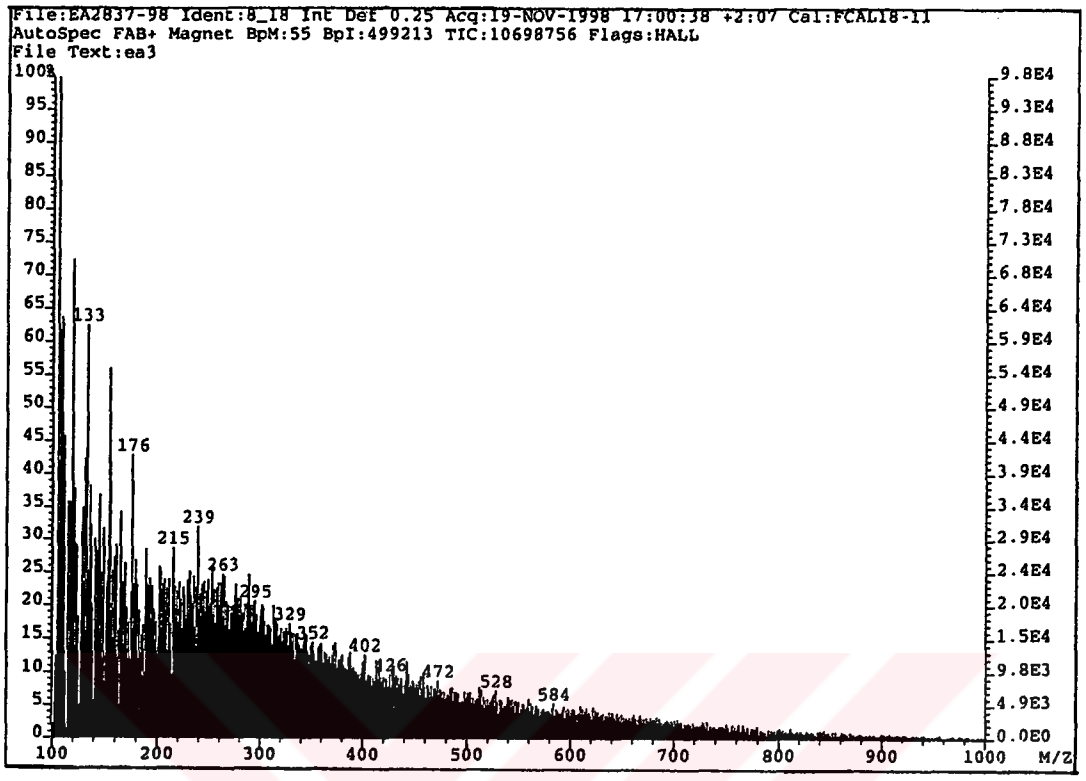

(b)

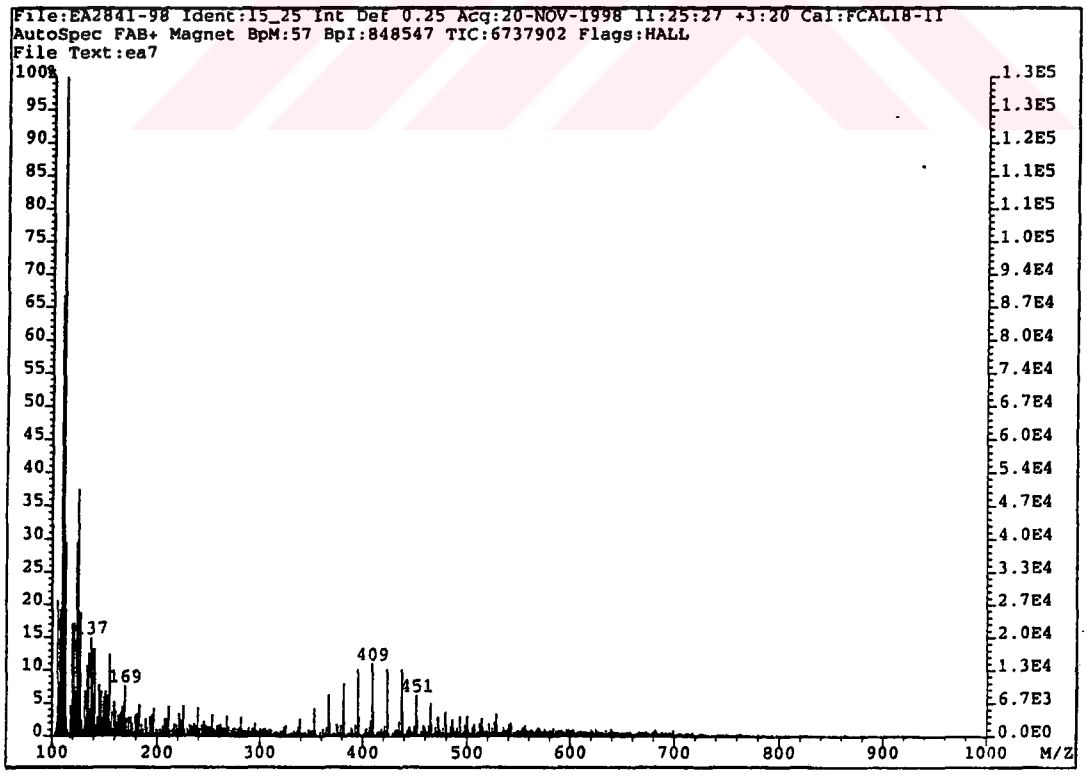

Figure 5.17 Mass spectra of S5A5-A4 pitch (a), and its hexane soluble fraction (b).

(a)

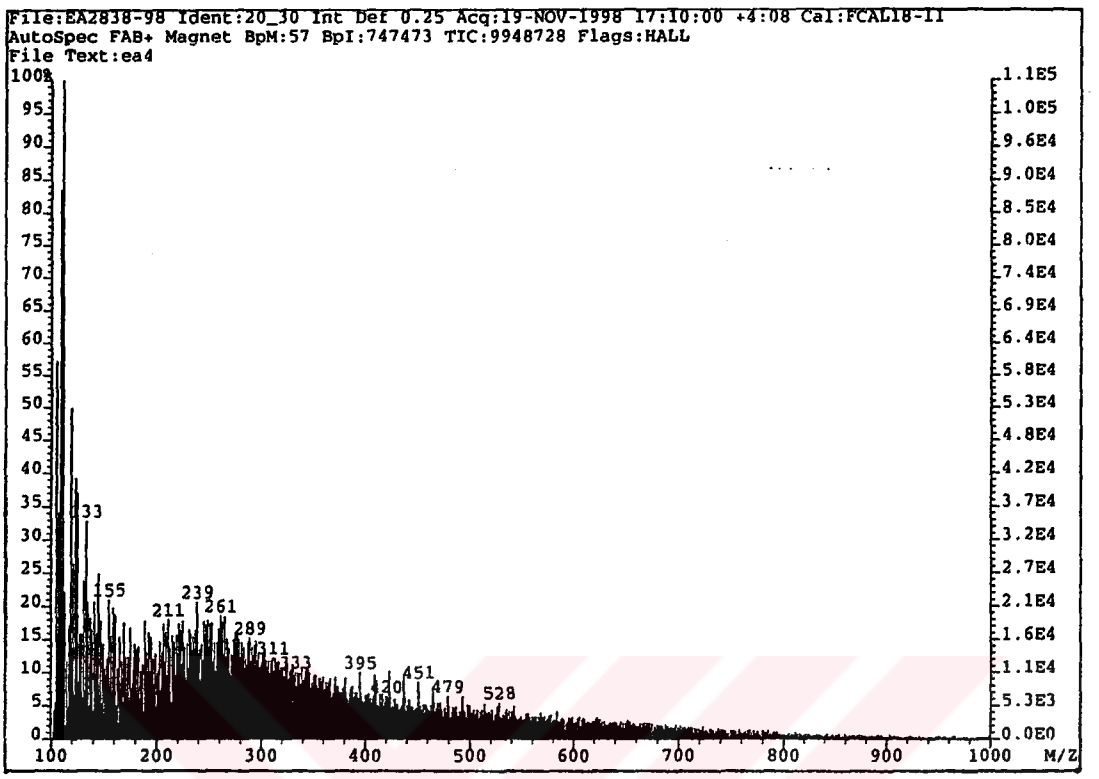

(b)

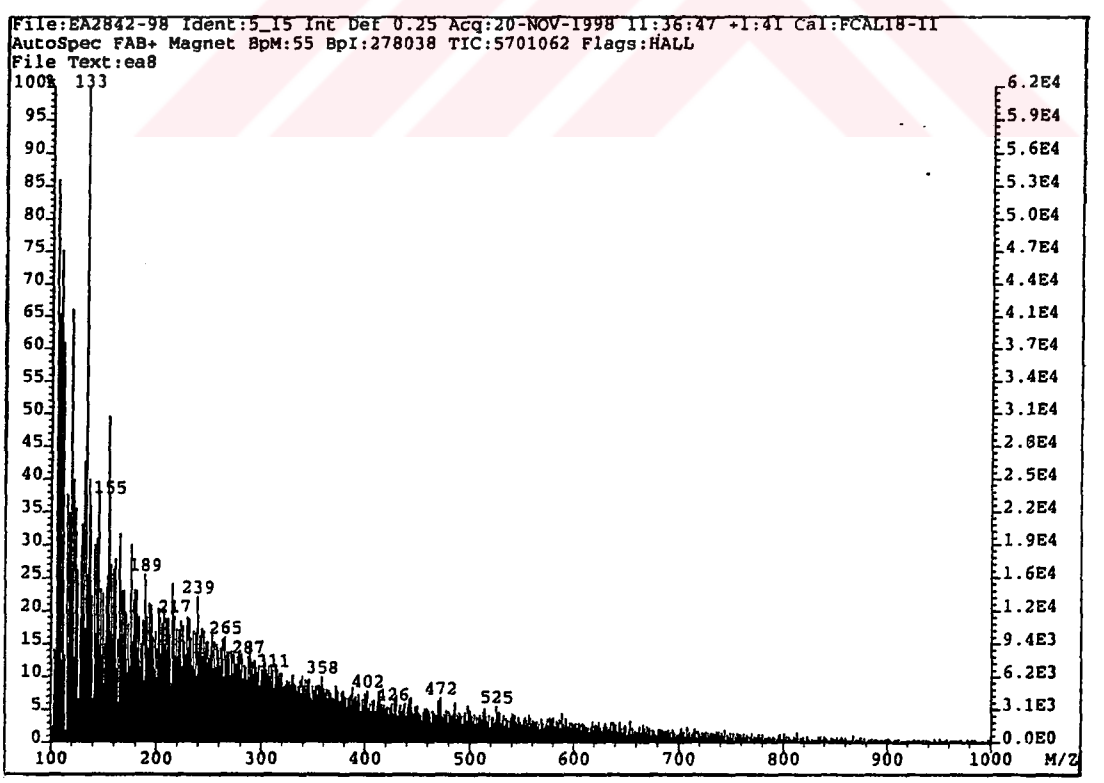

Figure 5.18 Mass spectra of S5A5-N3 pitch (a), and its hexane soluble fraction (b).

It is noted that since vertical scales were normalised with respect to the highest detected intensity in each graph, intensities shown in one mass spectrum are not directly comparable with those of another diagrams.

The mass spectra for S5A5-A4, and S5A5-N3 pitches (Figure 5.17a and Figure 5.18a) show a relatively wide ion distribution profile from 133 to 1000 Da, although the relative abundance of the ions higher than 800 Da are very small. The molecular ion distribution of the hexane soluble fraction of S5A5-N3 pitch (Figure 5.18b) was similar to that of the original S5A5-N3 pitch which means S5A5-N3 pitch is highly soluble in hexane. This suggests that S5A5-N3 pitch has mainly aliphatic structures. However, compared to hexane soluble fraction of S5A5-N3 pitch, the mass spectrum for the hexane soluble fraction of S5A5-A4 pitch (Figure 5.17b) illustrates a narrower ion distribution profile from137 to 700 Da. But the relative abundance of the ions is mainly less than 500 Da. This narrow ion distribution of the hexane soluble fraction of S5A5-A4 pitch is probably due to less solubility of the pitch in hexane. The solubility of this pitch in hexane suggests that S5A5-A4 pitch contains more aromatic structures than aliphatic compounds. All these findings are confirmed by the FTIR results, as the aromaticity index are 0.13 and 0.24 for S5A5-N3, and S5A5-A4 pitches, respectively.

The mass spectra of S7A3-V1 pitch (Figure 5.20a) shows a wider ion distribution from 133 to 800 Da while the ion distribution for S5A5-V1 pitch was between 133-700 Da (Figure 5.19a). However, the mass spectra for the hexane soluble fraction of S7A3-V1 pitch (Figure 5.20b) and S5A5-V1 pitch (Figure 5.19b) were similar and contained high molecular ions up to 600 Da which means these two pitches are also highly soluble in hexane. Hence, they have also aliphatic structures.

The complexity of the mass spectra of the pitches and their hexane soluble fractions indicates that the presence of a wide range of individual molecules. In all of the fast atom bombardment mass spectra, the complexity of m/z values is so great that no meaningful statements can be made as to the type of molecules being detected, apart from the obvious features such as molecular profile of the pitches and their fractions. Whilst mass spectrometer may be a very powerful technique it is evident that, in order to gain specific structural information, the method should be coupled with a

(a)

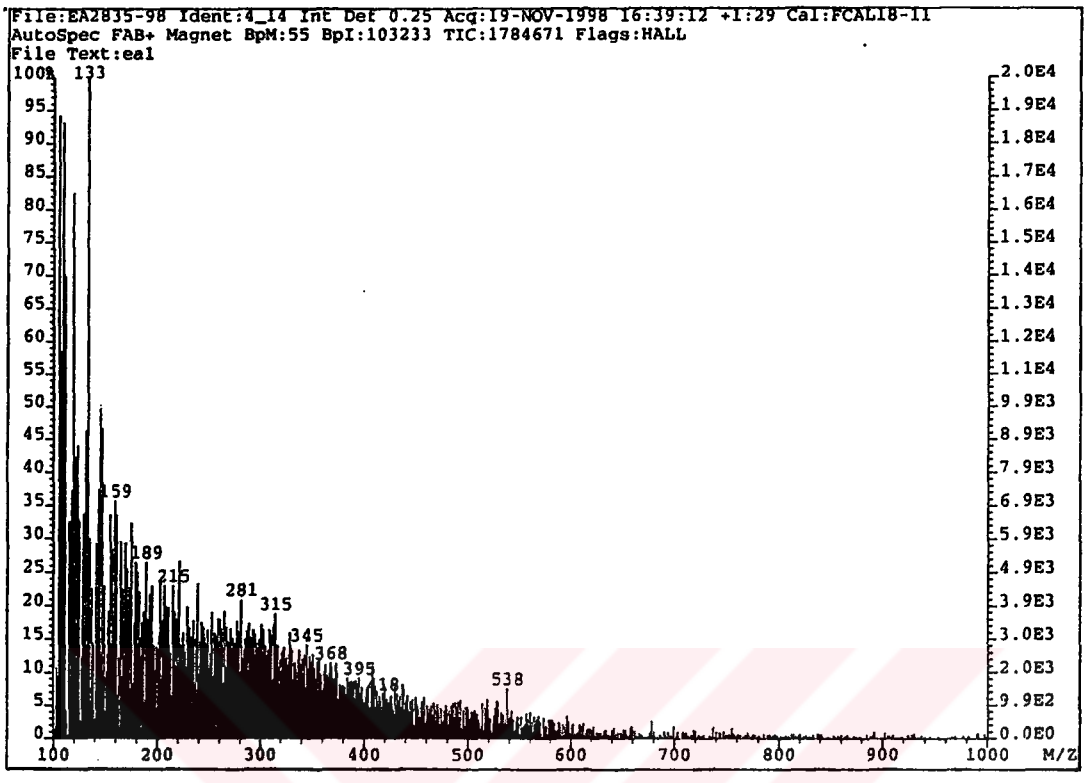

(b)

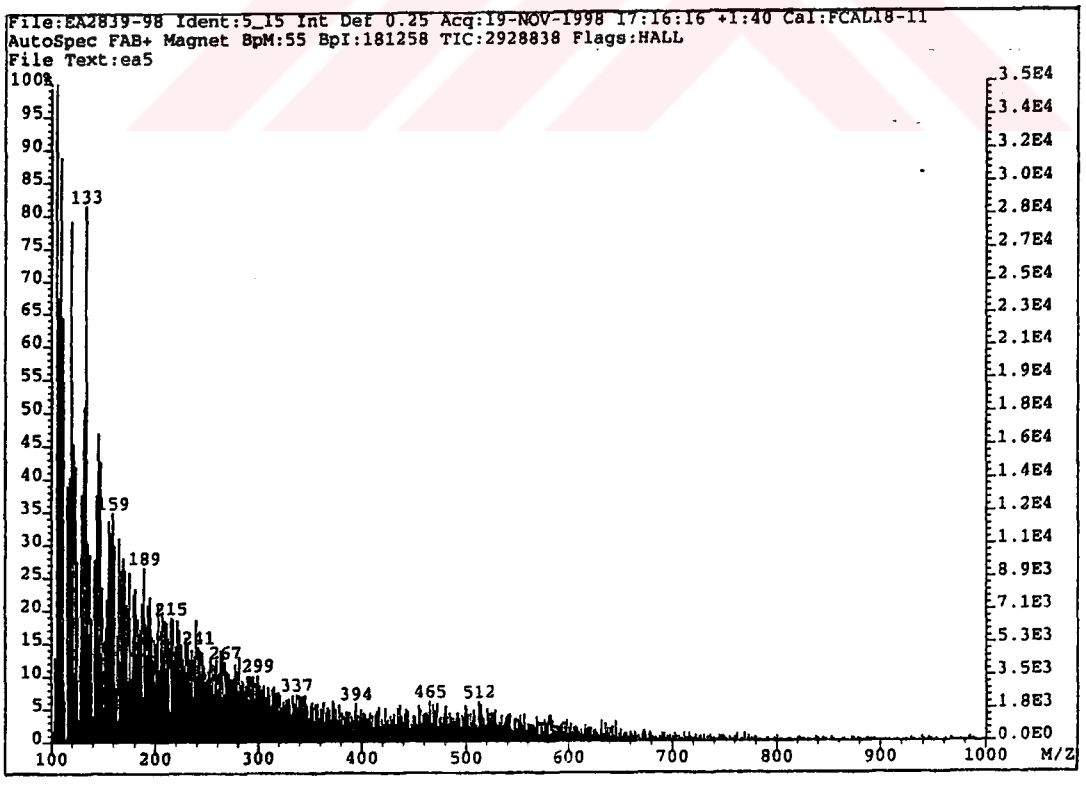

Figure 5.19 Mass spectra of S5A5-V1 pitch (a), and its hexane soluble fraction (b).

(a)

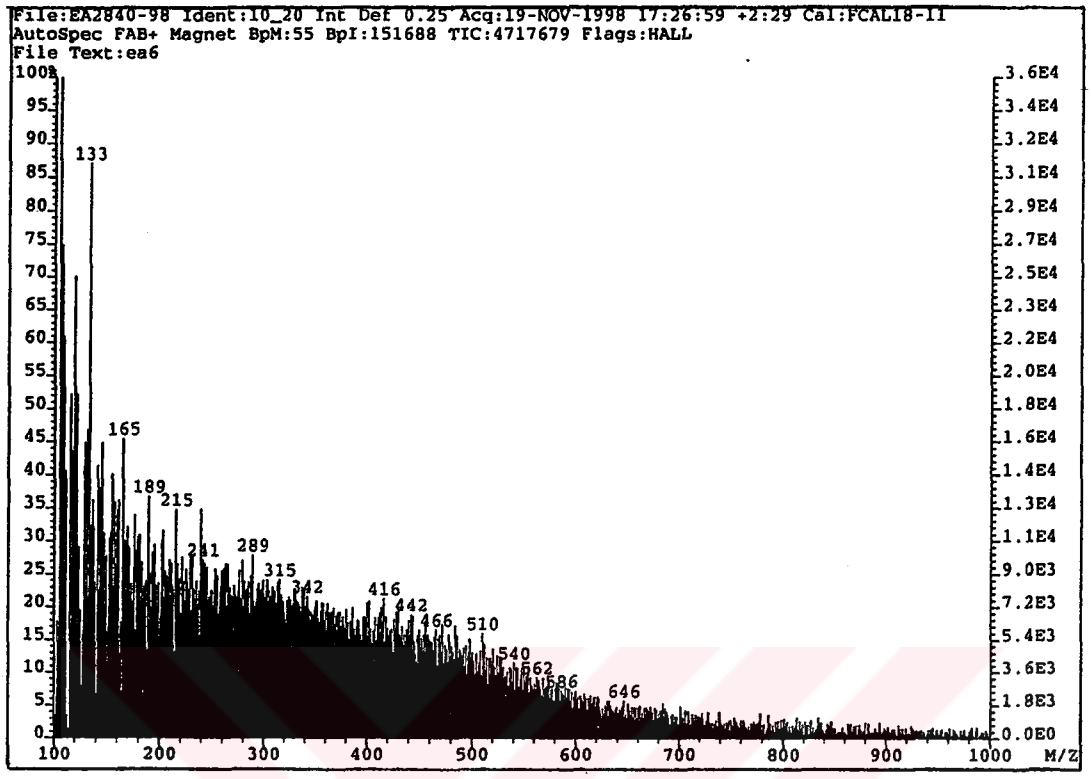

(b)

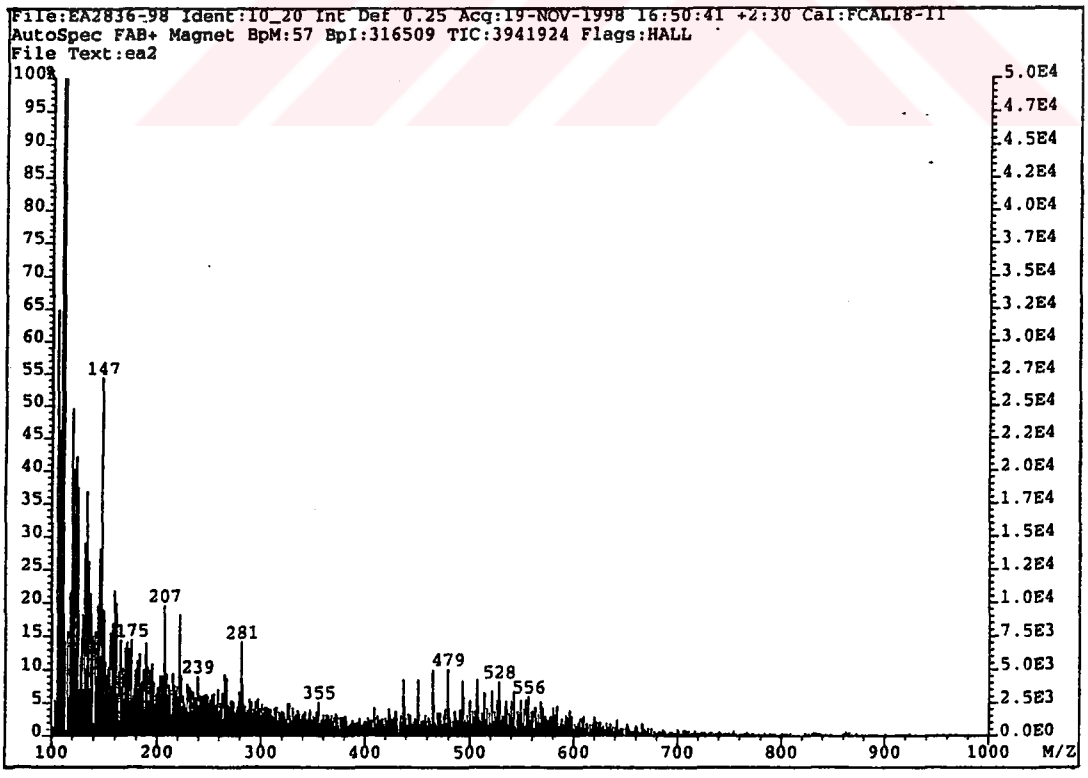

Figure 5.20 Mass spectra of S7A1-V1 pitch (a), and its hexane soluble fraction (b).

suitable fractionation scheme such as extrography. Only in this way can sufficiently simple molecular ion spectra be obtained.

5.7.3 Infrared Spectroscopy

Pitch precursors are very complex materials containing between a hundred and a thousand compounds with different functions and molecular structures and a broad molecular weight distribution. For this reason, the study of their composition, which is the key for a more rational use of these materials, is very difficult [177].

Fourier transform infrared spectroscopy, which provides information about functional groups in a particular substance, is one of the most versatile analytical techniques available for the study of complex mixtures like coals and related materials [178].

It must be taken into account that all carbonaceous solids essentially give the same bands in their IR spectra, which differ from each other by their intensities. Typically, infrared spectroscopy is sensitive to the presence of specific functional groups in organic materials. Thus, IR spectroscopy is widely used in the characterisation of these materials. The examination of IR spectra intensity provides a sort of semiquantitative functional analysis of the complex materials [179].

FTIR spectra of a series of whole Göynük oil shale-Avgamasya asphaltite tar, air-blown pitches, nitrogen-blown pitches, vacuum distilled pitches, and vacuum distilled and then solvent extracted pitch are quite similar showing only differences in their relative intensities.

Figure 5.21 shows the infrared spectra of 100%GOS tar, 50%GOS-50%AA tar, and 70%GOS-30%AA tar. The characteristic absorption bands corresponding to aromatic structures are at 3050, 1600, 870, 813, and 750 cm^{-1}, and aliphatic structures are at 2960, 2918, 2850, and 1377 cm^{-1}. The bands in the region 1600-1470 cm^{-1} are assigned to the stretching of C=C groups, and the bands in the region 900-750 cm^{-1} are assigned to the out-of-plane bending of aromatic C-H groups, bands at 3050 cm^{-1} to the stretching of aromatic groups. The bands at 2968 cm^{-1}, and in the 1450-1377 cm^{-1} region are due to the stretching and bending modes of saturated aliphatic

hydrocarbons [169,180]. The assignments of the bands in the infrared spectra are given in Table 5.8.

Table 5.8. Functional groups and corresponding band frequencies in the infrared spectra of the green fibre [179].

Functional groups	IR vibrational frequency (cm^{-1})	
$-CH_3$ (mostly methyl substituents on aromatic ring	ν-CH δ-CH	2968,2866 1444,1377
$-CH_2$ (mostly methylene linking aromatic rings)	ν-CH δ-CH	2918, ~2850[a] 1478
Unsaturated aliphatic hydrocarbons	ν=CH νC=C	3050 1600
Aromatic rings	ν=C-H	3078-3035
Aromatic rings containing 4 adjacent hydrogens	γ=C-H	750
Aromatic rings containing 2 adjacent hydrogens	γ=C-H	810
Aromatic rings containing isolated hydrogens	γ=C-H	870
-C=O	ν	1697
-OH (free)	ν	~3450
-OH (hydrogen bonded)	ν	~3550

[a]Overlapping bands.

S5A5 tar exhibited a very weak band at 3050 cm^{-1}, and the intensity of this band was weaker for S7A3 and S tars. The aliphatic C-H bands (2855-2960 cm^{-1}) and methylene/naphthenic C-H bending bands (1450 cm^{-1}) of S7A3 and S tars were similar to each other. The band at 1377 cm^{-1} of the S5A5 tar was also more intense compared to the other two samples, indicating presence of more methyl substituents on the aromatic ring systems. GOS has aliphatic nature (H/C=1.44) while AA has aromatic nature (H/C=0.99). The synergistic effect of the copyrolysis of GOS and AA was reflected to the aromaticity of the tars through S, S7A3, and S5A5 tars. S5A5 tar showed the highest aromatic nature followed by S7A3 tar and S tar as deduced from the absorption at 3050 cm^{-1} and 700-900 cm^{-1}. These findings are consistent with H/C ratio where S5A5 tar has the lowest H/C ratio.

Figure 5.22 shows the FTIR spectra of the parent and air-blown pitches. In general, the major air blowing products are carbonyl C=O (1697 cm^{-1}), phenoxyl (1280 cm^{-1}),

and hydroxyl functional groups formed at aliphatic side chain. Both S5A5-A4 and S-A2 pitches showed a slight increase in the peak intensity at about 1700 cm^{-1} related to the formation of carbonyl groups. The absorbances around 1700 cm^{-1} are ascribed to carboxylic ketone, acid, or aldehyde functionality. Akrami [181] has found similar results for the pitches produced by the air-blowing of Avgamasya asphaltite at 330°C for 240 and 360 minutes. The S5A5-A4 pitch displayed an intense signal compared to others near 750 cm^{-1}, which indicates that substituted aromatic rings are present. This intense signal in the absorption of the out-of-plane deformation vibration of aromatic group C-H indicates the generation of ortho-para-positioned two substituted aromatic components. This means that the reaction with air blowing is marked by cross-linked bonding. The aliphatic C-H stretching (2955-2855 cm^{-1}) as well as the methylene/naphthenic C-H bending band (1450 cm^{-1}) was relatively more intense in S5A5-A4 pitch than those of the S-A2 pitch. However, the aromatic C-H stretching band at 3050 cm^{-1} and the aromatic C=C stretching band at 1600 cm^{-1} have been increased in both S5A5-A4 and S-A2 pitches, indicating the occurrence of aromatisation. To compare the two pitches, the increases in aromatic C-H and C=C stretching bands are clearer in S5A5-A4 pitch than the S-A2 pitch. The slight decrease in the peak intensity of 2923 cm^{-1} due to the methylene hydrogen bonding indicates the quantitative consumption of aliphatic material which could be attributed to dehydrogenative aromatisation during air-blowing.

Table 5.9. The relation between softening point and the parameters calculated from the FTIR spectra of the pitches produced by different processes.

Pitches	SP (°C)	H/C	R_1	R_2	R_3	R_4	R_5	I_S	I_{Ar}
S5A5	< 25	1.58	0.07	0.63	0.05	0.08	0.37	0.70	0.06
S5A5-V1	50	1.47	0.12	0.84	0.09	0.17	0.44	0.73	0.11
S5A5-A4	130	1.21	0.31	0.88	0.18	0.34	0.68	0.88	0.24
S5A5-N3	50	1.39	0.15	0.84	0.10	0.18	0.45	0.76	0.13
S5A5-N5	160	0.98	0.67	0.92	0.92	0.56	1.00	0.88	0.40
S7A3	< 25	1.78	0.12	0.59	0.04	0.07	0.33	0.35	0.11
S7A3-V1	50	1.50	0.19	0.90	0.12	0.24	0.57	0.86	0.16
S7A3-E1	136	1.08	0.35	0.79	0.20	0.36	0.75	0.86	0.26
S	50	1.55	0.05	0.58	0.04	0.06	0.24	0.78	0.05
S-A2	110	1.32	0.27	0.90	0.14	0.27	0.61	0.93	0.21

R_1, aromatic C-H(3050 cm^{-1})/CH_2(2925 cm^{-1}); R_2, CH_3(2855 cm^{-1})/CH_2(2925 cm^{-1}); R_3, aromatic C=C(1600 cm^{-1})/[CH_2(2925 cm^{-1})+CH_3(2855 cm^{-1})]; R_4, aromatic C=C(1600 cm^{-1})/CH_2(2925 cm^{-1}) ; R_5, aromatic C=C(1600 cm^{-1})/aliphatic C-H(1450 cm^{-1}); I_S, substitution number, (870 cm^{-1})/(750 cm^{-1}); I_{Ar}, hydrogen aromaticity index, C-H(3050 cm^{-1})/[aromatic C-H(3050 cm^{-1})+ CH_2(2925 cm^{-1})].

From Table 5.9 the highest aromatic hydrogen concentrations (absorbencies at 3050 cm^{-1}) among the air-blown pitches can be observed for S5A5-A4 pitch. The hydrogen aromaticity (I_{Ar}) of S5A5-A4 and S-A2 pitches were similar and 0.24, and 0.21, respectively. There is a significant increase in hydrogen aromaticity for both pitches compared to parent tar. The increase in aromaticity index is an indicative of an increase in the degree of polymerisation of the sample [88]. This clearly illustrates that the aromaticity of air-blown pitches increases with increasing softening point. Between two air-blown pitches, S5A5-A4 is the most aromatic product. This is also confirmed by the low H/C atomic ratio calculated from elemental analysis results.

The infrared spectra of nitrogen-blown pitches are presented in Figure 5.23. It should be noted that the relative intensity of the bands in the region 900-700 cm^{-1}, 3050 cm^{-1}, and 1600 cm^{-1} are dependent on the blowing time and temperature, since the increase in the relative intensities of aromatic C-H (3050 cm^{-1}) and the out-of-plane aromatic C-H bending (900-700 cm^{-1}) bands in the spectra of S5A5-N5 pitch indicates that S5A5-N3 pitch is less aromatic than S5A5-N5 pitch. However, it is clear that both nitrogen blowing processes increased the aromaticities of these pitches when they are compared with the parent S5A5 tar. This is confirmed by the sharp increase in the band intensity at 1600 cm^{-1} due to aromatic C=C stretching in both S5A5-N3 and S5A5-N5 pitches. This result is consistent with the H/C ratio. Nitrogen-blowing resulted in the decrease in the peak intensity at about 1700 cm^{-1} related to carbonyl groups. The decrease in the intensity of 1700 cm^{-1} band should be attributed to the distillation of oxygen containing compounds by the effect of temperature during nitrogen-blowing.

The main difference between S5A5-N3 and S5A5-N5 pitches, for S5A5-N5 pitch there is a simultaneous decrease in the intensity of both the aliphatic C-H stretching bands (2850 cm^{-1} to 2968 cm^{-1}) and the CH_2 stretching and bending bands (2918 cm^{-1} and 1455 cm^{-1}) respectively, compared to parent S5A5 tar. This result indicates that S5A5-N5 pitch contains more aromatic structure than that of S5A5-N3 pitch although S5A5-N3 pitch was treated for a long time (240 minutes) at 250°C. This is confirmed with low H/C atomic ratio and high hydrogen aromaticity (I_{Ar}) of S5A5-N5 pitch.

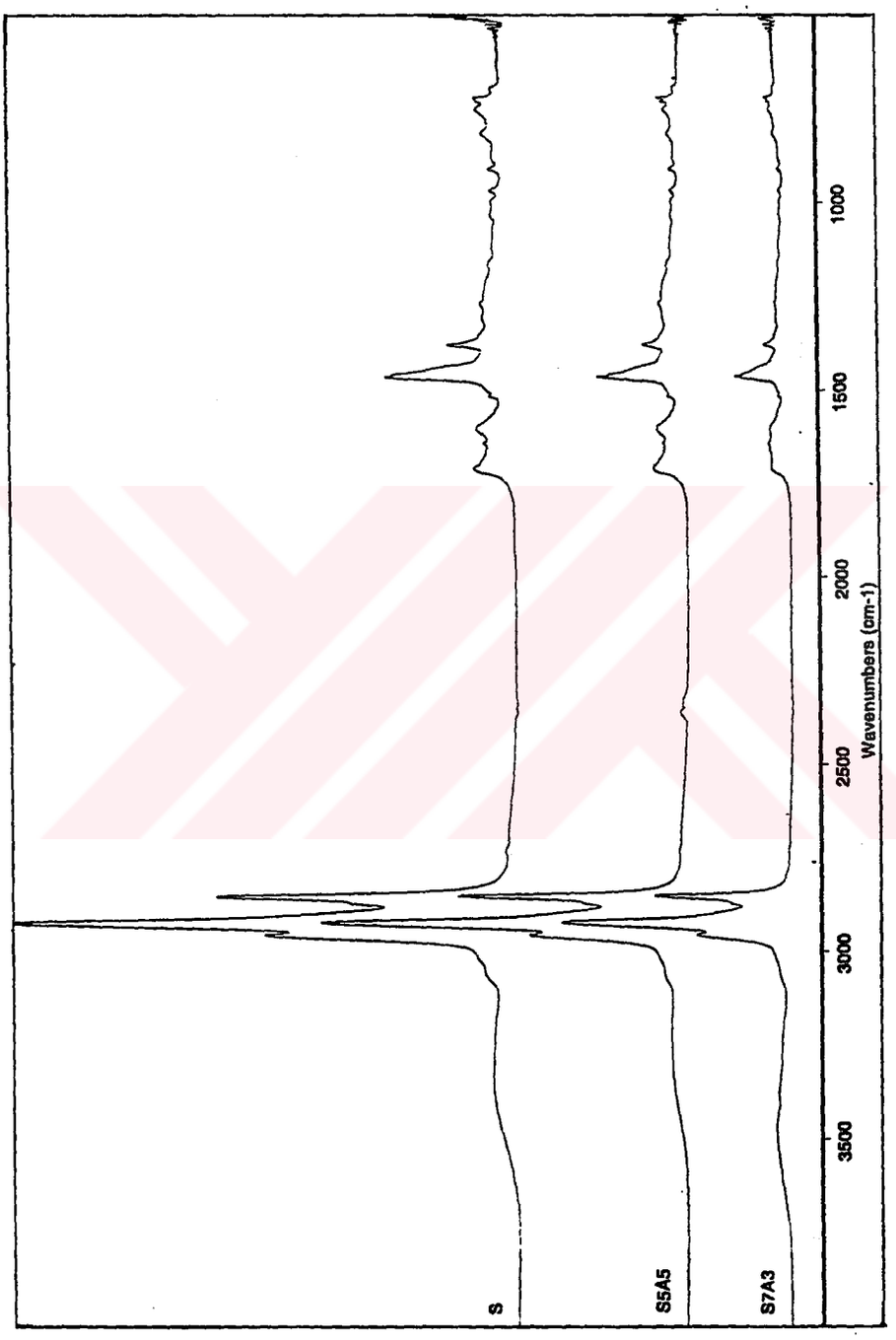

Figure 5.21 FTIR spectra of S, S5A5, and S7A3 tars.

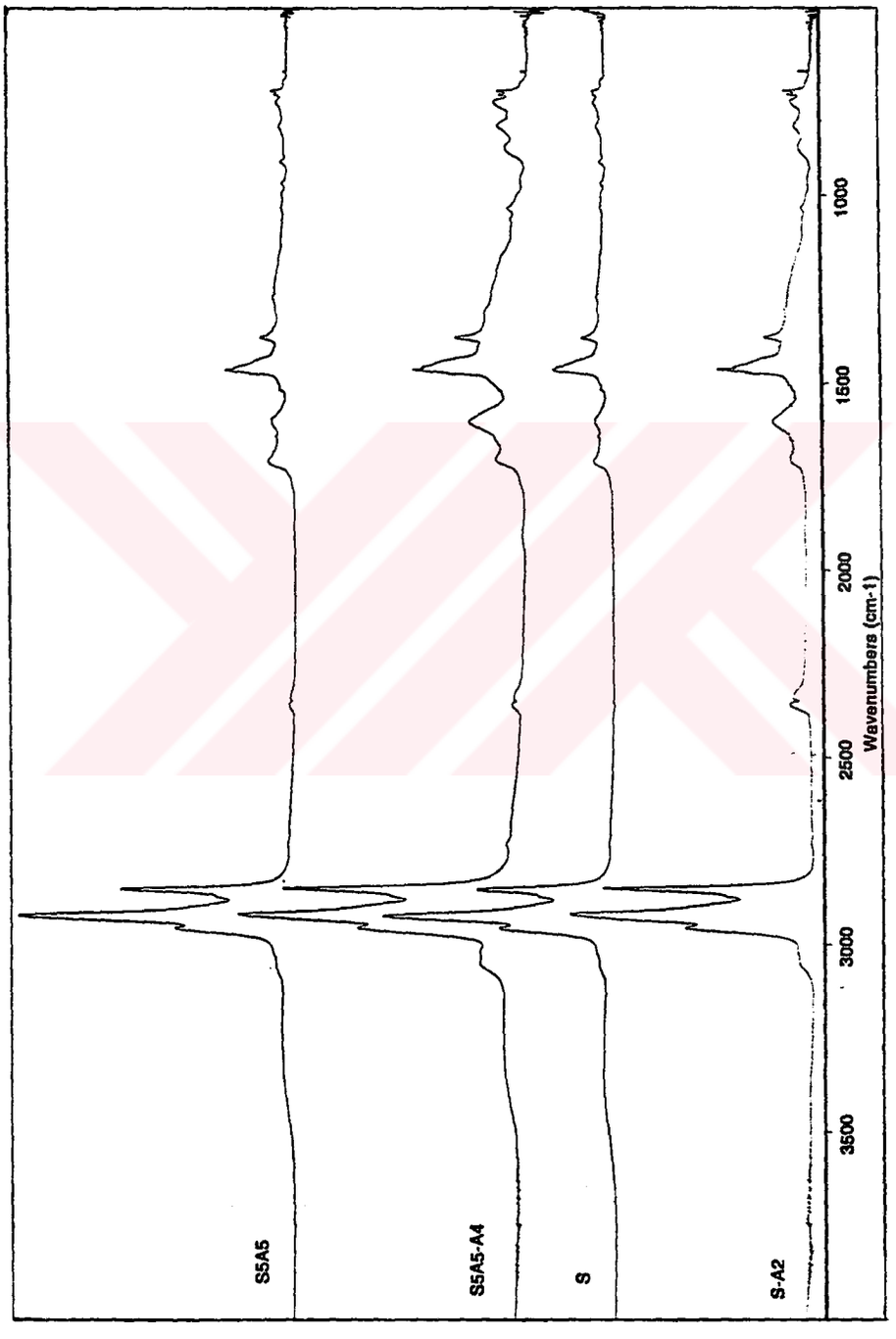

Figure 5.22 FTIR spectra of the parent tar and air-blown pitches.

It can be revealed that the FTIR results are in good agreement with previously reported results that blowing temperature is more effective than the blowing time.

The FTIR spectra of the vacuum distilled (S5A5-V1 and S7A3-V1) pitches and vacuum distilled and then extracted pitch (S7A3-E1) are compared in Figure 5.24. The FTIR spectra of the vacuum distilled pitches showed that the relative intensities of aliphatic C-H bands at 2850 cm^{-1} and 2968 cm^{-1} were intense. This indicates that these pitches contain significant amounts of aliphatic components. The strong bands at 2918 cm^{-1} arise from the saturated C-H stretching vibrations of alkyl substituents (methlyene groups $-CH_2$) and the weak bands near 3050 cm^{-1}, suggest that the aromatic rings are highly substituted. The aliphatic C-H stretching bands at 2918-2950 cm^{-1} and methylene/naphthenic C-H bending band at 1480 cm^{-1} of S7A3-V1 pitch were less intense than S5A5-V1 pitch indicating that S5A5-V1 pitch contains more methylene substituents on the aromatic ring system than S7A3-V1 pitch. The intensities of the bands at 750-870 cm^{-1} were the same for both pitches.

There is a significant difference between vacuum distilled S7A3 pitch (S7A3-V1) and vacuum distilled and then hexane extracted S7A3 pitch (S7A3-E1). Extraction with hexane of vacuum distilled S7A3-V1 pitch resulted in a decrease in the intensity of the aliphatic carbon-hydrogen bands. The bands at 2700-2970 cm^{-1} and 1450 cm^{-1} decreased with increasing softening point while the bands at 3050 and 1600 cm^{-1} were almost unchanged. The band at 1377 cm^{-1} (methyl groups $-CH_3$) decreased in intensity. All of these findings found for S7A3-E1 pitch are confirmed by the low H/C atomic ratio and high hydrogen aromaticity (I_{Ar}).

Figure 5.25 shows the comparison of FTIR spectra of S5A5 pitches derived by different methods: air-blown (S5A5-A4), nitrogen-blown (S5A5-N3 and S5A5-N5), and vacuum distilled (S5A5-V1).

Among the various methods studied, S5A5-N5 pitch showed the highest aromatic nature followed by S5A5-A4, S5A5-N3, and S5A5-V1, respectively, as indicated by the relative intensities of aromatic C-H (3050 cm^{-1}) and aromatic intensities of C-H out-of-plane bending modes (700-900 cm^{-1}) in the FTIR spectra in Figure 5.25. This result is consistent with the H/C atomic ratio, aromaticty index (I_{Ar}), and therefore with softening points of the pitch materials.

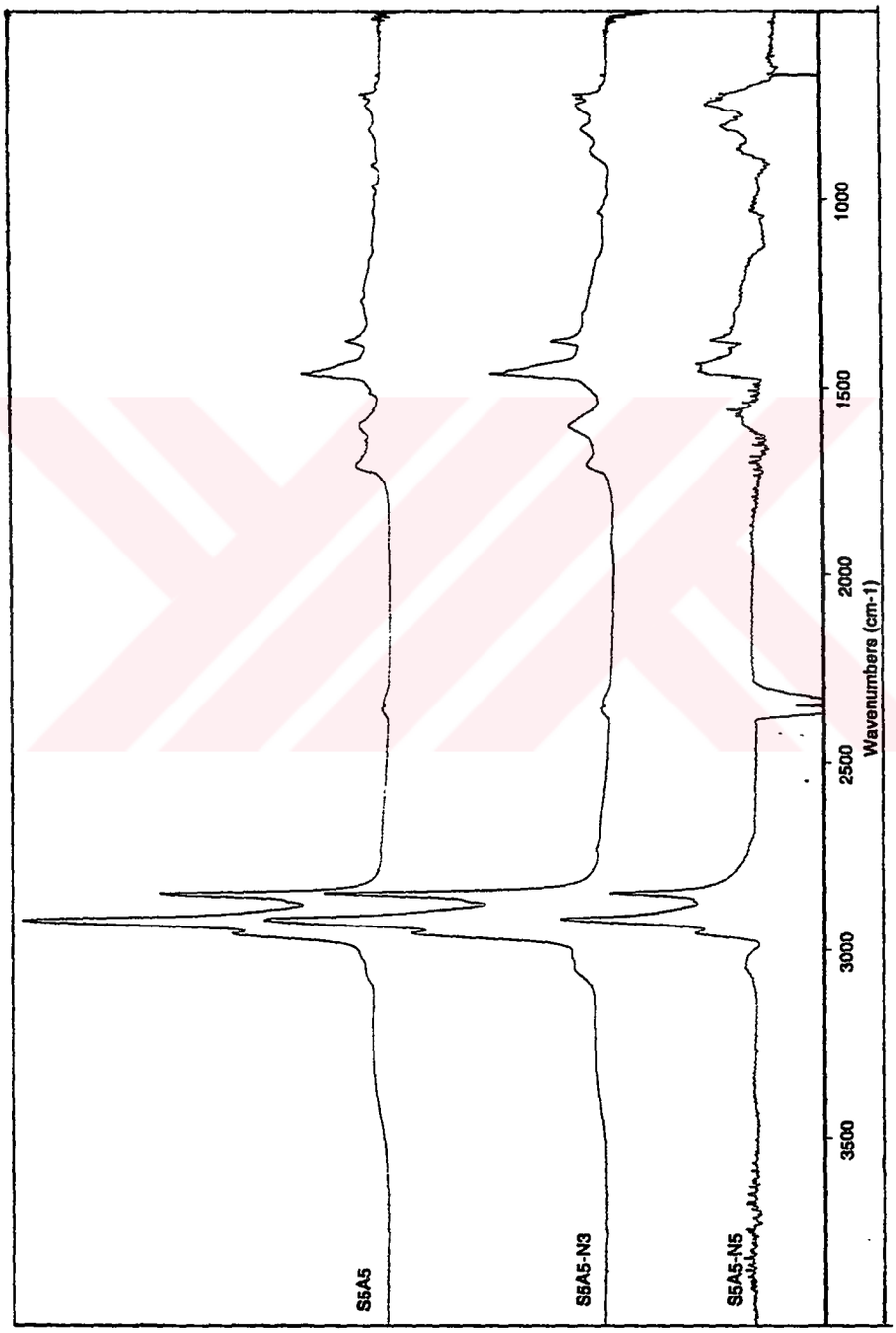

Figure 5.23 FTIR spectra of the parent tar and nitrogen-blown pitches.

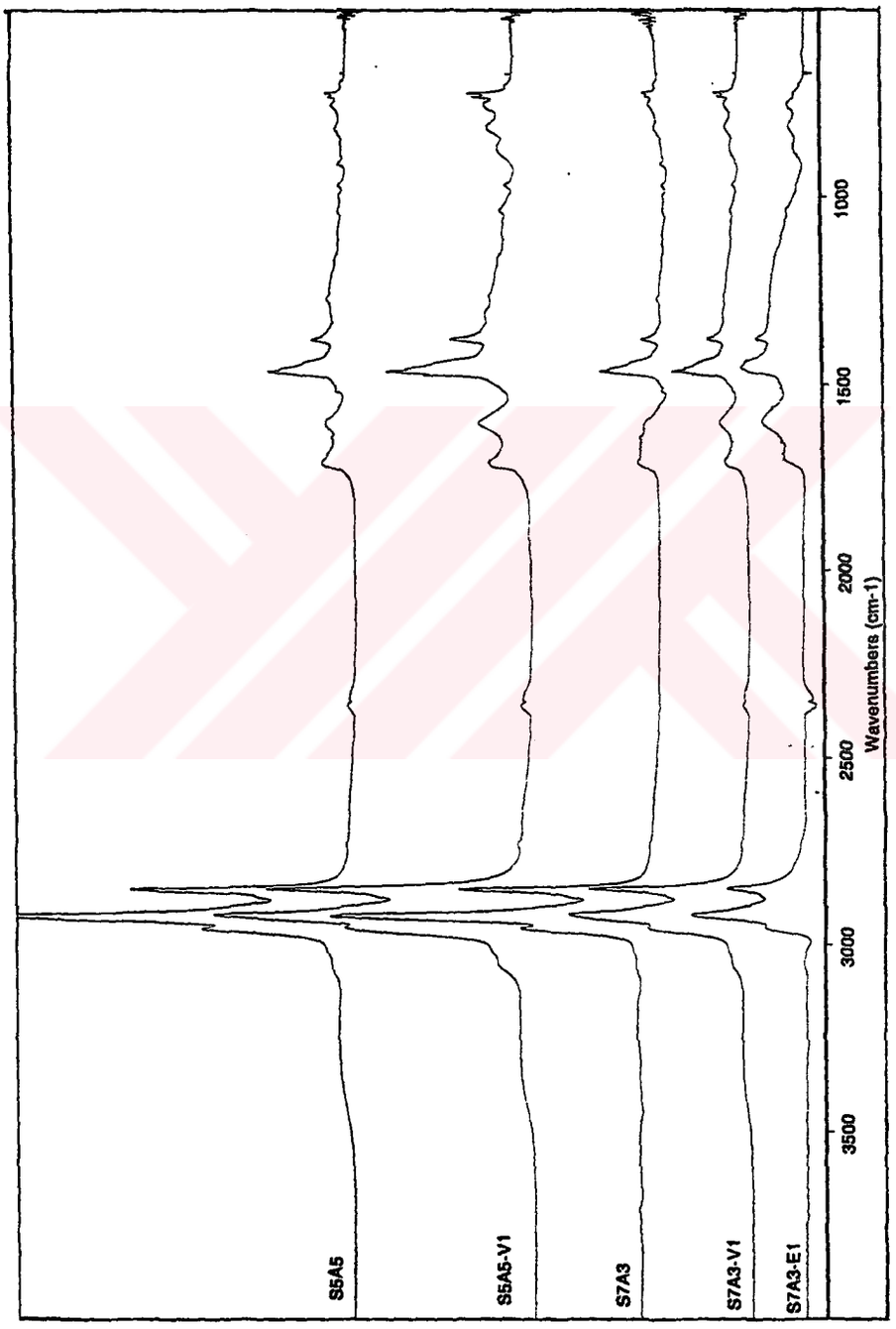

Figure 5.24 FTIR Spectra of parent tars, vacuum-distilled, and vacuum-distilled-solvent extracted pitches.

All pitches essentially have the same bands in their infrared spectra, but differ in intensity. For example, the band near 3050 cm^{-1}, which is due to aromatic C-H stretching vibrations, is observed more or less for every pitch, and it suggests that the aromatic rings are sparsely substituted. The peak at ~ 2920 cm^{-1} is clearly seen for every pitch and it arises from the saturated C-H stretching vibrations of alkyl substituents. Thus the intensity ratios need to be examined to be able to evaluate more precisely the effect of various preparation processes and operation conditions on the molecular structures of pitches [182].

Several parameters calculated from the intensity ratios of characteristic absorption bands were designated as R_1 to R_5, I_{Ar}, and I_S [180] . These parameters of air-blown, nitrogen-blown, vacuum distilled and vacuum-distilled-hexane extracted pitches were calculated and the results were shown in Table 5.9.

For S5A5 tar derived pitches it should be noted that R_1 increased from 0.07 to 0.12, 0.15, 0.31, and to 0.67 for S5A5 tar, S5A5-V1, S5A5-N3, S5A5-A4, and S5A5-N5 pitches, respectively. For S7A3 tar derived pitches, vacuum distilled-hexane extracted pitch showed the highest R_1 value as 0.35. These results indicate that the ratio of aromatic to aliphatic hydrogen increased with increasing softening point for the same originated pitches.

R_2 and R_3 reflect the relative abundance of CH_3 and CH_2 groups as well as aromatic carbon and aliphatic carbon. There was an increase in R_2 and R_3 values from S5A5 to S5A5-V1, S5A5-N3, S5A5-A4, and S5A5-N5. The extend of increase in the values of R_2 and R_3 was correlated with H/C atomic ratios. Unexpectedly, the value of R_2 for S7A3-V1 was greater than that of S7A3-E1. The intensity ratios of R_4 and R_5 indicate the aromaticity, and there is an increase in the order of S5A5 < S5A5-V1 < S5A5-N3 < S5A5-A4 < S5A5-N5, for S5A5 derived pitches and S7A3< S7A3-V1 < S7A3-E1 for S7A3 derived pitches, respectively. Comparison of the different methods for S5A5 derived pitches show that nitrogen-blowing at 300°C and 60 minute gave the largest values of R_4 and R_5, indicating the higher aromaticity. The absorbencies at 3050 and 2920 cm^{-1} allow evaluation of the concentrations of aromatic and aliphatic C-H bonds in pitches. Hydrogen aromaticity indices (I_{Ar}),

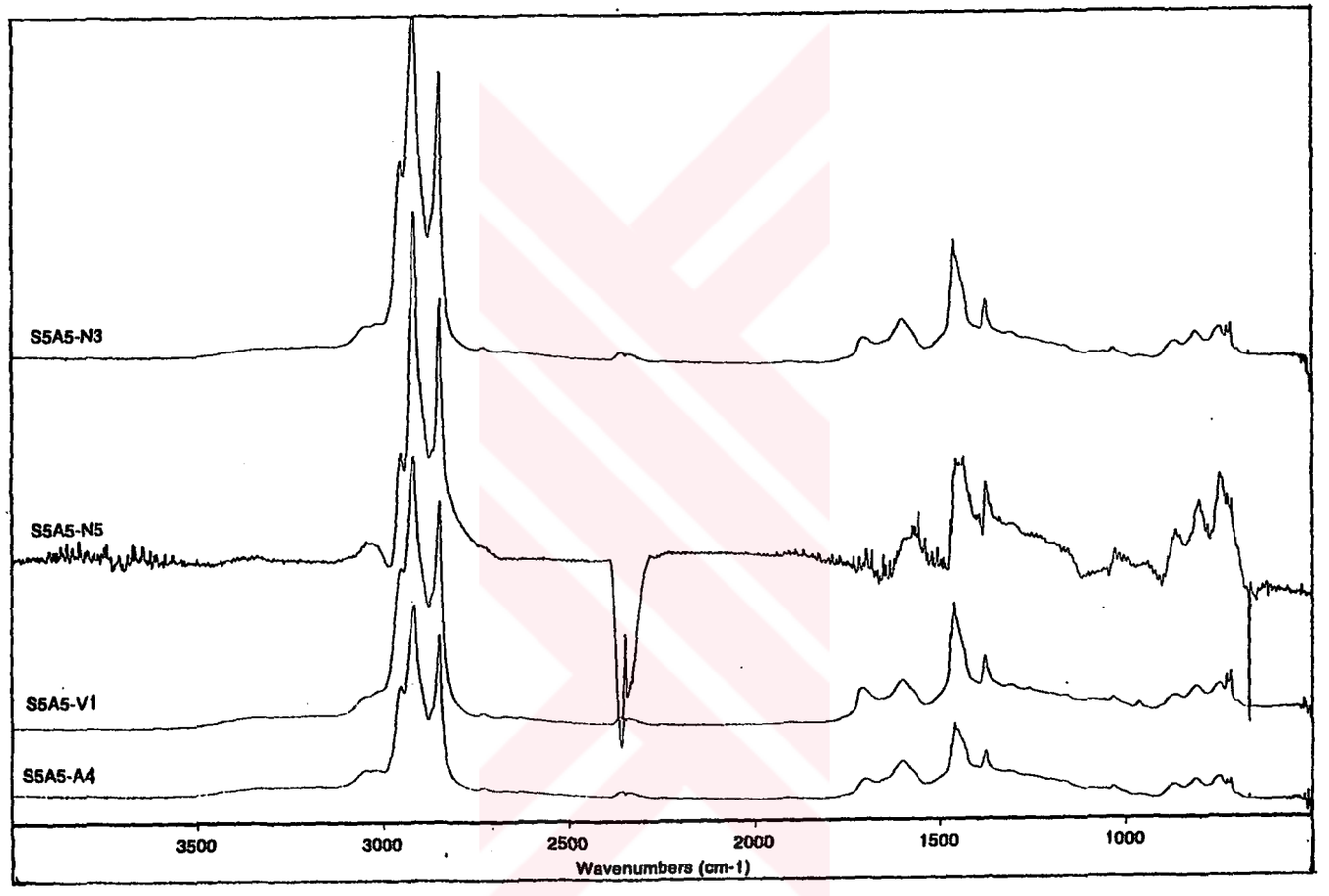

Figure 5.25 Comparison of FTIR spectra of the S5A5 derived pitches by different methods: air-blowing (S5A5-A4), nitrogen blowing (S5A5-N3 and S5A5-N5), and vacuum distillation (S5A5-V1).

were also calculated. The highest value for I_{Ar} was obtained for S5A5-N5 and S7A3-E1 pitches. These data indicate a preponderance of aliphatic hydrogen and the relative degree of saturation of aromatic rings.

5.8 Estimation of Structural Parameters of Pitches by ^{1}H and ^{13}C NMR

5.8.1 Characterisation of pitches by ^{1}H NMR

^{1}H NMR is a technique which can be used very effectively to analyse hydrogens of chemically different types. It can distinguish not only between hydrogen atoms in aromatic and non-aromatic systems but also between those hydrogen atoms on carbon atoms in α-position with respect to the aromatic ring and those, which are not immediately adjacent to aromatic rings. In addition, the integrated intensities of the different peaks in the NMR spectrum are directly proportional to the numbers of hydrogen atoms involved, independent of their chemical nature.

The different proton types producing absorption in the ^{1}H NMR spectrum were defined by the following chemical shift ranges shown in Table 5.10: aromatic protons, 9.0-6.8 ppm; α-protons on alkyl side chains, 4.0-2.0 ppm; and protons other than α on side chains, 2.0-0.5 ppm. Olefinic proton absorptions (6.0-4.0 ppm) were hardly detected since none of the samples produced significant absorption in this region. The integrated aromatic hydrogen and total aliphatic hydrogen intensities were normalised over the complete spectrum (9.0-0.5 ppm). The clearly defined peak at around 7.25 ppm is due to deuterochloroform ($CDCl_3$) used as solvent for all the samples.

Figures 5.26-5.30 present ^{1}H NMR spectra of the pitches produced under different methods such as air-blowing (S-A2 and S5A5-A4), nitrogen-blowing (S5A5-N5), vacuum-distillation (S7A3-V1), and vacuum distillation followed by solvent extraction (S7A3-E1), respectively.

The proton absorptions for S5A5-A4, S5A5-N5, and S7A3-E1 pitches are mostly broad and there are few sharply defined peaks. However, the proton absorptions for S-A2 and S7A3-V1 pitches are sharply defined. The peak at 0.96 ppm is overlapped

by the peak at 1.35 ppm in the spectra of S5A5-A4 pitch while it is separate in all other spectra.

Table 5.10 ^{1}H NMR spectral assignments [152].

H_A: 6.8-9.0 ppm	Hydrogens attached to aromatic ring carbons.
H_{OL}: 4.0-6.0 ppm	Hydrogens attached to carbons forming double bonds.
H_α: 2.0-4.0 ppm	Hydrogens attached to carbons in alkyl substitution α to aromatic ring.
$H_{\alpha 1}$: 2.0-2.3 ppm	Hydrogen in methyl group α to aromatic ring.
$H_{\alpha 2}$: 2.3-4.0 ppm	Hydrogen in CH_2 and CH groups of saturates.
H_β: 1.0-2.0 ppm	Hydrogens in alkyl substitution β- or further from aromatic rings.
H_{CH}: 1.6-2.0 ppm	Hydrogens in CH groups of saturates.
H_{CH2}: 1.0-1.6 ppm	Hydrogens in CH_2 groups of saturates (including cycloparaffins).
H_γ or H_{CH3}: 0.5-1.0 ppm	Hydrogen in terminal or isolated CH_3 groups of saturates or hydrogens in alkyl groups substituted in position γ- and further from aromatic ring.

Figures 5.26 and 5.29 present proton nuclear magnetic resonance spectra of the air-blown pitch (S-A2) and vacuum-distilled pitch (S7A3-V1), respectively. The proton spectrum of these two pitches display clear peaks at around 0.91, 0.94, and 0.96 ppm which is due to methyl protons attached to carbon positioned γ or further from the aromatic rings. However, these three peaks are overlapped in the spectra of other pitches.

The proton NMR spectrum of S-A2 pitch resembles to that of S7A3-V1 pitch while the proton NMR spectrum of S5A5-N5 pitch resembles to that of S7A3-E1 pitch. The main difference between the four spectra is the relative concentrations of the various structural groups indicated by peak intensities in specific chemical shift ranges. For S-A2 and S7A3-V1 pitches, aromatic-hydrogen signals are weak compared to S5A5-A4, S5A5-N5, and S7A3-E1 pitches, showing the presence of low quantity of aromatic structures. The H_β and H_γ signals are narrow and are consistent with long alkyl side chains as discussed later in Table 5.11.

The peak at 1.25, 1.31, 1.35, 1.29, and 1.33 ppm for S7A3-V1, S-A2, S5A5-A4, S7A3-E1, and S5A5-N5 pitches, respectively, are due to long alkyl side chain methylene, i.e., $(CH_2)_M$, where M≥8. This region also contains methyl protons

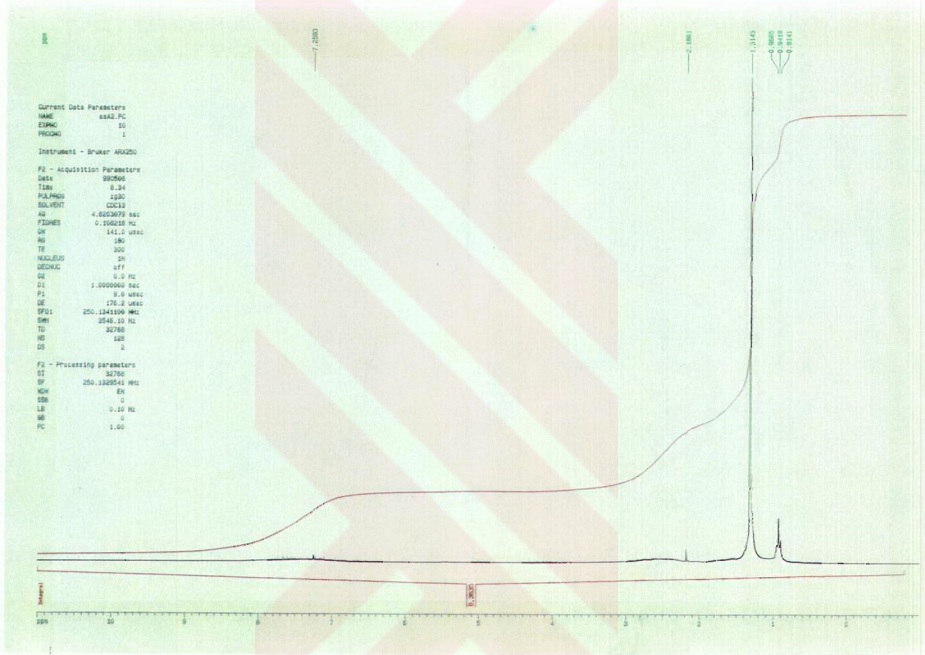

Figure 5.26 ^{1}H NMR spectrum of S-A2 pitch.

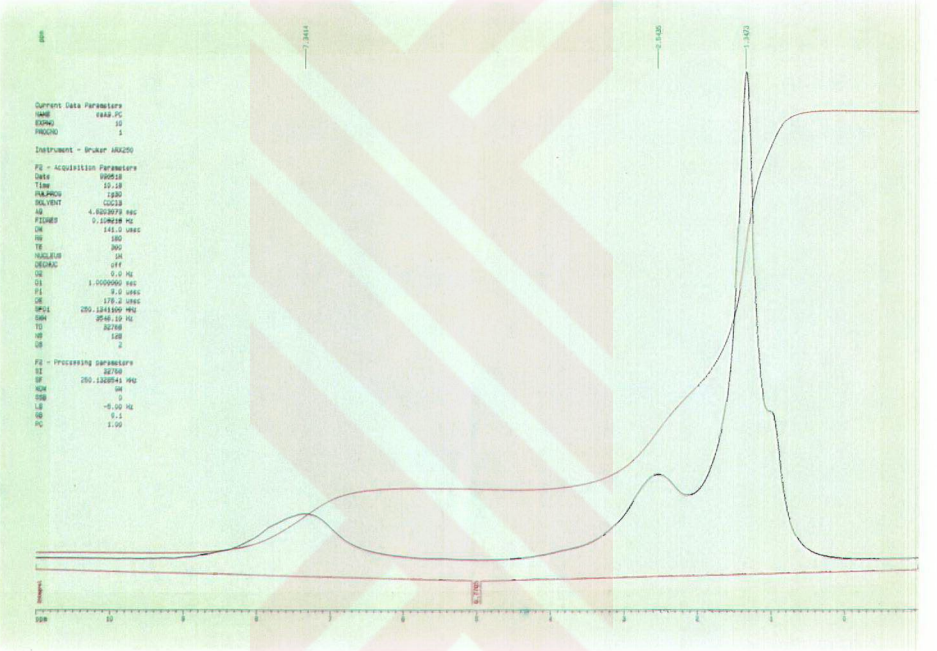

Figure 5.27 ^{1}H NMR spectrum of S5A5-A4 pitch.

attached to a carbon positioned β to an aromatic ring. The proton data of S5A5-N5 pitch shows the highest increase while S7A3-E1 pitch shows a slight increase in aromatic-hydrogen content as 0.25 and 0.15, respectively (Table 5.11). This indicates an increase in condensation with heat treatment under nitrogen and with solvent extraction. This result is accompanied by a decrease in protons attached to carbon in the CH, CH_2 (β) hydrocarbon groups, 0.45 for S5A5-N5 and 0.46 for S7A3-E1 pitches.

Table 5.11. Hydrogen distribution of pitches.

Band (ppm)	S-A2	S5A5-A4	S5A5-N5	S7A3-V1	S7A3-E1
H_A	0.14	0.14	0.25	0.09	0.15
H_{OL}	$5x10^{-3}$	$5x10^{-3}$	0.01	$5x10^{-3}$	$5x10^{-3}$
$H_{\alpha 1}$	0.03	0.06	0.03	0.04	0.06
$H_{\alpha 2}$	0.12	0.16	0.18	0.12	0.21
H_{α}	0.15	0.22	0.21	0.16	0.27
H_{CH}	0.04	0.10	0.07	0.06	0.08
H_{CH2}	0.56	0.45	0.38	0.57	0.38
H_{β}	0.60	0.55	0.45	0.63	0.46
H_{γ} or H_{CH3}	0.11	0.09	0.09	0.12	0.12

As seen from Table 5.11, S5A5-N5 pitch contains the highest aromatic hydrogens while S7A3-V1 pitch contains the highest aliphatic hydrogens. This result is also consistent with the aromaticity index (I_{Ar}) data which was obtained by FTIR. It is very obvious that air-blowing was not as successful as nitrogen-blowing and solvent extraction to increase the aromaticity. Moreover, hydrogens attached to carbons forming double bonds were negligible.

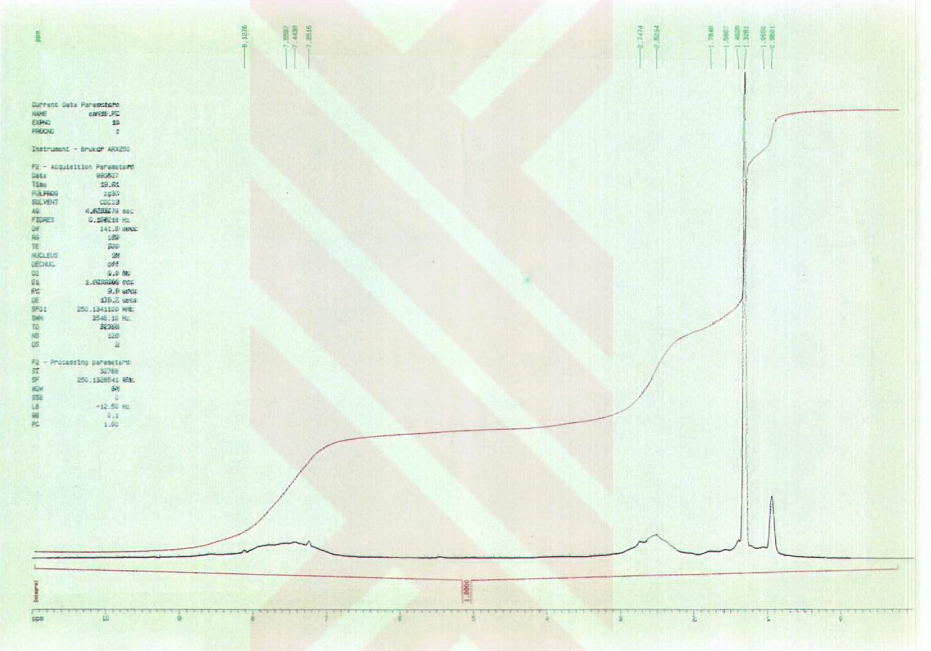

Figure 5.28 ^{1}H NMR spectrum of S5A5-N5 pitch.

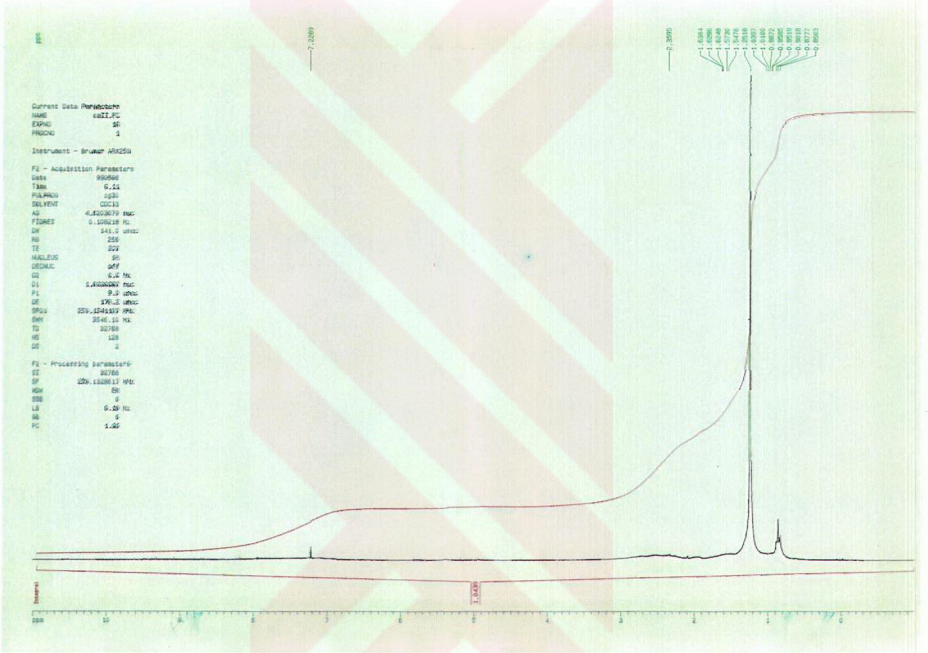

Figure 5.29 ^{1}H NMR spectrum of S7A3-V1 pitch.

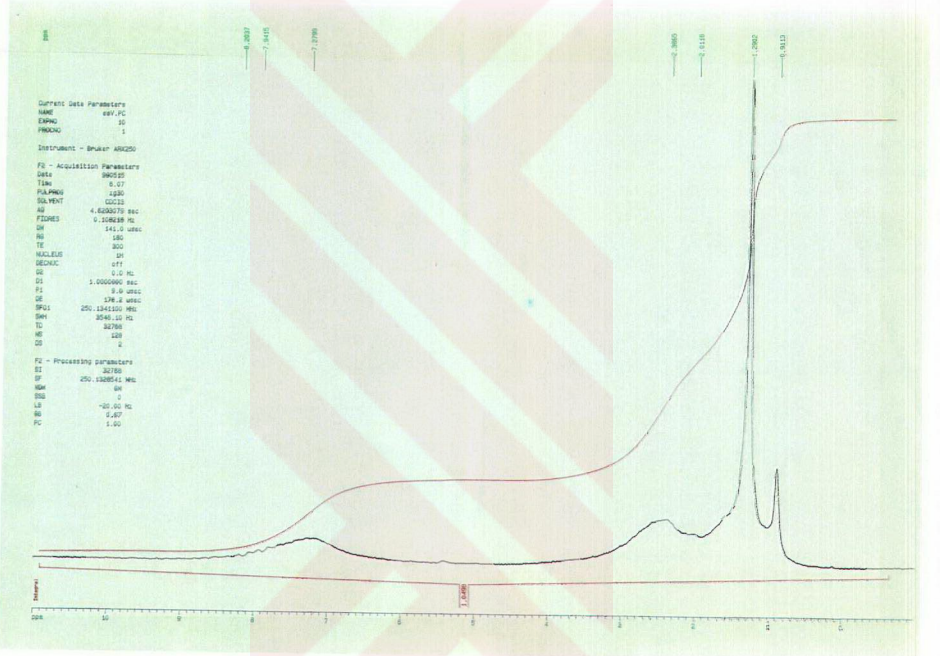

Figure 5.30 ^{1}H NMR spectrum of S7A3-E1 pitch.

5.8.2 Characterisation of pitches by ^{13}C NMR

From the ^{13}C NMR spectra of the samples, aromatic carbon (150-117 ppm) and aliphatic carbon (60-8.5 ppm) absorptions were integrated, and the aromaticity (C_{Ar}) of the samples were calculated (fraction of aromatic over total carbon) depending on the ^{13}C NMR spectral assignments shown in Table 5.12. The calculated results of carbon distribution of pitches are summarised in Table 5.13.

Table 5.12. ^{13}C NMR spectral assignments [152,183].

Band (ppm)	Assignments
ALIPHATIC	
C_{Ali} : 8.5-54.0	Aliphatic carbon atoms
$C_{Al.1}$: 8.5-21.9	Methyl carbon
C_{Al-2} : 21.9-54.0	Methylene carbon
AROMATIC	
C_{Aro} : 117-150	Aromatic carbon atoms
CH_{Aro} : 117-127	Protonated carbon atoms
C_q : 127-150	Quaternary carbon atoms
C_{oq} : 127-133	Outer carbon atoms
C_s : 133-138	Substituted carbon atoms
C_{qs} : 138-150	Substituted quaternary carbon atoms or internal benzonaphthenic carbons.

The ^{13}C spectra of S-A2, S5A5-A4, S5A5-N5, S7A3-V1, and S7A3-E1 pitches are shown in Figures 5.31-5.35. In all five spectra, absorptions are confined to two ranges from 10 to 60 ppm and 110 to 160 ppm, corresponding to aliphatic and aromatic resonances, respectively. The peaks around 77 ppm are due to the carbon of the solvent, deuteriochloroform, used.

All the spectra displayed well-resolved, rather big and sharp absorption bands in the aliphatic region. However, big lumps are obtained in the aromatic region in each spectrum.

It should be noted that from the chemical shift value, the combination of lines around 14.2, 22.8, 29.8, and 31.9 ppm, which were observed in the spectrum of S-A2, S5A5-

A4, S5A5-N5, and S7A3-E1 pitches, would be compatible with a straight-chain alkane structure. The 21.5 ppm signal in the spectrum of S7A3-V1 pitch, 22.7 ppm signal in the spectra of S-A2 and S7A3-E1 pitches, and 22.8 ppm signal in the spectra of S5A5-A4 and S5A5-N5 pitches can be assigned to methyl groups. The 29.8 ppm signal observed in the spectrum of S-A2, S5A5-A4, and S5A5-N5 pitches and 29.6 ppm signal in S7A3-E1 pitch and 28.4 ppm signal in S7A3-V1 pitch can be assigned to internal methylene carbons of longer paraffinic chains. The resonances of the corresponding terminal methyl and the methylene functions were found around 14.2, 22.7, and 32.0 ppm, respectively.

Compared with the aliphatic carbon resonances, big lumps are observed in the aromatic region for all pitch materials. The main absorption band in the aromatic region does not appear structured into a number of well-resolved single resonance. The signal at around 127 ppm must be associated with the quaternary carbons of the polycyclic structures, and this band is very strong in the spectrum of S5A5-N5 pitch.

S5A5-N5 pitch has the largest number of tertiary carbons (CH_{Aro}), which means that nitrogen blowing increased unsubstituted carbon (protonated carbon, CH_{Aro}). For nitrogen-blown pitch S5A5-N5, the highest value for the number of aromatic carbon was observed. This is mainly due to an increase in the quaternary carbons, C_{oq}, which is a measure of condensation reactions. Carbons in methylene group ($CH_{Al.2}$) decreased and those in methyl groups ($CH_{Al.1}$) increased as a result of hydrogen transfer to radicals formed after opening of naphthenic rings.

Vacuum distillation was not a successful technique to increase the aromaticity as S7A3-V1 pitch has the highest amounts of aliphatic carbons. The intensity of aliphatic signals at 12.9, 21.5, and 30.6 ppm is high as shown in Figure 5.34 for S7A3-V1 pitch.

S5A5-N5 pitch was followed by S7A3-E1 pitch as the second highly aromatic pitch, since the methylene carbon, $CH_{Al.2}$, values are lower and the higher values in the aromatic carbons. The C_s carbon and CH_{Aro} carbon (unsubstituted aromatic carbons) were also high in S7A3-E1 pitch. This indicates that the naphthalene structure was converted to an aromatic structure by dehydrogenation. These results are consistent with the data obtained by ^1H NMR.

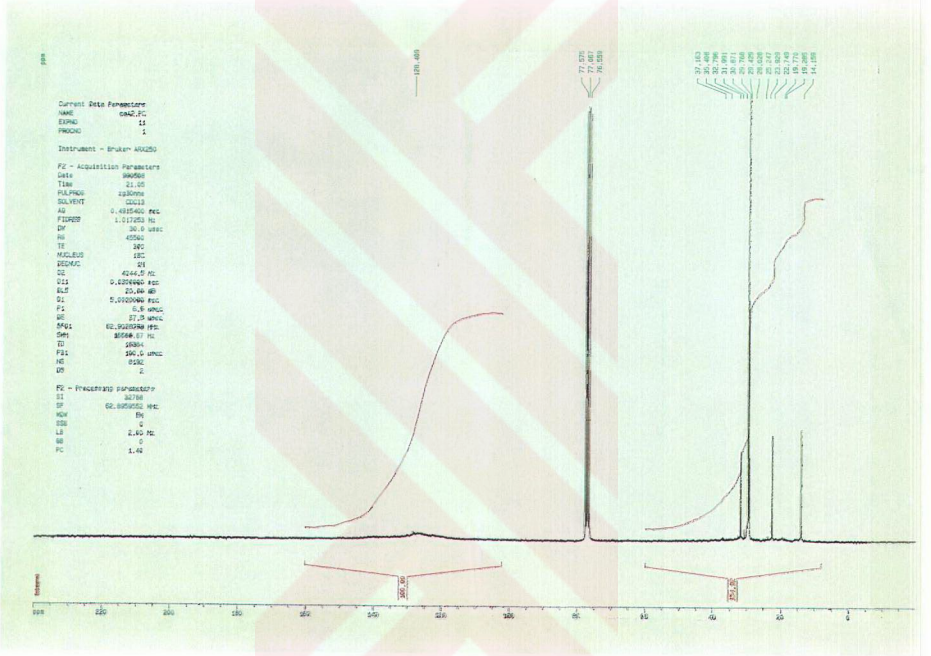

Figure 5.31 ^{13}C NMR spectrum of S-A2 pitch.

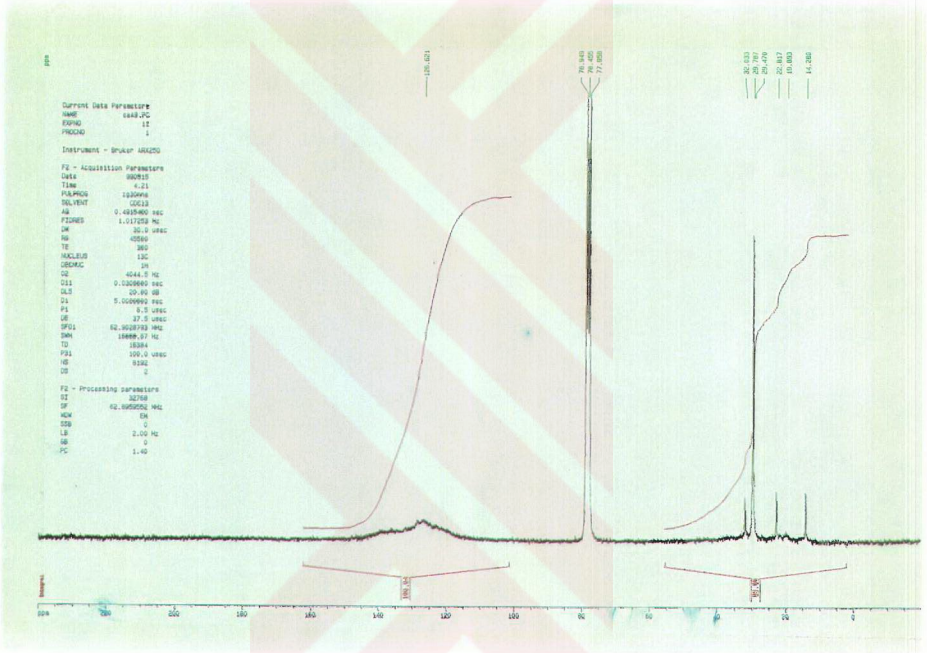

Figure 5.32 ^{13}C NMR spectrum of S5A5-A4 pitch.

Table 5.13. Carbon distribution of pitches.

Band (ppm)	S-A2	S5A5-A4	S5A5-N5	S7A3-V1	S7A3-E1
$C_{Al.1}$	0.16	0.16	0.22	0.18	0.19
C_{Al-2}	0.81	0.79	0.72	0.77	0.76
C_{Ali}	0.97	0.95	0.94	0.95	0.95
CH_{Aro}	0.35	0.36	0.42	0.29	0.37
C_q	0.54	0.57	0.60	0.36	0.59
C_{oq}	0.25	0.29	0.31	0.17	0.29
C_s	0.12	0.14	0.23	0.10	0.17
C_{qs}	0.12	0.14	0.12	0.08	0.15
C_{Aro}	1.42	1.50	1.68	1.00	1.57
$C_{Al-2}/ C_{Al.1}$	5.06	4.94	3.27	4.28	4.00
$C_{Ali}+ C_{Aro}$	2.39	2.45	2.62	1.95	2.52
FRACTIONS					
C_{Ali}	0.41	0.39	0.36	0.49	0.38
C_{Aro}	0.59	0.61	0.64	0.51	0.62

S-A2 pitch has the largest $CH_{Al.2}/ CH_{Al.1}$ ratio than the others. This indicates that S-A2 pitch has a greater number of methylene carbon than methyl carbon.

The calculated structural parameters for the S-A2, S5A5-A4, S5A5-N5, S7A3-V1, and S7A3-E1 pitches by using the equations listed in Table 5.I4 [152] are summarised in Table 5.15.

There are significant differences in some of the important structural parameters for the pitches. The hydrogen distribution data show that S5A5-N5 pitch contains the largest amounts of H_{Aro}, around 25% leading to the highest fa^{13} (aromaticity) of around 55%. On the other hand, S7A3-V1 pitch contains the smallest amount of aromatic hydrogen (9%), and therefore, the aromaticity fa^{13} is low (43%). It should be noted that nitrogen blowing emphasised the dehydrogenative condensation, as previously mentioned, of the pitch by lowest substitution percent of the aromatic rings, σ.

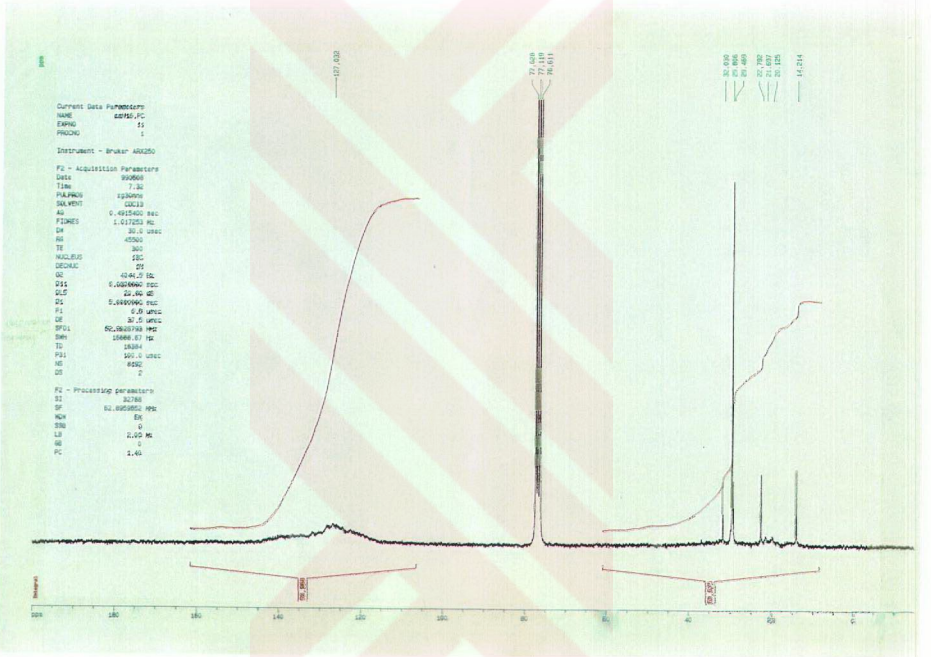

Figure 5.33 ^{13}C NMR spectrum of S5A5-N5 pitch.

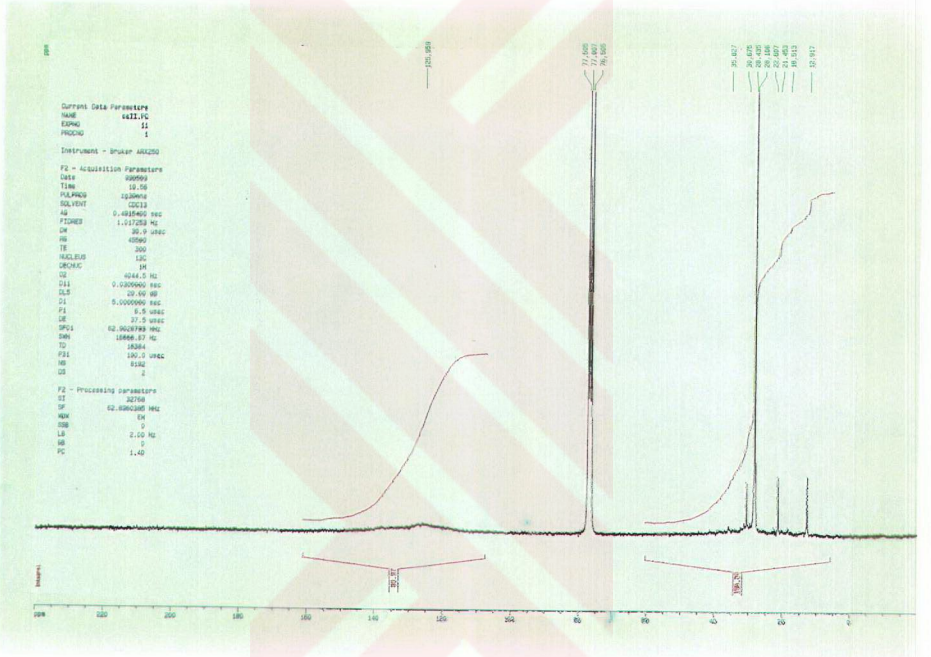

Figure 5.34 ^{13}C NMR spectrum of S7A3-V1 pitch.

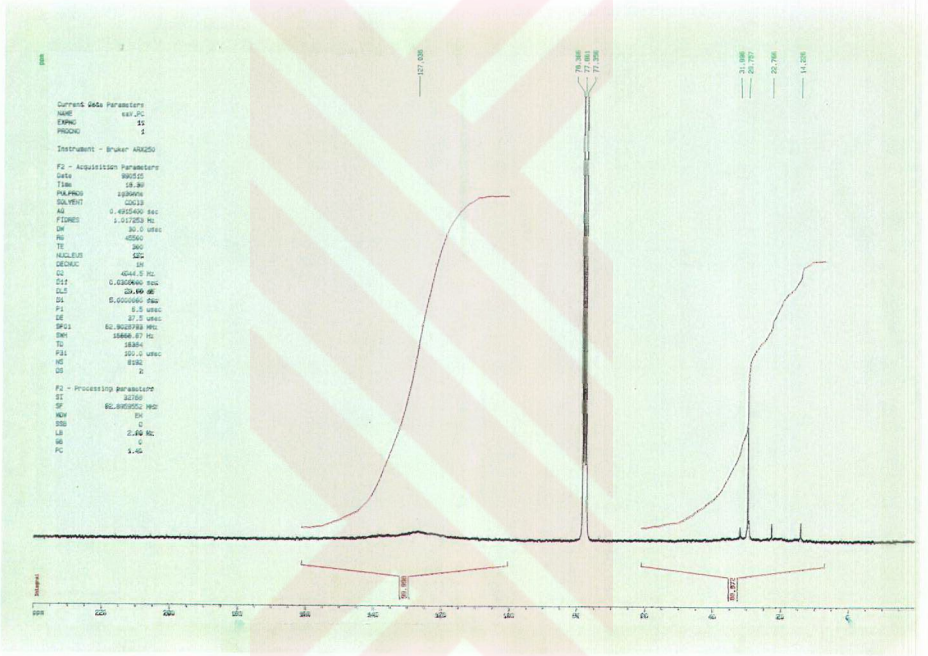

Figure 5.35 ^{13}C NMR spectrum of S7A3-E1 pitch.

Table 5.14. The calculated structural parameters [152].

Notation	Equation	Description
fa^{13}	C_{Aro}/C	Aromaticity
f	$[C_{Ali}(H/C)]/[H_\alpha + H_\beta + H_\gamma]$	Hydrogen to carbon atomic ratio in alkyl groups
n	C_{Ali}/C_{Aqs}	Average number of carbon atoms per alkyl substituent
r	(n+0.5)-(n/2f)	Number of naphthenic rings per alkyl substituent
C^s_1	C_{Ali} (C/n)	Weight fraction of non-bridge aromatic rings by alkyl groups
C^u_1	$12\ H_{Ar}H/(H_{Ar}+H_\alpha+H_\beta+H_\gamma)$	Weight fraction of non-bridge aromatic rings which are unsubstituted.
C_1	$C^s_1+C^u_1$	Weight fraction of non-bridge aromatic rings which are unbridged
σ	C^s_1/C_1	Degree of substitution of non-bridge aromatic rings by alkyl groups
H/C	------	Hydrogen/carbon atomic ratio

Table 5.15. Structural parameters of pitches.

Notation	S-A2	S5A5-A4	S5A5-N5	S7A3-V1	S7A3-E1
H_{Aro}	0.14	0.14	0.25	0.09	0.15
H_{Ali}	0.86	0.86	0.75	0.91	0.85
H_α	0.15	0.22	0.21	0.16	0.27
H_β	0.60	0.55	0.45	0.63	0.46
H_γ	0.11	0.09	0.09	0.12	0.12
C_{Aro}	0.59	0.61	0.64	0.51	0.62
C_{Ali}	0.41	0.39	0.36	0.49	0.38
fa^{13}	0.52	0.52	0.55	0.43	0.51
f	0.63	0.55	0.47	0.81	0.48
n	8.08	6.79	7.83	11.88	6.33
r	2.17	1.12	2.1×10^{-4}	5.05	0.24
C^s_1	0.04	0.05	0.04	0.03	0.05
C^u_1	0.16	0.15	0.21	0.11	0.13
C_1	0.20	0.20	0.25	0.14	0.18
σ	0.20	0.25	0.16	0.21	0.28
H/C	1.32	1.21	0.98	1.50	1.08

Hydrogen to carbon atomic ratio in alkyl groups, f, is also less in S5A5-N5 pitch (0.47), while it is the highest in S7A3-V1 pitch (0.81) which is expected because of the higher H/C atomic ratio of the parent S7A3 tar. S5A5-N5 pitch is also rich in aromatic carbon. For S5A5-N5 pitch, the H_β value is about 45%, while it is 63% for S7A3-V1 pitch. This suggests that S7A3-V1 pitch has higher number of naphthenic hydrogen and alkyl substitution than S5A5-N5 pitch. This result is consistent with the data shown in Table 5.15 where the S7A3-V1 pitch contains more substitution percentage of the aromatic rings (σ=0.21) and larger alkyl substituents (n=11.88) than that of S5A5-N5 pitch (σ=0.16; n=7.83). Therefore, S7A3-V1 pitch has lower carbon aromaticity (fa^{13}=0.43).

Table 5.15 shows that S5A5-N5 pitch has the highest aromatic ring carbons which are unbridged (C_1=0.25) and S7A3-V1 pitch has the lowest (C_1=0.14). Among all these processing methods nitrogen-blowing appears to be an effective method for pitch modification.

5.9 Characterisation of Pitch Cokes by Optical Microscopy

The quality of a graphitizable carbon is directly related to its optical texture, which is controlled by the development of mesophase during the carbonisation process which depends on the reactivity of pitch components. The reactivity of pitch, defined in terms of its ability to generate mesophase, can be related to the chemical composition of the pitches. The optical texture is defined by the size, shape and orientation of the different crystalline structures present in a material, as determined by optical microscopy on polished sections of samples [2]. There are different classification systems, all of them similar and based on the same criteria, being that proposed by Forrest and Marsh [184], one of the more widely used.

The formation of mesophase during pyrolysis of organic materials is not restricted to the presence of a specific type of compounds. As a result of the occurrence of different mechanisms of mesogen formation, these can be different size, structure, and planarity. On the other hand, the nucleation, growth, and coalescence of mesophase spheres require a system where the mesogens have the necessary mobility to contact one to each other. Optimum conditions will mean very fluid systems with

a high concentration of mesogens. According to these requirements, a good mesophase precursor must generate a high amount of mesogens in a medium of low viscosity [2].

The purpose of such a study was to determine the properties of carbons from the carbonisation of pitches. This was done by examining the polished surfaces of these carbons under a polarising optical microscope to determine their optical textures.

S5A5-A4, S5A5-N3, S5A5-V1, S7A3-V1, and S7A3-E1 pitches were selected to be examined under the optical microscope.

It was expected that changes in size and chemical structure of pitch components produced by air-blowing, nitrogen-blowing, vacuum distillation, and vacuum distillation followed by solvent extraction will affect the development of mesophase during the pitch carbonisation.

Table 5.16 summarises the coking yields and optical texture of the cokes from pitches produced by methods mentioned above.

Figures 5.36(a)-(e) show the optical textures of cokes produced from the five different pitches. The optical texture of the cokes were found to be different.

Table 5.16. Optical texture of the cokes obtained from the pitches.

Pitch	CY(wt%)	Optical texture
S5A5-A4	19.80	Flow domains
S5A5-N3	16.70	Coarse-grained mosaics
S5A5-V1	13.40	Coarse grained mosaics, medium-flow domains
S7S3-V1	12.40	Medium-grained mosaics
S7A3-E1	37.80	Isotropic

For the coke resulted from S5A5-A4 pitch, the development of mesophase had progressed to an extensive flow-domains, as shown in Figure 5.36a. Generally, molecular cross-linking induced by oxygen functionality at low temperatures increases the molecular weight of some molecules during air-blowing, preventing their distillation and removal at the carbonisation stage. Such treatments result in a viscosity increase and, simultaneously, the lamellar orientation of the aromatic molecules becomes more difficult to achieve. Both factors limit the growth and coalescence of mesophase formed during pitch heat treatment [185]. However, in the

case of S5A5-A4 pitch, very well oriented and big size of optical texture has been observed. This should be attributed to the lack of oxygen incorporation into the molecules during air-blowing which is confirmed by FTIR results. Oxygen molecules might react with the more reactive aliphatic hydrogens, leaving the more stable aromatic hydrogens. During the carbonisation of S5A5-A4 pitch, the stable aromatic hydrogens might move to the free radicals to block their reactivity. The carbonisation reaction consists of pyrolytic radical reactions, which proceed through radical initiation, propagation, condensation, and termination. The radicals are stabilised through hydrogen transfer or coupling to terminate the chain reaction [185]. Carbonisation reaction might be delayed through this slow reaction leading to flow-domains since in low reactive systems, polymerisation occurs at higher temperatures, being the formation of mesophase coincident with maximum fluidity conditions. Association of mesogens could be more easily accomplished because of their mobility, producing mesophase of big size which the coalesce to form anisotropic carbons with big size of optical texture.

Cokes resulting from nitrogen-blowing (S5A5-N3) and vacuum-distillation (S5A5-V1) cannot be precisely distinguished as seen in Figure 5.36b-c. Both of the cokes are mainly composed of coarse-grained mosaics while the coke from S5A5-V1 pitch has also medium-flow anisotropy. During thermal treatment and vacuum distillation, the light components are removed from the system. Therefore, the only difference between the two processes could be the amount of light components removed by these two methods. S5A5-N3 and S5A5-V1 pitches are the least aromatic ones still containing light components. During carbonisation, the aliphatic substituents of these pitches might be broken and the stabilisation of the free radicals by aromatic hydrogen could not be happened since the pitches contain mainly aliphatic hydrogens. Therefore, the reaction would be very fast leading molecules to grow up rapidly. This should be resulted in high viscosity in the system and consequently, would create coarse-grained mosaic texture.

S7A3-V1 pitch gave a coke with different optical texture than S5A5-V1 pitch although both of the pitches were produced by vacuum-distillation. The coke of S7A3-V1 pitch has mainly medium-grained mosaics as seen in Figure 5.36d. These differences between two vacuum-distilled pitches establish that the coke structure should be dependent upon the feedstock composition. S5A5-V1 pitch contains more

(a)

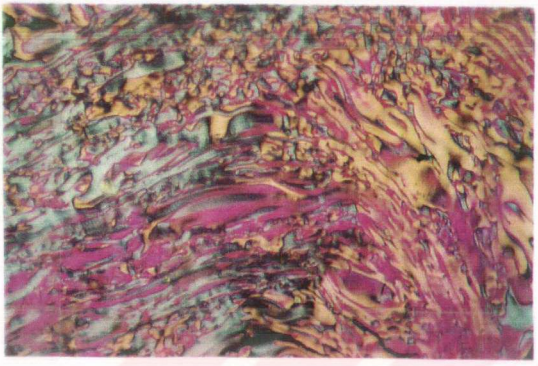

(b)

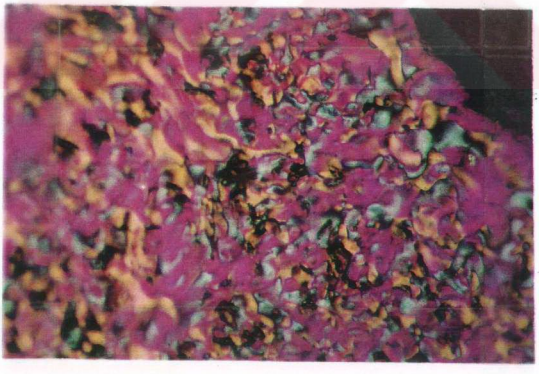

Figure 5.36. Optical micrographs of the cokes obtained from;
(a): S5A5-A4, (b): S5A5-N3

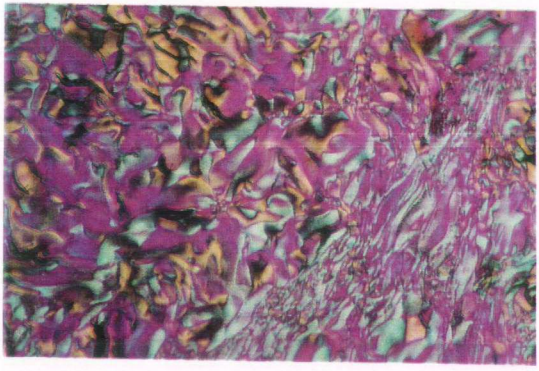

(c)

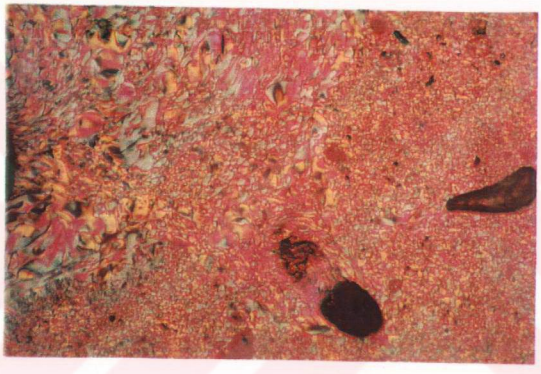

(d)

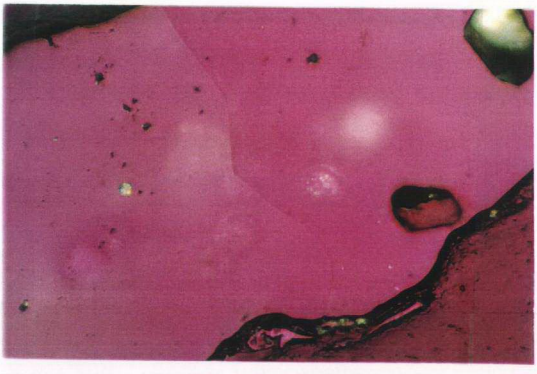

(e)

Figure 5.36 Optical micrographs of the cokes obtained from;
(c): S5A5-V1 pitch. (d): S7A3-V1, (e): S7A3-E1 pitch.

amounts of light components while S7A3-V1 pitch is more aromatic and this is confirmed by FTIR results. The light components might give the S5A5-V1 pitch a lower viscosity during the carbonisation, resulting a coke with a bigger optical texture than that of the coke of S7A3-V1 pitch.

S7A3-E1 pitch has a high content of heteroatoms, mainly oxygen and hydrogen. The high content of heteroatoms resulted in increasing viscosity and decreasing the facility to coalesce, which means that the mesophase development had been restricted. Therefore, vacuum distillation followed by hexane extraction maintained the pitch optically isotropic as shown in Figure 5.36e.

5.10 Spinning

For a precursor to be spinnable, it must be able to form an unbroken filament between the spinneret capillary exit and the wind-up device. The spinnability of a pitch precursor then is defined by the maximum length of the filament that can be drawn from its melt [186]. The spinning temperature has to be carefully controlled. There is a temperature range during which the viscosity appeared to be ideal for drawing out the filament. If the melt temperature is too high, the extruding jet of material can break up into drops, breaking the filament.

The softening point and the temperature at which the precursor became fluid are helpful to determine the spinning temperature, but the actual spinnability has to be determined by the spinning itself. The precursor with the good spinnability can be spun at high draw-down speed, thus producing thin fibres. The high fluidity of the precursor with good spinnability allows the melt fibre to have a smooth surface.

Table 5.17. Properties and spinning results of S7A3-E1 pitch.

Precursor	SP(°C)	Spinning Temp. (°C)	Spinnability
S7A3-E1	136	155	spinnable

The sign of poor spinnability is frequent breaks during wind-up. The fibre draw-down speed must be kept low, as spinnability decreases, and as a result thick fibres

are obtained. Poor spinnability produces fibres with more defects such as voids and cracks [83].

The spinning precursor S7A3-E1 pitch was spun with the spinning results shown in Table 5.17. It was found that the spinning temperature was about 20°C higher than the softening point of the S7A3-E1 pitch. The spinnability of the S7A3-E1 pitch was good, and was continuously spun but with a slower draw-down speed. The diameter the fibre filaments was between 15-20μ.

5.11 Stabilisation

When pitch-based carbon fibres are spun, they must be prepared to undergo the coking reaction, in which much of the hydrogen in the fibre is removed and the fibre becomes infusible [187]. In order to retain the fibre shape, spun fibres have to be stabilised to render them infusible before further heat treatment, which is carbonisation [84]. The usual means of stabilisation is through oxidation, in which the spun fibres are heat-treated in an oxygen-containing atmosphere to temperatures between 200 and 350°C for a period of time, sufficient to prevent fibres from deformation and/or sticking during carbonisation.

The spun fibres are thermoplastic, and have to be carefully oxidised for the prevention of viscous flow and consequent loss of the fibrous shape during the succeeding carbonisation. The oxidative stabilisation is rather slow at low temperatures, but the fibre deformation may occur or they may stick to each other at too high temperatures. The glass transition temperature, T_g, increases as the stabilisation proceeds, and finally the fibres become infusible. It is thought that the glass transition temperature of the fibres increases by the formation of three-dimensional crosslinking, lower fusibility of oxygen-containing molecules, and evaporation or condensation of low molecular weight compounds. Since the stabilisation process is exothermic and the heat release may cause the actual fibre temperature to exceed its glass transition temperature leads to fibre-fibre fusion, usually the stabilisation temperature is kept below the T_g [83].

In general, the stabilisation of pitch fibre is carried out in gases such as air, ozone, or oxygen, or it should be done with chemical treatment. However, in this study, the

spun fibre S7A3-E1 was stabilised by nitric acid. Although S7A3-E1 pitch is the highest softening point pitch among the other pitch precursors produced, its softening point is still too low compared to commercial pitches. Therefore, the stabilisation of S7A3-E1 green fibre by ordinary oxidative stabilisation would be at a lower temperature so that an extremely long time would be required to fully stabilise the fibres and it would not be economical. Regarding to these evaluations, S7A3-E1 green fibre was stabilised by nitric acid instead of oxidative stabilisation in order to shorten the stabilisation time and reduce the cost.

Table 5.18. Stabilisation conditions of S7A3-E1 pitch fibre and the results.

Acid to water ratio	Time (min)	Results
Concentrated HNO_3	1	not interfused
2 : 1	10	interfused
2 : 1	30	slightly interfused
1 : 9	5	interfused

The spun-fibre stabilisation results are listed in Table 5.18. It is clear from the results that nitric acid acts as an accelerator of the stabilisation reactions. As the reactivity of the nitric acid is too high, 1 minute stabilisation period was enough for S7A3-E1 green fibre.

Fibres stabilised by 2 parts nitric acid to 1 part water for 10 minutes and by 1 part nitric acid to 9 parts water for 5 minutes were found to be fusible when observed by naked eye. This must be due to insufficient stabilisation because of the short stabilisation period and in the mean time the less concentrated nitric acid used. The dilution of acid with water decreased the reactivity of the nitric acid. However, when the stabilisation period was extended to 30 minutes for 2 parts nitric acid to 1 part water the stabilisation was performed but still slightly interfused fibres were observed.

In each case of stabilisation conditions applied, the fibres were shrunk because of the reactivity of the acid but this result was much clearer in the fibres stabilised by the concentrated nitric acid. The shrinkage during stabilisation consists of a physical contribution called entropy shrinkage, which is completed below 200°C, and a chemical contribution called reaction shrinkage, which starts at about 200°C.

Entropy shrinkage is the initial contraction of the molecules that have been highly aligned during stretching prior to stabilisation. Reaction shrinkage is due to the shortening of the molecules during cyclisation and oxygen-group formation [23].

It must be noted that when the fibre was dipped into the nitric acid and nitric acid-water solution, an exothermic reaction occurred. However, in the case of stabilisation by nitric acid-water solution, before dipping the fibres into the solution, the heat of association of the solution was increased when water was added to acid. Due to the increase in the heat of association of the solution and the exothermic reaction occurred during the dipping of fibres into the solution, the total reaction temperature might be increased above the glass transition temperature (43°C) of the S7A3-E1 green fibre. As a result of insufficient stabilisation and the increase of medium temperature over T_g of the S7A3-E1 fibre the interfusion was observed in the fibres.

5.12 Carbonisation

After stabilisation, the pitch fibres are carbonised by heating in a series of heating zones at higher temperatures ranging from 700 – 2000°C. An inert atmosphere is used to prevent oxidation of the final carbon fibres [23]. During carbonisation, most of the non-carbon elements in the stabilised fibre are driven off as low molecular weight gases [27]. This accompanied by the evolution of volatiles, so a graded series of heating zones is needed to prevent excessive disruption of the structure. Below 1000 °C, the greatest quantity of gases as CH_4 and H_2 are released. Hydrogen is the main gas evolved above 1000 °C. During carbonisation, intermolecular cross-linking occurs through oxygen-containing groups or through dehydrogenation, and the cyclised sections coalesce by cross-linking to form a graphite-like structure in the lateral direction [23].

In this study, two of the spun fibres, which were stabilised by concentrated nitric acid for a minute (infusible) and 2 parts nitric acid to 1 part water for 30 minutes (slightly fusible), were pre-treated with air at lower temperatures in order to complete stabilisation before further carbonisation process.

The rate of heating during the pre-treatment, was kept low to prevent the fast release of the volatiles and the pores or surface irregularities in the fibre. The heating steps

during the pre-treatment is shown in Figure 5.37. The carbonisation took place between 300 – 1000°C, and higher heating rate (10°C/min) was used under the flow of nitrogen.

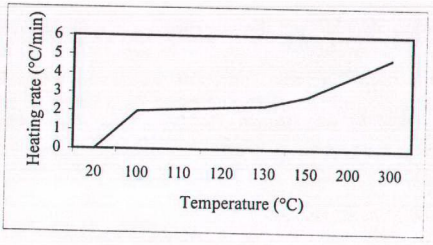

Figure 5.37. The heating steps of pre-treatment.

During carbonisation, weight loss and volume shrinkage was determined. The volume of the remaining fibres appeared approximately 50% of the original fibre. The volume shrinkage of the fibres led to microcracks and porosity along the fibre axis.

Figure 5.38(a) presents the scanning electron microscopy (SEM) image observed on the bundle of carbonised fibre which was stabilised by 2 parts nitric acid to 1 part water for 30 minutes. It is very obvious from the SEM image that the fibres did not keep their original cylindrical form. They fused and stuck together which is the result of insufficient stabilisation.

Figure 5.38(b) shows the SEM image observed on the carbonised single fibre which was stabilised by 2 part nitric acid to 1 part water for 30 minutes. The circular pores and a wavy slit are seen on the surface of the fibre. These pores and the slit must be due to the release of the volatiles.

About 50% by weight of the pitch fibre was lost as H_2O, CO_2, CO, and to a lesser extent as H_2 and CH_4. During carbonisation, as the temperature was increased the volatiles occurred tried to be released out of the surface of the fibres, and they caused the formation of the bubbles on the surface of the fibres. These bubbles are seen in the Figures 5.39(a)-(c).

The fibre shows the distortions, and rough surface due to the pitch composition and insufficient stabilisation.

(a)

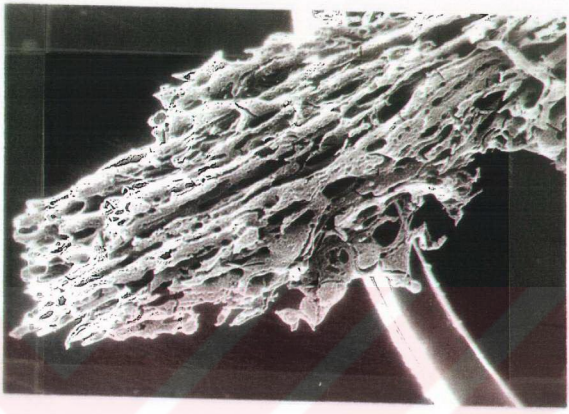

(b)

Figure 5.38. SEM images of the carbonised fibres (stabilised by 2 part HNO_3 to 1 part H_2O): (a) a bundle of fibres, (b) a single fibre.

(a)

(b)

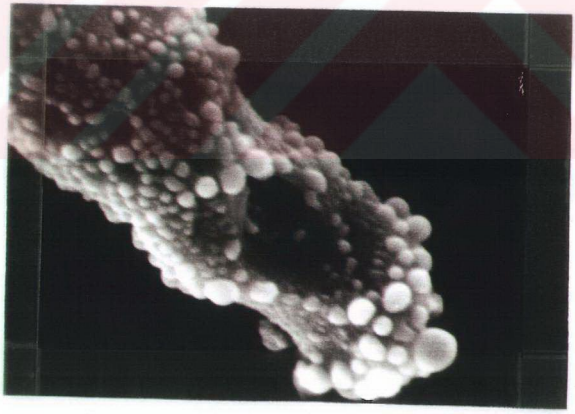

Figure 5.39. SEM images of the carbonised fibres (stabilised by concentrated HNO_3): (a) along the fibre axis, (b) tip of the fibre.

(c)

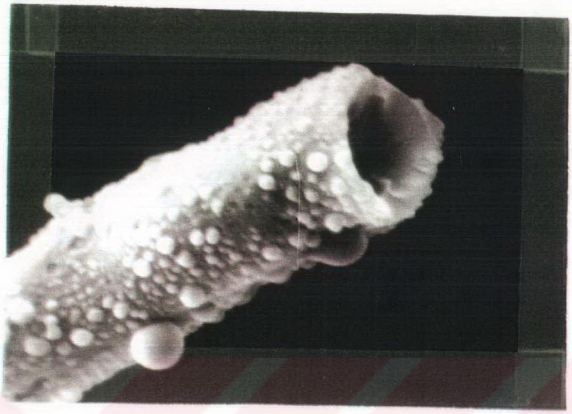

Figure 5.39. SEM images of the carbonised fibres (stabilised by concentrated HNO_3): (c) tip of the fibre.

5.13 Supercritical Fluid Extraction (SFE)

Supercritical fluid extraction (SFE) appears to be ideally suited to the extraction of the lower molecular weight component from pitch. Although there have been a limited number of reports about supercritical fluid extracted pitch, the aim of reports of these studies generally has been to extract the pitch from the undesirable particulate impurities present in the pitch rather than to "strip" off the "lights" from the pitch [188]. A unique feature of SFE compared to conventional solvent extraction is that not only the temperature but also the pressure can be used to effect changes in the strength of the solvent [189].

In order to compare the resultant pitches, an air-blown pitch (S-A2), a nitrogen-blown pitch (S5A5-N5), a vacuum-distilled and then hexane extracted pitch (S7A3-E1), and a high softening point pitch (Aerocarb75) were extracted by CO_2 and CO_2 modified by hexane as a co-solvent, at temperatures of 100, 150°C and of pressures 200, 400 atm. Extracts (light fractions) were analysed by size exclusion chromatography (SEC), and mass spectroscopy (MS). Residues (heavy fractions) were analysed by SEC, MS, FTIR, and DDSC.

Table 5.19 shows the percentage of the extract recovered from pitch materials for various temperatures and pressures with CO_2. The density of CO_2 is increased when the pressure is increased at constant temperature, which enhances the stability of various solutes. The results showed that the extraction recoveries of pitch materials were increased with increasing temperature and pressure. However, the effect of the temperature was not as significant as the effect of pressure.

The increase in pressure from 200 to 400atm when the temperature was constant at 100°C, increased the extraction yield from 30.6% to 38.3%, 28.9% to 40.3, 3.4% to 7.1%, and 0.2% to 1.6% for S-A2, S5A5-N5, S7A3-E1, and Aerocarb75 pitches, respectively. But when the pressure was decreased to 200atm while the temperature was increased to 150°C, the extraction yield decreased except for S-A2 pitch. It seems possible that the contact between the CO_2 and pitch would be less efficient at lower pressures.

The increase in the extraction yield was, expectedly, inversely proportional with the softening points of the pitches (Tables 5.19-5.20). As high softening point pitches (S7A3-E1 and Aerocarb75) contain less amount of light fractions, the extraction yields were low for these pitches.

Table 5.19. Extraction recovery of pitches at various temperatures and pressures using CO_2.

Conditions		Percent Recovery (wt%)			
Temp (°C)	Pressure (atm)	S-A2	S5A5-N5	S7A3-E1	Aerocarb75
100	200	30.6	28.9	3.4	0.2
100	400	38.3	40.3	7.1	1.6
150	200	40.6	31.9	4.0	0.6
150	400	59.3	35.7	12.3	2.5

Addition of a small amount of solvent to the supercritical fluid can result in an increase in the solubility of solutes. Polar solvents usually cannot be used as pure supercritical fluids because their critical temperatures are too high. Instead CO_2 is used as a main solvent and a small amount of modifier including polar, acidic, or basic groups is added in order to increase the polarity and the density of the solvents [160].

Table 5.20. General properties of the pitches.

Pitches	C (wt%)	H (wt%)	[a]O (wt%)	H/C	CY (wt%)	SP (°C)
S-A2	87.55	9.60	0.10	1.32	ND	110
S5A5-N5	86.45	7.10	1.90	0.98	ND	160
S7A3-E1	81.95	7.35	4.45	1.08	62.20	136
Aerocarb75	93.15	5.10	0.25	0.66	75.00	230

[a]: difference, ND: not determined.

As seen from FTIR results, the pitch materials mainly have aliphatic structures. Therefore, an aliphatic solvent, hexane, was chosen as the supercritical solvent modifier for investigation of the extraction parameters. 0.3ml of hexane was used for each extraction. Table 5.21 shows that 62% of the light fraction of S-A2 pitch was successfully removed under high temperature (150°C) and high pressure (400 atm) during 30 minutes dynamic extraction. The solubility of light molecular weight fraction was increased sharply with increasing pressure. The high recovery of extract from S-A2 pitch is probably due to the greater content of low molecular weight hydrocarbons in this material. An increase in the extraction yield with increasing pressure was expected as the solvent density increases as the pressure increases.

Table 5.21. Extraction recovery of pitches at various temperatures and pressures using CO_2 modified with hexane.

Conditions			Percent recovery (wt%)			
Temp (°C)	Pressure (atm)	Time (min)	S-A2	S5A5-N5	S7A3-E1	Aerocarb75
100	200	30	35.9	8.9	5.6	0.3
100	400	30	39.6	9.4	13.2	-
150	200	30	43.9	33.3	6.7	1.1
150	400	30	62.0	36.2	29.1	-
150	400	15	46.0	-	-	-

The extraction yield was slightly lower at 150°C, and 200atm for S7A3-E1 pitch than at 100°C, 400atm, reflecting the decrease in solvent density with increasing temperature. As the light molecular content of Aerocarb75 pitch is lower, the extraction yield was also low for this pitch.

Kershaw et.al. [190] also reported an increase in yield with pressure for extraction of a coal-tar pitch with toluene at 25MPa and 350°C.

S-A2 pitch was subjected to SFE at 150°C, 400atm, 100°C, 400atm and 100°C, 200atm with CO_2 modified by toluene. However, in each case, the selected pitch was dissolved ~100% in supercritical toluene. The reason should be the aliphatic nature of the pitch. As toluene is a powerful aromatic solvent, the pitch was totally dissolved in the toluene.

5.13.1 Analysis of SFE products

5.13.1.1 Size exclusion chromatography

To determine the effectiveness of the extraction process, samples of the original pitch materials, their SFE extracts, and residues (150°C, 400atm, CO_2 modified by hexane) were analysed by SEC to compare the molecular weight distributions.

Original pitch materials, extracts, and residues were dissolved in NMP in ultrasonic bath. All SEC analysis were performed on a Polymer Labs Mixed E Bed Column (polyvinylbenzene co-polymer packing), with NMP as a mobile phase, as described elsewhere.

Figure 5.40 (1-2) shows the size exclusion chromatogram of S-A2 pitch, its SFE residues and extracts which were produced by 15, and 30 minute extraction time. In each extraction period, both original pitch and the residue showed peaks between 450-700s correspond to material excluding above 20000 at the exclusion limit of the column. The intensities of the retained (separated) material, giving peaks between 750-1500, and 750-1350s for 15, and 30 minute extractions, respectively, were considerably greater than those of the excluded material. This suggests that the retained fraction to contain relatively smaller aromatic ring systems than the excluded material. The extract did not give any indication of the presence of excluded material in either case. As the extraction time increased to 30 minutes, the peak correspond to the residue shifted to the lower retention times. This result indicates that longer extraction times were more efficient to remove the light molecules from the pitch. Hence, longer extraction times resulted in the residue which contains higher molecular components.

Figure 5.41 shows the size exclusion chromatogram of S5A5-N5 pitch, its SFE extract, and residue. The peak corresponds to the original pitch was close to the peak

corresponds to the extract meaning the S5A5-N5 pitch contains large amounts of lower molecular weight components. These findings are supported by H/C atomic ratio of the pitches. The peak of the residue shifted to the lower retention times, which is the signal of higher molecular weight components in the residue. Both original pitch and the extract showed peaks between 450-600s correspond to material excluded above 20000. The apparent molecular weight distribution was between 100-16000, 100-8000, and 100-2500 for the residue, pitch, and the extract, respectively, depending on the calibration curve (Figure 4.7).

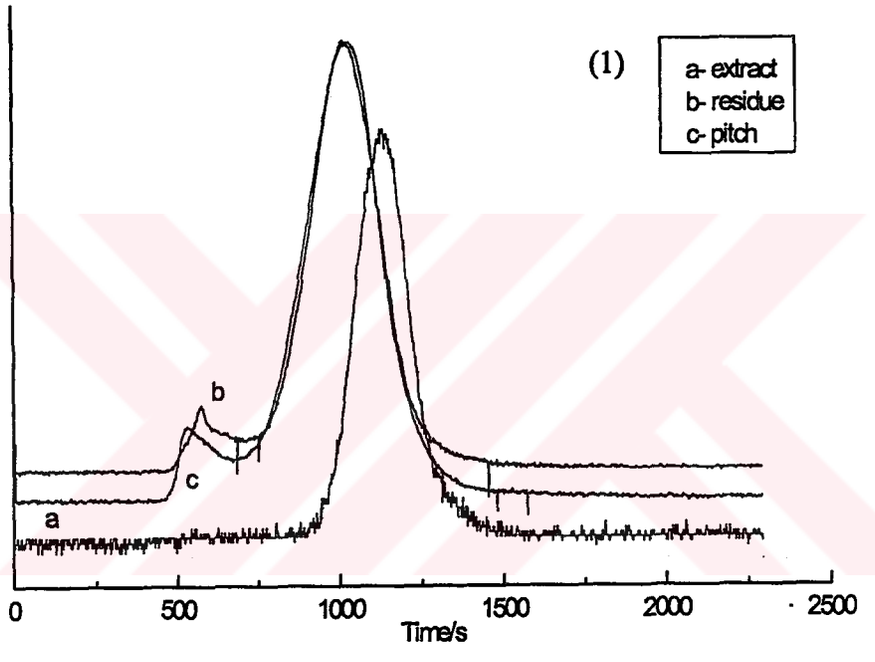

Figure 5.40. Size exclusion chromatograms of S-A2 pitch, its SFE extract, and residue: (1) 15 min extraction

Figure 5.42 shows the size exclusion chromatogram of S7A3-E1 pitch, its SFE extract, and residue. Both original pitch and the residue showed peaks between 400-600s correspond to material excluding. The intensity of the excluded material of the residue was remarkably high. This suggests that the excluded material to contain relatively high molecular weight components. The peak corresponds to the extract was close to the peak of the residue which means the pitch does not contain high amounts of extractable compounds. This is confirmed with MS results of the SFE of S7A3-E1 pitch extract.

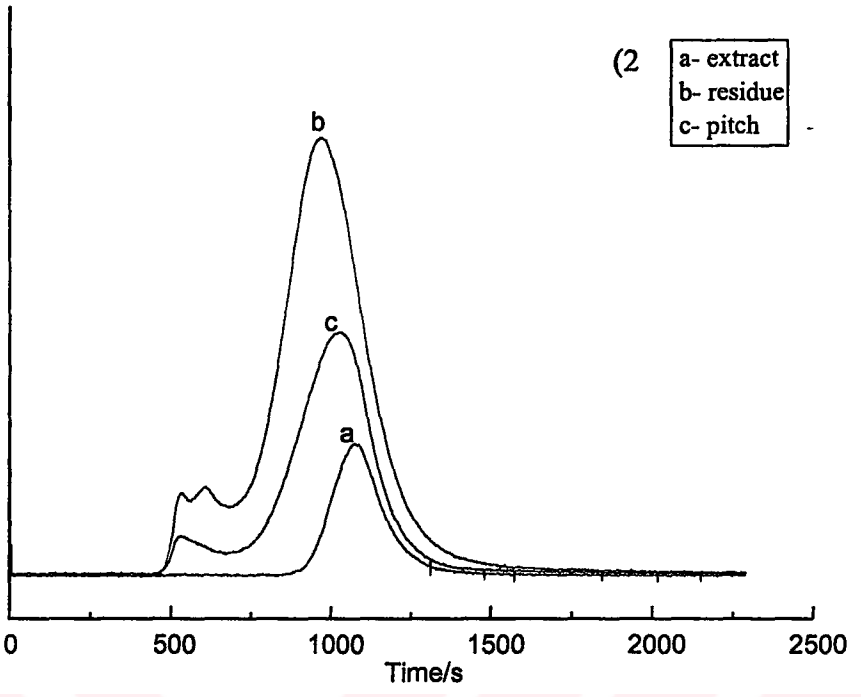

Figure 5.40. Size exclusion chromatograms of S-A2 pitch, its SFE extract, and residue: (2) 30 min extraction.

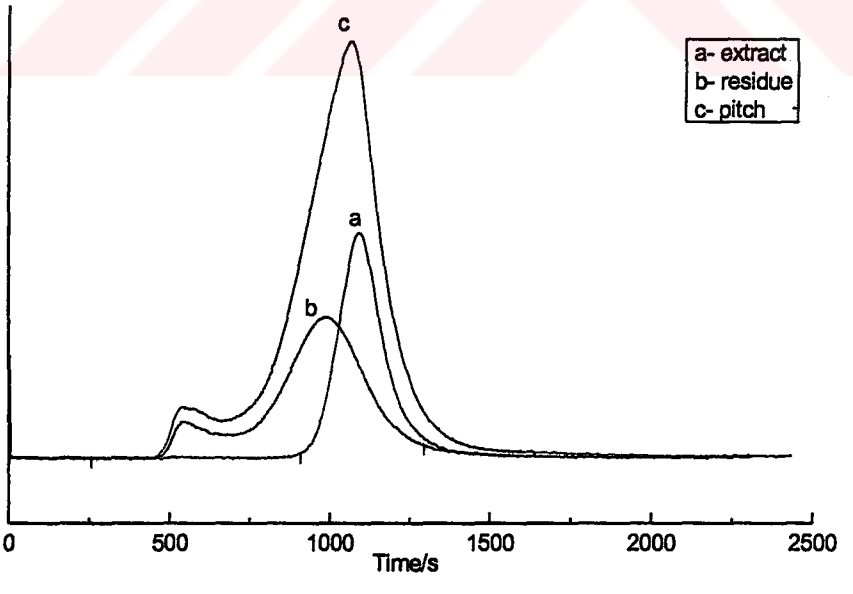

Figure 5.41. Size exclusion chromatogram of S5A5-N5 pitch, its SFE extract, and residue.

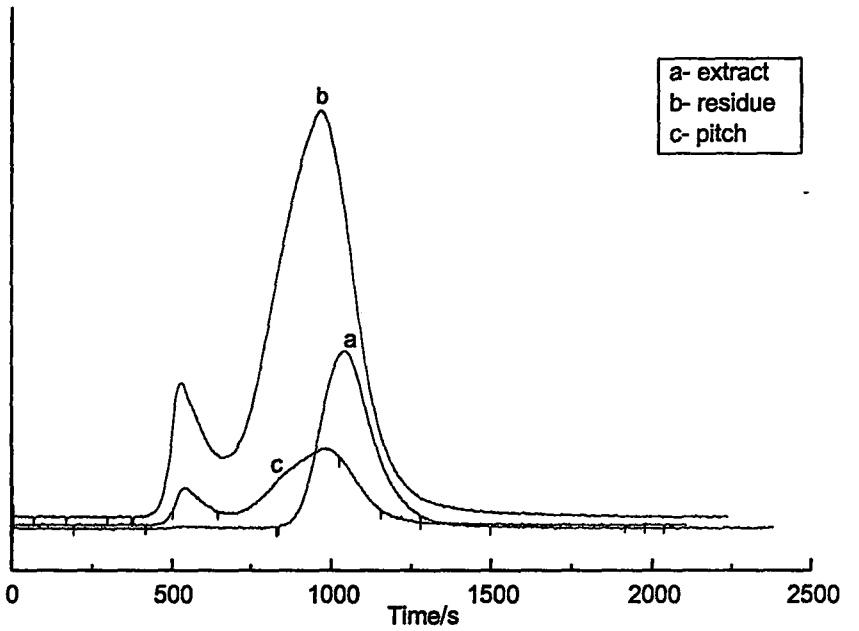

Figure 5.42. Size exclusion chromatogram of S7A3-E1 pitch, its SFE extract, and residue.

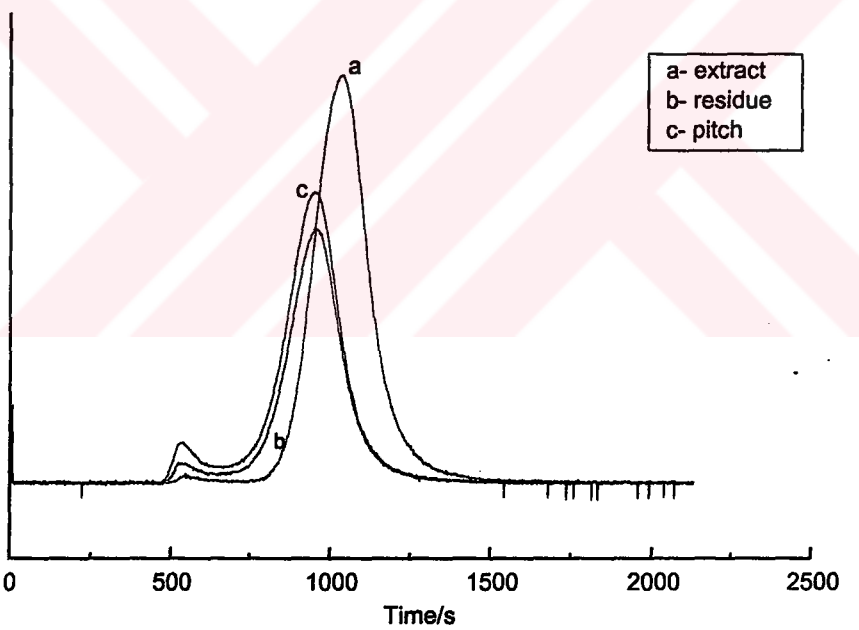

Figure 5.43. Size exclusion chromatogram of Aerocarb75 pitch, its SFE extract, and residue.

Figure 5.43 shows the size exclusion chromatogram of Aerocarb75 pitch, its SFE extract, and residue. The peaks for the original pitch and the residue look quite similar and were close to the each other. These two peaks shifted to the early retention times. These findings show that the pitch material and the residue do not contain low molecular weight materials. The extract contains excluded material as

the residue and the pitch. This is the indication of high molecular weight components in the extract. The other finding related to the extract, which differs than the other pitch extracts, is that the peak for the extract slightly shifted to the early retention times. This is another indication of high molecules place in the extract. These findings are consisted by the MS results.

5.13.1.2 Mass spectroscopy

Fast atom bombardment mass spectra (FAB-MS) of the SFE extracts of S-A2 and S5A5-N5 pitches and S7A3-E1 and Aerocarb75 pitches were similar to each other with major ions at 69, 71, 83, 97, 111, 265, and 285. However, as the H/C atomic ratio of the pitches (Table 5.22) decreases, the ion profile becomes more complex with the appearance of higher molecular weight components in both the extracts and residues.

It is noted that since vertical scales were normalised with respect to the highest detected intensity in each group, intensities shown in one mass spectrum are not directly comparable with those of other diagrams.

Figure 5.44 shows the FAB-MS spectra of S-A2 pitch, extract, and residue (150°C, 400atm, 0.3ml hexane, 30 min extraction), respectively. The spectra of these three fractions demonstrate similar trends to those in the SEC chromatograms. However, MS produces molecular weight profiles and these profiles are much more informative than the results obtained by SEC.

Comparison of these three spectra shows that the S-A2 pitch contains large amounts of lower molecular weight components. There is a slight shifting to higher molecular compounds in the spectra. Although high amounts of the low molecular weight material (62%) was extracted, the residue still contains low molecular weight carbonaceous materials. This shows that SFE did not completely extract the light fraction from the S-A2 pitch. Supercritical CO_2 modified with hexane only extracted a part of the lower molecular weight components. However, those remaining after the extraction were very similar to those extracted for S-A2 pitch.

Table 5.22. Elemental analysis of pitch materials and their residues after SFE (150°C, 400atm, 0.3ml hexane).

Samples	C(wt%)		H(wt%)		N(wt%)		S(wt%)		[a]O(wt%)		H/C		T_g	
	pitch	residue	pitch	residue	pitch	residue	pitch	residue	pitch	residue	pitch	residue	pitch	residue
S-A2-15	87.55	84.75	9.60	7.00	1.05	1.95	1.70	1.70	0.10	4.6	1.32	0.99	ND	ND
S-A2-30	87.55	85.55	9.60	8.75	1.05	1.15	1.70	1.60	0.10	4.10	1.32	1.23	ND	21.68
S5A5-N5	86.45	84.00	7.10	5.80	1.25	1.10	3.30	2.90	1.90	6.20	0.98	0.82	19.27	66.25
S7A3-E1	81.95	81.10	7.35	6.95	2.40	2.20	3.85	2.05	4.45	7.70	1.08	1.03	43.23	76.75
Aerocar75	93.10	92.40	5.10	4.65	T/N	T/N	1.50	1.70	0.25	1.25	0.66	0.60	166	135

[a] by difference.

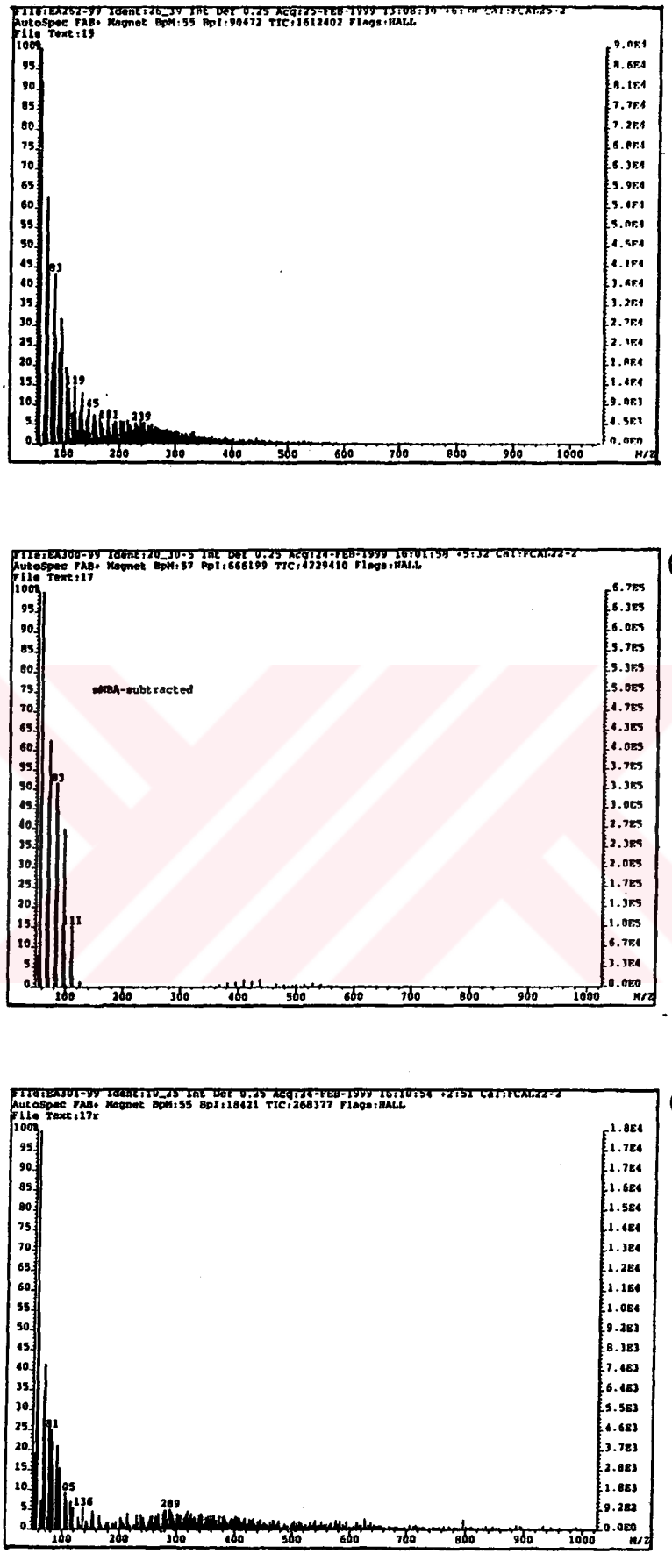

Figure 5.44 Mass spectra of S-A2 pitch (a), extract (b), and residue (c).

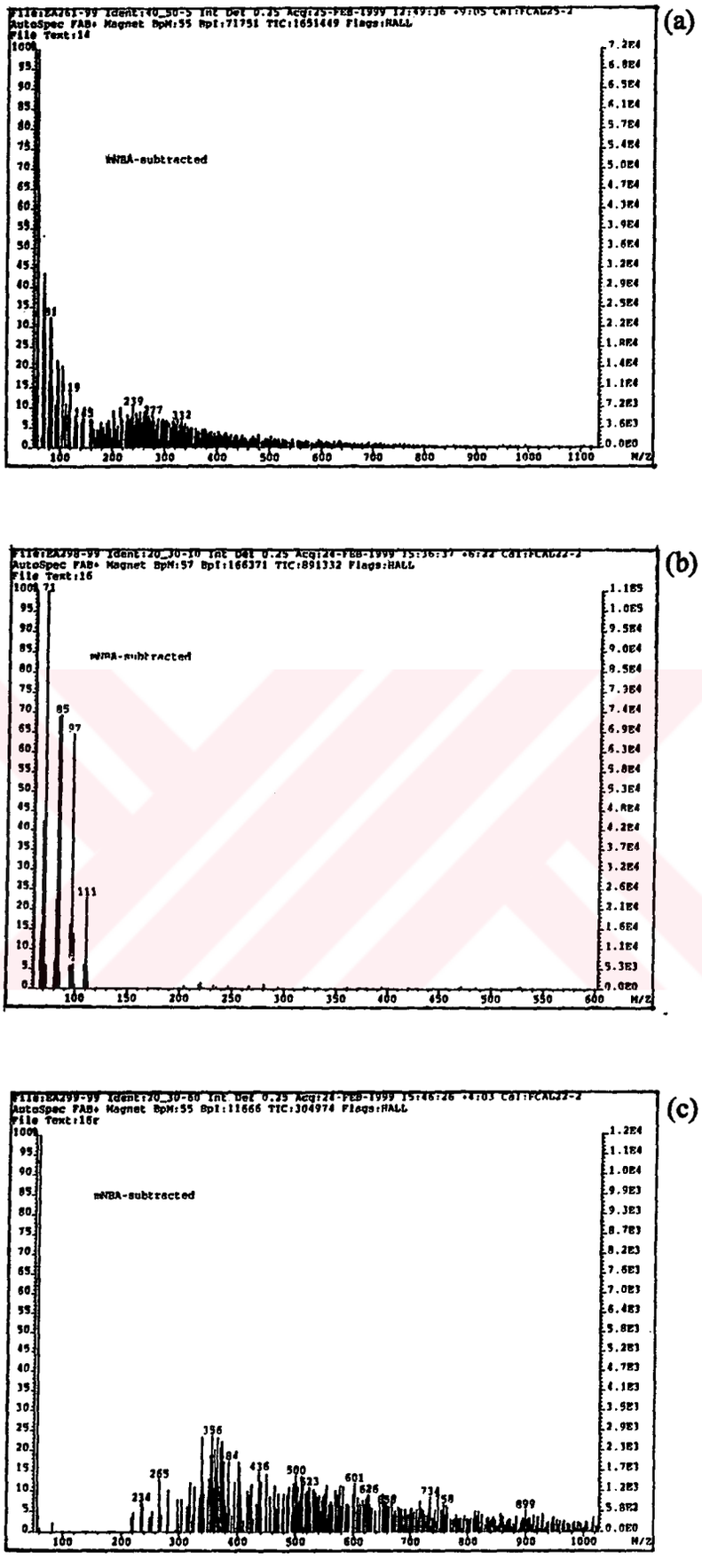

Figure 5.45 Mass spectra of S5A5-N5 pitch (a), extract (b), and residue (c).

Figure 5.45 displays the FAB-MS spectra of S5A5-N5 pitch, extract, and residue (150°C, 400atm, 0.3ml hexane), respectively. The spectra show that supercritical CO_2 modified with hexane efficiently separated the light fraction from the pitch material, as there is an obvious shift to higher molecular compounds in the spectra. The ion distribution is between 234-900 Da for the residue, whereas between 85-111 Da for the extract.

Figure 5.46 and Figure 5.47 show the FAB-MS spectra of S7A3-E1 and Aerocarb75 pitches, their extracts, and residues (150°C, 400atm, 0.3ml hexane), respectively. As these two pitches have higher softening points compared to the other two, the extraction yields of these pitches decreased. However, these pitches contain low amounts of lower molecular weight components. Therefore, those remaining after the extraction were similar to those extracted for both pitches. The ion distribution of S7A3-E1 and Aerocarb75 residues is between 81-400 Da and 74->1000 Da, respectively.

It is obvious that great amounts of low molecular weight components were removed from S5A5-N5 pitch by CO_2 modified with hexane. This finding is supported by H/C atomic ratio of the residue. Because there is a definite decrease in H/C ratio of the residue. This shows that the residue do not contain light molecules.

There is a slight shift to higher molecular weight components in the spectra of S-A2, S7A3-E1, and Aerocarb75 pitch residues. The signals are stretching beyond 1000 Da for Aerocarb75 residue. However, the molecular weight range shown by FAB-MS is limited by the instrumentation.

SFE was successful in removing the lower molecular weight materials from the pitches. However, still light molecular weight components can be observed in the spectra of the residue of S-A2 pitch. The reason should be the fragmentation of the high molecular weight materials into lower molecular weight components by ^{+}Cs ions. The second reason should be the breaking of some loose bonded compounds into lower molecular weight components as the probe of the spectrometer was heated.

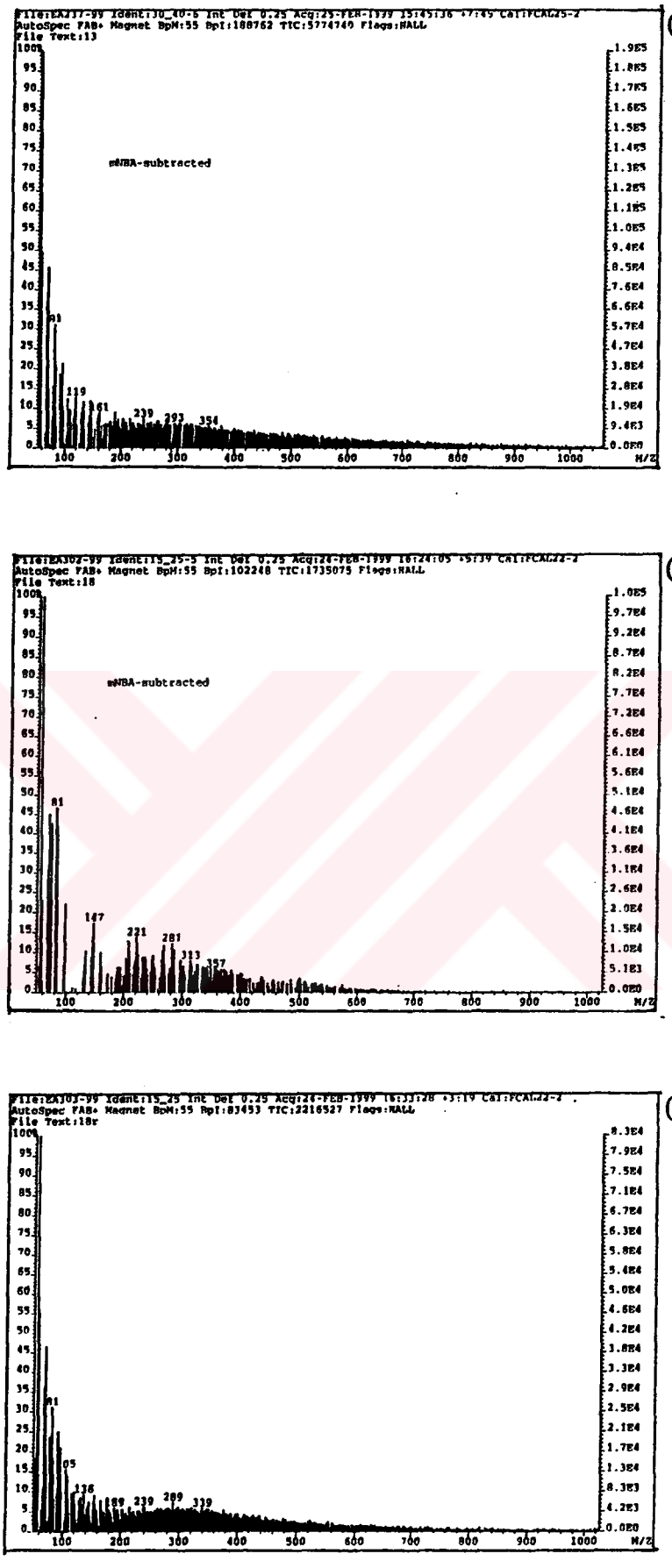

Figure 5.46 Mass spectra of S7A3-E1 pitch (a), extract (b), and residue (c).

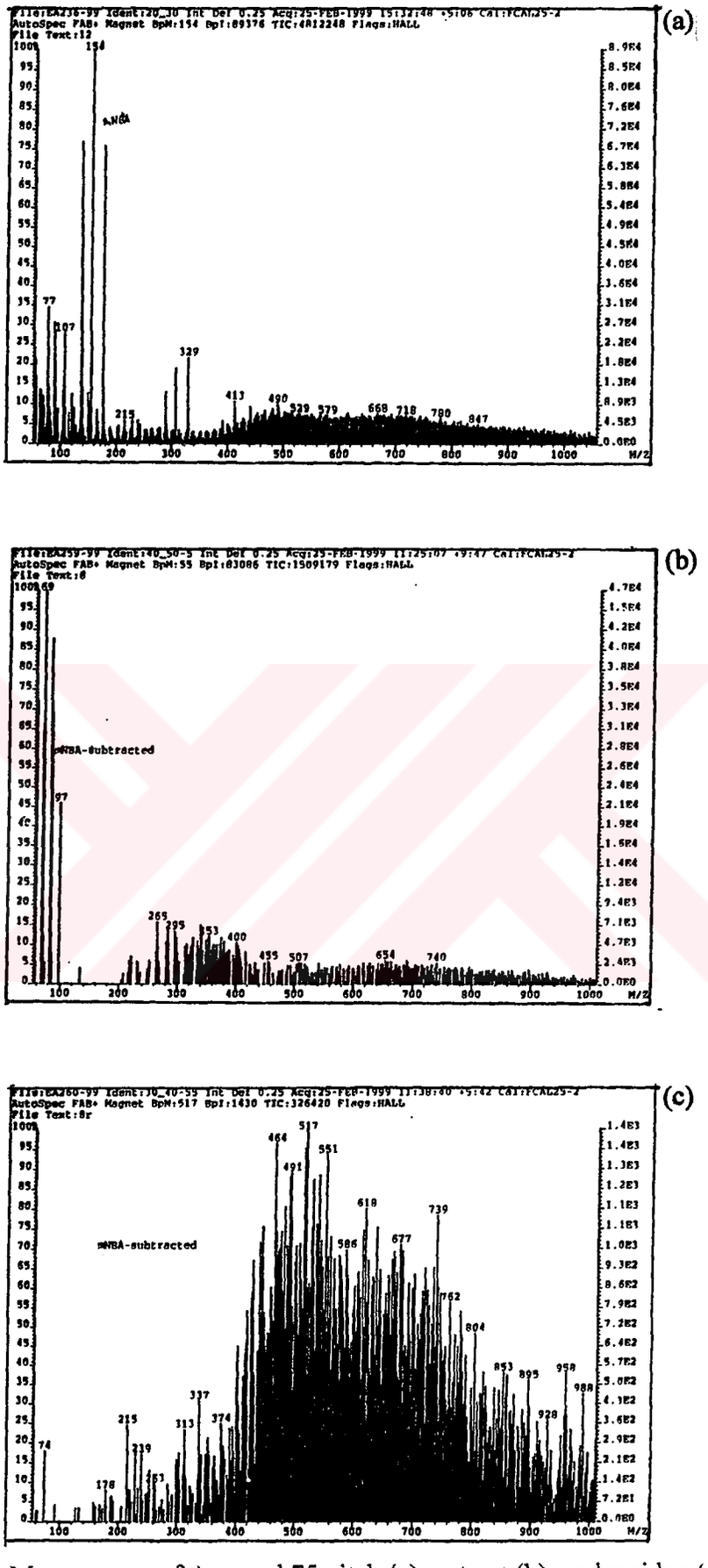

Figure 5.47 Mass spectra of Aerocarb75 pitch (a), extract (b), and residue (c).

5.13.1.3 Infrared spectroscopy

Figures from 5.48 to Figure 5.52 show the infrared spectra of S-A2 pitch and its 15 minute SFE residue and extract, S-A2 pitch and its 30 minute SFE residue and extract, S5A5-N5, S7A3-E1, and Aerocarb75 pitches and their 30 minute SFE residues and the extracts.

Figures 5.48 and 5.49 show the infrared spectra of S-A2 pitch and its 15 minute and 30 minute SFE extracts and residues, respectively. The bands at 2954 and 2920 cm^{-1} in the spectra are related to the asymmetric stretching of CH_3- and – CH_2- groups, respectively. The intensities of these bands increased in the infrared spectra of the extracts while they decreased in the spectra of the residues compared to those of the original S-A2 pitch spectra. Additionally, the aliphatic C-H band at 2850 cm^{-1} and methylene/naphthenic C-H bending bands at 1450 cm^{-1} decreased their intensities in the spectra of the residues and increased their intensities in the spectra of the extracts compared to those of the original S-A2 pitch spectra. This clearly illustrates that the aliphaticity of the extracts increased with the supercritical fluid extraction (SFE). However, the increase in the intensity of the bands at 2954, 2920, 2850, and 1450 cm^{-1} was greater for 30 minute extraction while was lower for 15 minute extraction. This suggests that as the extraction time increases the aliphaticity of the extracts also increases.

The band at 3036 cm^{-1} related to the stretching of aromatic groups was disappeared in the spectrum of the extract of 15 minute SFE of S-A2 pitch while it was visible in the spectrum of the extract of 30 minute SFE of S-A2 pitch. Moreover, the intensities of the absorption peaks at 750, 870, and 1600 cm^{-1} related to the 1,2-substituted aromatic rings, out-of-plane bending of C-H substituted aromatic rings, and aromatic ring-stretching mode, respectively, are stronger in the spectrum of the extract of 30 minute SFE than those of the 15 minute SFE. This clearly shows that as the extraction time increases the aromatic compounds begin to be extracted slightly. However, the aromaticity of the residue increases related to the increase in the intensities of these bands in the spectrum of the residue of 30 minute SFE. This shows that longer extraction period is more effective to remove the aliphatic compounds from the pitch and leads the residue to contain more amounts of aromatic compounds.

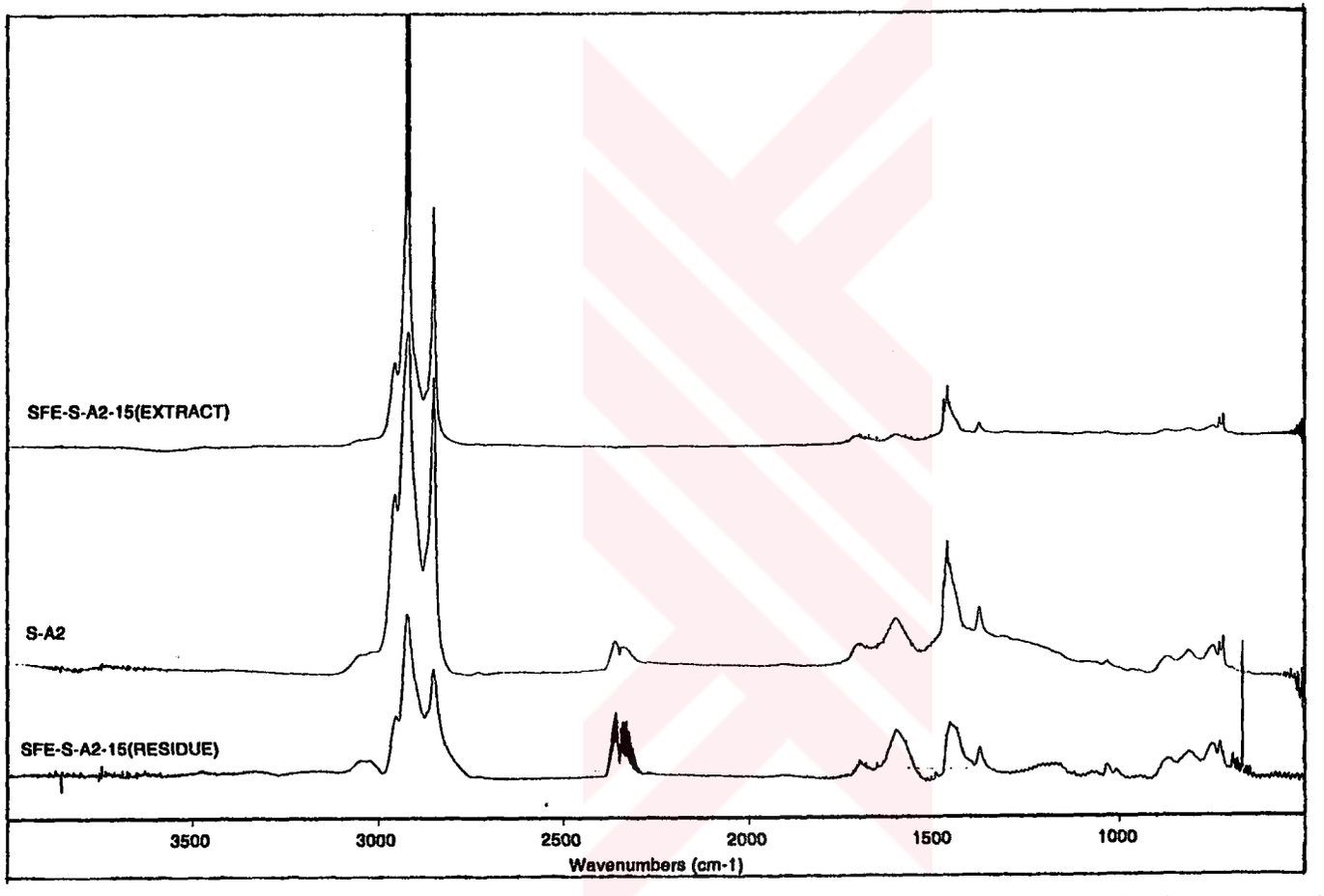

Figure 5.48 Infrared spectra of S-A2 pitch, its SFE residue and the extract (15 minute extraction).

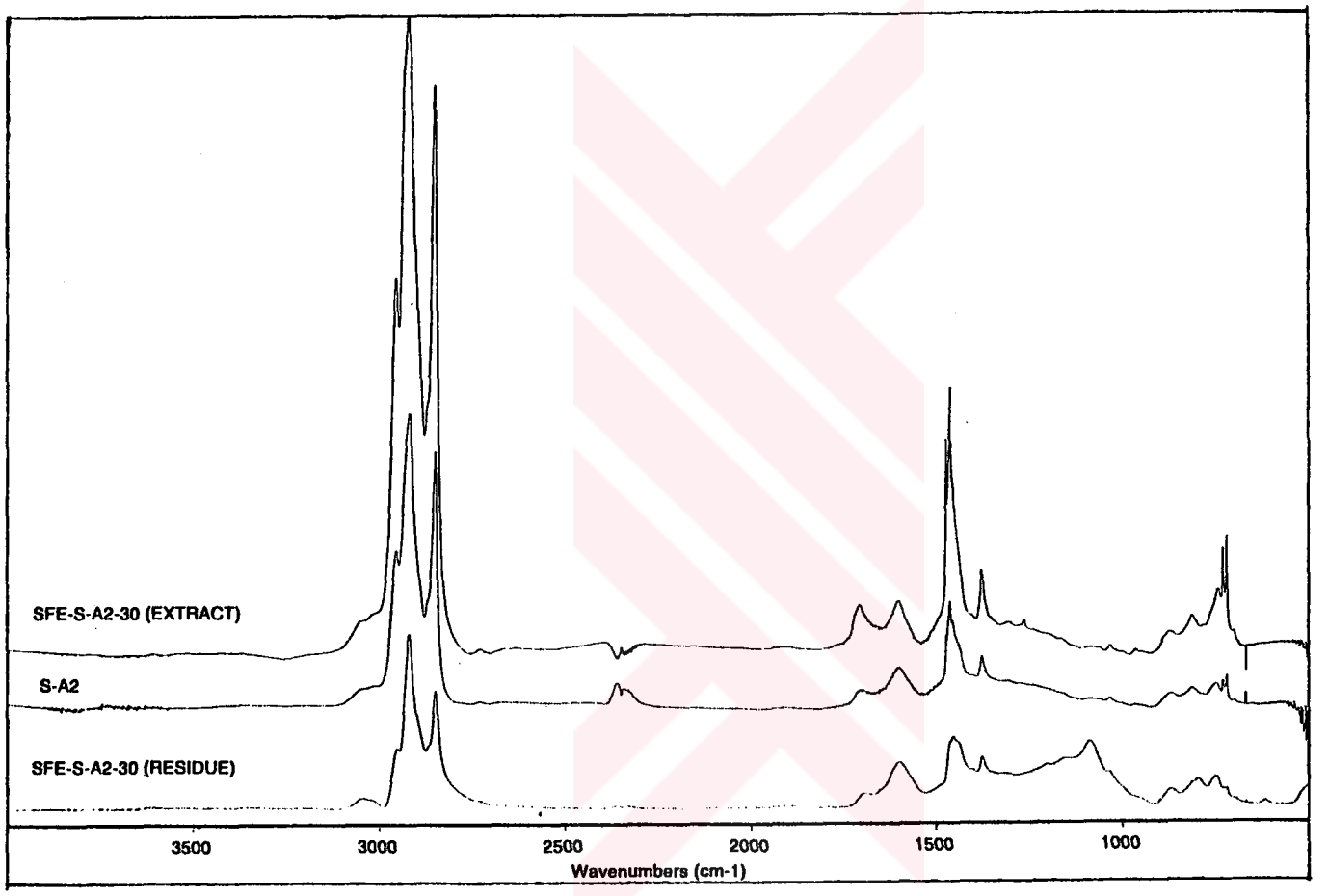

Figure 5.49 Infrared spectra of S-A2 pitch, its SFE residue and the extract (30 minute extraction).

Figure 5.50 shows the infrared spectra of S5A5-N5 pitch and its SFE residue and the extract. The bands at 2954, and 2920 cm^{-1} related to the asymmetric stretching of CH_3- and – CH_2- groups increased their intensities in the spectrum of the extract of S5A5-N5 pitch. The bands at 2848, 1450, and 1377 cm^{-1} are due to the CH_3- groups, and stretching and bending modes of saturated aliphatic hydrocarbons, respectively, and their intensities increased in the extract as well. Evidently, the aliphatic hydrocarbons were concentrated in the extract of S5A5-N5 pitch, as it was extracted by supercritical CO_2 modified by hexane which is an aliphatic solvent.

The intensity of the band at 3036 cm^{-1} related to the stretching of aromatic groups increased in the spectrum of the residue compared to that of the extract. The band at 750 cm^{-1} is assigned to 1,2-substituted aromatic rings, i.e., aromatic rings with four neighbouring hydrogens and the band at 870 cm^{-1} is probably due to the out-of-plane bending of isolated C-H substituted aromatic ring. These two bands can be clearly observed in the spectrum of the residue with a higher intensity than those of the extract. The aromatic structures have low solubility in hexane. Therefore, the relative quantity of CH_3- containing groups increased while the relative quantity of aromatic components was reduced in the extract of S5A5-N5 pitch.

Figures 5.51 and 5.52 show the infrared spectra of S7A3-E1 pitch, Aerocarb75 pitch, and their SFE residues and the extracts. The bands at 2950 and 2920 cm^{-1} related to the asymmetric stretching of CH_3- and – CH_2- containing groups, respectively, and also the symmetric stretching band (CH_2-) at 2850 cm^{-1} increased their intensities in the spectra of the extracts of the S7A3-E1 and Aerocarb75 pitches. Additionally, the bands at 1450 and 1377 cm^{-1} associated to methyl substituents on aromatic rings were very intense in the extracts of both pitches. This indicates the presence of more amounts of methyl substituents were extracted from the pitches into their extracts. However, the intensities of the bands at 2950, 2920, 2850, 1450, and 1377 cm^{-1} are higher in the spectrum of the extract of S7A3-E1 pitch than those of the Aerocarb75 pitch. Depending on these data, the comparison of the spectra of the extracts of the two pitches shows that the extract of S7A3-E1 pitch contains more amounts of aliphatic compounds than that of the Aerocarb75, which is expected.

On the other hand, the intensities of the bands at 2950, 2920, and 2850 cm^{-1} due to methyl and methylene substituents on aromatic ring systems are higher in the

spectrum of the residue of S7A3-E1 pitch than those of Aerocarb75 pitch. This clearly identifies that the residue of the S7A3-E1 pitch might contain some aliphatic compounds. This possible result should be due to the presence of more amounts of aliphatic groups in the S7A3-E1 pitch and the insufficient time to recover the aliphatic compounds from the pitch to leave the residue less aliphatic.

An intense band at 1273 cm^{-1} in the extract of the Aerocarb75, which is not visible in the spectrum of the original pitch, in the residue, or in the spectra related to the SFE of S7A3-E1 pitch, is probably associated with the C-H in-plane bending of 1,2-substituted aromatic rings.

The intensity of the bands at 3036, 1600, 870, and 750 cm^{-1} related to the stretching of aromatic groups, the stretching of C=C groups, out-of-plane bending of C-H substituted aromatic rings, and 1,2-substituted aromatic rings are higher in the spectrum of the residue of Aerocarb75 than those of S7A3-E1 pitch. This finding is confirmed by the H/C atomic ratio of these two pitches. The H/C atomic ratio of Aerocarb75 pitch is less than that of the S7A3-E1 pitch, and subsequently, its softening point is higher than that of S7A3-E1 pitch. Therefore, SFE of Aerocarb75 pitch by CO_2 modified by hexane resulted in high amounts of aromatic structures in the residue of Aerocarb75. All these results listed above are also supported by the FAB-MS results.

Hydrogen aromaticity indices (I_{Ar}) were calculated for S-A2, S5A5-N5, S7A3-E1, and Aerocarb75 pitches and their 30 minute SFE residues and the results are given in Table 5.23.

The highest value for I_{Ar} was obtained for Aerocarb75 and S5A5-N5 pitches and for their SFE residues. The extend of increase in the value of I_{Ar} was conversely correlated with the H/C atomic ratios of the pitches and with their SFE residues.

Table 5.23. Hydrogen aromaticity indices of the pitches and their SFE residues.

	H/C		I_{Ar}	
	Pitch	Residue	Pitch	Residue
S-A2	1.32	1.23	0.21	0.03
S5A5-N5	0.98	0.82	0.40	0.17
S7A3-E1	1.08	1.03	0.26	0.04
Aerocarb75	0.66	0.60	0.43	0.42

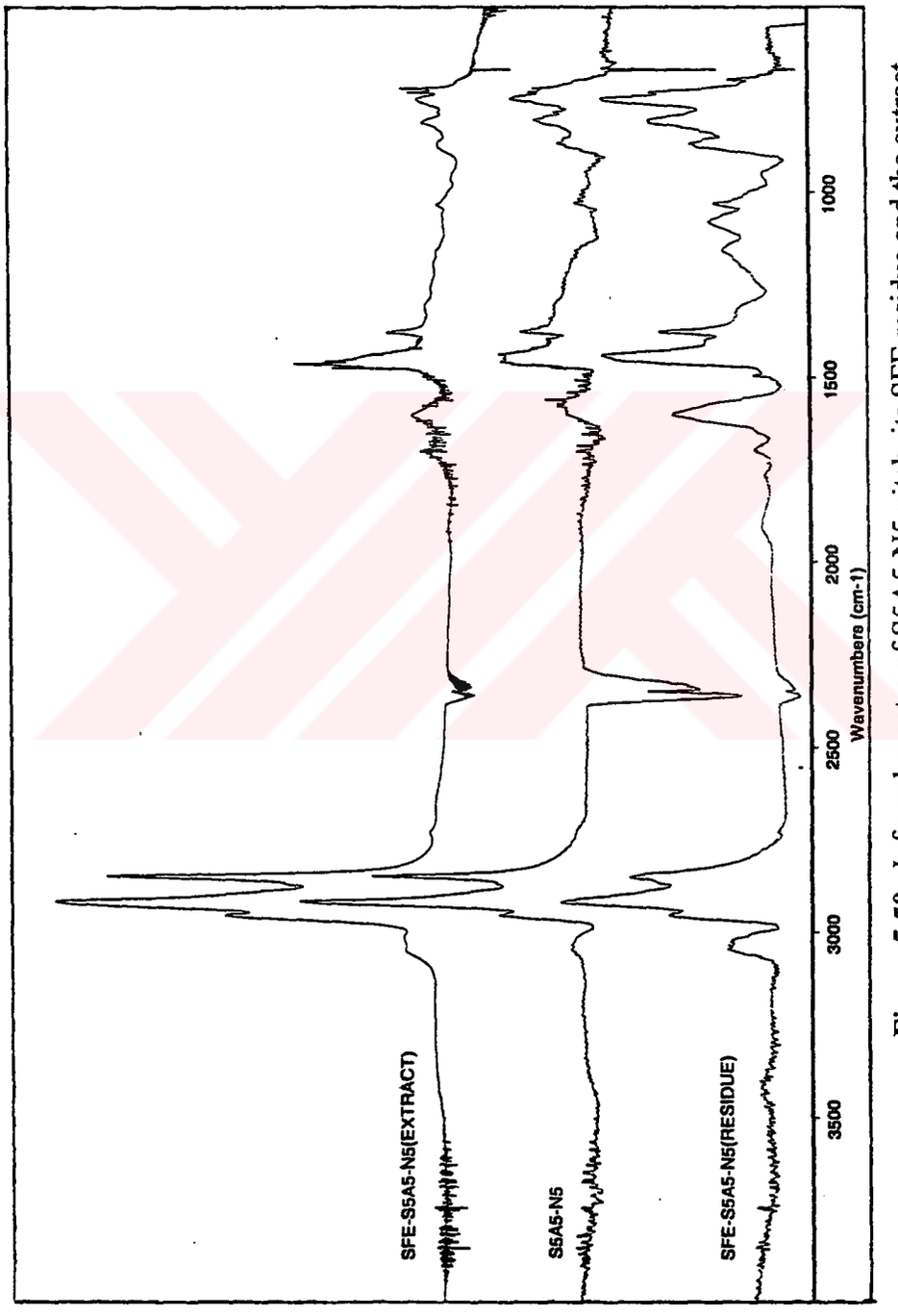

Figure 5.50 Infrared spectra of S5A5-N5 pitch, its SFE residue and the extract.

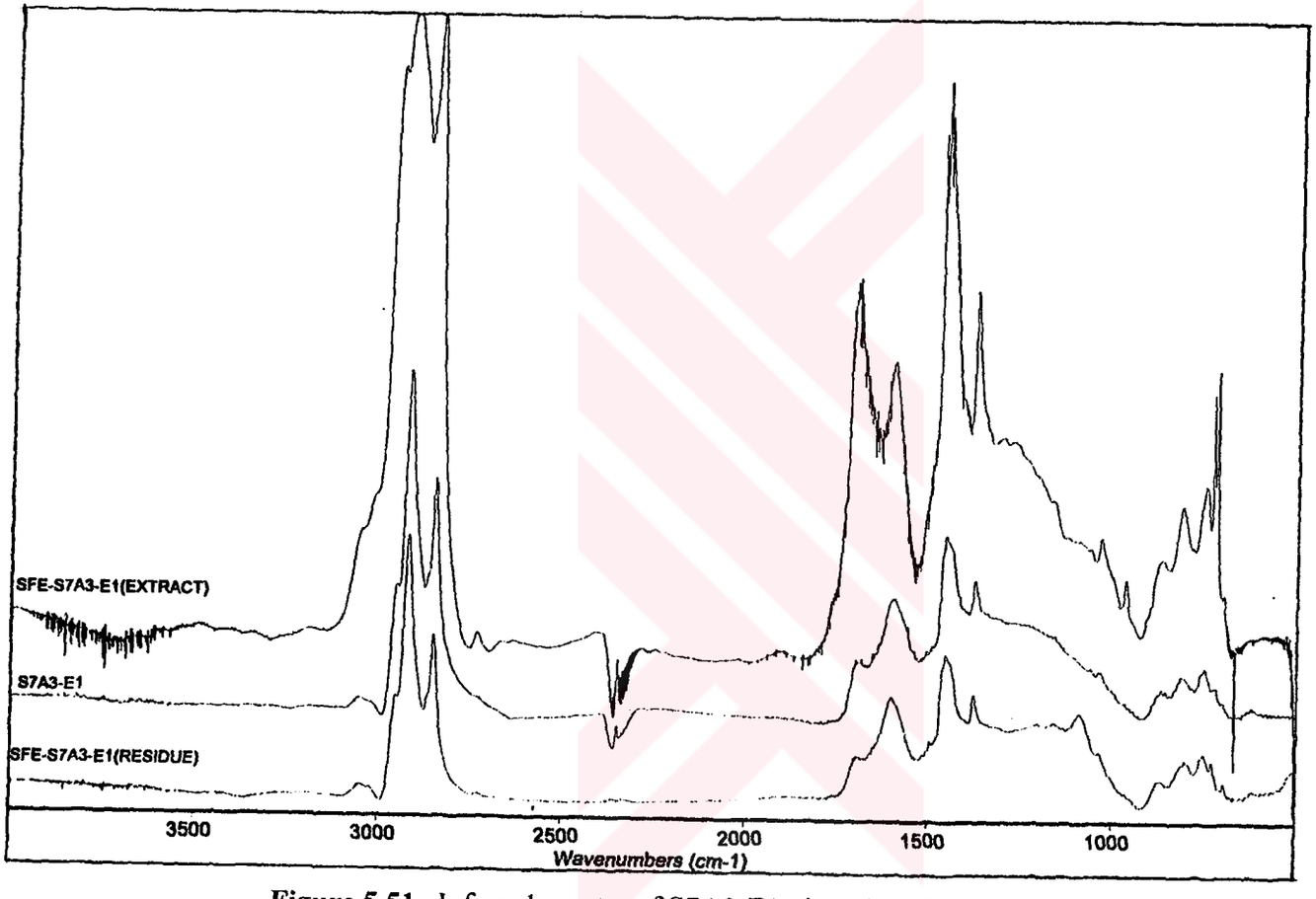

Figure 5.51 Infrared spectra of S7A3-E1 pitch, its SFE residue and the extract.

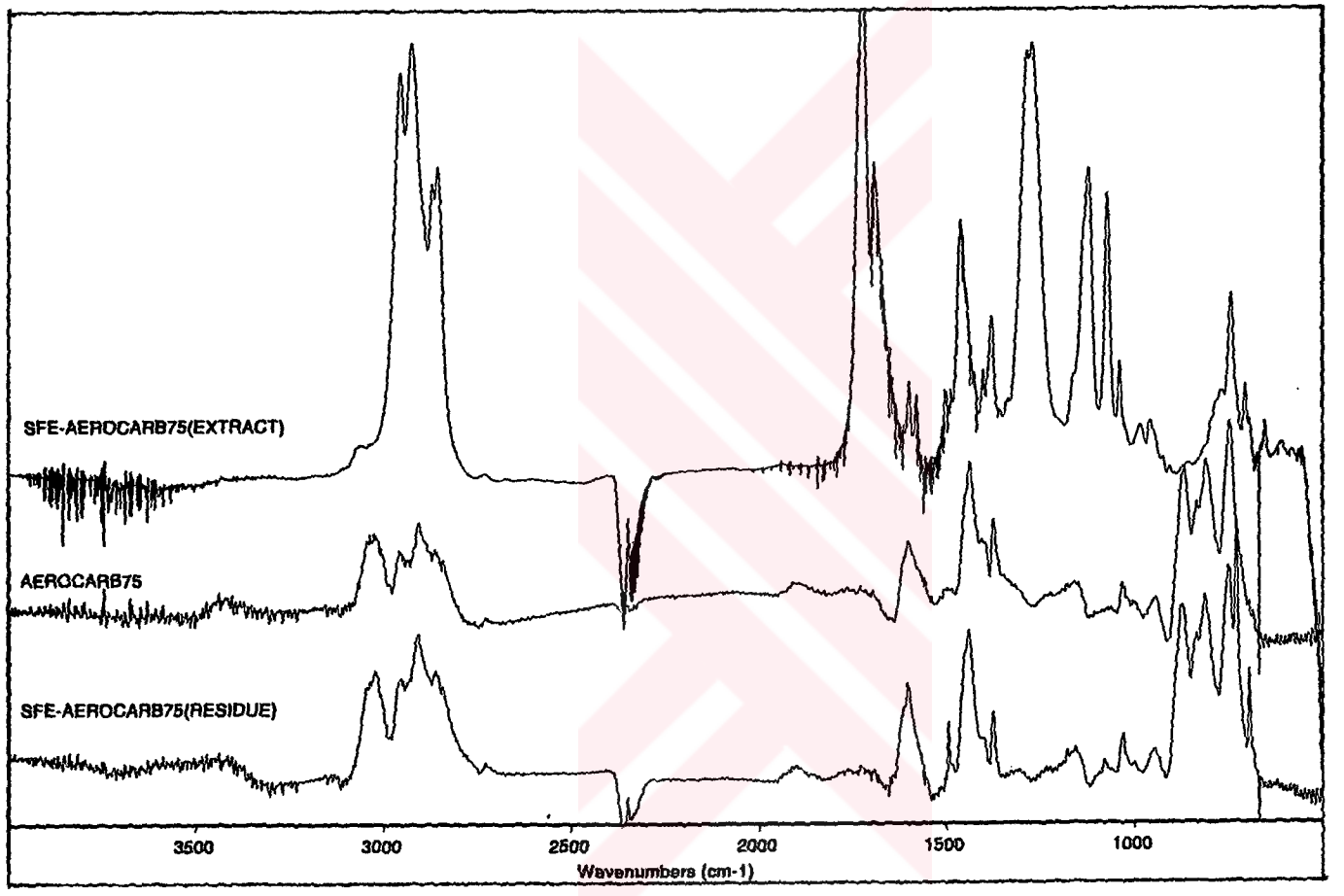

Figure 5.52 Infrared spectra of Aerocarb75 pitch, its SFE residue and the extract.

6. CONCLUSIONS

In order to improve the economics of oil shale and asphaltite, which comprise large amounts of reserves in Turkey, Göynük oil shale and Avgamasya asphaltite have been used as possible new candidate hydrocarbon sources for the production of pitch precursors and general purpose carbon fibres. The direct application of specific treatments to parent tar has been thought to simplify the pitch preparation procedure and reduce the costs. Therefore, parent tar has been produced by the co-pyrolysis of Göynük oil shale and Avgamasya asphaltite.

Several methods such as air-blowing, nitrogen-blowing (thermal treatment), vacuum-distillation, and vacuum-distillation followed by solvent extraction have been applied to parent tars in order to produce pitch precursors and to modify their compositions.

To monitor the chemical changes in tar and pitch precursors, various techniques have been used including elemental analysis, TI measurement, thermal analysis (TGA and DDSC), size exclusion chromatography (SEC), softening point measurement, mass spectroscopy (FAB-MS), infrared spectroscopy (FTIR), and nuclear magnetic resonance spectroscopy (^{1}H and ^{13}C NMR). Optical microscopy has been used to investigate the optical texture of the cokes obtained from the pitch precursors. The surface characteristics of the fibres produced from one of the selected pitches have been observed by using scanning electron microscopy (SEM). Depending on the results of these analysis, following conclusions can be proposed:

1. The co-pyrolysis of GOS and AA mixture in some ratios has resulted in a slight synergistic effect. The difference between the experimental yield and calculated yield has also been slight. However, as the percentage of the GOS decreases in the raw mixture, the yield of all the tars and the H/C atomic ratio for S7A3 and S5A5 tars decreases.

2. The pitch yield decreases with the extent of air-blowing, and nitrogen-blowing. Besides time and temperature, the use of high air and nitrogen flows during treatments might lead to low pitch yield. However, vacuum-distillation has resulted in the least pitch yield among the other modification methods. This should be attributed to the significant removal of the volatiles during vacuum-distillation.

3. Air-blowing and nitrogen-blowing have found to be useful methods for increasing the softening points of the tar materials to the values between 110-160°C. On the contrary, vacuum-distillation has not been successful to increase the softening points. However, vacuum-distillation followed by hexane extraction has been found as an effective method in increasing the softening point of the S7A3-V1 pitch.

4. The H/C atomic ratios of the pitches have been decreased with the severity of air-blowing and nitrogen-blowing. The carbon yield of the pitches is diversely proportional with the H/C atomic ratio since the carbon yield increases with decreasing H/C ratio. The decrease in the H/C ratio should be due to dehydrogenative condensation during air-blowing and the removal of the light molecular weight components during heat treatment. This should be resulted in high carbon yield during carbonisation of the pitches.

Vacuum-distillation has resulted in highest H/C atomic ratio and lowest carbon yield.

5. The pitches have shown high reactivity with air during air-blowing. The severe air-blowing conditions have resulted in the formation of cokes from the pitches. This should be due to the high reactivity of Göynük oil shale in the mixtures.

6. Air-blowing has resulted in mild oxidation in the pitches. The polymerisation of oxygen with methylene which leads to partial conversion to carbonyl has been reflected by the slight increase of absorption intensity band at around 1697 cm^{-1} in the FTIR spectra.

7. Relation has been found between the softening points, H/C atomic ratios, and hydrogen aromaticity indices (I_{Ar}) of the pitches produced by several methods. As H/C atomic ratio decreases the softening point and the I_{Ar} value increase. Among all processing methods, nitrogen-blowing has appeared to be an effective method for pitch modification. S5A5-N5 pitch, which was produced by nitrogen-blowing at

300°C for 60 minutes, has been found the most aromatic pitch and FTIR, ^{1}H and ^{13}C NMR analysis results have confirmed each other.

8. The cokes obtained by the carbonisation of pitches produced by several methods have given different optical textures. The cokes resulted from nitrogen-blown and vacuum-distilled pitches have shown coarse and medium grained mosaics while the coke obtained from air-blown pitch has shown flow domains. Flow domains are not the familiar optical textures of the cokes obtained from air-blown pitches. However, in the case of studied coke, the lack of oxygen incorporation into the molecules of pitch during air-blowing might lead to flow domains at the end of carbonisation stage. The pitch produced by vacuum-distillation followed by hexane extraction has resulted in a coke totally isotropic.

9. Vacuum-distillation followed by hexane extraction has resulted in a spinnable pitch. However, since the softening point of the S7A3-E1 pitch is not high enough to result in a successful oxidative stabilisation, the green fibres have been stabilised by nitric acid. The SEM images of the carbonised fibres have shown some surface distortions, probably due to the pitch composition and/or insufficient stabilisation.

10. Supercritical fluid extraction (SFE) of pitches with CO_2 modified by hexane at 150°C and 400 atm for 30 minutes have removed a great percentage of the light fractions of the pitches. Therefore, SFE has resulted in pitch residues with lower H/C atomic ratios. Since S-A2 pitch is mainly aliphatic, SFE of S-A2 pitch with CO_2 modified by toluene has lead to 100% dissolution of the pitch.

SFE has been found to be a clean and an effective extraction technique to remove the light components from the pitch.

7. RECOMMENDATIONS AND FUTURE WORK

The present study has shown that the modification of Göynük oil shale-Avgamasya asphaltite co-pyrolysis tar by some methods resulted in pitches with intermediate and low aromaticities and softening points. These pitches can be used as new substitute source for the production of general purpose carbon fibres. However, some further studies may be interesting to investigate such as:

1. The use of some additives to improve the chemical and structural characteristics of the pitches.

2. The investigation of the effect of composition of GOS and AA in the optical texture of pitches derived by different methods.

3. Pyrolysis is one of the most relevant method for tar production from the GOS. However, tar yield from pyrolysis of AA is very low. SFE can be substitute method in terms of higher tar yield and chemical composition of the GOS and AA mixture for tar production.

4. One of the aims of this research was to produce isotropic pitch. However, the development of mesophase structure in the pitch precursors has been observed during optical texture analysis. In this context, mesophase development and the qualification will be interesting to investigate for further studies.

REFERENCES

[1] **Özsöz, E.K.,** 1999. Carbon Fibres and Their Economics, *BSc Dissertation*, İ.T.Ü., Chemical Engineering Department, Istanbul.

[2] **Menendez, R., Granda, M., and Bermejo, J,** 1997. Pitch Pyrolysis Chemistry, Mesophase Chemistry and Coking, *Introduction to Carbon Technologies*, pp.461-484, Eds. Marsh, H., Heintz, E.A., and Rodriguez-Reinoso, F., Universidad de Alicante, Secretariado de Publicaciones.

[3] **Lu, S., Rand, B., Bartle, K.D., and Reid, A.W.,** 1997. Novel Oxidation Resistant Carbon-Silicon Alloy Fibres, *Carbon*, **35**, 10-11, 1485-1493.

[4] **Wang, C.Y., and Inagaki, M.,** 1998. Oxidation Resistance of Pitch-Based Carbon Fibres During Heat-Treatment in Carbon Dioxide, *Proceedings of the International Symposium of Carbon,* Tokyo, Japan, 242-243.

[5] **Ismail, M.K. Ismail,** 1992. Modelling Carbon Fibers Oxidation in Air at Constant Heating Rates, *Carbon*, **30**, 3, 419-427.

[6] **Yonemoto, T., Nitta, H., Kawata, T., and Tadaki, T.,** 1992. Modelling of Isothermal Oxidative Stabilisation of Mesophase Pitch Fibre, *Journal of Chemical Engineering*, **49**, 133-139.

[7] **Savage, G.,** 1993. Carbon-Carbon Composites, Chapman and Hall, London.

[8] **Lewis, I.C.,** 1998. Preparation and Properties of Novel Pitches, *Extended Abstracts of the EUROCARBON'98*, Strasbourg. France, 39-40.

[9] **Prada, V., Granda, M., Bermejo, J., and Menendez, R.,** 1998. Carbon Precursors from Tar Air-Blowing, *Extended Abstracts of the EUROCARBON'98*, Strasbourg. France, 231-232.

[10] **Edie, D.D.,** 1989. Pitch and Mesophase Fibers, *Carbon Fibers Filaments and Composites,* pp.43-94, Eds. Figueiredo, J.L., Bernardo, C.A., Baker, R.T.K., and Huttinger, K.J., NATO ASI Series, Kluwer Academic Publishers, Dordrecht.

[11] **Derbyshire, F., Jacques, D., Jagtoyen, M., Kimber, G., Rantell, T., and Vego, A.,** 1998. Activated Carbon Fibres from Non-Conventional Pitch Precursors, *Extended Abstracts of the EUROCARBON'98*, Strasbourg. France, 63-64.

[12] **Kimber, G.M., Fei, Y.Q., Jagtoyen, M., and Derbyshire, F.J.,** 1995. Coal Based Activated Carbon Fiber Composites for Gas Separation, Coal Science, Eds. Pajares, J.A., and Tascon, J.M.D., *Proceedings of the 8th ICCS*, Elsevier, Amsterdam, 1157-1160.

[13] **Thwaites, M.W., Steward, M.L., McNeese, B.E., and Sumner, M.B.,** 1993. Synthesis and Characterisation of Activated Pitch-Based Carbon Fibres, *Fuel Processing Technology*, **34**, 137-145.

[14] **Ekinci, E., Akar, A., Okutan, H., Yardım, M.F., Çıtıroğlu, M., Özdemir, M., Hilmioğlu, B., ve Apak, E.,** 1996. Bitümlü Şistlerden Petrol Üretimi, DPT Teknolojik Araştırma Projesi, Proje No: 90K120760, İstanbul, Türkiye.

[15] **Erdem-Senatalar, A.,** 1984. Avgamasya Asfaltitinin Sıvılaşma Potansiyelinin ve Ekstrakt Yapılarının İncelenmesi, *Doktora Tezi*, İ.T.Ü. Fen Bilimleri Enstitüsü, İstanbul.

[16] **Edwards, I.A.S.,** 1989. Structure in Carbons and Carbon Forms, *Introduction to Carbon Science,* pp.1-36, Ed. Marsh, H., Butterworths, London.

[17] **Ehrburger, P.,** 1996. Carbon: A Material for Modern Technology, *Proceedings of the of the 2nd Turkish Chemical Engineering Congress,* Istanbul, Turkey, 60-71.

[18] **Ruland, W.,** 1968. X-Ray Diffraction Studies on Carbon and Graphite, *Chemistry and Physics of Carbon,* 4, pp.1-80, Ed. Walker, P.L., Jr., Marcel Dekker, Inc., New York.

[19] **Griffiths, J.,** 1982. High Resolution Electron Microscopy Study of Graphitization of Graphitizable Carbons, *Proceedings of the International Symposium on Carbon*, Toyohashi, Japan, 81.

[20] **Brooks, J.D., and Taylor, G.H.,** 1968. The Formation of Some Graphitizing Carbons, *Chemistry and Physics of Carbon,* 4, p.243, Ed. Walker, P.L., Jr., Marcel Dekker, Inc., New York.

[21] **Marsh, H., and Menendez, R.,** 1989. Mechanisms of Formation of Isotropic and Anisotropic Carbons, *Introduction to Carbon Science*, p.38, Ed. Marsh, H., Butterworths, London.

[22] **Miura, K., Nakagawa, H., and Hashimoto, K.,** 1995. Examination of the Oxidative Stabilisation Reaction of Pitch Based Carbon Fibres Through Continuous Measurement of Oxygen Chemisorption and Gas Formation Rate, *Carbon*, **33**, 3, 275-282.

[23] **Chung, D.L., Deborah,** 1994. Carbon Fibre Composites, Butterworths-Heinemann, Boston.

[24] **Diefendorf, J., R,** 1987. Carbon/Graphite Fibres, *Engineered Materials Handbook*, Composites, **1**, p.49, ASM Int., Ohio, USA.

[25] **Hansen, W., N,** 1987. Carbon Fibres, *Engineered Materials Handbook*, **1**, p.112, Composites, ASM Int., Ohio, USA.

[26] **Fitzer, E.,** 1989. Carbon Fibres-Present State and Future Expectations, *Carbon Fibres Filaments and Composites,* p.6, Eds. Figueriredo, J.L., Bernardo, C.A., Baker, R.T.K., and Huttinger, K.J., NATO ASI Series, Kluwer Academic Publishers, Dordrecht.

[27] **Fitzer, E., and Heine, M.,** 1988. Carbon Fibre Manufacture and Surface Treatment, Composite Materials Series, *Fibre Reinforcement for Composite Materials,* **2**, pp.37-148, Ed. Russel, A.R., Elsevier, Amsterdam.

[28] **Otani, S.,** 1965. The Fundamental Structure of MP Carbon Fibre, *Carbon*, **3**, 213.

[29] **Fitzer, E., Muller, K., and Schafer, W.,** 1971. Chemistry and Physics of Carbon, **7**, pp.237-283, Ed. Walker, P.L., Jr., Marcel Dekker, Inc., New York.

[30] **Bacon, R.,** 1973. Chemistry and Physics of Carbon, **9**, p.7, Ed. Walker, P.L., Jr., Marcel Dekker, Inc., New York.

[31] **Pilato, A.L., and Michno, J.M.,** 1994. Advanced Composite Materials, Springer-Verlag, Berlin.

[32] **Tibbets, G.G.,** 1989. Vapor-Grown Fibres, *Carbon Fibres Filaments and Composites*, p.73, Eds. Figueriredo, J.L., Bernardo, C.A., Baker, R.T.K., and Huttinger, K.J., NATO ASI Series, Kluwer Academic Publishers, Dordrecht.

[33] **Koyama, T.,** 1972. Formation of Carbon Fibres from Benzene, *Carbon*,**10**, p.757.

[34] **Alig, B.,** 1996. Process Produces Vapor-Grown Carbon Fibres Using Coal, *ENERGEIA.*, CAER-University of Kentucky, Center for Applied Energy Research,.**7**, 1, 1-4.

[35] **Tibbets, G.G., Bernardo, C.A., Gorkiewicz, D.W., and Alig, R.L.,** 1994. Role of Sulfur in the Production of Carbon Fibres in the Vapor Phase, *Carbon*, **32**,4, 569.

[36] **Katsuki, H., Matsugana, K., Egashira, M., and Kawasumi, S.,** 1981. Formation of Carbon-Fibres from Naphthalene on Some Sulfur-Containing Substrates, *Carbon*, **19**, 4, 148.

[37] **Tibbets, G.G., Bernardo, C.A., Gorkiewicz, D.W., and Alig, R.L.,** 1993. Effect of Sulfur on the Production of Carbon Fibres in the Vapor Phase, *Extended Abstracts of the 21st Biennial Conference on Carbon*, Buffalo, USA, 185.

[38] **Otani, S.,** 1981. Carbonaceous Mesophase and Carbon Fibres, *Mol. Cryst. Liq. Cryst.,* **63**, 249-264.

[39] **Donnet, J.B., and Bansal, R.C.,** 1990. Carbon Fibres, *International Fibre Science and Technology,***10**, Marcel Dekker, New York, USA.

[40] **Lewis, I.C.,** 1980. Thermal Polymerisation of Aromatic Hydrocarbons, *Carbon,***18**, 191.

[41] **Riggs, D.M., and Diefendorf, R.J.,** 1983. Solvent Extracted Pitch Precursors for Carbon Fibre, *Extended Abstracts of the 16th Biennial Conference on Carbon*, San Diego, USA, 24-25.

[42] **Zander, M.,** 1987. On the Composition of Pitches, *Fuel*, **66**, 1536.

[43] **Riggs, D.M., and Diefendorf, R.J.,** 1980. Factors Controlling the Thermal Stability and Liquid Crystal Forming Tendencies of Carbonaceous Materials, *Preprints of the 3rd International Carbon Conference,* Baden-Baden, Germany, 330-333.

[44] **Rand, B., and Shephard, P.M.,** 1980. Glass Transition in Some Pitch Materials, *Fuel*, **59**, 814.

[45] **Nazem, F.F.,** 1982. Flow of Molten Mesophase Pitch, *Carbon*, **20**, 345.

[46] **Romey, I., and Hein, M.,** 1981. Carbon Fibres from Coal Tar Pitch, *Fuel*, **60**,.848.

[47] **Yoon, H.S., Korai, Y., and Mochida, I.,** 1993. Microtexture of Precursor Pitch on the Texture and Microstructure of Pitch Fibre, *Extended Abstracts of the 21st Biennial Conference on Carbon,* Buffalo, USA, 256-257.

[48] **Dhami, T.L., Manocha, L.M., and Bahl, O.P.,** 1991. Oxidation Behavior of Pitch Based Carbon Fibres, *Carbon*, **29**, 1.

[49] **Monge-Alcaniz, J., Amoros-Cazorla, D., Solano-Linares, A., Oya, A., Sakamoto, A., and Hoshi, K.,** 1995. Preparation and Properties of Carbon Fibres Derived from a Spanish Coal Tar Pitch, Coal Science, Eds. Pajares, J.A., and Tascon, J.M.D, *Proceedings. of the 8th ICCS,* , Elsevier, Amsterdam, **2**, 1161.

[50] **Monge-Alcaniz, J., Amoros-Cazorla, D., Solano-Linares, A., Oya, A., Sakamoto, A., and Hoshi, K.,** 1997. Preparation of General Purpose Carbon Fibres from Coal Tar Pitches with Low Softening Point, *Carbon*, **35**, 8, 1079-1087.

[51] **Liu, G.Z., Edie, D.D., and Fain, C.C.,** 1991. Processing Isotropic Pitch Based Carbon Fibres, *Extended Abstracts of the 20th Biennial Conference. on Carbon*, Santa Barbara,, USA, 264.

[52] **Otani, S., Yamada, K., Koitabashi, T., and Yokoyama, A.,** 1966. On the Raw Materials of MP Carbon Fibres, *Carbon*, **4**, 425-432.

[53] **Mochida, I., Korai, Y., Nakamura, M., and Zeng, S.M.,** 1989. Preparation of Precursor Pitch for Isotropic Carbon Fibres, *Carbon*, **27**, 3, 498-500.

[54] **Fitzer, E., and Liu,G.Z.,** 1989. The Effect of Sulfur Addition to Coal Tar and Petroleum Pitch As Precursor for Isotropic Carbon Fibres, *Extended Abstracts of the 19th Biennial Conference on Carbon,* University Park, PA, USA, 254-255.

[55] **Arai, Y., Tomioka, T., Matsumoto, M., and Kobayashi, K.,** 1992. Determination of Solid Impurities in Mesophase Pitch by a Filtration Model of a Binary Cake, *Journal of Chem. Eng. of Japan*, **25**, 4, 415.

[56] **Otani, S.,** 1965. On the Carbon Fibre from the Molten Pyrolysis Products, *Carbon*, **3**, 31-38.

[57] **Singer, L.S.,** 1981. Carbon Fibres from Mesophase Pitch, *Fuel*, **60**, 839.

[58] **Korai, Y., and Mochida, I.,** 1991. Change in Molecular Assembly of Mesophase Pitch at Higher Temperature, *Extended Abstracts of the 20th Biennial Conference on Carbon*, Santa Barbara, USA, 148-149.

[59] **Mochida, I., Shmizu, K., Korai, Y., Otsuka, H., SAKAI, Y., and Fujiyama, S.,** 1990. Preparation of Mesophase Pitch from Aromatic Hydrocarbons by the Aid of HF/BF_3, *Carbon*, **28**, 2/3, 311-319.

[60] **Lewis, I.C.,** 1984. Chemistry and Development of Mesophase in Pitch, *Journal de Chimie Physique*, 11/12, 751.

[61] **Lee, Y.H., Liu, A.M., and Shao, C.H.,** 1990. Surface Characteristics of the Meophase of Coal-Tar Pitch as an Industrial Application, *Proceedings of the International Symposium. on Carbon*, Tsukuba, Japan, 22-25.

[62] **Brooks, J.D., and Taylor, G.H.,** 1965. The Formation of Graphitizing Carbons from the Liquid Phase, *Carbon,* **3**, 185-193.

[63] **Mochida, I., Shmizu, K., Korai, Y., Sakai, Y., Fujiyama, S., Toshima, H., and Sakai, T.,** 1992. Mesophase Pitch Catalytically Prepared from Anthracene with HF/BF_3, *Carbon*, **30**, 1, 55-61.

[64] **Lafdi, K., Bonnamy, S., and Oberlin, A.,** 1991. Mechanism of Anisotropy Occurrence in a Pitch Precursor of Carbon Fibres: Part 1-Pitches A and B, *Carbon*, **29**, 7, 831-847.

[65] **Chwastiak, S., and Lewis, I.C.,** 1978. Solubility of Mesophase Pitch, *Carbon*, **16**, 156.

[66] **Park, Y.D., Korai, Y., and Mochida, I.,** 1989. Preparation of Anisotropic Mesophase Pitch by Carbonisation Under Vacuum, *Journal of Materials Science*, **21**, 97.

[67] **Toshima, H., Mochida, I., Korai, Y., and Hino, T.,** 1992. Modification of Petroleum-Derived Mesophase Pitch by Blending Naphthalene-Derived Partially Isotropic Pitches, *Carbon*, **30**, 5, 773-779.

[68] **Singer, L.S., Riffle, D.M., and Cherry, A.R.,** 1987. High-Temperature Centrifugation: Application to Mesophase Pitch, *Carbon*, **25**, 249-257.

[69] **Lewis, R.T.,** 1975. Hot Stage Microscopy of Mesophase Pitches, *Extended Abstracts of the 12th Biennial Conference on Carbon,* Pennsylvania, USA, 215.

[70] **Riggs, D.M., and Diefendorf, R.J.,** 1980. A Phase Diagram for Pitches, *Preprints of the 3rd International Carbon Conference,* Baden-Baden, Germany, 326-329.

[71] **Yudate,K., Ohsugi, Y., and Kamisita, M.,** 1990. Preparation of Mesophase-Pitch with Low Viscosity, *Proceedings of the International Symposium on Carbon*, Tsukuba, Japan, 38.

[72] **Lewis, I.C.,** 1982. Chemistry of Carbonisation, *Carbon*, **20**, 6, 519-529.

[73] **Huttinger,K.J., and Rosenblatt, U.,** 1977. Pressure Effects on the Yield and on the Microstructure Formation in the Pyrolysis of Coal Tar and Petroleum Pitches, *Carbon*, **15**, 69.

[74] **Singer,L.S., and Lewis, I.C.,** 1978. ESR Study of the Kinetics of Carbonisation, *Carbon*, **16**, 417.

[75] **Greinke, R.A.,** 1986. Kinetics of Petroleum Pitch Polymerisation by Gel Permeation Chromatography, *Carbon*, **24**, 6, 677.

[76] **Greinke, R.A., and Lewis, I.C.,** 1984. Carbonisation of Naphthalene and Dimethylnaphthalene, *Carbon*, **22**, 2, 305.

[77] **Riggs, D.M., and Diefendorf, R.J.,** 1979. The Solubility of Aromatic Compounds, *Extended Abstracts of 14th Biennial Conference on Carbon,* PennState, USA, 413.

[78] **Greinke, R.A.,** 1990. Quantitative Influence of Dealkylation and Polymerisation Reactions on Mesophase Formation, *Carbon*, **28**, 5, 701-706.

[79] **Bhatia, G., Fitzer, E., and Kompalik, D.,** 1986. Mesophase Formation in Defined Mixtures of Coal Tar Pitch Fractions, *Carbon*, **24**, 4,489-494.

[80] **Chwastiak, S., Lewis, I.C., and Ruggiero, J.D.,** 1981. Quantitative Determination of Mesophase Content in Pitch, *Carbon*, **19**, 5, 357-363.

[81] **Honda, H., Kimura, H., Sanada, Y., Sugawara, L., and Furata, T.,** 1981. Optical Mesophase Texture and X-Ray Diffraction Pattern of the Early-Stage Carbonisation of Pitches, *Carbon*, **8**, 181-189.

[82] **Park, Y.D., and Yoon, S.H.,** 1990. Pyrolytic Behaviours of Pitch Materials-Synthesis of Mesophase Pitch by Heterogeneous Nucleation Method, *Proceedings of the International Symposium on Carbon*, Tsukuba, Japan, 16.

[83] **Lu, S.,** 1997. Carbon-Silicon Alloy Fibres From Polymeric Precursors, *PhD Thesis*, University of Leeds, Department of Materials, UK.

[84] **Lin, S.S.,** 1991. Oxidative Stabilisation in Production of Pitch Based Carbon Fibre, *SAMPE Journal*, **27**, 1, 9-14.

[85] **Korai, Y., Mochida, I., and Matsumoto, T.,** 1987. Stabilisation Process of Pitch Based Carbon Fibre, *Extended Abstracts of the 18th Biennial Conference on Carbon*, Worcester, USA, 411-412.

[86] **Bhat, G.S., Cook, F.L., Peebles, L.H. JR., and Abhiraman, A.S.,** 1989. New Aspects in the Stabilisation of PAN-Based Precursors for Carbon Fibres, *Proceedings of the 19th Biennial Conference on Carbon*, University Park, PA, USA, 252-254.

[87] **Ma, A.C., Chen, S.H., and Diefendorf, R.J.,** 1989. Oxidative Stabilisation of Pitch-Based Carbon Fibres, *Proceedings of the 19th Biennial Conference on Carbon*, University Park, PA, USA, 128-129.

[88] **Lavin, J.G.,** 1992. Chemical Reactions in the stabilisation of Mesophase Pitch-Based Carbon Fibre, *Carbon*, **30**, 3, 351-357.

[89] **Drbohlav, J., and Stevenson, W.T.K.,** 1995. The Oxidative Stabilisation and Carbonisation of a Synthetic Mesophase Pitch, Part II: The carbonisation process, *Carbon*, **33**, 5, 713-731.

[90] **Korai, Y., Nakamura, M., and Mochida, I.,** 1991. Mesophase Pitches Prepared from Methylnaphthalene by the Aid of HF/BF_3, *Carbon*, **29**, 561.

[91] **Drbohlav, J., and Stevenson, W.T.K.,** 1995. The Oxidative Stabilisation and Carbonisation of a Synthetic Mesophase Pitch, Part I: The oxidative stabilisation process, *Carbon*, **33**, 5, 693-711.

[92] **Benson, S.W.,** 1965. Effetcs of Resonance and Structure on the Thermochemistry of Organic Peroxy Radicals and the Kinetics of Combustion Reactions, *Journal of American Chemical Society,* **87**, 972-979.

[93] **Woodward, A.E., and, Mesorbian, R.B.,** 1953. Low Temperature Autoxidation of Hydrocarbons. The Kinetics of Tetralin Oxidation, *Journal of American Chemical Society*, **75**, 6189.

[94] **Lietke, V., Huttinger, K.J.,** 1996. Mesophase Pitches as Matrix Precursor of Carbon Fibre Reinforced Carbon: II. Stabilisation of Mesophase Pitch Matrix by Oxygen Treatment, *Carbon*, **34**, 9, 1067-1079.

[95] **White, J.L., and Sheaffer, P.M.,** 1989. Effect of Oxidation Stabilisation on Carbonisation Yield, *Carbon*, **28**, 1, 235-236.

[96] **Mochida, I., Shimizu, K., Korai, Y., Otsuka, H., and Fujiyama, S.,** 1988. Structure and Carbonisation Properties of Pitches Produced Catalytically from Aromatic Hydrocarbons with HF/BF_3, *Carbon*, **26**, 6, 843-852.

[97] **Politis, T.G., and Chang, C.F.,** 1985. Pitch Carbonisation, *Extended Abstracts of the 17th Biennial Conference on Carbon,* Lexington, Kentucky, USA, 8-9.

[98] **Ryu, S.K., Lee, J.K., In, S.J., and Rhee, B.S.,** 1991. Carbonisation of Isotropic Pitch Fibre Oxidised by Nitric Acid Vapor, *Extended Abstracts of the 20th Biennial Conference on Carbon,* Santa Barbara, USA, 280-281.

[99] **Oberlin, A., 1984.** Carbonisation and Graphitization, *Carbon*, **22**, 6, 521-541.

[100] **Daji, J.,** 1998. Rheological Characterisation of Pitch Based Precursors, *PhD Thesis*, The University of Leeds, Department of Materials, UK.

[101] **Fric, K.C.J.,** 1969. An Introduction to Thermogravimetry, Heyden and Son Ltd., Bath.

[102] **Wendlant, W.W.M.,** 1974. Thermal Methods of Analysis, **19**, John Wiley and Sons, New York.

[103] **Rand, B., and Benn, M.,** 1989. Thermogravimetric Study of the Pyrolysis of Pitch and Mesophase Pitch, *Extended Abstracts of the19th Biennial Conference on Carbon,* University Park, PA, USA, 100-101.

[104] **Bermejo, J., Granda, M., Menendez, R., and Tascon, J.,M.D.,** 1991. Comparative Characterisation by TG and DTA of Different Kinds of Pitches, *Extended Abstracts of the 20th Biennial Conference on Carbon*, Santa Barbara, USA, 116-117.

[105] **Martinez-Alonso, A., Bermejo, J., Granda, M., and Tascon, J.M.D.,** 1992. Suitability of Thermogravimetry and Differential Thermal Analysis Techniques for the Characterisation of Pitches, *Fuel*, **71**, 611-617.

[106] **Alula, M., Cagniant, D., Lauer, J.C.,** 1990. Contribution to Characterisation of Pyrolysis Coal Products by Means of Thermal Analysis, *Fuel*, **69**, 177-182.

[107] **Ehrburger, P., Martin, C., Lahaye, J., and Couderc, P.,** 1987. Glass Transition Characteristics of Coal Tar Pitches, *Extended Abstracts of the 18th Biennial Conference on Carbon,* Worcester, USA, 165-166.

[108] **Khandare, P.M., Zondlo, J.W., and Pavlovic, A.S.,** 1996. The Measurement of Glass Transition Temperature of Mesophase Pitches Using a Thermomechanical Device, *Carbon*, **34**, 5, 663-669.

[109] **Wunderlich, B.,** 1990. Thermal Analysis, Academic Press, Inc., San Diego.

[110] **Lahaye, J., Ehrburger, P., Saint-Romain, J.L., and Couderc, P.,** 1987. Physicochemical Characterisation of Pitches by Differential Scanning Calorimetry, *Fuel*, **66**, 11, 1467-1471.

[111] **Rand, B.,** 1987. Pitch Precursors for Advanced Carbon Materials - Rheological Aspects, *Fuel*, **66**, 1491.

[112] **Preiss, H., Szulzewsks, K., and Kotsch, P.,** 1993. Characterisation of Pitches by X-Ray Scattering and Differential Scanning Calorimetry, *Fuel*, **72**, 9, 1301-1303.

[113] **Stadelhofer, J.W.,** 1979. The Glass Transition of Coal-Derived Low-Volatile Residues, *Carbon*, **17**, 301-303.

[114] **Hayward, J.S., Ellis, B., and Rand, B.,** 1988. Characterisation of Pyrolysis Products of Pitch Materials by Broad Line Proton NMR Spectroscopy and Thermogravimetry, *Carbon*, **26**, 1, 71.

[115] **Ehrburger, P.,** 1994. Glassy Properties of Coal Tar Pitch Materials, *ENERGEIA*, CAER-University of Kentucky, Center for Applied Energy Research, **5**, 3.

[116] **Barr, J.B., and Lewis, I.C.,** 1982. Characterisation of Pitches by Differential Scanning Calorimetry and Thermomechanical Analysis, *Thermochimica Acta*, **52**, 297-304.

[117] **Rand, B., Turpin, M., and Cheung, T.,** 1990. The Use of Controlled Stress Rheology for the Characterisation of Precursors for Carbon Materials, *Proceedings of the International Symposium on Carbon,* Tsukuba, Japan, 42-45.

[118] **Rand, B., West, S.C., Ellis, B., and Turpin, M.,** 1995. Effect of Composition on the Glass Transition and Rheological Properties of Pitch, *Extended Abstracts of the 22nd Biennial Conference on Carbon,* San Diego, USA, 1998-1999.

[119] **Turpin, M., Cheung, T., and Rand, B.,** 1996. Controlled Stress, Oscillatory Rheometry of Mesophase Pitches, *Carbon*, **34**, 2, 265-271.

[120] **Daji, J., and Rand, B.,** 1997. Elasticity of Isotropic Pitches Observed by Dynamic and Creep Rheology, *Extended Abstracts* of the *23rd Biennial Conference on Carbon*, PennState, USA, 184.

[121] **Menendez, R., Figueiras, A., Bermejo, J., Fleurot, O., and Edie, D.,** 1997. The Influence of Thermal Treatment on the Rheology of Coal Tar Pitches, *Extended Abstracts* of the *23rd Biennial Conference on Carbon*, PennState, USA, 204.

[122] **Daji, J., and Rand, B.,** 1998. The Rheological and Thermal Behaviour of Pitch Based Precursors, *Proceedings of the International Symposium of Carbon*, Tokyo, Japan, 572-573.

[123] **Collet, G.W., and Rand, B.,** 1978. Rheological Investigation of Coal Tar Pitch During Its Transformation to Mesophase, *Fuel*, **57**, 3, 162-170.

[124] **Balduhn, R., and Fitzer, E.,** 1980. Rheological Properties of Pitches and Bitumina up to Temperatures of 500°C, *Carbon*, **18**, 155-161.

[125] **Nazem, F.,** 1980. Rheology of Carbonaceous Mesophase Pitch, *Fuel*, **59**, 851-858.

[126] Annual Book of ASTM Standards, 1987. **4**, 359-367.

[127] **Romovacek, G.R.,** 1987. New Analytical Methods for Pitch Characterisation and Production Control, *Extended Abstracts of the 18th Biennial Conference on Carbon,* Worcester, USA, 163-164.

[128] **Cao, J., Buckley, A.N., and Lynch, L.,** 1994. Measurement of an Intrinsic Softening Temperature for Coal-Tar Pitch by Proton Magnetic Resonance Thermal Analysis, *Carbon*, **32**, 3, 493-497.

[129] **Mulligan, M.J., Thomas, K.M., and Tytko, A.P.,** 1987. Functional Group Fractionation and Characterisation of Tars and Pitches, *Fuel*, **66**, 11, 1472-1480.

[130] **Edstrom, T., and Petro, B.A.,** 1968. Gel Permeation Chromatographic Studies of Polynuclear Aromatic Hydrocarbon Materials, *Journal of Polymer Sciences*: Part C, 21, 171-182.

[131] **Bartle, K.D., Collin, G., Stadelhofer, J.W., and Zander, M.J.,** 1979. Recent Advances in the Analysis of Coal-derived Products, *Chem. Tech. Biotechnol*, **29**, 531-551.

[132] **Altgelt, K.H.,** 1979. Chromatography in Petroleum Analysis, p.287, Eds. Altgelt, K.H., and Gouw, T.H., Marcel Decker, New York.

[133] **Schanne, L., and Haenel, M.W.,** 1981. Preparative Gel Permeation Chromatography of Coal-derived Products, *Fuel*, **60**, 556.

[134] **Zander, M., and Collin, G.,** 1993. A Review of the Significance of Polycyclic Aromatic Chemistry for Pitch Science, *Fuel*, **72**, 1281.

[135] **Mayer, H.K.,** 1995. Characterisation of Pitches Using Gel Permeation Chromatography, *Extended Abstracts of the 22nd Biennial Conference on Carbon*, San Diego, USA, 202-203.

[136] **Mayer, H.K., Nanni, E.J., and Lewis, I.C.,** 1997. Fractionation of Pitches by Gel Permeation Chromatography, *Extended Abstracts of the 23rd Biennial Conference on Carbon*, PennState, 31-35.

[137] **Zander, M.,** 1987. Recent Advances in Pitch Characterisation, *Fuel*, **66**, 11, 1459-1466.

[138] **Southard, W.M., Snow, T.A., McEwen, C.N., Lavin, J.G., Romine, H.E., and Nanni, E.J.,** 1997. Molecular Weight Characterisation of Isotropic and Mesophase Pitches by Matrix Assisted Laser Desorption Ionisation Mass Spectrometry, *Extended Abstracts of the 23rd Biennial Conference on Carbon,* PennState, USA, 188-189.

[139] **Yau, W.W., Kirkland, J.J., and Bly, D.D.,** 1979. Modern Size Exclusion Chromatography, Wiley-Interscience, New York.

[140] **Bartle, K.D., Mills, D.G., Mulligan, M.J., Amaechina, I.O., and Taylor, N.,** 1986. Errors in the Determination of Molecular Mass Distributions of Coal Derivatives by Size Exclusion Chromatography, *Analytical Chemistry*, **58**, 2403-2408.

[141] **Billingham, N.C.,** 1977. Molar Mass Measurements in Polymer Science, Kogan Page, London.

[142] **Willard, H.H, Merritt, L.L.Jr., Dean, J.A., and Settle, F.A.Jr.,** 1981. Instrumental Methods of Analysis, 177, Wadsworth Com., Belmont, California.

[143] **Guillen, M.D., Iglesias, M.J., Dominguez, A., and Blanco, C.G.,** 1995. Fourier Transform Infrared Study of Coal Tar Pitches, *Fuel*, **74**, 11, 1595-1598.

[144] **Blanco, C.G., Dominguez, A., Iglesias , M.J., and Guillen, M.D.,** 1994. Relation Between Solubility of Coal Tar Pitches and Composition of Their Volatile Fraction., *Fuel*, **73**, 510.

[145] **Guillen, M.D., Dominguez, A., Iglesias, M.J., and Gutierrez, C.G.,** 1995. Semiquantitative Gas Chromatographic Analysis of the Volatile Fraction in Several Extracts Obtained by Treatment of Coal Tar Pitches with Different Organic Solvents, *Fuel*, **74**, 233.

[146] **Blanco, C.G., Blanco, J., Bernad, P., and Guillen, M.D.,** 1991. Capillary Gas Chromatographic and Combined Gas Chromatography-Mass Spectrometric Study of the Volatile Fraction of a Coal-Tar Pitch Using OV-1701 Stationary Phase, *Journal of Chromatography*, **539**, 157-167.

[147] **Karr, C. Jr.,** 1978. Analytical Methods for Coal and Coal Products, **2**, Academic Press.

[148] **Brown, J.K., and Ladner, W.R.,** 1960. A Study of the Hydrogen Distribution in Coal-Like Materials by Higher Resolution Nuclear Magnetic Resonance Spectroscopy II- A Comparison with Infra-red Measurement and the Conversion to Carbon Structure, *Fuel*, **39**, 87.

[149] **Sohar, P.,** 1983. Nuclear Magnetic Resonance Spectroscopy, **2**, CRC Press, Inc.

[150] **Kershaw, J.R., and Black, K.J.T.,** 1993. Structural Characterisation of Coal-Tar and Petroleum Pitches, *Energy and Fuels*, 7, 3, 420-425.

[151] **Abrahim, R.J., and Loftus, P.,** 1978. Proton and ^{13}C NMR Spectroscopy, Heydon.

[152] **Gupta, L.P., Dogra, P.V., Kuchhal, R.K., and Kumar, P.,** 1986. Estimation of Average Structural Parameters of Petroleum Crudes and Coal-Derived Liquids by ^{13}C and ^{1}H NMR, *Fuel*, 65, 515-519.

[153] **Forrest, R.A. and Marsh, H.,** 1977. Reflection Interference Colours in Optical Microscopy of Carbon, *Carbon*, **15**, 348-349.

[154] **Unurlu, S., Özen, S., Mısırlı, Z., Yörücü, H., and Özkan, T.,** 1986. Enerji Dağılım Analiz Tekniği ile Mikroanaliz, Tübitak Gebze Araştırma Merkezi Marmara Bilimsel ve Endüstriyel Araştırma Enstitüsü Malzeme Araştırma Bölümü, Proje No: 03 1201 8503, Gebze-Kocaeli, Türkiye.

[155] **Özer, M.Z,** 1998. Applications of Supercritical Fluid Extraction for Environmental Remediation, *PhD Thesis*, University of Leeds, School of Chemistry, UK.

[156] **Hutchenson, K.W., Roebers, J.R., and Thies, M.C.,** 1991. Fractionation of Petroleum Pitch by Supercritical Fluid Extraction, *Carbon*, **29**, 2,215-223.

[157] **Cotton, N.J., Rayner, M.W., and Bartle, K.D.,** 1993. Coupled Supercritical Fluid Extraction - Capillary Supercritical Fluid Chromatography, *Supercritical Fluid Extraction In Use In Chromatographic Sample Preparation*, pp.87-110, Ed. Westwood, S.A., Blackie, London.

[158] **Hawthorne, S.B.,** 1993. Methodology for Off-Line Supercritical Fluid Extraction, *Supercritical Fluid Extraction In Use In Chromatographic Sample Preparation*, pp.39-63, Ed. Westwood, S.A., Blackie, London.

[159] **Rabiah, Ali-Al, H.,** 1997. Supercritical Fluid Fractionation of Petroleum Crude Oil, *PhD Thesis*, University of Leeds, School of Chemistry, UK.

[160] **Clifford, A.A.,** 1993. Introduction to Supercritical Fluid Extraction in Analytical Science, *Supercritical Fluid Extraction In Use In Chromatographic Sample Preparation*, pp.1-38, Ed. Westwood, S.A., Blackie, London.

[161] **Williams, D.F.,** 1981. Extraction with Supercritical Gas, *Chemical Engineering Science*, **36**, 11, 1769-1788.

[162] **McHugh, M.A., and Krukonis, V.J.,** 1994. Supercritical Fluid Extraction Principles and Practice, Butterworth-Heinemann, USA.

[163] **Bolanos, G., Hochgeschurtz, T., and Thies, M.C.,** 1991. Production of Mesophase Pitch by Supercritical Fluid Extraction, *Proceedings of the 2nd International Symposium on Supercritical Fluids,* Boston, 164-165.

[164] **Tanaka, A.,** 1997. Characterisation of Coal-Tar Pitches in Air-Blowing Reaction by Ultrasonic Method, *Extended Abstracts of the 23rd Biennial Conference on Carbon*, PennState, USA, 195-196.

[165] **Kershaw, J.R., and Smart,P.J.,** 1994. Extraction of Coal-Tar Pitch and the Effect on Carbonisation, *Carbon*, 32, 1, 85-92.

[166] **Dean, J.R., and Murray, G.S.,** 1998. Carbon from Phenolic Resins – What is the Carbon Yield?, Carbon As a Material, *A Meeting of the British Carbon Group*, University of Bath, UK.

[167] The Manual of VG AutoSpec Mass Spectrometry.

[168] **Fernandez, J.J., Figueras, A., Granda, M., Bermejo, J., and Menendez, R.,** 1995. Modification of Coal-Tar Pitch by Air-Blowing- I. Variation of Pitch Composition and Properties, *Carbon*, 33, 3, 295-307.

[169] **Prada, V., Granda, M., Bermejo, J., and Menendez, R.,** 1999. Preparation of Novel Pitches by Tar Air-Blowing, *Carbon*, 37, 97-106.

[170] **Yamaguchi, C., Matsuyoshi, H., Mondori, J., Matsui, H., Kumagai, H., and Sanada, Y.,** 1997. Properties and Molecular Structure of Pitch Produced in Air-Blowing Reaction, *Extended Abstracts of the 23rd Biennial Conference on Carbon,* PennState, USA, 192-193.

[171] **Daji, J., Rand, B., Martin, Y., Moinelo, S.R., and Garcia, R.,** 1998. Viscoelasticity of Air-Blown Pitches, *Proceedings of the International Symposium of Carbon,* Tokyo, Japan, 250-251.

[172] **Barr, J.B., and Lewis, I.C.,** 1978. Chemical Changes During the Mild Air Oxidation of Pitch, *Carbon*, 16, 439-444.

[173] **Maeda, T., Zeng, S.M., Tokumitsu, K., Mondori, J., and Mochida, I.,** 1993. Preparation of Isotropic Pitch Precursors for General Purpose Carbon Fibres (GPCF) by Air-Blowing- I. Preparation of Spinnable Isotropic Pitch Precursor from Coal Tar by Air-Blowing, *Carbon*, 31, 3,407-412.

[174] **Almugerhiy, A.A.,** 1998. Preparation and Characterisation of Göynük Oil Shale Derived Pitch Precursors for Production of Carbon Materials, *PhD Thesis*, Istanbul Technical University, Institute of Science and Technology, Chemical Engineering Department, Turkey.

[175] **Herod,A.A., Zhang, S.F., Johnson, B.R., Bartle, K.D., and Kandiyoti, R.,** 1996. Solubility Limitations in the Determination of Molecular Mass Distributions of Coal Liquefaction and Hydrocracking Products; 1-Methyl-2-pyrrolidinone as Mobile Phase in Size Exclusion Chromatography, *Energy and Fuels*, **10**, 743-750.

[176] **Lewis, I.C., and Petro, B.A.,** 1976. Molecular Weight Analysis of Pitches and Polymeric Pitches by Gel-Permeation Chromatography, *Journal of Polymer Science*, **14**, 1975-1985.

[177] **Blanco, C.G., Iglesias, M.J., Dominguez, A., and Guillen, M.D.,** 1994. Fourier Transform Infrared Study of Coal Tar Pitches, *Extended Abstracts of the Biennial Conference on Carbon,* Granada, Spain, 92-93.

[178] **Solomon, P.R., and Miknis, F.P.,** 1980. Use of Fourier Transform Infrared Spectroscopy for Determining Oil Shale Properties, *Fuel*, **59**, 893-896.

[179] **Guillen, M.D., Iglesias, M.J., Dominguez, A., and Blanco, C.G.,** 1992. Semiquantitative FTIR Analysis of a Coal Tar Pitch and Its Extracts and Residues in Several Organic Solvents, *Energy and Fuels*, **6**,518-525.

[180] **Charles, Q.Y., and John, R.S.,** 1993. Infrared Spectroscopy Studies of the Petroleum Pitch Carbon Fibre – I. The Raw Materials, the Stabilisation, and Carbonisation Processes, *Carbon*, **31**, 3, 451-459.

[181] **Akrami, H.A., 1997.** Preparation and Characterisation of Avgamasya Asphaltite and Raman-Dinçer Crude Oil Derived Pitches for Production of Stabilised Fiber, *PhD Thesis*, Istanbul Technical University, Institute of Science and Technology, Chemical Engineering Department, Turkey.

[182] **Akrami, H.A., Yardım, M.F., Akar, A., and Ekinci, E.,** 1997. FTIR Characterisation of Pitches Derived from Avgamasya Asphaltite and Raman-Dincer Heavy Crude, *Fuel*, **76**, 14/15, 1389-1394.

[183] **Fischer, P., Stadelhofer, J.W., and Maximilian, Z.,** 1978. Structural Investigation of Coal-Tar Pitches and Coal Extracts by C NMR Spectroscopy, *Fuel*, **57**, 345-352.

[184] **Forrest, R.A. and Marsh, H.,** 1983. The Carbonisation of Blends of Pitches and Resins to Produce Anisotropic Carbon and the Effects of Pressure, *Journal of Materials Science,* 18, 991-997.

[185] **Mochida, I., Oyama, T., Korai, Y., and Fei, Y.Q.,** 1988. Study of Carbonisation Using a Tube Bomb: Evaluation of Lump Needle Coke, Carbonisation Mechanism and Optimisation, *Fuel*, 1171-1181.

[186] **Shi, J.L., Zha,Q.F., Ji, Y., and Liu, L.,** 1991. The Evaluation of Spinnability of Mesophase Pitch, *Extended Abstracts of the 20th Biennial Conference on Carbon*, Santa Barbara, USA, 282-283.

[187] **Lavin, J.G.,** 1998. Mesophase Precursors for Advanced Carbon Fibres, *The Abstracts of Design and Control of Structures of Advanced Carbon Materials for Enhanced Performance,* NATO-ASI, Antalya, Turkey, 106

[188] **Kershaw, J.R., and Smart, P.J.,** 1994. Supercritical Fluid Extraction of Coal-Tar Pitch: Part2. Extraction of the Lower Molecular Weight Species with Aliphatic Solvents, *Fuel Processing Technology*, **38**, 1-15.

[189] **Dauche, F.M., Bolanos, G., Blasig, A., and Thies, M.C.,** 1998. Control of Mesophase Pitch Properties by Supercritical Fluid Extraction, *Carbon*, **36**, 7-8, 953-961.

[190] **Kershaw, J.R., and Smart, P.J.,** 1993. Extraction of Coal-Tar Pitch with Supercritical Toluene, *The Journal of Supercritical Fluids*, **6**, 155-163.

CURRICULUM VITAE

Mevlude Ebru APAK was born in Istanbul, Turkey in September, 1970. Upon her graduation from Özel Tarhan Lisesi in 1987, she attended to Istanbul Technical University (ITU), Chemical Engineering Department. She received her B.Sc degree in June, 1991, and in the same year she started to study as a Master student at the same department. She received her M.Sc degree in September, 1994. Subsequently, she started to her PhD degree in the same year at ITU, Chemical Engineering Department. One year later in July 1995, she got a scholarship from British Council and studied at the University of Strathclyde, Pure and Applied Chemistry Department, UK, for three months. She studied on the characterisation of the pyrolysis products of tyre crumbs. After returning back to Turkey, she started to her experimental work about her PhD study. In 1998, she was awarded by British Council – TÜBİTAK scholarship and joined to the Carbon Group at the University of Leeds, School of Materials, UK, for nine months. She made a research on pitch characterisation and carbon fibre production related to her PhD study. She has been working as a research and teaching assistant at ITU, Chemical Engineering Department since January, 1994.